MODELLING A BATCH BIOFILM PASSIVE AERATION PROCESS USING AN ACTIVATED SLUDGE PROCESS AND A BIOFILM PROCESS

A thesis submitted to the National University of Ireland, Galway, in fulfilment of the requirement for the Doctor of Philosophy

by

Noelle Jones O'Connell

BSc, MSc, CEng MIEI Chartered Engineer

Scoil na hInnealtóireacht,
Ollscoil na hÉireann,
Gaillimh

An tOllamh Padraic O'Donoghue

Department of Civil Engineering,
National University of Ireland,
Galway

Dr. Eoghan Clifford

A dissertation submitted to the National University of Ireland in fulfilment of the requirements for the degree of Doctor of Philosophy.

April 2015

The National University of Ireland requires the signatures of all persons using or photocopying this thesis. Please sign below, and give the address and date.

"*Think where man's glory most begins and ends,*

And say my glory was I had such friends."

William Butler Yeats (1865 – 1939)

ACKNOWLEDGEMENTS

I would like to sincerely thank the following people.

Dr. Eoghan Clifford whom I am extremely grateful and indebted to for giving me the opportunity to conduct this research. For your enthusiasm and immense knowledge in every area of my work. I appreciate the freedom you gave me to progress at my own pace and also allowing me time off when needed. Thank you.

An tOllamh Padraic O'Donoghue for his encouragement and guidance throughout my research.

Dr. Edmond O'Reilly and Shane Fox for allowing me to use their data in my research and for their help throughout this project. Maebh Grace for presenting this work at the 7th International Congress on Environmental Modelling and Software in California on my behalf. Dr. Bryan McCabe for his support throughout my time in NUIG.

Galway Mayo Institute of Technology (GMIT) for the financial support provided throughout my research.

To my very good friends and lecturers in the engineering department.

My wonderful parents, Daniel and Margaret and sisters and brothers.

Eleanor, Lillian and Stephen your help in writing this thesis is greatly appreciated.

Leonie Kelly – if convention allowed, your name would be on the title page also.

My three extra chapters that were a huge part of this thesis Clíodhna (aged 4), Siún (aged 3) and Fia (8 months).

Finally my husband Eoghan for his love, patience, understanding and support.

ABSTRACT

Recently, mathematical modelling of wastewater treatment plants has become a widely used tool for planning, designing, optimising and evaluating wastewater treatment plants (WWTPs). While wastewater models can provide insights into plant upgrades, new plant designs, optimised operational regimes and enable discharge effluent limits to be met, they are not been widely applied, particularly in informing the development of new technologies or optimising small-scale WWTPs. This is frequently due to the significant resources necessary to develop calibrated models for individual wastewater treatment processes.

The pumped flow biofilm reactor (PFBR), a batch biofilm technology, is a recent example of a new technology targeted at urban areas of about 5000 persons or less. This biofilm-based passive aeration system has been shown to have potential as an energy efficient and low maintenance alternative for the treatment of municipal wastewater. However, the modelling of biofilm-based PAS can present challenges, particularly where new technologies are not easily simulated using existing commercial modelling software. As a relatively new technology a predictive model for the PFBR system has yet to be developed. Indeed for novel passive aeration systems in general, it can be time consuming and difficult to develop new models that accurately describe performance. Nevertheless, if the modeller is concerned only with simulating "macro" plant performance (e.g. key effluent concentrations and cycle analysis), it may be possible to model these technologies using "surrogate" unit process systems (e.g. using an activated sludge process to model a biofilm process). While in practice biofilm systems may have been modelled as activated sludge systems, there has been limited research conducted on how such models can be systematically developed and what the merits or otherwise are of using activated sludge models as surrogates for biofilm systems.

The present investigation serves to investigate the possibility of (1) modelling the PFBR using an activated sludge object in GPS-X in order to quickly study the PFBR (2) predicting effluent results and contaminant concentration changes (nitrogen and organic carbon) during individual treatment cycles using the activated sludge object (3) modelling different operational scenarios and thus optimising operational efficiency and (4) modelling the PFBR using AQUASIM in order to study the cycle performance, biofilm thickness and biofilm composition of the PFBR.

The PFBR was modelled and calibrated at laboratory and field scale. In each case, after calibration, the models were verified using independent data. The models resulted in good predictions of effluent results and contaminant concentration changes (nitrogen and organic carbon) during individual treatment cycles and could thus be used for process optimisation; or eventually real time process simulation. In all cases there was limited data available due to minimal on site monitoring. This is typical of small scale systems and thus the study demonstrates that even limited monitoring, if strategically targeted, can lead to good model calibration.

The work done in this study has demonstrated that it is possible to model a novel wastewater technology using 'surrogate' processes in existing software. This has the potential to provide substantial benefits as such simulations can in turn can lead to cost savings during technology development and on-site operation. The calibrated model can enhance the understanding of the technology in question and thus lead to better design and more cost-effective wastewater treatment systems. The use of "surrogate" unit processes as described in this research could be applied to other technologies to provide rapid performance simulation. Thus the study demonstrates simple approaches to modelling novel technologies where new technologies are not easily modelled using existing commercial modelling software.

TABLE OF CONTENTS

I, Noelle Jones, certify that this Thesis is all my own work and I have not obtained a degree in this University or elsewhere on the basis of any of this work.

1. INTRODUCTION

1.1 BACKGROUND

One of the main threats to water comes from untreated sewage. Over 90% of all wastewater in developing countries is discharged untreated, polluting rivers, lakes and seas. In developed countries, while compliance levels may be higher, there are still considerable challenges regarding small scale wastewater treatment systems, energy consumption by facilities and wide variations in operational efficiency.

Mathematical modelling and computer simulation have become useful tools in evaluating the operation of wastewater treatment plants. Improvements in modelling techniques and computational power mean such tools can be deployed to help optimise wastewater plant operation and minimise environmental costs. Over the last number of years, mathematical modelling has become increasingly popular as a supporting tool for the design, operation and control of activated sludge systems and biofilm systems.

Wastewater treatment modelling can enhance plant efficiencies, resulting in significant cost and energy savings. Once implemented and calibrated correctly, a model can offer many advantages, such as optimising daily operation, determining maximum flow conditions, evaluating proposed operational or infrastructural changes, and evaluating the suitability of existing wastewater treatment facilities for more stringent regulations.

While wastewater treatment modelling is developing and making important contributions to practice, it must be remembered that treatment systems are complex and that further challenges for engineers remain. Areas requiring greater focus include (i) the modelling of new technologies which are still in their infancy; (ii) the model calibration process; (iii) the modelling of biofilm-based passive aeration systems, (iv) the quantity and quality of data necessary for calibration; in many cases infrequent and basic data only is available, and (v) scaling up laboratory-scale data to full-scale models.

The pumped flow biofilm reactor (PFBR); a batch biofilm process, is an example of a new wastewater treatment technology. The PFBR is a two reactor technology that employs a unique hydraulic regime and enables aerobic, anoxic and anaerobic conditions to be sequenced. Biofilm, growing on plastic media modules within the two reactors, is aerated passively as wastewater is moved alternately between the reactors during an aeration sequence. Thus as the two reactors empty and fill a number of times during a typical aeration sequence, the biofilm is exposed, in turn, to atmospheric air and

wastewater. Furthermore while the PFBR has many of the features of a sequencing batch reactor the fill and discharge from the system typically take place in Reactors 1 and 2 respectively.

In this study, using the PFBR as a case study, predictive models were developed using two different modelling packages. There are numerous methods and commercial wastewater simulators used to model wastewater treatment processes, including BioWin (EnviroSim Associates Ltd, Canada), EFOR (Danish Hydraulic Institute, Denmark), SIMBA (Institut für Automation und Kommonikation (IFAK), Germany), STOAT (Water Research Centre, UK) and WEST (Hemmis, Belgium). In this study the modelling packages GPSX (Hydromantis Inc, Canada) and AQUASIM (EAWAG, Switzerland) were chosen to model the PFBR. As the PFBR is a relatively new technology, a predictive wastewater treatment model for the PFBR system has yet to be developed. There are no commercially available unit processes to correctly model the PFBR, and commissioning bespoke software would not be feasible for many company's and thus this study focused on how existing packages could be adapted to model technologies that may have unique operating characteristics.

1.2 OBJECTIVES

The key objectives of this study were:

1. To investigate if robust, calibrated models (using GPS-X software) of laboratory and site-scale PFBR systems could be developed using activated sludge unit processes in existing software in order to predict effluent results and contaminant concentration changes (nitrogen and organic carbon) during individual treatment cycles.
2. To use the above models to inform optimal system operation, (e.g. maximizing contaminant removal per unit energy input) and compare various treatment scenarios from an economic and effluent quality point of view.
3. To develop a biofilm-based model for the PFBR, using the modelling package AQUASIM, that (i) predicts the effluent characteristics, (ii) the cycle performance of the PFBR and (iii) simulate biofilm composition.
4. To investigate rapid modelling methodologies that can inform the development of newly developed technologies 'using surrogates processes', which in turn will

minimise the time and costs necessary to model new, similar technologies using commercial software. Issues considered included the relative impacts on model accuracy of key operational data, including reactor hydraulics, oxygen transfer characteristics and influent data (which may often be limited on site).

5. To inform new approaches for rapidly developing and calibrating models without the need for developing bespoke unit processes. The use of "surrogate" unit processes could be applied to other technologies to provide rapid performance simulation for newly developed technologies. This would ensure that the development or design stage for new technologies would be theoretically tested and optimised before the physical unit was constructed, while minimising the use of resources.

1.3 RESEARCH METHODOLOGY

The study is based on the use of a new passive aeration technology (the pumped flow biofilm reactor) as the case study to be modelled. Initially, data obtained during a long-term laboratory study of the system was used to develop, build and calibrate the models. Given that the PFBR is a new technology, existing software packages do not have a specific process object for this system. Thus, alternative processes were used to model the PFBR. As the PFBR is operated as a sequencing batch biofilm reactor type process with typical phases, including fill/draw, anoxic, aerobic and settle, an initial analysis indicated sequencing batch reactor objects could be most efficiently adapted to model the characteristics of the PFBR. The model was calibrated using experimental data obtained from laboratory studies and validated against a second set of independent data from the laboratory studies.

The laboratory model was then used as the basis for modelling site scale PFBR units. In the site studies, data during steady state operation were used in conjunction with data obtained during intensive monitoring periods to calibrate and subsequently validate the model.

The GPS-X model was only concerned with simulating the effluent from the PFBR and predicting individual treatment cycles. The AQUASIM model involved modelling the PFBR as a biofilm process in order to develop a unique biofilm model for the PFBR in

order to calibrate the effluent characteristics and the cycle performance of the PFBR and identify the biofilm thickness and composition.

In order to assess the ability of the model to predict the treated effluent quality and biofilm composition for different PFBR plants, the developed models in GPS-X and AQUASIM were applied to a second PFBR plant. The results show that once a PFBR model is built and calibrated correctly, it can easily be adapted and used for a different PFBR plant.

1.4 STRUCTURE OF THE DISSERTATION

Chapter 2 reviews the current literature relevant to this study, including wastewater treatment technologies, modelling theory, model calibration and validation and wastewater modelling software.

Chapter 3 details the design and operation of the laboratory and field scale PFBR and discusses the previous experimental work conducted.

Chapters 4 and 5 respectively present the development of models for the laboratory and field scale PFBRs. The chapters demonstrate the use of surrogate processes to model the new PFBR system. These models were used to simulate effluent quality and predict concentration changes (nitrogen and organic carbon) during individual treatment. The field scale models were then used to predict the optimal operational regimes.

In Chapter 6, the development of a biofilm-based model for the PFBR using the modelling package AQUASIM capable of predicting the effluent characteristics and the cycle performance of the PFBR and identifying the biofilm composition in the PFBR is presented. The chapter also demonstrates the use of a simplified surrogate process to model the PFBR system.

Chapter 7 involves applying a step-wise procedure developed in Chapter 4 in adapting the developed GPS-X and AQUASIM models to a second field-scale PFBR in order to assess its ability to predict the treated effluent quality for different PFBR plants.

Chapter 8 discusses the five main causes of uncertainty in wastewater treatment modelling encountered as part of this research: (i) modelling the hydraulics of new technologies, (ii) modelling the passive aeration process in new technologies, (iii) modelling new technologies with minimal performance datasets, (iv) accurate

undertaking/execution of the calibration process and (v) scaling up laboratory-scale data to full-scale models.

Finally, in Chapter 9 conclusions from each of the studies and recommendations for further research are presented.

2 LITERATURE REVIEW

2.1 INTRODUCTION

The growth of wastewater treatment modelling has gained momentum in the past decade with the global wastewater challenges now being faced. Over 90% of all wastewater in developing countries is discharged untreated or from poorly designed wastewater treatment plants, polluting rivers, lakes and seas. Mathematical modelling of wastewater treatment processes has become a widely established tool in the past decade for planning, designing, optimizing and evaluating wastewater treatment plants (WWTPs). Such modelling software has also shown significant potential in the areas of wastewater research and education. Wastewater modelling could have significant potential in developing new technologies and processes by minimising the expenses incurred at the research and piloting stage. However, the use of modelling software to inform research in the area of technology development and optimisation has been limited to date.

Due to pressures such as increasingly stringent discharge limits and energy efficiency biofilm-based passive aeration systems (PAS) have attracted attention recently as alternative, sustainable technologies in the wastewater sector. However, the simulation of biofilm-based PAS (and indeed many new process configurations) can present unique challenges for process modellers, particularly where new technologies are not easily simulated using existing commercial modelling software. Thus, the potential of models to drive technology research and development can be underutilised.

This chapter presents an overview of wastewater systems and wastewater models and reviews some of the major challenges experienced by process modellers. The review finally summarises these challenges and proposes key solutions that are investigated in this thesis.

2.2 WASTEWATER TREATMENT TECHNOLOGIES

Modern wastewater treatment techniques have been in use for over a century. In that period, numerous processes have been developed, each of which can have site specific variations. In general, biological-based technologies are most widely applied, and these can be broadly divided into (i) activated sludge processes, and (ii) biofilm processes.

In the activated sludge process, the wastewater to be treated is aerated in the presence of a suspended bacterial biomass that stabilises biodegradable organic matter in the wastewater. In general, the bacteria stabilising the organic matter require a supply of dissolved oxygen in order to function. Examples of activated sludge processes include conventional activated sludge systems, completely mixed systems, plug flow systems and sequence batch reactors.

In biofilm processes (also known as attached growth processes), a bacterial biomass attached to a supporting media in a reactor is responsible for the removal of pollutants. The microorganisms that treat the wastewater are generally attached to an inert media material (e.g. plastic, stone, sand). Biofilms processes have been used in engineered wastewater treatment since the 1870s, when stone pebbles were used as media. Such processes drove the earlier examples of wastewater treatment processes (O'Reilly et al., 2008). Examples of biofilm processes include trickling filters, rotating biological contactors and PFBRs. Given the large variation in technology and processes configuration, the following sections review the technologies employed in the wastewater sector that are most relevant to this study.

2.2.1 Sequencing Batch Reactor (SBR)

The SBR is an activated sludge process designed to accommodate both biological reactions and solid-liquid separation in a time sequence in the same tank. The SBR process generally comprises a number of distinct steps that occur in a single reactor, namely (i) fill, (ii) mix and react (with or without air as required), (iii) settle, (iv) draw, and (v) idle periods, as required (Vesilind, 2003). For example, a typical treatment cycle comprises five steps, as illustrated in Figure 2.1.

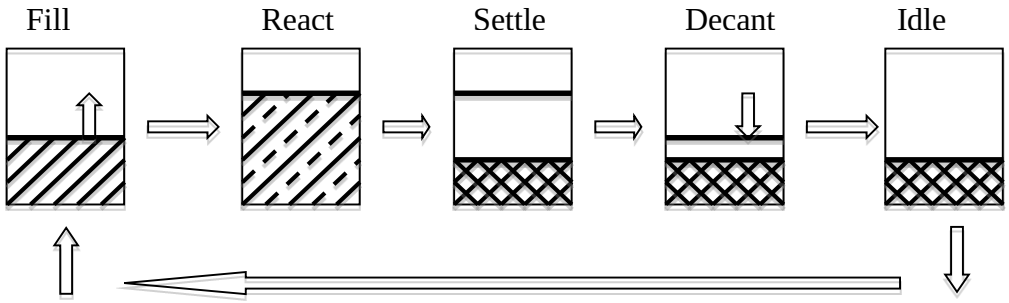

Figure 2.1 - Sequencing batch reactor process (Henry, 2013)

Wastewater is treated in batches, and the sequence of successive stages can be adjusted to create the required combination of growth conditions necessary for different groups of microorganisms to remove targeted contaminants from wastewater, i.e. aerobic for chemical oxygen demand (COD) removal only, aerobic/anoxic for COD/nitrogen removal and aerobic/anoxic/anaerobic for COD/nitrogen/phosphorus removal (Hank et al., 2006).

SBR technology is widely used and tested, and can have advantages, including (i) a relatively low cost, (ii) a small footprint, (iii) flexibility of operation, and (iv) that it can achieve nitrification, denitrification and phosphorus (P) removal. The disadvantages include (i) high energy consumption, (ii) all processes occur in one tank, and (iii) it can be difficult to adjust cycle times in the SBR for small communities.

2.2.2 Sequencing Batch Biofilm Reactors (SBBR)

Sequencing batch biofilm reactors (SBBRs) are a modification of the SBR but they utilise biofilm technology instead of activated sludge. They have a similar operational regime to SBRs and are used for the biological removal of nitrogen and phosphorus in wastewater (Wildered & McSwain, 2004; Zhang et al., 2009; Fu et al., 2010). The layout of the SBBR is similar to the SBR shown in Figure 2.1.

The advantages of SBBRs are that can achieve (i) land and energy savings (ii) greater volumetric loads, and (iii) nitrification, denitrification and P removal (Rodgers & Zhan, 2003). The main disadvantage of the SBBR is that a higher level of sophistication is

required (compared to conventional systems) especially for larger systems, of timing units and controls (US EPA, 1999).

2.2.3 Rotating Biological Contactor (RBC)

The RBC is a biofilm-based treatment process and has been extensively tested for carbon removal and biological nitrogen removal from municipal wastewaters (Grady, 1983; Akunna & Jefferies, 2000; Griffin & Findlay, 2000; Nowak, 2000) (Figure 2.2). RBCs generally comprise disks fitted on an axis that are partially submerged in wastewater. The disks are rotated as wastewater flows through and the microbial community is alternately exposed to atmosphere and wastewater. This allows the aerobic processing of contaminants dissolved in the wastewater (Pylnik et al., 2012).

Typical advantages of the RBC are listed as including (i) simplicity of operation, (ii) low energy consumption, (iii) low operating and maintenance cost, and (iv) high BOD removal and good nitrification (Cortez et al., 2008). The main disadvantages can include the excessive biofilm build-up that can occur on the media and the high capital costs associated with the RBC (Cortez et al., 2008).

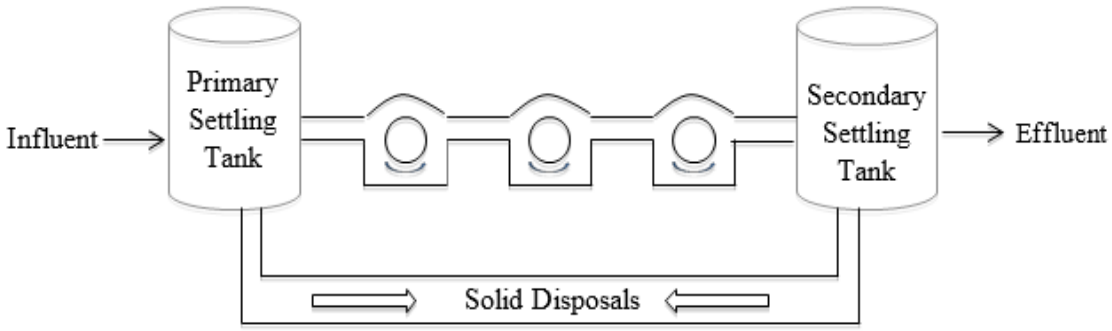

Figure 2.2 – Rotating biological contactor

2.2.4 Submerged Biological Contactor (SBC)

A SBC is a variation of the RBC and works on the same basic principle except the SBC media is submerged underwater for longer periods (ETC, 2013) (Figure 2.3). The SBC is designed to impose reduced loads on the shaft bearings when compared to the RBC. The

biomass forms a thinner film than is found on the RBC, and as the reactor vessel can be deeper, the volume of liquid in contact with the media is greater.

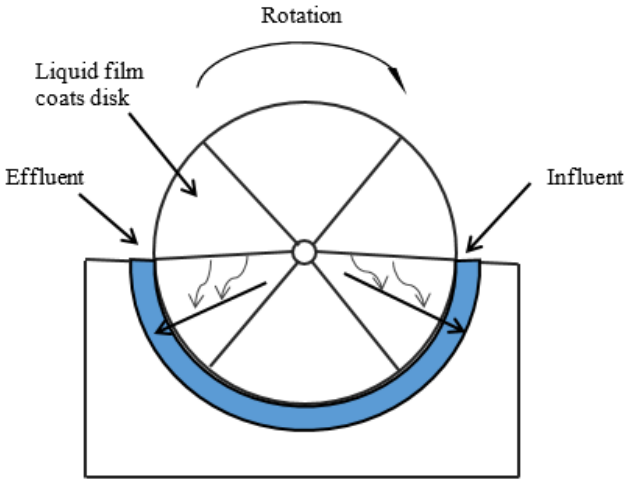

Figure 2.3 – Submerged biological contactor

Typical advantages of the SBC are reported as (i) limited odour production, (ii) the enclosure raises the operating temperatures and improve nitrification, and (iii) it is suited to high-strength industrial wastewater applications with limited available space (ETC, 2014). Similar to the RBC, the main disadvantages can include excessive biofilm build-up that can occur on the media and the high capital costs (ETC, 2014).

2.2.5 Trickling Filters (TF)

Trickling filters use a static medium such as rocks or plastic within a reactor to support biofilm growth. In most variations of the TF, wastewater is pumped on a continuous or intermittent basis over the static media; biofilm growing on the media then biologically degrades organic matter within the wastewater (Vesilind, 2003). A well operated trickling filter in combination with a secondary settling tank may remove 75% to 90% BOD and produce highly nitrified effluent (EPA, 1997).

The main advantages of the TF can include (i) it is a simple and reliable process, (ii) it is effective in treating high concentrations of organic material depending on the type of media used, (iii) that it is very efficient in removing ammonia from water, (iv) its ability to handle and recover from shock loads, and (v) its low power requirements and therefore

low operating costs. The main disadvantages of trickling filters are their (i) large land requirements, (ii) odour problems, and (iii) high capital costs (US EPA, 2000).

2.2.6 Moving Bed Biofilm Reactor (MBBR)

The MBBR process is a fixed film (or attached growth) biological process. The biomass in the MBBR exists in two forms: suspended flocs and a biofilm attached to carriers. The MBBR was introduced in the late 1980s and has been widely applied when upgrading and retrofitting existing wastewater treatment plants (Ferrai et al., 2010).

The MBBR is a completely mixed, continuous flow through process, which combines the advantage of fixed film and suspended growth processes. The main advantages of MBBRs are reported as including (i) compact units with small sizes, (ii) increased treatment capacity, (iii) complete solids removal (Borkar et al., 2013), (iv) it can be operated at high organic loads and it is less sensitive to hydraulic overloading (Ødegaard, 2006), and (v) it achieves high nitrification efficiencies under severe climate conditions (Andreottola et al., 2000). The main disadvantages of the MBBR can include the relatively high energy consumption due to aeration (Weiss et al., 2005) and high chemical costs.

2.2.7 Pumped Flow Biofilm Reactor (PFBR)

The PFBR is a two-reactor technology that employs a unique hydraulic regime and enables aerobic, anoxic and anaerobic conditions to be sequenced. Biofilm growing on plastic media modules within the two reactors (Reactors 1 and 2) is aerated passively as wastewater is moved alternately between the reactors during an aeration sequence. Thus, as the two reactors empty and fill a number of times during a typical aeration sequence, the biofilm is exposed, in turn, to atmospheric air and wastewater. Furthermore, while the PFBR has many of the features of a sequencing batch reactor, the fill and discharge from the system typically take place in Reactors 1 and 2 respectively (O'Reilly, 2005, O'Reilly et al., 2008, O'Reilly et al., 2011). The PFBR can achieve BOD_5, COD, and SS removal, nitrification and denitrification.

The main advantages of the PFBR include (i) a low land requirement, (ii) low construction costs, (iii) low maintenance costs, (iv) infrequent sludge disposal, and (v) it can be

operated without continuous supervision (Zhan et al., 2006). The PFBR is discussed in further detail in Chapter 3.

2.3 WASTEWATER CHARACTERISTICS

2.3.1 Introduction

Wastewater entering treatment plants comprises various organic and inorganic materials and about 99.9% water (Gray, 2004). The concentrations of pollutant constituents in municipal wastewater (WW) are usually measured in the following way:

(i) organic carbon (C), measured in terms of COD, and 5-day biochemical demand BOD_5;

(ii) nitrogen (N), measured as total N (TN), ammonium-nitrogen (NH_4-N), nitrate-nitrogen (NO_3-N) and nitrite-nitrogen (NO_2-N);

(iii) phosphorus (P), measured as total P (TP), and inorganic P usually in the form of orthophosphate-phosphorus (PO_4-P) and microorganisms;

(iv) solids, measured as suspended solids (SS) or total SS (TSS);

(v) bacterial contamination, measured in terms of coliforms (total coliforms and faecal coliforms).

Table 2.1 presents the typical composition of raw municipal wastewater. It shows the influent nitrogen composition, COD and TSS, which are most relevant to this discussion.

Table 2.1 - Range of municipal wastewater characteristics (Henze et al., 2002)

Parameter	Concentration (mg/l)
TSS	120-450
BOD_5	150-530
Total COD	210-740
TN	20-80
Organic N	8-30
NH_4-N	12-50
NO_2-N	0.01
NO_3-N	0.5
Total P	4-10
Organic P	1-3
Inorganic P	3-7

The measurement of influent and effluent parameters at a wastewater treatment plant can often be an expensive undertaking. However, the quality of the data used to calibrate a wastewater treatment model will have a direct impact on the reliability of the predictions made when using the final calibrated model. Table 2.2 shows a range of effluent parameters measured at a treatment plant alongside the parameters used in wastewater treatment modelling. These are discussed in more detail in Section 2.5.2.1.

Table 2.2 - Parameters typically measured on site and parameters required for modelling

Parameters measured on site	Parameters required for modelling
BOD_5	BOD_5
COD	Total COD (COD_t)
	Filtered COD (COD_f)
	Readily biodegradable substrate (Ss)
	Inert soluble organic matter (Si)
	Slowly biodegradable substrate (Xs)
	Particulate inert organic matter (Xi)
Dissolved oxygen (DO)	DO
TN	TN
NH_4-N	NH_4-N
NO_3-N	NO_3-N
	Soluble biodegradable organic nitrogen
SS	SS
pH	pH
	Active heterotrophic biomass $X_{B,H}$
	Active autotrophic biomass $X_{B,A}$

2.3.2 Organic Carbon Removal

Biodegradable organic matter in wastewater is usually expressed in terms of BOD_5 and COD. It is removed from wastewater through biological degradation by the aerobic or anaerobic growth of heterotrophic bacteria, using soluble organic carbon as an energy source. The main factors limiting aerobic growth of heterotrophic bacteria include the lack of sufficient nutrients (N and P) and oxygen, and incorrect temperature and pH (Henze et al., 2002).

2.3.3 Nitrification and denitrification

The nitrogen present in influent wastewater to a municipal WWTP is typically in the form of NH_4-N or organic nitrogen (N_{org}). Ammonium-nitrogen and total N removal is generally accomplished by the nitrification processes followed by denitrification. In nitrification, ammonium is first oxidised to nitrite and then to nitrate by the aerobic growth of autotrophic bacteria (Eq. 2.1 and 2.2). Soluble NH_4-N serves as the energy source for the growth of nitrifies (Henze, 2000). The nitrification process is highly dependent on a number of factors including the substrate and oxygen concentrations, temperature, pH, alkalinity and the presence of toxic or inhibiting substances.

$$NH_4 + 1.5O_2 \longrightarrow NO_2 + H_2O + 2H^+ \qquad \text{(Eq. 2.1)}$$

$$NO_2 + 0.5O_2 \longrightarrow NO_3 \qquad \text{(Eq. 2.2)}$$

Denitrification occurs when oxidised nitrogen produced during nitrification is converted to nitrogen gas (Eq. 2.3). This process occurs in an anoxic environment, that is, in the absence of oxygen (Sincero et al., 2003).

$$2NO_3 + 12H^+ \longrightarrow N_2 + 6H_2O \qquad \text{(Eq. 2.3)}$$

Anoxic zones are necessary for denitrification, whereas aerobic zones are necessary for nitrification. The main factor limiting denitrification is the absence of an anoxic zone.

2.4 WASTEWATER TREATMENT MODELLING

The use of mathematical modelling and computer simulation has become a useful tool in evaluating the operation of wastewater treatment plants since the mid-1990s (Vanrolleghem & Jeppsson, 1995; Gabaldon et al., 1998; Gernaey et al., 2004). A number of factors have contributed to, this such as the publication of the Activated Sludge Models (ASM1, ASM2, ASM2d and ASM3) by Henze et al. (2000) and the publication of the Anaerobic Digestion Model No. 1 by Batstone et al. (2002).

Wastewater treatment plant modelling can effectively inform plant capacity assessments and improved plant operation, and thus enable better environmental performance, reducing energy and chemical costs. Models can also provide important benefits for

planning and designing of new wastewater treatment plants (Dupont & Sinkjaer, 1994; Suescun et al., 1994; Dudley & Chambers, 1995).

Most commercial software comprises a number of process modules that can be configured and connected by flow streams to represent a specific WWTP. The algorithms for each of these modules can vary greatly. Some modules include empirical removal rates while others consist of complex mathematical models that are based on detailed modelling of individual substrate removal and biomass growth processes (Boltz et al., 2010).

Simulations, based on high quality calibration and validation studies, can lead to improved plant performance, along with reduced energy and chemical costs. Devisscher et al. (2006) noted that mathematical modelling can optimise plant efficiencies, resulting in cost savings of (i) aeration energy of between 10 and 20%, and (ii) chemical dosing of up to 30%. Once implemented and calibrated, a model can offer many advantages, including (Pena-Tijerina et al. (2007)):

(i) determining maximum flow conditions,
(ii) optimising daily operation,
(iii) energy saving evaluations,
(iv) preparing existing wastewater treatment facilities for upcoming regulations.

Wastewater treatment processes are complex because of the large variations in the influent wastewater flow rate, concentration and composition. Computer simulations can describe, predict and control the complicated interactions of the processes (Jeppsson, 1996), however while wastewater treatment modelling is advancing and making important contributions to practice, it must be remembered that these are complex systems, and further challenges to modellers remain. The main challenges which are discussed in this study are the modelling of new technologies that are not easily simulated using existing commercial modelling software.

2.5 ACTIVATED SLUDGE BIOLOGICAL MODELS

The modern age of wastewater treatment modelling began with the publication of the International Water Association (IWA) Activated Sludge Model (ASM) 1 and has advanced significantly since (Daigger, 2011). The models of the ASM family (ASM1, ASM2, ASM2d, ASM3) are used in most modelling and simulation studies are thus the basis of most of today's commercial and non-commercial simulation platforms (Henze et

al., 2008). The ASMs have been successfully applied both in research and practice, and serve as the benchmark for new or expanded activated sludge models (Morgenroth et al., 2000a).

2.5.1 Activated Sludge Models used in Development of Model for the PFBR

Selecting the ASM model to use in the calibration of a wastewater treatment is usually dependent on:

(i) the biological process occurring in the treatment plant (e.g. COD removal, N removal or P removal or combinations thereof), and

(ii) the purpose of the model application.

In general, it is recommended that ASM models should be chosen depending on the situation being modelled (Sin, 2004) (Table 2.3).

Table 2.3 – ASM family and application

ASM Family	Application
ASM1	modelling biological removal of organic carbon, NH_4-N and TN removal
ASM2	modelling COD, N and P removing biological wastewater treatment plants
ASM2d	modelling biological phosphorus removal with simultaneous nitrification-denitrification. ASM2d is based on ASM2 and is expanded to include the denitrifying activity of the phosphorus accumulating organisms (PAOs)
ASM3	modelling biological removal of organic carbon, NH_4-N and TN

In sections 2.5.2, 2.5.3 and 2.5.4, the model concepts of ASM1 (Henze et al., 1987) and the recent modifications leading to ASM3 (Gujer et al., 1999) are described. A detailed description of ASM2/ASM2d (Henze et al., 1995, 1999) is, however, not included as biological phosphorus removal was not considered during this study.

2.5.2 ASM1

In 1982, the International Association on Water Pollution Research and Control (IAWPRC) (now known as the IWA) established a task group to develop a standard mathematical modelling basis for the design and operation of activated sludge processes.

The outcome was ASM1, which was published in 1987 (Henze et al., 2000). ASM1 was developed mainly for activated sludge plants and includes biological nitrogen and organic matter removal with simultaneous consumption of oxygen and nitrate as electron acceptors; however, it does not contain biological phosphorous removal (Henze et al., 2002; Henze et al., 2008). ASM1 is presented in a matrix format in Tables 2.4 – 2.6. The model components are given in the first row of Table 2.6. The first column contains the processes included in ASM1 and the last column contains the process rates (kinetics) of these processes. The stoichiometric coefficient of each component for each process is given in the cell, corresponding to the intersection of the row of the process and the column of the component. In total, eight processes are modelled in ASM1:

- growth of biomass (three processes),
- decay of biomass (two processes),
- ammonification of organic N (one process),
- hydrolysis (two processes).

In the eight process equations, 19 parameters are used and are discussed below (Petersen, Gernaey, Henze, & Vanrolleghem, 2000) (Table 2.6). A summary of the state variables and parameters included in ASM1 are included in Tables 2.4 and 2.5.

Table 2.4 – State Variables included in ASM1

Symbol	Units	Description
S_S	(g COD/m^3)	Readily biodegradable substrate
S_I	(g COD/m^3)	Soluble inert organic matter
S_{NH}	(g N/m^3)	Free and ionized ammonia
S_{NO}	(g N/m^3)	Nitrate and nitrite nitrogen
S_{ND}	(g N/m^3)	Soluble biodegradable organic nitrogen
S_O	(g O_2/m^3)	Dissolved oxygen
S_{ALK}	(mol/m^3)	Alkalinity
X_S	(g COD/m^3)	Slowly biodegradable substrate
X_I	(g COD/m^3)	Particulate inert organic matter
$X_{B,H}$	(g COD/m^3)	Active heterotrophic biomass
$X_{B,A}$	(g COD/m^3)	Active autotrophic biomass
X_P	(g COD/m^3)	Particulate production from biomass decay
X_{ND}	(g N/m^3)	Particulate biodegradable organic nitrogen

Table 2.5 - ASM1 kinetic parameters

Symbol	Units	Description
$\hat{u}_H$	d^{-1}	Maximum growth rate for heterotrophic biomass
$\hat{u}_A$	d^{-1}	Maximum growth rate for autotrophic biomass
K_S	g COD / m^3	Half-saturation coefficient for heterotrophic biomass
K_{NO}	g N / m^3	Nitrate half-saturation coefficient for denitrifying heterotrophic biomass
K_{NH}	g N / m^3	Ammonia half saturation coefficient autotrophic biomass
$K_{O,A}$	g O_2 / m^3	O_2 half-saturation coefficient autotrophic biomass
$K_{O,H}$	g O_2 / m^3	O_2 half-saturation coefficient heterotrophic biomass
K_X	g COD/g COD	Half-saturation coefficient for hydrolysis of slowly biodegradable substrate
η_g	(/)	Correction factor for $\hat{u}_H$ under anoxic conditions
η_h	(/)	Correction factor for hydrolysis anoxic conditions
k_a	m^3 /g COD day	Ammonification rate
k_h	d^{-1}	Maximum specific hydrolysis rate
b_H	d^{-1}	Decay coefficient for heterotrophic biomass
b_A	d^{-1}	Decay coefficient for autotrophic biomass

Table 2.6 - The ASM1 process matrix (Henze et al., 1987)

Component	index	1	2	3	4	5	6	7	8	9	10	11	12	13	Process Rate, ρ_j
j	Process ↓	S_I	S_S	X_I	X_S	$X_{B,H}$	$X_{B,A}$	X_P	S_O	S_{NO}	S_{NH}	S_{ND}	X_{ND}	S_{ALK}	$[ML^{-3}T^{-1}]$
1	Aerobic growth of heterotrophs		$-\frac{1}{Y_H}$			1			$-\frac{1-Y_H}{Y_H}$		$-i_{XB}$			$-\frac{i_{XB}}{14}$	$\hat{u}_H\left(\frac{S_S}{K_S+S_S}\right)\left(\frac{S_O}{K_{O,H}+S_O}\right)X_{B,H}$
2	Anoxic growth of heterotrophs		$-\frac{1}{Y_H}$			1				$-\frac{1-Y_H}{2.86Y_H}$	$-i_{XB}$			$\frac{1-Y_H}{14*2.86Y_H}-\frac{i_{XB}}{14}$	$\hat{u}_H\left(\frac{S_S}{K_S+S_S}\right)\left(\frac{S_O}{K_{O,H}+S_O}\right)\times\left(\frac{S_{NO}}{K_{NO}+S_{NO}}\right)\eta_g X_{B,H}$
3	Aerobic growth of autotrophs						1		$-\frac{4.57-Y_A}{Y_A}$	$\frac{1}{Y_A}$	$-i_{XB}-\frac{1}{Y_A}$			$-\frac{i_{XB}}{14}-\frac{1}{7Y_A}$	$\hat{u}_A\left(\frac{S_{NH}}{K_{NH}+S_{NH}}\right)\left(\frac{S_O}{K_{O,A}+S_O}\right)X_{B,A}$
4	Decay' of heterotrophs				$1-f_P$	-1		f_P					$i_{XB}-f_p i_{XP}$		$b_H X_{B,H}$
5	Decay' of autotrophs				$1-f_P$		-1	f_P					$i_{XB}-f_p i_{XP}$		$b_A X_{B,A}$
6	Ammonification of soluble organic nitrogen										1	-1		$\frac{1}{14}$	$k_a S_{ND} X_{B,H}$
7	Hydrolysis' of entrapped organics		1		-1										$k_h\frac{\frac{X_S}{X_{B,H}}}{KX+(\frac{X_S}{X_{B,H}})}\left[\left(\frac{S_O}{K_{O,H}+S_O}\right)+\eta_h\left(\frac{K_{O,H}}{K_{O,H}+S_O}\right)\left(\frac{S_{NO}}{K_{NO}+S_{NO}}\right)\right]X_{B,H}$
8	Hydrolysis' of entrapped organic nitrogen											1	-1		$\rho_7\left(\frac{X_{ND}}{X_S}\right)$
Observed Conversion Rates $[ML^{-3}T^{-1}]$		$ri=\sum_j v_{ij}\rho_j$													
Stoichiometric Parameters: Heterotrophic Yield: Y_H Autotrophic Yield: Y_A Fraction of biomass yielding particulate products: f_P Mass N/Mass COD in biomass: i_{XB} Mass N/Mass COD in products from biomass: i_{XP}		Soluble inert organic matter $[M(COD)L^{-3}]$	Readily biodegradable substrate $[M(COD)L^{-3}]$	Particulate inert organic matter $[M(COD)L^{-3}]$	Slowly biodegradable substrate $[M(COD)L^{-3}]$	Active heterotrophic biomass $[M(COD)L^{-3}]$	Active autotrophic biomass $[M(COD)L^{-3}]$	Particulate products arising from biomass decay $[M(COD)L^{-3}]$	Oxygen (Negative COD) $[M(-COD)L^{-3}]$	Nitrate and nitrite nitrogen $[M(N)L^{-3}]$	NH_4^++NH_3 nitrogen $[M(N)L^{-3}]$	Soluble biodegradable organic nitrogen$[M(N)L^{-3}]$	Alkalinity - Molar units		Kinetic Parameters: Heterotrophic growth and decay: $\hat{u}_H$, K_S, $K_{O,H}$, K_{NO}, b_H Autotrophic growth and decay: $\hat{u}_A$, K_{NH}, $K_{O,A}$, b_A Correction factor for anoxic growth of heterotrophs: η_g Ammonification: k_a Hydrolysis: k_h, K_X Correction factor for anoxic hydrolysis: η_h

1. Aerobic growth of heterotrophs: This process is the growth of heterotrophic biomass when oxygen is present in the treatment system. It is the main contributor to the production of new biomass and the removal of organic carbon. The kinetics of this process is represented by:

$$\frac{dX_{B,H}}{dt} = \hat{u}_H \left(\frac{S_S}{K_S + S_S} \right) \left(\frac{S_O}{K_{O,H} + S_O} \right) X_{B,H} \qquad \text{(Eq. 2.4)}$$

Five components are considered in the aerobic growth of heterotrophs: S_S, $X_{B,H}$, S_O, S_{NH}, and S_{ALK}. The parameter Y_H, heterotrophic yield is utilised to describe the S_S reduction kinetics by Eq. 2.5.

$$\frac{dS_S}{dt} = -\frac{1}{Y_H} \frac{dX_{B,H}}{dt} \qquad \text{(Eq. 2.5)}$$

2. Anoxic growth of heterotrophs: This simulates the growth of heterotrophic biomass under anoxic conditions where nitrate is used as the terminal electron acceptor, leading to denitrification. The kinetic equation for this process is:

$$\frac{dX_{B,H}}{dt} = \hat{u}_H \left(\frac{S_S}{K_S + S_S} \right) \left(\frac{K_{O,H}}{K_{O,H} + S_O} \right) \left(\frac{S_{NO}}{K_{NO} + S_{NO}} \right) \eta_g X_{B,H} \qquad \text{(Eq. 2.6)}$$

Denitrification allows for the release of alkalinity (S_{ALK}), as shown in Eq. 2.7.

$$\frac{dS_{ALK}}{dt} = \left(\frac{1 - Y_H}{14 * 2.86 Y_H} - \frac{i_{XB}}{14} \right) \frac{dX_{B,H}}{dt} \qquad \text{(Eq. 2.7)}$$

3. Aerobic growth of autotrophs: This models the growth of autotrophic biomass under aerobic conditions. This process results in nitrification within the model. The kinetic equation for this process is:

$$\frac{dX_{B,A}}{dt} = \hat{u}_A \left(\frac{S_{NH}}{K_{NH} + S_{NH}} \right) \left(\frac{S_O}{K_{O,A} + S_O} \right) X_{B,A} \qquad \text{(Eq. 2.8)}$$

The kinetics of the S_{NH} reduction can be expressed by Eq. 2.9, where Y_A, is the yield coefficient for autotrophic biomass.

$$\frac{dS_{NH}}{dt} = \left(-i_{XB} - \frac{1}{Y_A} \right) \frac{dX_{B,A}}{dt} \qquad \text{(Eq. 2.9)}$$

The nitrification process reduces alkalinity as follows:

$$\frac{dS_{ALK}}{dt} = \left(-\frac{i_{XB}}{14} - \frac{1}{7Y_A} \right) \frac{dX_{B,A}}{dt} \qquad \text{(Eq. 2.10)}$$

4. Decay of heterotrophs: This models the decay of heterotrophic biomass under aerobic, anaerobic and anoxic conditions where:

$$\frac{dX_{B,H}}{dt} = -b_H X_{B,H} \qquad \text{(Eq. 2.11)}$$

5. Decay of autotrophs: This models the decay of autotrophic biomass during aerobic, anaerobic and anoxic conditions. The kinetic equation of this process is:

$$\frac{dX_{B,A}}{dt} = -b_A X_{B,A} \qquad \text{(Eq. 2.12)}$$

6. Ammonification of soluble organic nitrogen: This process converts S_{ND} to S_{NH}.

$$\frac{dS_{NH}}{dt} = k_a S_{ND} X_{B,H} \qquad \text{(Eq. 2.13)}$$

7. Hydrolysis of entrapped organics: This process controls how readily biodegradable substrate is produced when slowly biodegradable substrate contained in the sludge mass is broken down extra-cellular. The readily biodegradable substrate becomes available to the organisms for growth. The kinetic equation of this process is:

$$\frac{dS_S}{dt} = k_h \frac{X_S / X_{B,H}}{K_X + (X_S / X_{B,H})} \left[\left(\frac{S_O}{K_{O,H} + S_O} \right) + \eta_h \left(\frac{K_{O,H}}{K_{O,H} + S_O} \right) \left(\frac{S_{NO}}{K_{NO} + S_{NO}} \right) \right] X_{B,H} \qquad \text{(Eq. 2.14)}$$

S_S is produced in this process and X_S is consumed.

8. Hydrolysis of entrapped organic nitrogen: This process models the breakdown of biodegradable particulate organic nitrogen to soluble organic nitrogen. The kinetics of this process is shown in the following equation (Henze, 1987; Petersen et al., 2000; Henry, 2013):

$$\frac{dS_{ND}}{dt} = p_7\left(\frac{X_{ND}}{X_S}\right) \qquad \text{(Eq. 2.15)}$$

When using the matrix form of ASM1, the rate equations and stoichiometric coefficients can be combined to simulate the differential processes within the model. These values are combined using the conversion rate equation:

$$r_i = \sum_j v_{ij} p_j \qquad \text{(Eq. 2.16)}$$

where r_i is the component to be simulated, v_{ij} is the stoichiometric coefficient of the component for the relevant processes and ρ_j is the kinetic equations of the processes relevant to the component. By utilising these equations with calibrated kinetic and stoichiometric parameters, the various dynamics of the activated sludge process can be simulated. The ASM1 model can still be considered the core system for modelling activated sludge systems.

2.5.2.1 State Variables in ASM1

Wastewater treatment modellers use two terms to describe a collection of wastewater components: state variables and composite variables. State variables refer to the basic variables in wastewater that are continuously integrated over time. Composite variables are those variables in wastewater that are calculated from (or composed of) the state variables. The state variables of ASM1 relate to the wastewater characteristics in the bulk fluid, expressed in terms of COD, nitrogen compounds, dissolved oxygen and alkalinity. The wastewater characteristics for carbonaceous components are shown in Figure 2.4.

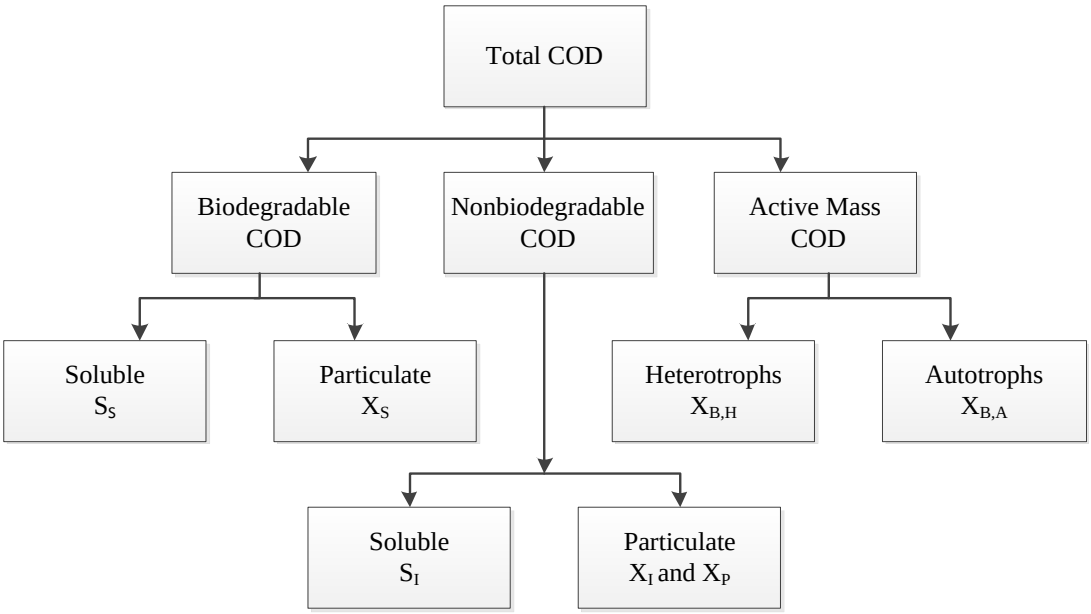

Figure 2.4 - Wastewater characteristics for carbonaceous components (Jeppsson, 1996)

The total COD balance of ASM1 is defined by Eq. 2.17 (Petersen et al., 2000).

$$COD_{tot} = S_I + S_S + X_I + X_S + X_{BH} + X_{BA} + X_P \qquad \text{(Eq. 2.17)}$$

The wastewater characterization for nitrogenous components is shown in Figure 2.5.

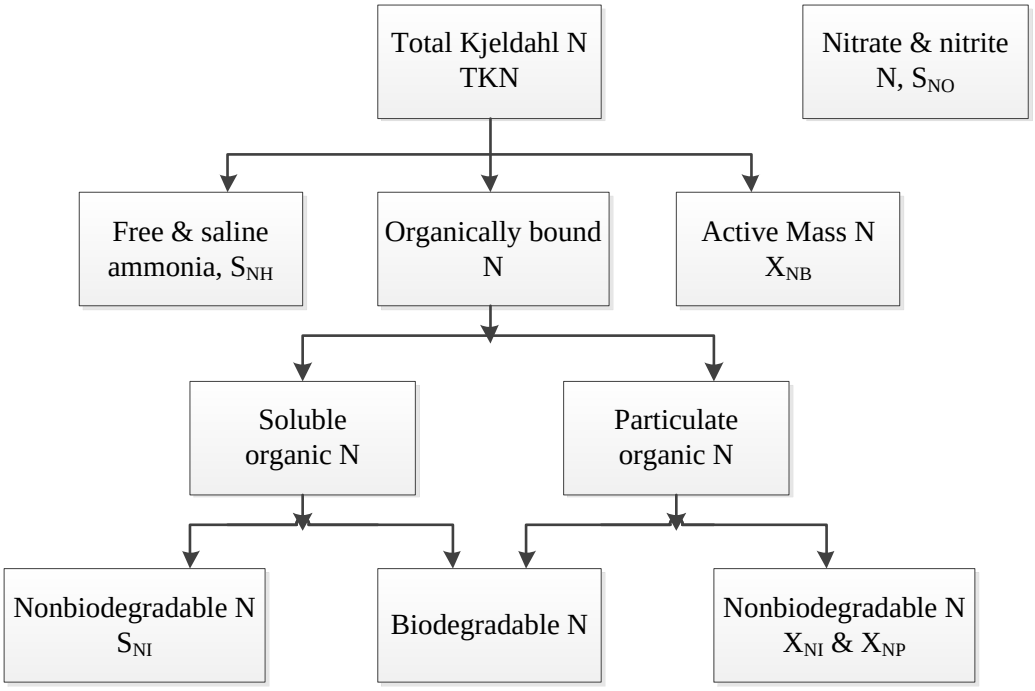

Figure 2.5 – Wastewater characterization for nitrogenous components (Jeppsson, 1996)

There are three forms of nitrogen that are commonly measured in wastewater ammonia, nitrates and nitrites. Total nitrogen is the sum of total kjeldahl nitrogen and nitrate-nitrite. The total nitrogen balance for the components in ASM1 is defined by Eq. 2.18 (Petersen et al., 2000).

$$N_{tot} = S_{NH} + S_{ND} + S_{NO} + X_{ND} + X_{NI} + i_{XB}(X_{BH} + X_{BA}) + i_{XP}.X_P \qquad \text{(Eq. 2.18)}$$

ASM1 is probably the most widely-used model for describing wastewater treatment. However, there are a number of limitations associated with it, some are as follows (Jeppsson, 1996):

- The model operates at a constant temperature, but temperature variations affect many biological process kinetics.
- The rate equation coefficients are assumed to be constant, despite the fact that they vary with time.
- The coefficients for nitrification are assumed to be constant and to incorporate any inhibitory effects that other waste constituents are likely to have on them.
- The denitrification correction factors are constant and are therefore not affected by variations in system configuration.
- The hydrolysis processes are coupled and are assumed to occur simultaneously at equal rates.

In order to address the limitation in ASM1 constant research has been carried out and further ASM models have been developed in order to achieve more accurate simulations. Another typical problem related to the calibration of ASM1 is that more than one combination of parameters can give the same description of the collected data. This indicates that a calibration procedure based on changing the parameters by trial and error is not advisable (Hellstedt, 2005). In order to address these issues ongoing research is continually being carried out to try and develop a universal calibration procedure.

2.5.3 ASM2 and ASM2D

The ASM2 and ASM2D models combine the biological processes for COD, N and P removals and was developed by Henze et al. (1995). To achieve these simulations, the ASM1 model was extended and the number of processes considered was increased. There

are 19 processes and 20 components in the ASM2 model. The process matrix table for ASM2 is shown in Appendix B.

2.5.4 ASM3

ASM3 describes the same processes as ASM1. However, ASM3 was introduced to address some of the identified deficiencies of ASM1. One of the most important reasons for introducing ASM3 was the recognition of the importance of oxygen consumption in biological treatment processes, namely (i) the rapid oxygen consumption rates for the degradation of readily biodegradable COD, (ii) the slow oxygen consumption rates associated with the degradation of slowly biodegradable COD, and (iii) slower endogenous oxygen uptake rate (OUR) (Haimi et al., 2009). The ASM3 process rates are presented in matrix form in Table 2.7. For a complete description of the ASM3 stoichiometric matrix, refer to Gujer et al. (1999). Similarly to ASM1, in ASM3 there are four basic processes as follows, which, however, vary in nature from ASM1 (Gujer et al., 1999; Petersen et al., 2000):

1) Storage of readily biodegradable substrate,

2) Growth of biomass,

3) Decay of biomass,

4) Hydrolysis of particulate organic matter.

In ASM1 a single decay process (cell lysis) was introduced to describe the sum of all decay processes under all environmental conditions (aerobic, anoxic). The primary amendment to the ASM1 model during the development of ASM3 is that a more realistic description of decay processes was introduced, known as ‘endogenous respiration’. In ASM1 the decay process is expressed as one process however according to Friedrich et al., (2013) the decay process actually occurs over distinguishable phases. The first phase involves the degradation of easily degradable storage compounds and active biomass simultaneously. The second phase involves the degradation of active biomass that is regarded to consist mainly of slower degradable active heterotrophic biomass (Friedrich et al., 2013).

The substrate flows in ASM1 and ASM3 are outlined in Figure 2.6. In ASM3 the conversion processes of the autotrophs and heterotrophs are clearly separated whereas in

ASM1 the decay regeneration cycles of the autotrophs and heterotrophs are strongly interrelated. This change (and the introduction of the storage step) enables more points for oxygen utilisation resulting in, at some points, easier separation and characterisation of the processes. Second, there is a shift of emphasis from hydrolysis to storage of organic matters. This alters how wastewater characterisation should be defined since the separation between readily biodegradable substrate (Ss) and slowly biodegradable substrate (Xs) now should be based on the storage process rather than on the growth process. Still, the separation remains somewhat based on biodegradation rates. In ASM3 hydrolysis is a less dominant influence for the rates of oxygen consumption, when compared to ASM1, since only hydrolysis of Xs in the influent is considered (Petersen et al., 2000).

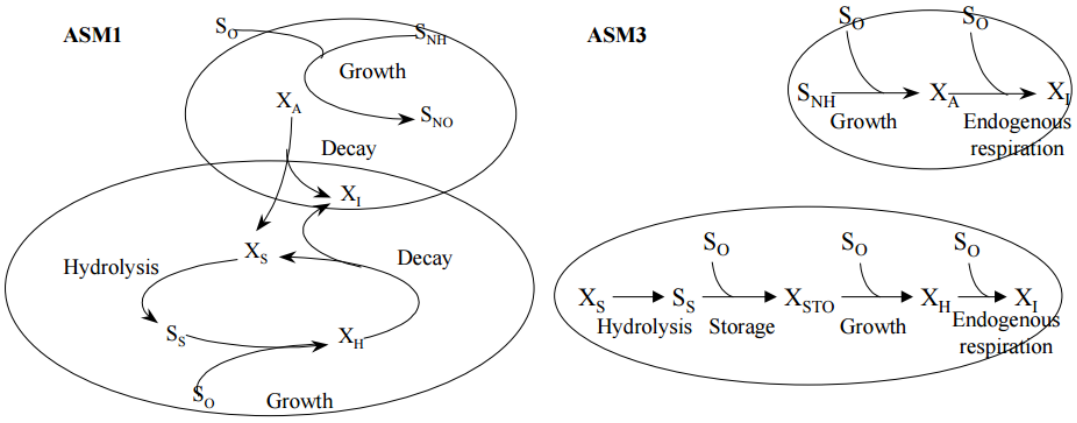

Figure 2.6 - Substrate flows in ASM1 and ASM3 (Peterson et al., 2006)

There is considerable agreement among practitioners that using endogenous respiration processes is better than using decay processes when modelling biofilms (Brockmann, 2013). Biological wastewater treatment involves the transformation of dissolved and suspended organic contaminants to biomass and gases (Low & Chase 1999). It has been observed that endogenous respiration results in incoming substrate being respired to carbon dioxide and water, and thus reducing biomass production (Low & Chase 1999; Abbassi et al. 2000; Liu & Tay 2001).

Table 2.7 – Process rate expressions of ASM3 (Gujer et al., 1999)

Component	index	1	2	3	4	5	6	7	8	9	10	11	12	13	Process Rate, ρ_j
j	Process ↓	S_{O2}	S_I	S_S	S_{NH4}	S_{N2}	S_{NOX}	S_{ALK}	X_I	X_S	X_H	X_{STO}	X_A	X_{SS}	$[ML^{-3}T^{-1}]$
1	Hydrolysis		f_{SI}	x_1	y_1			z_1		-1				$-i_{XS}$	$k_H\left(\frac{X_S/X_H}{K_X+X_S/X_H}\right)X_H$
Autotrophic organisms, nitrifying activity															
2	Aerobic storage of S_S	x_2		-1	y_2			z_2						t_2	$k_{STO}\left(\frac{S_{O2}}{K_{O2}+S_{O2}}\right)\left(\frac{S_S}{K_S+S_S}\right)X_H$
3	Anoxic storage of S_S			-1	y_3	$-x_3$	x_3	z_3						t_3	$k_{STO}\eta_{NOX}\left(\frac{K_{O2}}{K_{O2}+S_{O2}}\right)\left(\frac{S_{NOX}}{K_{NOX}+S_{NOX}}\right)\frac{S_S}{K_S+S_S}X_A$
4	Aerobic growth of X_H	x_4			y_4			z_4			1		$Y_{STO,O2}$	t_4	$\mu_H\left(\frac{S_{O2}}{K_{O2}+S_{O2}}\right)\left(\frac{S_{NH4}}{K_{NH4}+S_{NH4}}\right)\frac{S_{ALK}}{K_{ALK}+S_{ALK}}\frac{X_{STO}/X_H}{K_{STO}+X_{STO}/X_H}X_H$
5	Anoxic growth (denitrification)				y_4	$-x_5$	x_5	z_5			1		$Y_{STO,NOX}$	t_5	$\mu_H\eta_{NOX}\left(\frac{K_{O2}}{K_{O2}+S_{O2}}\right)\left(\frac{S_{NOX}}{K_{NOX}+S_{NOX}}\right)\frac{S_{NH4}}{K_{NH4}+S_{NH4}}\frac{S_{ALK}}{K_{ALK}+S_{ALK}}\frac{X_{STO}/X_H}{K_{STO}+X_{STO}/X_H}X_H$
6	Aerobic endogenous respiration	x_6			y_6			z_6	f_I		-1	-1	$-1/Y_{H,O2}$	t_6	$b_{H,O2}\frac{S_{O2}}{K_{O2}+S_{O2}}X_H$
7	Anoxic endogenous respiration		1		y_7	$-x_7$	x_7	z_7	f_I		-1		$-1/Y_{H,NOX}$	t_7	$b_{H,O2}\frac{S_{O2}}{K_{O2}+S_{O2}}\frac{S_{NOX}}{K_{NOX}+S_{NOX}}X_H$
8	Aerobic respiration of X_{STO}	x_8										1	-1	t_8	$b_{STO,O2}\frac{S_{O2}}{K_{O2}+S_{O2}}X_{STO}$
9	Anoxic respiration of X_{STO}					$-x_9$	x_9	z_9					-1	t_9	$b_{STO,O2}\frac{S_{O2}}{K_{O2}+S_{O2}}\frac{S_{NOX}}{K_{NOX}+S_{NOX}}X_{STO}$
Autotrophic organisms, nitrifying activity															
10	Aerobic growth of X_A	x_{10}			y_{10}		$1/Y_A$	z_{10}						t_{10}	$\mu_A\left(\frac{S_{O2}}{K_{A,O2}+S_{O2}}\right)\left(\frac{S_{NH4}}{K_{A,NH4}+S_{NH4}}\right)\frac{S_{ALK}}{K_{A,ALK}+S_{ALK}}X_A$
11	Aerobic endogenous respiration	x_{11}			y_{11}			z_{11}	f_I					t_{11}	$b_{A,O2}\frac{S_{O2}}{K_{A,O2}+S_{O2}}X_A$
12	Anoxic endogenous respiration				y_{12}	$-x_{12}$	x_{12}	z_{12}	f_I					t_{12}	$b_{A,O2}\frac{S_{O2}}{K_{A,O2}+S_{O2}}\frac{S_{NOX}}{K_{A,NOX}+S_{NOX}}X_A$
	Compostion Matrix $i_{k,I}$														
k	*Conservatives*														
1	ThOD	gThOD	-1	1	1		-1.71	-4.57		1	1	1	1	1		
2	Nitrogen	gN		$i_{N,SI}$	$i_{N,SS}$	1	1	1		$i_{N,XI}$	$i_{N,XS}$	$i_{N,BM}$		$i_{N,BM}$		
3	Ionic Charge	Mole +				1/14		−1/14	-1							
	Observables															
4	SS	gSS								$i_{SS,XI}$	$i_{SS,XS}$	$i_{SS,BM}$	0.6	$i_{SS,BM}$		
Observed Conversion Rates $[ML^{-3}T^{-1}]$		$ri=\sum_j v_{ij}\rho_j$														
Stoichiometric Parameters: f_{SI}, $Y_{H,O2}$, $Y_{H,NOX}$, $Y_{STO,O2}$, $Y_{STO,NOX}$, Y_A, f_{XI}, $i_{N,SI}$, $i_{N,SS}$, $i_{N,XI}$, $i_{N,BM}$, $i_{SS,XI}$, $i_{SS,XS}$, $i_{SS,BM}$		Oxygen (Negative COD) $[M(-COD)L^{-3}]$	Soluble inert organic material $[M(COD)L^{-3}]$	Readily biodegradable substrate $[M(COD)L^{-3}]$	$NH_4^+ + NH_3$ nitrogen $[M(N)L^{-3}]$	Dinitrogen, N_2 $[M(N)L^{-3}]$	Nitrate and nitrite nitrogen $[M(N)L^{-3}]$	Alkalinity $[mole(HCO_3)L^{-3}]$	Particulate inert organic matter $[M(COD)L^{-3}]$	Slowly biodegradable substrate $[M(COD)L^{-3}]$	Heterotrophic Organisms $[M(COD)L^{-3}]$	A cell internal storage product of heterotrophic organisms $[M(COD)L^{-3}]$	Nitrifying Organisms $[M(COD)L-3]$	Suspended Solids $[M(SS)L^{-3}]$	Kinetic Parameters: Heterotrophic organisms, aerobic and denitrifying activity: μ_H, K_S, K_{O2}, K_{NOX}, K_{NH4}, k_{STO}, K_{STO}, K_{ALK}, η_{NOX}, $b_{H,NOX}$, $b_{STO,O2}$, $b_{STO,NOX}$, $b_{H,O2}$ Autotrophic growth and decay: μ_A, $K_{A,NH4}$, $K_{A,O2}$, $K_{A,ALK}$, $b_{A,O2}$, $b_{A,NOX}$ Hydrolysis: k_h, K_X

2.6 BIOFILM MODELLING

2.6.1 Introduction to Biofilms

A biofilm is defined as ‘microorganisms attached to a surface’. However, a more comprehensive definition of a biofilm is ‘a group of cells immobilised in an organic polymer matrix of microbial origin’ (Van Loosdrecht et al., 2002). Biofilms have been successfully used in water treatment for over a century (Lazarova & Manem, 1995). There are four main compartments considered in a biofilm system: the substratum, the biofilm, the bulk liquid and the boundary layer (Figure 2.7).

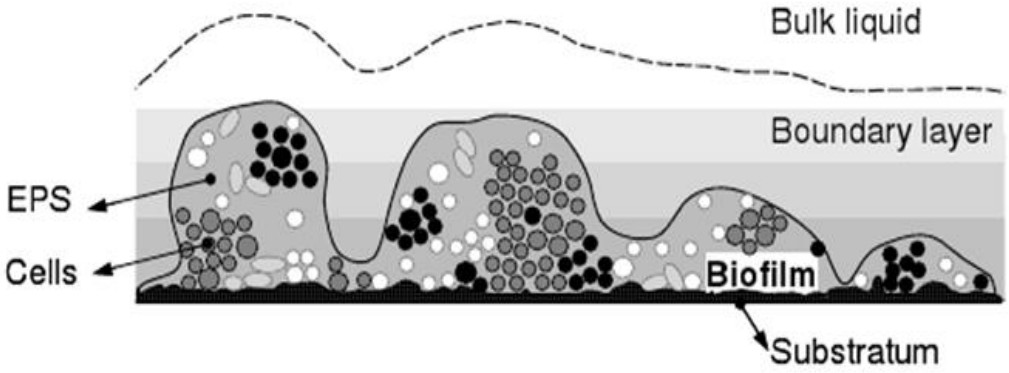

Figure 2.7 – The four compartments of a biofilm system: the substratum, the biofilm, the bulk liquid and the boundary layer (Eberl et al., 2006)

The substratum is the solid surface on which the biofilm grows. It can be any surface and in most cases it is inert and impermeable. The biofilm compartment contains both liquid and solid matter. The liquid in the biofilm usually constitutes the majority of the biofilms mass. The solids in the biofilm give the biofilm its reactive and structural properties. The solids include active cells, organic and inorganic particles and extracellular polymeric substances (EPS). The bulk liquid is the medium in which the biofilm grows. The bulk liquid compartment lies over the biofilm compartment. Dissolved and particulate components can be exchanged between the biofilm and the bulk liquid. Nutrients and substrates for biofilm growth are contained within the bulk liquid (Eberl et al., 2006). The boundary layer is a thin film between the bulk liquid and biofilm.

2.6.2 Biofilm Modelling

Mathematical modelling of biofilm reactors can be complicated and time-consuming due to the complexity of the biofilms, and a wide range of models have been developed to simulate biofilm reactors. Biofilm modelling has proved to be a powerful tool for studying biofilm processes in the treatment of wastewater. However, there can be significant uncertainties in biofilm models relating to (i) biofilm thickness, (ii) biofilm composition and (iii) biofilm reactor model calibration protocols. The modelling of biofilm reactors is complicated and requires a high level of understanding of the biofilm reactor technology and the mathematical concepts behind this; indeed this can limits its application in many cases (J. Boltz et al., 2013; Brockmann, Boltz, Morgenroth, Daigger, & Henze, 2012).

Historically, biofilm models were used for evaluating biofilm systems that had one dominant process (e.g. nitrification or BOD removal). The biofilm models then progressed to one-dimensional (1D) models, which represented multi-species and multi-substrate biofilms growing in one dimension perpendicular to the substratum. Following this, 2D and 3D numerical models were developed, which were used to describe the heterogeneous characteristics of biofilms (Wanner, 1997). The optimal choice of a biofilm model depends on the type of biofilm system studied, the objectives of the model user and the modelling capability of the user (Noguera et al., 1999; Eberl et al., 2006).

The modelling of biofilm processes and activated sludge processes are similar in many aspects but biofilm models are more complex. The ASMs are also used to model biofilm based systems in terms of kinetics and stoichiometric calculations. However, the biofilm models also need to account for a number of additional considerations, encompassing (Boltz et al., 2012; Van Loosdrecht et al., 2002).

1. *Attachment and Detachment rates:* The main issue to be considered when modelling biomass in the biofilm reactor is the attachment and detachment rate of biofilm from the substratum.
2. *Biofilm thickness* (L_F): The biofilm thickness (depth) is influenced by biofilm biomass concentration, substrate conditions, oxygen concentrations and attachment and detachment rates.
3. *Aeration*: Modelling aeration in a biofilm reactor requires knowledge or estimation of oxygen transfer characteristics, which are linked to factors such as mass transfer coefficient (k_La).

4. *Soluble biodegradable organic substrate*: Model predictions of soluble biodegradable organic substrate concentrations can be sensitive to the boundary layer thickness in the biofilm (L_L).
5. *Nitrification / Denitrification:* Model predictions of ammonium, nitrite, nitrate and organic nitrogen can be sensitive to the boundary layer thickness in the biofilm.

2.6.2.1 Nutrient Transport

The nutrients necessary for bacterial growth are dissolved in the liquid stage and reach the cells after they pass first through the boundary layer (external mass transfer) and then through the biofilm matrix (internal mass transfer) (Picioreanu et al., 1999). Fick's first law is used to model nutrient diffusion in biofilms (Metcalf & Eddy, 2003).

$$J = \eta . D . \frac{dS}{dZ} \qquad \text{(Eq. 2.19)}$$

J = the flux of a substrate S in the direction normal to the substratum.

η = the coefficient controlling mass transfer within biofilms or in the bulk water where:

$\eta < 1$ is when the nutrient is transporting within the biofilm matrix and

$\eta = 1$ is for the nutrient transporting in the bulk water

D is the diffusivity coefficient of S.

2.6.2.2 Biofilm Growth

Similarly to activated sludge models a Monod expression is used in biofilm modelling to represent biofilm growth (Levenspiel, 1980).

$$\mu = \mu_{max} \frac{C_S}{K_S + C_S} \qquad \text{(Eq. 2.20)}$$

μ = the specific growth rate
μ_{max} = the maximum specific growth rate
Cs = the substrate concentration
Ks = the half saturation coefficient (the substrate concentration at which $\mu = 0.5\ \mu_{max}$)

2.6.2.3 Biofilm Detachment

Biofilm detachment is the primary process used to balance microbial growth and decay (Chaudhry & Beg, 1998). Biofilm detachment can generally be described by the following equation (Wanner & Reichert, 1996; Wolf et al., 2007):

$$r_d = k.r_g \qquad \text{(Eq. 2.21)}$$

r_d = the biofilm detachment rate
k = the biofilm detachment coefficient
r_g = the biofilm growth rate

2.6.3 The Oxygen Transfer Process in Biofilm Modelling

A diagram showing the transfer of oxygen from the atmosphere to the biofilm is shown in Figure 2.8.

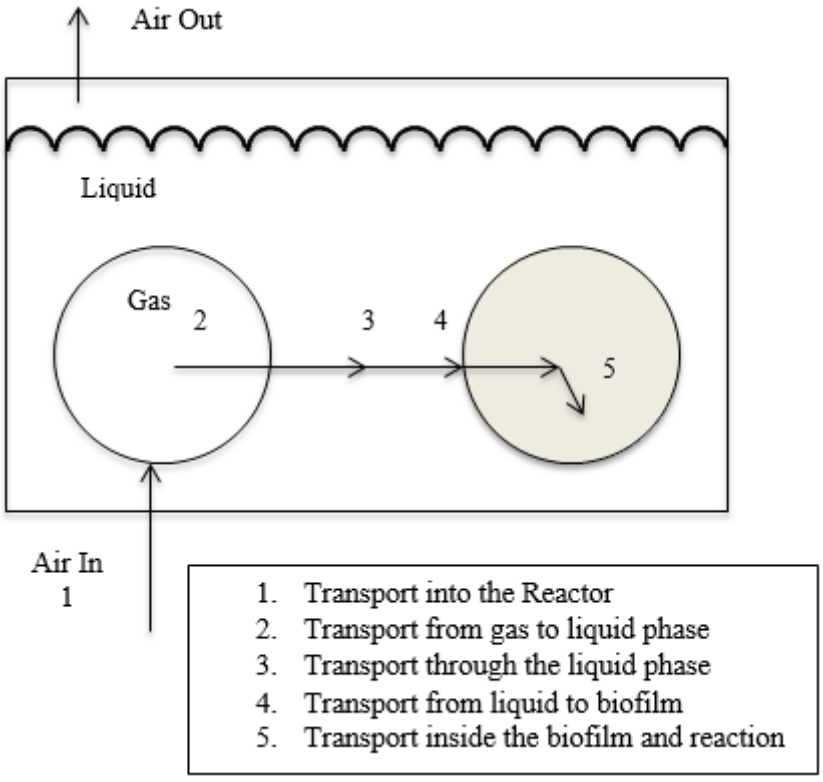

Figure 2.8 – Transfer of oxygen from the atmosphere to the biofilm

The transfer process in the biofilm system is the exchange of the mass of dissolved or particulate components between the bulk liquid and the biofilm or between the bulk liquid and the atmosphere. The mass transfer between the bulk liquid and the biofilm is a vital process as the source of the substrates in most biofilm systems is the bulk liquid. At the interface between the bulk liquid and the biofilm, a continuity condition for the component concentration C and the flux (j) of the exchanged mass must be fulfilled (continuity means that C and j are the same on both sides of the interface between, for example, the bulk liquid and the biofilm). The transport is driven by a concentration gradient across the mass transfer boundary layer (also known as the concentration boundary layer) (Eberl et al., 2006). The exchange of oxygen between the bulk liquid and the biofilm is described by Eq. 2.22. The mass flux of oxygen in the mass-transfer boundary layer is proportional to the difference between the oxygen concentration in the bulk liquid (C_B) and the concentration at the biofilm surface (C_{LF}), with the proportionality constant being the liquid-biofilm mass transfer coefficient *kc* (Eberl et al., 2006).

$$j_n = k_C \ (C_B - C_{LF}) \qquad \text{(Eq. 2.22)}$$

j_n = the mass flux perpendicular to the biofilm surface
kc = the mass transfer coefficient
C_B = the oxygen concentration in the bulk liquid
C_{LF} = the oxygen concentration at the biofilm surface

2.7 WWTP MODEL DEVELOPMENT

Initially, when developing a simulation for a WWTP, the modeller should decide the purpose and scope of the simulation. The model complexity, the data required and the level of model calibration depend on the purpose and scope of the model (Pena-Tijerina et al., 2007). A key rule of modelling (which, indeed, applies in general to all engineering domains) is that a model should be as simple as possible and only as complex as needed (Eberl et al., 2006). It is important to note that a model does not need to exactly represent the subject system in order to answer relevant questions. Over the past three decades, numerous calibration protocols have been developed. However, the model calibration process still represents one of the main bottlenecks to modelling (Mannina et al., 2011).

A model can be in run in steady state or dynamic mode. In steady-state modelling, the process variables do not vary with respect to time. In dynamic modelling the process variables vary with respect to time until the process is stabilised, assuming the system is not disturbed by external factors. The three main steps to model development and calibration are discussed below.

2.7.1 Step 1: Data Collection

The collection of data for model development can often be a costly and expensive undertaking. The quality of the data used to calibrate the model will have a direct impact on the reliability of the predictions made when using the final calibrated model (Melcer, 2003). Figure 2.9 illustrates the typical information that can be used for successful model development (Henze et al, 1987; Henze 1992; Lesouef et al, 1992; Pedersen & Sinkjaer, 1992; Siegrist & Tschui, 1992; Stokes et al., 1993; Dupont & Sinkjaer, 1994; Funamizu & Takakuwa, 1994; Xu & Hultma, 1996; Coen et al., 1997; Kristensen et al., 1998; Petersen et al., 2000). However, it should be noted that in many sites, the data available may be significantly less than that illustrated in Figure 2.9.

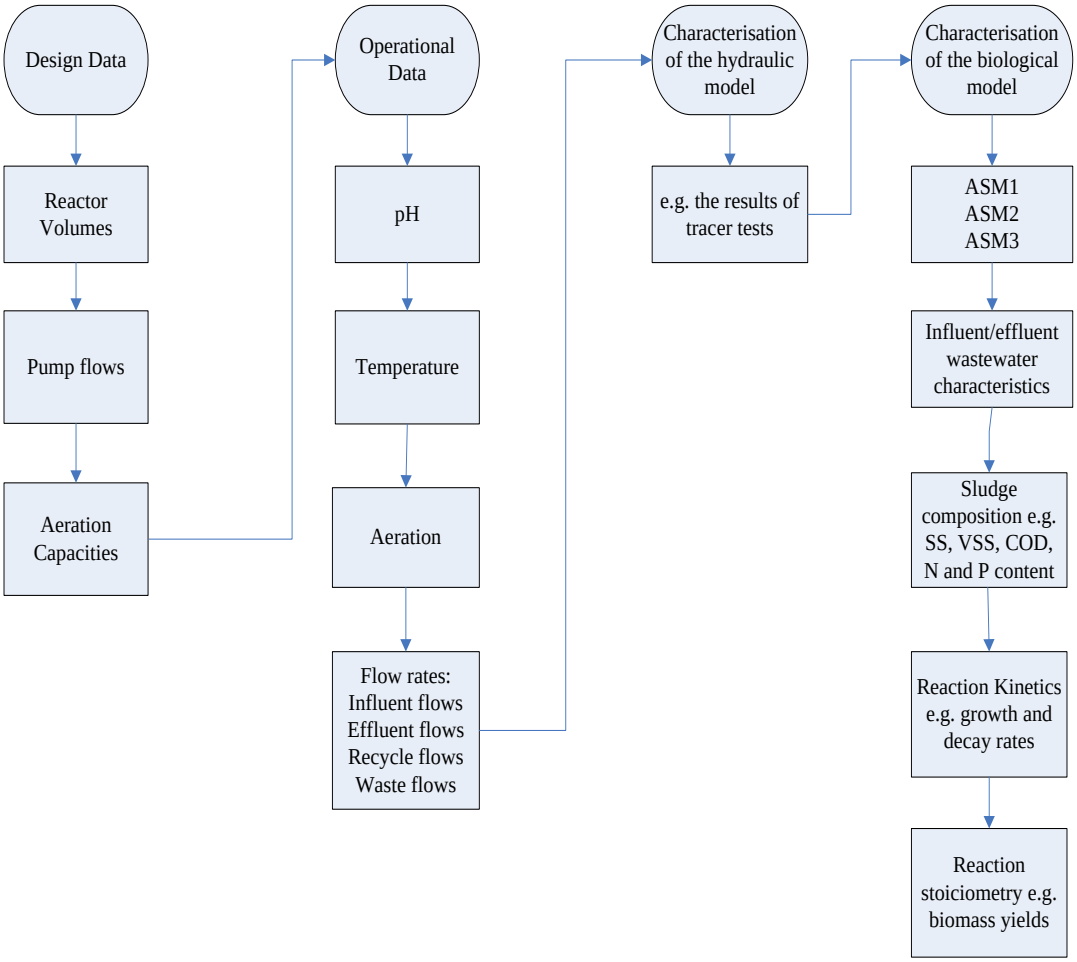

Figure 2.9 – Typical information used for successful model development

Influent characterisation is one of the dominant factors and involves translating data available from the WWTP into data that can be used in the model (Mannina, 2011). If an existing treatment plant is to be modelled, then the opportunity exists to gather available information on flow patterns and wastewater characteristics. Historical plant records can provide enough information to make a calibration of a simulator, although the accuracy of the calibration can depend on the quantity, quality and nature of the data available. In ideal circumstances, the modeller will initiate a sampling regime that can capture as much relevant data as is possible. For example, Melcer, (2003) recommended a sampling and monitoring program that:

- Gathers 24-hour composite samples of untreated wastewater, primary effluent and secondary effluent for analysis of a range of parameters (e.g. COD, BOD, VSS (volatile suspended solids), TSS (total suspended solids), TKN, NO_3-N, NH_4-N, Total P and alkalinity);

- Undertakes at least two, 24-hour phase studies, with influent and effluent samples collected on an hourly basis during the aforementioned average sampling period.

2.7.2 Step 2: Sensitivity Analysis and Model Calibration

The most relevant parameters to be estimated during calibration are determined by completing a sensitivity analyses as this identifies the parameters to be adjusted during calibration. Model calibration, also known as parameter estimation, is defined as the process of adjusting model parameters so that the differences between observed and simulated results are minimized (Hydromantis, 2006). Sensitivity analysis and model calibration are one of the most important components of any modelling project and can be challenging and be resource and time consuming tasks.

Since the introduction of ASM1 in 1987 (Henze et al., 1987), numerous studies have examined the calibration of activated sludge models. Petersen et al. (2003) carried out a review on the calibration of activated sludge models and documented that there are a large number of experimental methodologies proposed and applied for the calibration of activated sludge systems. Mannina et al. (2011) noted that numerous applications of ASMs have demonstrated that the ASM parameters are not universal in the sense that not all systems can be modelled using the same parameter values. Site-specific model parameters must be obtained by calibration with experimental data.

The choice of calibration approach depends heavily on the WWTP being modelled. As the complexity of the models has increased considerably with the discovery of new processes (Henze et al., 2000; Barker & Dold, 1997), the modelling task has become more time consuming, with ad hoc calibration of the model parameters occurring frequently (Sin, 2004). There is currently no unified approach towards calibration of activated sludge models worldwide. Moreover, there is a lack of systematic protocols to guide modellers during a calibration study (J. Boltz et al., 2013).

2.7.2.1 Objective of Sensitivity Analysis

Sensitivity analysis is used to identify the parameters to be adjusted during calibration. The influence of parameters on model calibration can vary due to the WWTP's operating conditions and influent composition. By examining the sensitivity of the model

parameters, an indication is given as to which parameters require adjusting to fit modelled and measured data.

2.7.3 Sensitivity Analysis – AQUASIM

With the sensitivity analysis function in AQUASIM, it is possible to examine whether the time series of the calculated values are affected by a change in the value of the model parameter. The sensitivity analysis feature allows the calculation of linear sensitivity functions of arbitrary variables with respect to each of the parameters included in the analysis (Reichert, 1995). The sensitivity analysis results in this study are those of the absolute-relative sensitivity function of AQUASIM (Eq. 2.23) that computes the absolute change in a model output variable, *y*, for a 100% change in any parameter of interest, *p*:

$$\partial_{y,p}^{a,r} = p\frac{\partial y}{\partial p} \qquad \text{(Eq. 2.23)}$$

This makes it possible to compare the impacts of the different parameters. The uncertainty is determined by using the error propagation formula (Eq. 2.24), which is based on the linearized propagation of standard deviations of the parameters of interest, neglecting their correlation (Mburu et al., 2014).

$$\sigma_y = \sqrt{\sum_{i=1}^{m}\left(\frac{\partial y}{\partial p}\right)^2 \sigma_{pi}^2} \qquad \text{(Eq. 2.24)}$$

p = model parameter of interest

pi = the uncertain model parameters

σ_{pi} = the standard deviations

σ_y = the approximate standard deviation of the model results

2.7.4 Sensitivity Analysis – GPS-X

In GPS-X the objective of the sensitivity analysis is to determine the sensitivity of the simulations model's output variables (dependent variables) to changes in its parameters (independent variables). This helps to identify the parameters that have the greatest impact on the model. The sensitivity analysis is set up after the model has been built.

There are three major steps in setting up a sensitivity analysis in GPS-X:

Step 1 - Specify the model parameters to serve as the independent variable.

Step 2 - Enter the minimum, maximum and increment value for the independent variable and specify the control window on which to display the analyse control.

Step 3 - Switch to a simulation model, turn on the desired analyse mode and start the simulation.

Once these steps are completed, the GPS-X will begin calculating the steady state values. When a solution is found for the current value of the independent variable, these points are displayed in the output windows, the independent variable is incremented and the solution procedure begins again.

2.7.4.1 Objective of Model Calibration

Calibration is the process in which model parameters are adjusted until the model predictions match selected sets of data from the actual WWTP. The objective is to minimize the error between the measured datasets and the model predictions. It is not necessary to achieve a perfect match between modelled and measured data, since the model is a simplified representation of the plant and often ignores some of the inputs and processes occurring at the actual plant. The exact matching of modelled and measured data is not necessary as while it might reduce the total error for one particular dataset, it can reduce the model's predictive power and increase model error for other datasets.

When evaluating the match of the modelled and measured data, it is crucial to observe all the important variables. It is preferable to fit most of the measured variables reasonably rather than fitting them perfectly to one selected component concentration and poorly to the others.

In steady state simulations of WWTPs, the effluent data being modelled should be matched to within 5% and 20% of the actual measured effluent data (Melcer, 2003).

2.7.4.2 Steps in Calibration

Model calibration cannot be described using a simple step-by-step procedure as calibration depends on the specific type of plant to be simulated and the specific questions

to be answered (Boltz et al., 2012). Thus, there are no 'one size fits all' recommendations for model calibration.

With ASM1, it is recognised that few parameters are subject to change during the calibration process. Thus, modellers in most cases rely on the default values or that the model outputs are not sensitive to these parameters (Hauduc et al., 2011). In an inter-model comparison study undertaking by Barker and Dold (1997), the following were identified as the parameters most often modified when calibrating an activated sludge plant:

- growth and decay rates of autotrophs,
- heterotrophic half-saturation coefficients for substrate and oxygen,
- autotrophic half-saturation coefficient for ammonia.

The IWA Scientific and Technical Report on Activated Sludge Model No. 2 (Henze et al, 1995) provides some general direction on model calibration. The report summarises a number of key principles on which model calibration should be based. The principles are summarized here:

- Most of the parameters in the model do not change significantly from case to case and therefore should not be changed without justification;
- It is not advisable to adjust a parameter to fit data unless the model predictions of that experimental data are sensitive to changes in that parameter;
- Only change one parameter at a time. If a parameter interacts (such as a growth rate or a decay rate), only the parameter with the largest relative influence should be changed.

Henze (1988) demonstrated how different sets of parameter values may lead to approximately the same model behaviour. This is due to the fact that many model coefficients are correlated. Some examples of such interrelations are given below.

- Growth rate and decay rate – increased growth and decay rate may produce an identical net growth rate but will increase the oxygen demand and speed up the substrate cycle.
- Yield and growth rate – increased yield and growth rate may outbalance each other with respect to substrate conversion rate but will increase the oxygen consumption.

- Yield and heterotrophs in the influent wastewater – high yield and a low concentration of heterotrophs in the influent wastewater are equal to a low yield and a high concentration of heterotrophs in the influent (Jeppsson, 1996).

Belia et al. (2009) identified model calibration as one of the main areas that introduce uncertainties to model predictions. If a reasonable match between data and model cannot be achieved, ensure that:

- The plant data are of good quality.
- An attempt is not being made to fit a process that is not accounted for in the model.

2.7.5 Step 3: Simulation, Model Validation and Verification

Once the model is calibrated, the modeller is ready to run numerous model simulations. In the first simulation, the model behaviour is validated. Model validation involves checking that the model responses generated during the model analysis agree with that obtained from the true process (Jeppsson, 1996). Model verification consists of comparing the simulation results to an independent set of data (Jeppsson, 1996).

2.8 WASTEWATER MODELLING SOFTWARE

There are numerous methods available for modelling wastewater treatment processes including:

1. Programming languages that implement model programs for specific systems, e.g. Visual basic, C, C+, FORTRAN and Delphi;

2 Using a general purpose simulator, such as MATLAB/Simulink (www.mathworks.com),

3. Using commercial simulators specifically for modelling of wastewater systems that contain a variety of process models.

In most engineering applications, commercial wastewater simulators are used. The modelling software packages listed below are Microsoft Windows-based simulators that simulate biological wastewater treatment systems.

2.8.1 BioWin

BioWin (EnviroSim Associates Ltd, Canada) (www.envirosim.com) model utilizes BioWin's full General Activated Sludge/Anaerobic Digestion Model (ASDM) that tracks over 50 components with more than 80 processes acting on these components (Copp, 2002).

2.8.2 EFOR

EFOR (Danish Hydraulic Institute, Denmark) (www.efor.dk) has in-built wastewater treatment processes, which make it easy to construct a wide variety of wastewater treatment plants. EFOR includes ASM1 and ASM2 models and is modified to include biological phosphorous removal (Haimi et al., 2009).

2.8.3 SIMBA

SIMBA (Institut für Automation und Kommonikation (IFAK), Germany) (www.ifak-system.com) is a custom-made version of Simulink for wastewater treatment applications. SIMBA allows for the complete consideration of sewer systems, wastewater treatment plants, sludge treatment and rivers. It extends Matlab/Simulink using block libraries for biological and chemical treatment processes (Haimi et al., 2009).

2.8.4 STOAT

STOAT (Water Research Centre, UK) (www.wrcplc.co.uk) is a modelling software tool designed to dynamically simulate the performance of a wastewater treatment works including sludge treatment processes. STOAT includes the implementation of ASM1, called IAWQ No.1, and the Takács settler model, called Generic. The software can be used together with commercial sewerage and river quality models (Haimi et al., 2009).

2.8.5 WEST

WEST (Hemmis, Belgium) (www.hemmis.com) includes a number of modules and features that enable the user to model and evaluate almost any kind of wastewater treatment plant application that exists. Most of the models in the WEST simulator are

open source and open code; thus, the models can be modified if necessary. WEST has been mainly used in the context of wastewater treatment research (Olsson et al., 1999).

2.8.6 GPS-X

GPSX (Hydromantis Inc, Canada) (www.hydromantis.com) is supplied with over 50 preconfigured layouts, covering most of the unit processes found in wastewater treatment plants. ASM1, ASM2d and ASM3 are available in GPSX. The biological unit processes include carbon, nitrogen and phosphorus removal in various suspended growth and fixed film configurations (Makinia, 2010). GPS-X uses over 20 process objects in its models, including a trickling filter, a rotating biological contactor and a membrane bioreactor.

2.8.7 AQUASIM

AQUASIM (EAWAG, Switzerland) (www.eawag.ch) was designed for the identification and simulation of natural and engineered aquatic systems and was developed by the Swiss Federal Institute for Environmental Science and Technology (EAWAG) (Reichert, 1998). AQUASIM uses an object-oriented approach, wherein the user defines variables and processes that can be selectively activated within a system of linked compartments. Reichert (1995) and Reichert (1998) provide a thorough description of the modelling package and its underlying concepts.

For this study, GPSX and AQUASIM were used, although other packages could also be used as many unit processes can be simulated using various software packages, such as those discussed above. AQUASIM was chosen as it allows users define relevant variables and processes; an approach that a lot of flexibility when compared to other software. GPS-X was chosen as it is user friendly and includes numerous process objects that were investigated for modelling the PFBR. GPS-X and AQAUSIM are discussed in more detail in Section 2.9 and 2.10.

2.9 GPS-X MODELLING SOFTWARE

The main components of GPS-X software and the process objects considered as part of this project are discussed in detail below.

2.9.1 Influent Advisor

Influent Advisor is an Excel-based tool that enables users to achieve influent characteristics most consistent with the available data. In many cases, detailed influent data may not be available, and influent advisor, when used by an experienced modeller, allows detailed characteristics of the influent wastewater to be estimated using only basic influent characteristics. The influent characterisation model used in Influent Advisor should be the same as the biological model used in the simulation itself (that is, ASM1, ASM2, ASM3 and Mantis).

2.9.2 GPS-X Objects

GPS-X objects model various physical components of a WWTP (e.g. influent processes, primary settlers and secondary treatment processes). Each object can be defined by some or all of the following user inputs:

- Hydraulic configuration (e.g. influent, effluent and sludge wastage flow rates);
- Physical attributes (e.g. the physical dimensions of biological reactors);
- Operational attributes (e.g. the actions performed by the object, stoichiometry, kinetics);
- Display variables (definition of the variables associated with an object that can be displayed to the user);
- Stream labels (these allow identification of flows into and out of objects);
- Sources (e.g. influent composition and volumes).

A user can use a combination of various objects to model their processes and define how each object interacts with other objects (this is known as the model layout). GPS-X translates the layout into a high-level computer language (ACSL) and generates an executable program. GPS-X achieves this using a specialized translator, which converts the layout into dynamic model equations. Once the executable code is generated, a fully featured interactive simulation control window enables simulations to be conducted (Hydromantis, 2010). The GPS-X objects that were studied as part of this project are discussed in Tables 2.8 to Table 2.12.

2.9.3 GPS-X Objects Relevant to this Study

Influent Objects

The influent objects in GPS-X are used to model the influent characteristics, both in terms of wastewater and flow characteristics.

Table 2.8 - Influent objects

Object	Description
Wastewater Influent 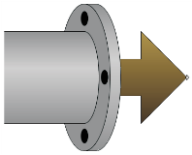	The wastewater influent object is used to characterise continuous wastewater flows (steady or dynamic). The flow is specified via a number of methods: 1) Data – users set the flow rate directly, via menu entry or read from file. 2) Sinusoidal – GPS-X applies a sinusoidal curve to the influent flow set in the menu or read from file. 3) Diurnal Flow – a daily diurnal pattern is set via flow rates at different times of the day (Hydromantis, 2006).

Preliminary Treatment Objects

Under the object heading 'preliminary treatment', the equalisation tank was investigated as part of this study.

Table 2.9 - Preliminary treatment objects

GPS-X Object	Description
Equalisation Tank 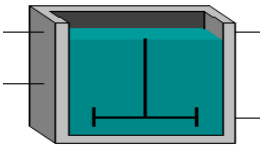	The equalization tank is a no-react model, where all the reaction rates are set to zero. There are no biological reactions occurring in the equalization tank (Hydromantis, 2006).

Suspended Growth Process Objects

There are 14 suspended growth process objects available in GPS-X. Only sequencing batch reactor (SBR) objects were considered as part of this study as this enabled the modelling of batch reactor systems. There are three different SBR objects in GPS-X: (i)

the simple SBR object, (ii) the advanced SBR object, and (iii) the manual SBR object. All three objects have the same functionality, appearance and choice of biological models. They differ in the manner in which the user specifies the operation of the SBR unit (Hydromantis, 2006).

Table 2.10 - Suspended growth process object

GPS-X Object	Description
SBR 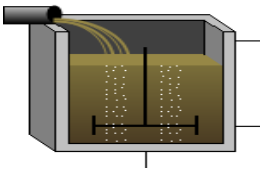	The SBR is discussed in detail in Chapter 4. The models associated with the SBR object are combinations of suspended-growth and sedimentation models. The various aerated and mixed stages use a suspended-growth model, assuming a completely mixed hydraulic configuration, while the settling and decanting stages use a reactive sedimentation model. The models are combined to form the whole unit process model (Hydromantis, 2006).

Attached Growth Process Objects

The major difference between the attached growth models and the suspended-growth models described is the inclusion of the diffusion process in the biofilm. A number of objects were examined in this study. These included the trickling filter, the rotating biological contactor (RBC) and the submerged biological contactor (SBC).

Table 2.11 - Attached growth process objects

GPS-X Object	Description
Trickling Filter 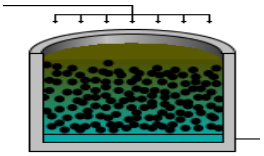	The trickling filter is divided into 'n' horizontal sections (default is 6 sections) each representing a cross-section of the trickling filter at a different depth. The biofilm in each of these horizontal sections is modelled as a number of layers. The transfer of soluble state variables between each of these layers is by diffusion only. The profiles of the various components through the biofilm are modelled so that different environments (aerobic, anoxic and anaerobic) can exist within the biofilm (Hydromantis, 2006).

Rotating Biological Contactor 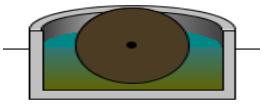	The rotating biological contactor is divided into 'n' stages (default is 1 stage), each representing a baffled RBC system. The transfer of the state variables between each of these stages is through the liquid flow. The biofilm in each stage is modelled as a number of layers. Similarly to the TF, the transfer of soluble state variables between each of these layers is by diffusion only (Hydromantis, 2006).
Submerged Biological Contactor 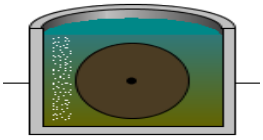	The submerged biological contactor (SBC) model is a modification of the RBC model for units that are air driven or are provided with supplemental aeration. The submerged biological contactor is divided into a number of stages (default is two stages), each representing a baffled SBC shaft (Hydromantis, 2006).

Modelling Tools

The Modelling Toolbox and the Black Box were each investigated when building the PFBR model.

Table 2.12 – Modelling tools

GPS-X Object	Description
Modelling Toolbox 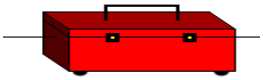	The tools used in the Modelling Toolbox are low-pass filtering, multivariable controllers, on-off controllers, pH tool, PID controllers, sampler controllers, timer controllers and feed-forward and feed-back controllers. The on-off function was investigated in the calibration of the PFBR.
Black Box 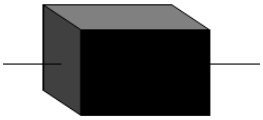	In the Black Box object, there are 18 predefined transfer functions for empirical modelling, which is user customizable.

2.9.4 Modelling the SBR Process

In order to successfully model the SBR in GPS-X, mass balance equations are used to help indicate the effects various components have on each other. The mass balance equation for the total reactor volume is:

$$V_T = V_O + QT_F \qquad \text{(Eq. 2.25)}$$

where V_T is total reactor volume, V_o is the initial reactor volume before the fill stage and during the idle stage, T_F is the fill time and Q is the flow rate in the fill stage. One commonly accepted assumption in SBR models is that biological conversion only occurs during the react stage and not during the settle, decant or idle stages. This means that soluble components are unchanged outside of the react stage, but particulate components are affected by wasting the sludge. The mass balance equation for particulate compounds is:

$$X_{io} = \frac{V_T X_{ie}(1-1)/m\theta_x}{V_O} \qquad \text{(Eq. 2.26)}$$

where X_{io} is the concentration of the particulate component at the beginning of the next cycle, V_T is the total reactor volume, X_{ie} is the concentration of the particulate at the end of the react stage, m is the number of treatment cycles in one day, V_o is the initial reactor volume and θ_x is the sludge age. This equation has two assumptions:

1. The excess sludge wasted at the end of the react stage is dependent on the SRT; and
2. The settling process is considered to be ideal with no solid loss in the effluent.

In the SBR, the oxygen transfer to the bulk liquid stage is modelled using a dynamic mass balance equation (Eq. 2.27).

$$V\frac{dC_L}{dt} = QC_{in} - QC_L + K_L a(C_\infty - C_L)V + rV \qquad \text{(Eq. 2.27)}$$

where V is the reactor volume (m^3), C_L is the concentration of dissolved oxygen (DO) in the reactor (mg/L), Q is the influent flow rate (m_3/d), C_{in} is the concentration of DO entering reactor (mg/L), K_La is the oxygen mass transfer coefficient at field conditions

(1/day), C_∞ is the DO saturation concentration at field conditions (mg/L) and *r* is the rate of use of DO by biomass (g/day) or the respiration rate.

The K_La is entered directly into the model and diffused aeration is calculated using Eq. 2.28.

$$K_L a_T = (\alpha F)\theta^{(T-20)} K_L a_{20} \qquad \text{(Eq. 2.28)}$$

Where $K_L a_T$ is the mass transfer coefficient at temperature T in oC (1/day), $K_L a_{20}$ is the mass transfer coefficient at 20^{o}C, θ is the temperature correction factor (default value in GPS-X is 1.024), α is the wastewater correction factor for 20 *K a L*, *F* is the diffuser fouling factor (default value in GPS-X is 1.0) and *T* is the wastewater temperature (^{o}C).

2.10 AQUASIM MODELLING SOFTWARE

The modelling software AQUASIM is described by Wanner (1996), Van Loosdrecht et al., (2002) and Picioreanu et al., (2004) as an excellent quantitative tool for understanding biofilm processes and modelling biofilm structures in wastewater. However, it is limited to 1-D profiles. The basic structure of the AQUASIM modelling software consists of links, compartments, processes and variables. Figure 2.10 shows the AQUASIM model structure and the inter link between the four subsystems: the variables, processes, compartments and links. The variables form the basic subsystem required for the formulation of processes, compartments and links. The processes are then activated in the compartments. Links are used to connect the compartments that are already defined.

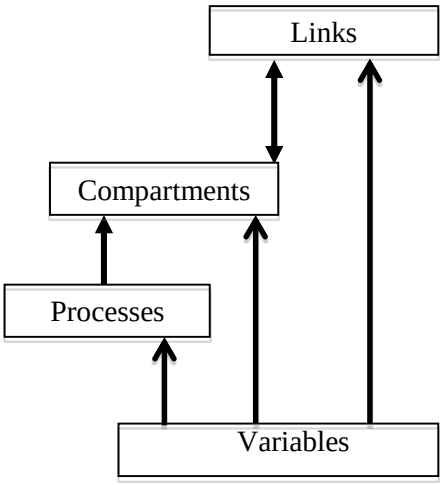

Figure 2.10 - Main elements of AQUASIM model structure (Reichert, 1998)

2.10.1 Variables

The basic objects for the formulation of models are variables. There are four main ranges of application of variables (Reichert, 1998):

- Variables can be used for quantities to be determined by the model (e.g. by the solution of algebraic or differential equations);
- Variables can have a predefined meaning in a compartment (e.g. time and space coordinates);
- Variables can be used to build functions depending on other variables (e.g. for the speciation of process rates or stoichiometric coefficients);
- Variables can be used as probes, which make the values of other variables evaluated at a given location in a compartment globally available.

There are seven types of variables available in AQUASIM: state variables, program variables, constant variables, real list variables, variable list variables, formula variables and probe variables (Table 2.13).

Table 2.13 - Description of variables in AQAUSIM (Reichert, 1998)

Variables	Description
State variables	Used to represent concentrations or other properties to be determined by a model according to user-selected transport and user-defined transformation processes.
Program variables	Used to make quantities such as time, space coordinates and discharge that are used for model formulation available as variables.
Constant variables	Used to describe single measured quantities that can also be used as parameters for sensitivity analyses or parameter estimations.
Real list variables	Used to provide measured data or to formulate dependencies on other variables with the aid of interpolated data pairs.
Variable list variables	Used to interpolate between other variables at given values of an arbitrary argument, e.g. for multidimensional interpolation.
Formula variables	Allow the user to build new variables as algebraic expressions of other variables.
Probe variables	Make the values of other variables evaluated at a given location in a compartment globally available.

State variables, program variables, constant variables, real list variables and formula variables were used in building the PFBR model.

2.10.2 Processes

In AQUASIM, the term "processes" refers to conversion reactions. These have to be specified by the user. There are two types of processes in AQUASIM that can be chosen from: dynamic processes and equilibrium processes (Reichert, 1998). In the model, the dynamic process describes the total transformation rate of a substance using Eq. 2.29. For example the dynamic processes can be used for the growth and decay rate of bacteria in a model.

$$r_i = \sum_j \nu_{ij} p_j \qquad \text{(Eq. 2.29)}$$

r_i = the component to be simulated,

ν_{ij} = the stoichiometric coefficient of the component for the relevant processes,

ρ_j = the kinetic equations of the processes relevant to the component.

Equilibrium processes are used to describe the effect of very fast processes which lead to permanent equilibrium values of the corresponding state values. A variable determined by such a process can be treated as always taking the value corresponding to its equilibrium state. Therefore, its value is given as the solution of an algebraic equation (Reichert, 1998).

$$r_{eq} = 0 \qquad \text{(Eq. 2.30)}$$

where r_{eq} depends on the variable involved and on other variables influencing the equilibrium value (Reichert, 1998).

2.10.3 Compartments

The AQUASIM software provides a number of compartment options, which include:

- Mixed Reactor Compartments, used to describe well-mixed domains, e.g. stirred reactors and mixed lakes;
- Biofilm Reactor Compartments, used to describe growth and population dynamics of biofilms in which substrate gradients over the depth are important;
- Advective-Diffusive Reactor Compartments, used to describe systems with a longitudinal given water flow, such as plug flow reactors;
- Saturated Soil Column Compartments, used to model transport, adsorption and transformation of substances in saturated soil columns, including exchange with dead zones or immobile pore volume;
- River Section Compartments, used to describe the hydraulics, transport and transformation processes in rivers;
- Lake Compartments, used to model stratification, mixing, transport and transformation processes in horizontally well-mixed lakes (Reichert, 1998).

The mixed reactor compartment and the biofilm reactor compartment were both considered as options to model the PFBR. The biofilm reactor compartment (BRC) was the preferred choice to model the PFBR as the biofilm composition and the biofilm growth could be more accurately studied using this compartment.

2.10.3.1 Biofilm Reactor Compartment

The biofilm reactor compartment of AQUASIM describes a reactor with a completely mixed bulk water volume and with a biofilm growing on a substratum surface in the reactor. Solids can attach or detach at the surface of the biofilm and in its interior. Any transformation processes can be defined. The BRC consist of three zones: bulk fluid, biofilm solid matrix and biofilm pore water. For all three zones, AQUASIM calculates the development over time of microbial species and substrates, as well as the biofilm thickness (Wanner & Morgenroth, 2004). The description of the biofilm in the BRC is one-dimensional. Only the direction perpendicular to the substratum, which has the largest concentration of gradients, is resolved. All variables are averaged over areas parallel to the substratum. Biofilm reactor compartments can be linked advectively or diffusively to other AQUASIM compartments (Reichert, 1998).

The AQUASIM User Manual (Reichert, 1998) details nearly 40 mathematical equations executed by the software to model the biofilm reactor compartment. However, the main process formulations that were reviewed in Section 2.6.2 were used to model the biofilm system, and these are: nutrient diffusion into the biofilm, in accordance with Fick's first law (Eq. 2.19), biofilm growth modelled by the Monod equation (Eq. 2.20), and biofilm detachment, described by a linear equation (2.21).

2.10.4 Links

The compartments in AQUASIM can be connected by links in order to model water and substance exchange between the compartments. Two types of links are available:

- Advective Links, used to describe water flow from one compartment to another;
- Diffusive Links model diffusive boundary layers or membranes between compartments (Reichert, 1998).

2.11 SUMMARY AND PROJECT OBJECTIVES

This chapter discusses the background and literature related to this study. The chapter briefly describes the wastewater treatment process and outlines a number of technologies of interest; particularly those that could inform the development of models for the PFBR. Modelling of activated sludge and biofilm systems is discussed as are the associated sensitivity analysis and calibration procedures. It was noted that while the application of modelling to WWTPs is increasingly popular it remains limited for small scale systems. The reasons for this can range from perceptions on cost, limited data availability or the lack of easy to use unit processes for modelling software that could aid modelling of new technologies. Furthermore it was noted that while modelling could become a very useful tool in informing systems design and operation for small scale treatment works; it is not widely applied. Finally the review discussed the PFBR technology and the key challenges that may be encountered in modelling this system. Based on the above review the main challenges discussed in this study are:

1. To investigate if robust calibrate models could be developed using activated sludge unit processes in existing software.
2. To investigate the impacts on model accuracy of key operational data, including reactor hydraulics, oxygen transfer characteristics and influent and effluent data.
3. To develop a model calibration protocol for the PFBR.
4. To inform new approaches for rapidly developing and calibrating models without the need for developing bespoke unit processes.

3 EXPERIMENTAL SYSTEMS

3.1 INTRODUCTION

This chapter describes pumped flow biofilm reactor in detail. The chapter also outlines the various experimental regimes applied to the laboratory and field-scale systems that formed the basis of this study. The chapter also describes the individual systems modelled in the study and their associated operating conditions.

The experimental data used in this study is based on previous work carried out by O'Reilly, 2005; O' Reilly, 2011 and Clifford et al., 2013. All of the experimental data, on which the modelling was based, was carried out before the commencement of this project.

3.2 PUMPED FLOW BIOFILM REACTOR

The PFBR is a two-reactor technology developed at NUI Galway that employs a unique hydraulic regime and enables aerobic, anoxic and anaerobic conditions to be sequenced. The PFBR operates as a sequencing batch biofilm reactor type process, with typical stages comprising fill/draw, anoxic, aerobic and settle. Biofilm, growing on plastic media modules within the two reactors, is aerated passively as wastewater is moved alternately between the reactors during an aeration sequence. The two reactors empty and fill a number of times during a typical aeration sequence, exposing, in turn, the biofilm to atmospheric air and wastewater (Figures 3.1). Furthermore, while the PFBR has many of the features of a sequencing batch reactor, the fill and discharge from the system typically take place in Reactor 1 (R1) and Reactor 2 (R2) respectively (patent no. S2004/0462) (Rodgers et al., 1997; O'Reilly, 2005; O'Reilly et al., 2008; O'Reilly et al., 2011). The two-reactor tank technology has been tested at laboratory scale and also at field scale for populations ranging from 15–750 population equivalents (PE).

The PFBR is suitable for treating both municipal wastewater and high strength wastewater. The first commercial PFBR is located in Moneygall, Co. Offally and the influent comprises a municipal wastewater. The PFBR is also suitable for high strength wastewater, however more typical for marts. There is a PRFBR located in a mart in Athenry, Co. Galway where it treats high strength wastewater.

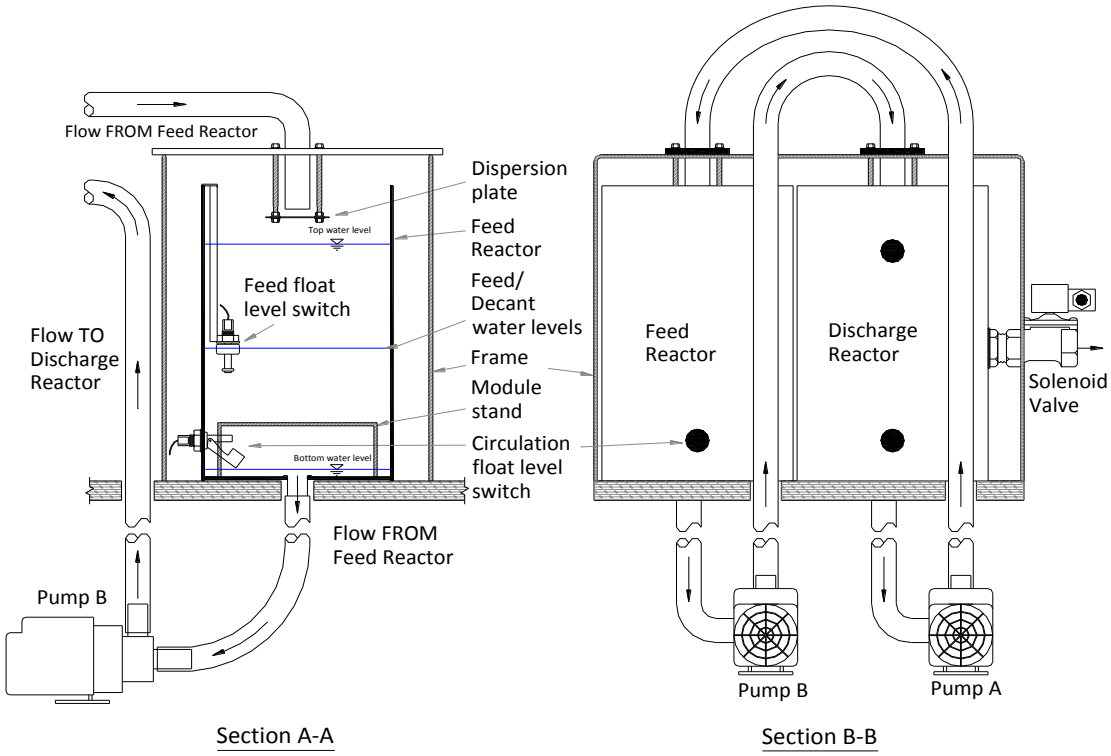

Figure 3.1 – Section view (left) and elevation view (right) of the laboratory scale PFBR (media not shown for clarity) (O'Reilly, 2005)

Three PFBR systems were modelled as part of this thesis: a laboratory-scale PFBR located in NUI Galway and two field-scale PFBRs located in Tuam, Co. Galway, and Moneygall, Co. Offaly, all of which are outlined below and in Table 3.1 The laboratory-scale PFBR (LS-PFBR) was operated using two wastewaters of varying strengths (Study 1, a high-strength synthetic wastewater and Study 2, a low-strength synthetic wastewater). The operating stages were the same for both studies. The field-scale PFBR located in Tuam, Co. Galway (FS-PFBR1), was operated under two different cycle regimes with influent wastewaters of varying strengths (Study 3 and Study 4). The field-scale PFBR located in Moneygall, Co. Offaly (FS-PFBR2), was operated under a one-cycle regime using one influent wastewater type (Study 5).

Table 3.1 – PRBRs studied

Laboratory scale PFBR (NUI Galway)		**Field scale PFBR (Tuam)**		**Field scale PFBR (Moneygall)**
LS-PFBR		FS-PFBR1		FS-PFBR2
Study 1 (Chapter 4)	Study 2 (Chapter 4)	Study 3 (Chapter 5, 6)	Study 4 (Chapter 5, 6)	Study 5 (Chapter 7)

3.2.1 PFBR Operating Regime

At the start of a typical PFBR treatment cycle, primary settled wastewater is pumped into R1 (fill stage = t_1 mins) while, simultaneously, treated effluent is discharged from R2. Where anoxic conditions are required, the wastewater is left quiescent in R1 (anoxic stage = t_2 mins). During the aerobic stage (aerobic stage = t_3 mins), water levels are initially equalised between R1 and R2 by gravity (typically using a motorised valve that connects R1 and R2). Once equalised, the remainder of the water is pumped to the receiving reactor, thus exposing the biofilm media in the emptied reactor to the atmosphere. This process is repeated a number of times (the process, whereby R1 (or R2) empties and fills again, is known as a pumping cycle). After the aerobic stage, a settle stage begins (settle stage = t_4 mins). At the end of the settle stage, treated wastewater is discharged from R1 (discharge stage = t_5 mins). Table 3.2 depicts a PFBR treatment cycle and details the treatment stage and water levels during each stage.

Table 3.2 – Typical PFBR treatment cycle for PFBR (O'Reilly, 2011)

Step	Stage	Water positions during each stage
1	Fill	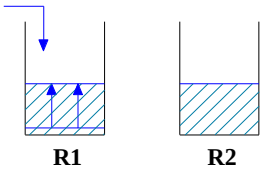
2	Anoxic	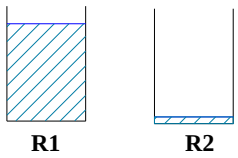
3	Aerobic	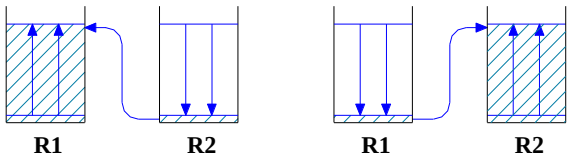 One circulation (from R1 to R2 and from R2 to R1) = one aerobic cycle and is repeated for the duration of the aerobic stage.
4	Settle	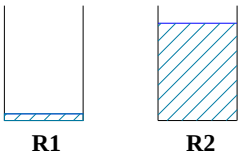
5	Discharge	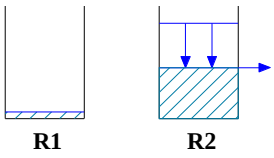

There is considerable flexibility available in the operation of the PFBR as it allows for a combination of different stages including anoxic and aerobic; anaerobic and aerobic; or anaerobic, anoxic and aerobic. The main purpose for the inclusion of an anaerobic stage is for the removal of phosphorus by the selective enrichment process known as enhanced biological phosphorus removal - EBPR (O'Reilly, 2011). EBPR occurs in two distinct stages under anaerobic and aerobic conditions. The anaerobic stage is effected by holding

the wastewater in either reactor for a defined period of time and this allows anaerobic conditions to develop. Phosphorus removal was not part of on-site operational requirements and therefore the anaerobic stage was not modelled in this study.

3.2.2 Aeration process and dissolved oxygen during typical treatment cycles

In the PFBR, aeration is achieved by alternately exposing the stationary biofilm media in either of its two reactors to air and wastewater though the movement of water using pumps (and a motorised valve in the field-scale systems) between the two reactors. While exposed to air, the microorganisms in the biofilm have access to atmospheric oxygen (Figure 3.2a). While submerged in wastewater, the microorganisms in the biofilm have access to organic carbon and nutrients, achieving carbonaceous oxidation and nutrient removal (Figure 3.2b). Anoxic conditions (or indeed anaerobic) are incorporated in the treatment cycle by holding the bulk fluid in either reactor for a period of time, allowing limited dissolved oxygen or oxidised nitrogen concentrations to develop in the bulk fluid.

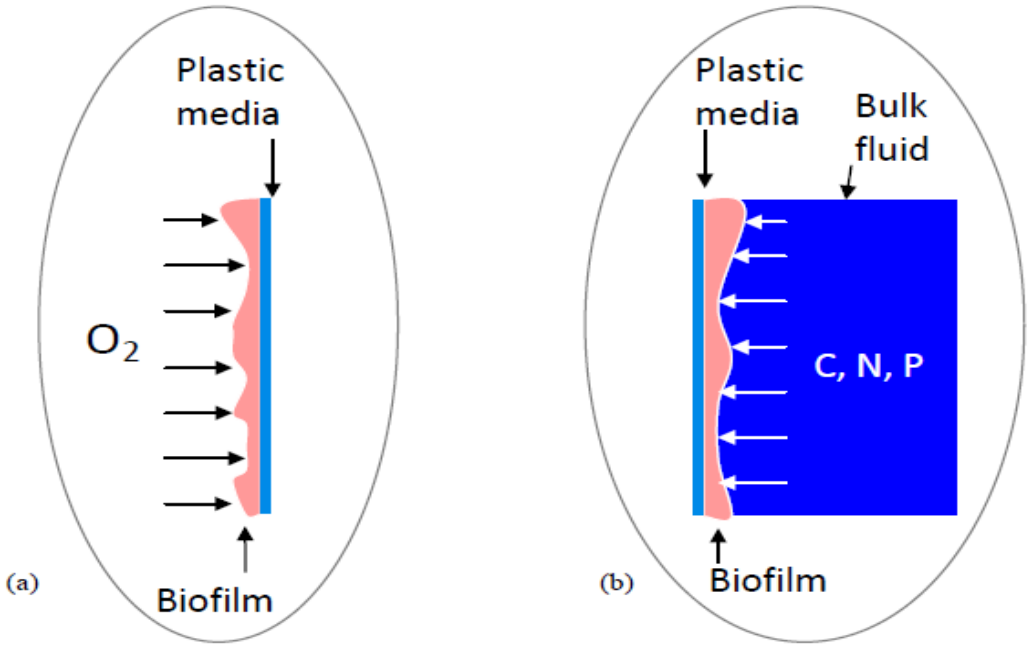

Figure 3.2 – (a) Biofilm exposed to atmospheric oxygen and (b) biofilm submerged with access to nutrients (O' Reilly, 2011)

In the LS-PFBR, two probes were used to measure the DO concentrations in R1, one positioned near the bottom of the reactor, and the other in the middle of the reactor. The

DO concentrations in R1 peaked after each pumping event and then began stabilising during the rest periods before starting to level out prior to the next pumping (Figure 3.3). The average of these DO concentrations were used in the calibration of the LS-PFBR model.

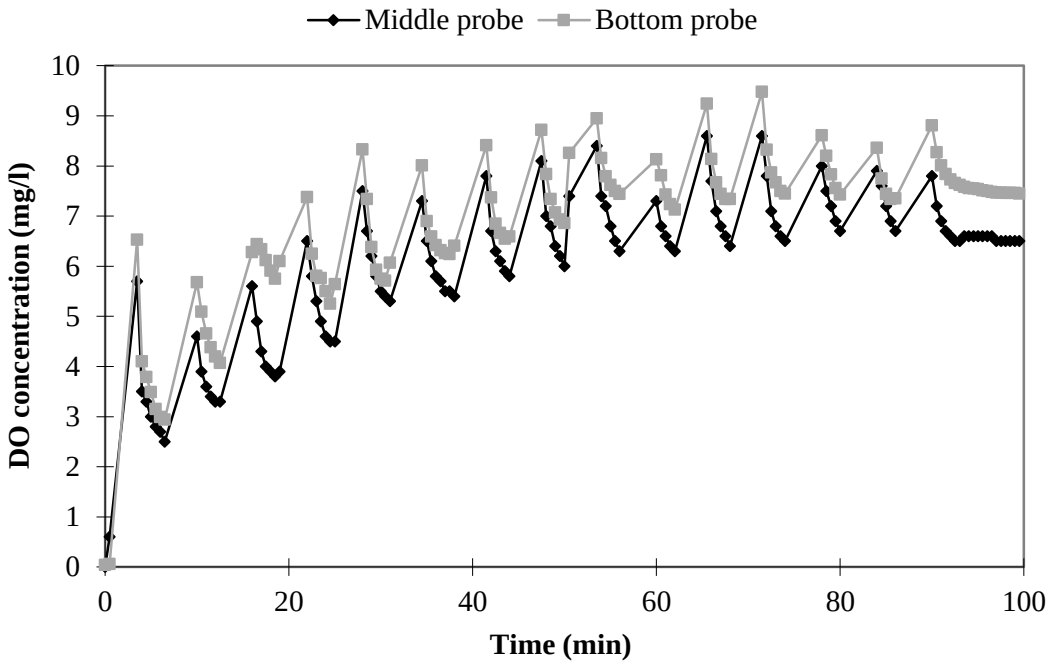

Figure 3.3 – LS-PFBR1 Study 1 DO profile

In FS-PFBR1 dissolved oxygen was measured in R1 and R2 by installing a set of DO probes near the top, middle and near the bottom of R1 and R2. The high probe and middle probe in the two reactors were exposed to atmospheric air every time water was transferred from one reactor to the other. The low probe remained submerged in wastewater throughout the cycle. The typical readings from the set of DO probes in Reactor 1 are shown in Figure 3.4.

During the fill stage at the start of a typical treatment cycle, primary settled wastewater was added to R1 and shortly afterwards the DO concentrations dropped. The bulk fluid was then pumped between the reactors during the aerobic stage. The alternate exposure of the biofilm in each reactor to the air during the aerobic stage was the main aeration mechanism by which diffusion of atmospheric oxygen directly into the biofilm occurred (as described in *Section 3.2.2*). Over the course of the aerobic stage, DO concentrations

increased steadily. During the settle stage, DO concentrations typically decreased; though this can depend on the quality of the treated wastewater.

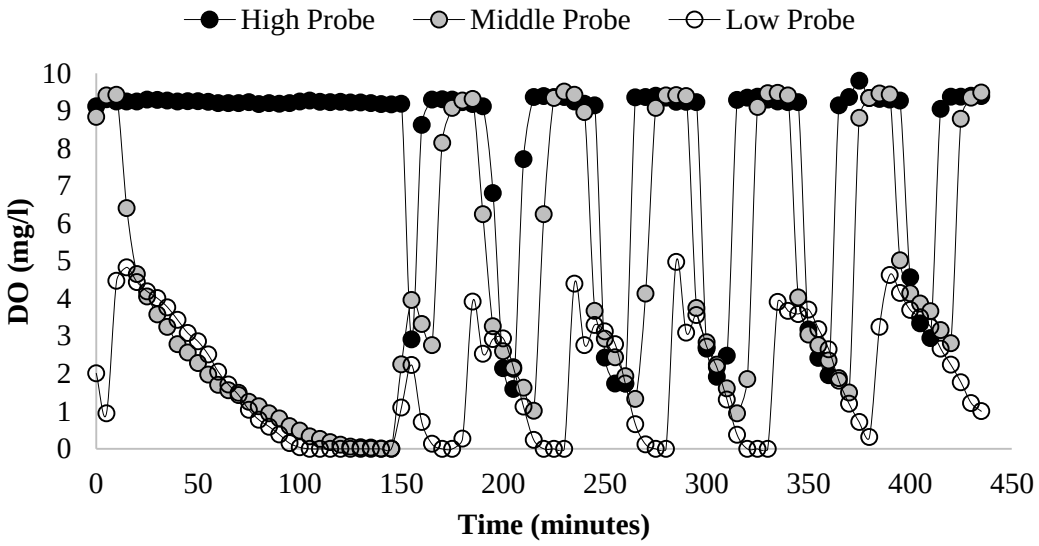

Figure 3.4 – FS-PFBR1 Study 3 DO profile

In order to present the DO data shown in Figure 3.4 during a phase study, the lower readings of each probe were used (Figure 3.5). This was utilised as the lower probes were the only ones not exposed to air during each cycle and it was felt best represented conditions in the bulk fluid.

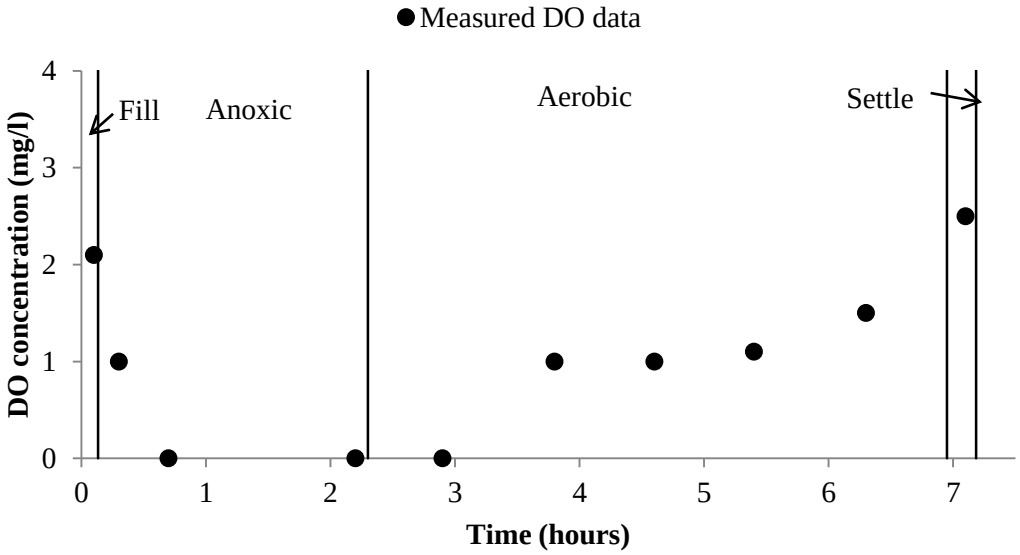

Figure 3.5 – FS-PFBR1 Study 3 DO phase study

In FS-PFBR2 one set of DO probes were installed in R1 and R2 near the bottom of the reactors. The DO probe remained submerged in wastewater throughout the cycle and results would be similar to the low probe in FS-PFBR1. Thus the data for FS-PFBR2 was presented as in FS-PFBR1 for each probe.

3.3 WASTEWATER SAMPLING AND ANALYSIS

A replicate laboratory unit of the PFBR was operated in order to gain an understanding of the physical unit (Figure 3.6) being modelled in this project. The dissolved oxygen work described in *Section 4.3.1* was performed on this unit.

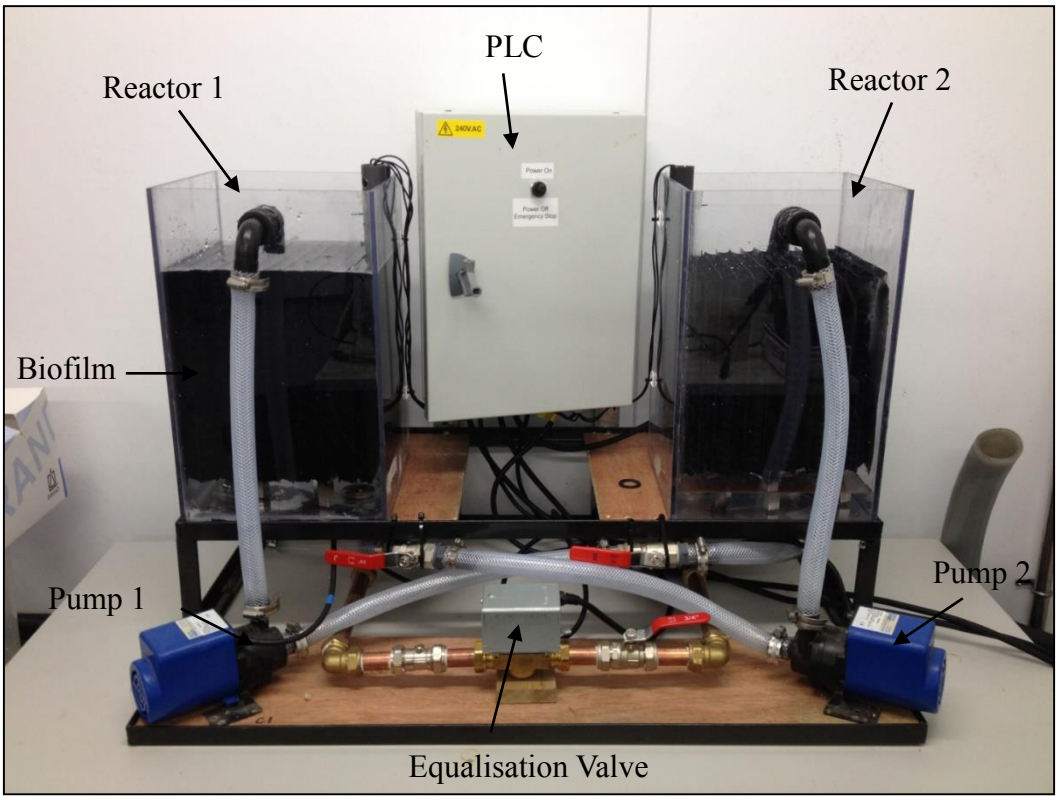

Figure 3.6 – LS-PFRR located at NUI Galway

For all studies, influent, effluent and in-reactor wastewater samples were tested for the following parameters, in accordance with the standard procedures detailed in Table 3.3 (APHA et al., 2005): SS, COD (unfiltered and filtered samples), TN (unfiltered and filtered samples), NH_4-N (filtered samples), NO_2-N (filtered samples), and NO_3-N (filtered samples). After filtration through 1.2µm Whatman GF/C microfiber filters, filtered samples were tested in accordance with Standard Methods (APHA, 2005).

Unfiltered samples were tested in a similar manner prior to filtration (Table 3.3). BOD_5 was measured using WTW Oxitop meters. Filtered and unfiltered TN was measured using a Biotector TOC TN TP Analyser. Filtered NH_4-N, total oxidised nitrogen (TON) and NO_3–N were measured using a Thermo Clinical Labsystem, Konelab 20 Nutrient Analyser. All analysers and equipment were maintained and calibrated as per manufacturer's guidelines.

Table 3.3 – Laboratory test for wastewater parameters (APHA et al., 2005)

Parameter	Laboratory Test
BOD_5	BOD_5 was measured in accordance with the Standard Methods for the Examination of Water and Wastewater (1995), method 5210-D.
COD	COD was measured using the Closed Reflux Titrimetric method in accordance with the Standard Methods for the Examination of Water and Wastewater (1995), method 5220-C.
DO	DO was measured using a Wissenschaftlich Technische Werkstatten (WTW) model CellOx 325 electrode that was connected to a WTW 330 meter.
TN	TN was measured using the HACH TNT Persuphate Digestion Method (method 10071) with the HACH DR/2000 spectrophotometer.
NH_4-N	NH_4-N was measured using a Thermo Clinical Labsystems, Konelab 20 Nutrient Analyser.
NO_3-N	NO_3-N was measured using a Thermo Clinical Labsystems, Konelab 20 Nutrient Analyser.
SS	The SS test measures the non-filterable residue of the sample. The test was carried out in accordance with the Standard Methods for the Examination of Water and Wastewater (1995), method 2540-D.
PO_4^{3-}-P	PO_4^{3-}P was measured using a Thermo Clinical Labsystems, Konelab 20 Nutrient Analyser.

3.4 LABORATORY-SCALE PFBR (LS-PFBR)

3.4.1 System overview

A laboratory-scale treatment unit was constructed and located in a temperature-controlled room (10^{o}C) in the Environmental Engineering laboratory, NUI Galway (O'Reilly, 2005). The LS-PFBR treatment unit comprised two reactors (R1 and R2), two biofilm media modules, three pumps (one feed pump and two circulation pumps), one equalisation valve, three float switches, one discharge valve and a PLC unit.

The reactors measured 240 mm x 240 mm x 400 mm high with straight sides. The reactors had a working fluid volume of 16.5 l each. The plastic media modules in R1 and R2 were 200 mm square in plan x 180 mm high. The module had a specific surface area of approximately 290 m^2/m^3, thus giving an effective media surface area of circa 2 m^2. The modules sat on a stand at the bottom of each reactor, 70 mm above the base. This provided room for a level switch that allowed the minimum water level to operate freely and separated the base of the module from sludge build-up at the bottom of the reactor. The pumps, valves and float switches and their functions in the operation of the LS-PFBR are outlined in Table 3.4.

Table 3.4 – LS-PRBR components and their functions

Equipment	Function
Feed pump	Filling R1 at the beginning of a cycle
Equalisation valve	Equalising the water levels between R1 and R2
Circulation pumps	Transferring the wastewater between R1 and R2
Float switches	Terminating circulation pumps

The LS-PFBR was operated using fill and anoxic, aerobic, settle and draw stages, each of which was controlled by a PLC unit. The inputs in the PLC included signals from the float level switches and user-inputted instructions, i.e. pumping and stage times and cycle numbers.

3.4.2 LS-PFBR operating conditions

LS-PFBR was operated in two distinct studies, Study 1 and Study 2. In Study 1, a high strength synthetic wastewater was used as the influent wastewater, and during Study 2, the influent comprised a low strength synthetic wastewater. The LS-PFBR system

operated a similar treatment cycle for both Study 1 and Study 2 (Table 3.5). The average volume per cycle for both Study 1 and 2 was 12 l.

Table 3.5 – Operational stages of LS- PFBR (Study 1 and 2)

PFBR Stage	Duration (minutes)
Fill (t_1)	8
Anoxic (t_2)	150
Aerobic (t_3)	106
Settle (t_4)	60
Draw (t_5)	5

3.4.3 Wastewater Characteristics

The influent wastewater for the LS-PFBR comprised a synthetic wastewater (detailed in Table 3.6). The synthetic influent wastewaters had a composition similar to that used by Odegaard and Rusten (1980).

Table 3.6 – Composition of domestic, low-strength synthetic wastewater (O'Reilly, 2005)

Constituents	Study 1 wastewater mg/l	Study 2 wastewater mg/l
Glucose	800	200
Yeast extract	120	30
Dried milk	480	120
Urea (NH_2CONH_2)	250	30
Ammonium chloride (NH_4Cl)	240	60
Sodium hydrogen phosphate ($Na_2H.12H_2O$)	200	100
Potassium hydrogen carbonate ($KHCO_3$)	200	50
Sodium hydrogen carbonate ($NaHCO_3$)	520	130
Magnesium sulphate ($MgSO_4.7H2O$)	200	50
Iron sulphide ($FeSO_4.7H_2O$)	8	2
Manganese sulphate ($MnSO_4.H_2O$)	8	2
Calcium chloride ($CaCl_2.6H_2O$)	12	3

During Study 1 and Study 2 influent and effluent wastewater samples were taken randomly over 90 days to provide a representative average of the influent and effluent parameter concentrations. Both influent and effluent wastewater samples were tested for the following parameters, in accordance with the standard procedures detailed in Table 3.3 (APHA et al., 2005): COD (unfiltered and filtered samples), TN_t (unfiltered and filtered samples), NH_4-N (filtered samples), NO_2-N (filtered samples), and NO_3-N

(filtered samples). There was 14 effluent samples taken and analysed in Study 1 and Study 2. Two phase studies were conducted during Study 2, where samples were taken at frequent intervals during the individual treatment cycles and tested for NH_4-N and NO_3-N. Details of the influent wastewater concentrations and the average steady-state effluent results from the LS-PFBR for both Study 1 and Study 2 are summarised in Table 3.7.

Table 3.7 – Typical average influent and effluent concentrations in the synthetic domestic wastewater. Standard deviations shown in ()

	Study 1		**Study 2**	
Parameters	Influent high strength wastewater (mg/l)	Effluent high strength wastewater (mg/l)	Influent low strength wastewater (mg/l)	Effluent low strength wastewater (mg/l)
COD_t	1021 (155)	76 (20)	346 (32)	40 (32)
TN_t	97 (3)	25 (7)	33 (2)	14 (6)
NH_4-N	62 (8)	10 (8)	18 (3)	0.4 (1)
NO_3-N	(not measured)	12 (5)	(not measured)	13 (3)
SS	(not measured)	10 (6)	(not measured)	3 (3)

Influent SS concentrations were negligible in the laboratory-scale studies due to the synthetic nature of the influent. Hence, influent COD_t and COD_f, concentrations were similar as were influent TN_t and TN_f, concentrations.

3.5 FIELD-SCALE PFBR – TUAM (FS-PFBR1)

3.5.1 System Overview

The FS-PFBR1 was installed as part of the EPA/NUI Galway Water Research Facility (WRF), located at the 25,000 population equivalent (PE) Galway County Council WWTP in Tuam, Co. Galway. Tuam is a medium-sized town with some industrial activity. The municipal WWTP was commissioned in 1996 with a design PE of 24,834 and has a current estimated load of 22,440 PE (EPA, 2010). A side stream of the influent wastewater entering the Tuam WWTP was pumped to the FS-PFBR1, with effluent returning to the Tuam WWTP prior to its primary settlement tanks. The Tuam WWTP received leachate from a nearby municipal waste landfill. The WRF processed about 1 – 2% of all influent wastewater to the main WWTP depending on the nature of the research being carried out at any given time.

The FS-PFBR1 system comprises seven identical, cylindrically-shaped pre-cast concrete tanks (with a base diameter of 2.89 m and a height of 3.85 m), and it includes primary settlement with primary sludge storage, secondary treatment and separate secondary sludge storages (Figure 3.7). Raw influent wastewater pumped to Primary Settlement Tank 1 flows by gravity to Primary Settlement Tank 2 and then to the Balance Tank. Settled wastewater is pumped at the beginning of each treatment cycle from the Balance Tank to the Reactor 1 for secondary treatment. Treated effluent from the Reactor 2 is pumped to the Clarifier at the end of each treatment cycle and it flows by gravity from the Clarifier through the Effluent Distribution and Effluent collection tanks. Thereafter, it ultimately returns to the Tuam WWTP.

Figure 3.7 – FS-PFBR1 located at NUI Galway/EPA Water Research Facility

The reactors have a total volume of 22.4 m^3 and a working volume of 20.9 m^3. There was approximately 11.5 m^3 of stationary biofilm media modules (with a specific surface area of 180 m^2/m^3). The plastic media in the reactor was maintained 600 mm from the base of the reactor tanks using a media stand (Figure 3.8). Reactors 1 and 2 were connected with a motorised valve.

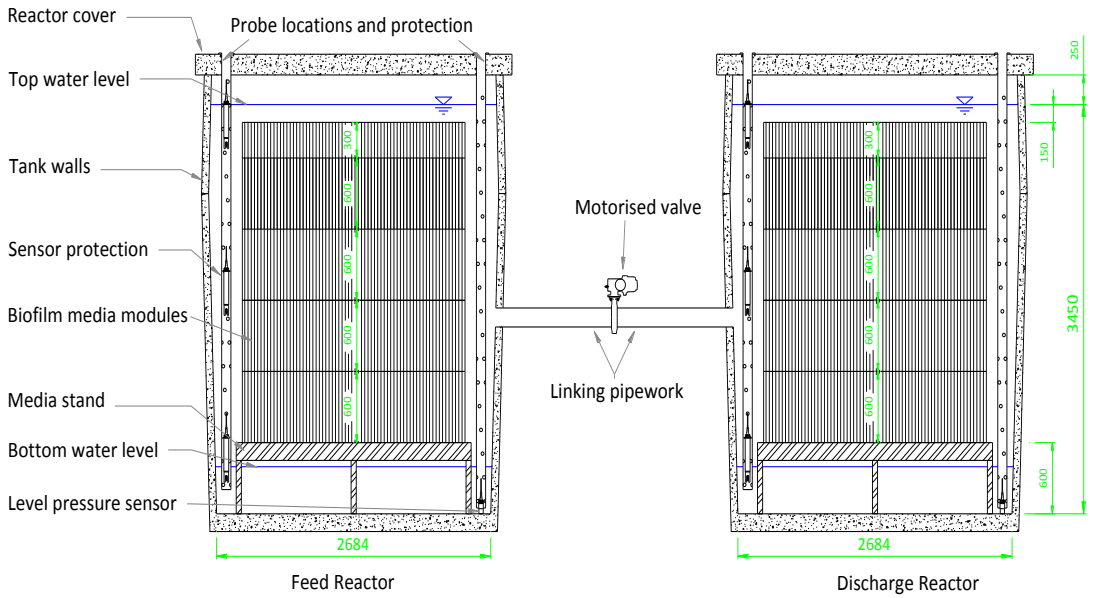

Figure 3.8 – Section view of R1 and R2 in FS-PFBR1 (O' Reilly, 2011)

3.5.2 FS-PFBR1 operating conditions

FS-PFBR1 was operated under two cycle regimes (Study 3 and 4). In each study, a typical treatment cycle comprised fill, anoxic, aerobic and settle stages of varying lengths. The fill stage provided for the addition of the influent to Reactor 1. The anoxic stage was effected by holding the wastewater, typically in Reactor 1, for a defined period of time. The aerobic stage was achieved by transferring wastewater between Reactor 1 and Reactor 2 using pumps. The settle stage allowed for separation of biosolids from the treated effluent.

The combination and timing of each stage of the PFBR makes the removal of carbon and nitrogen possible. Carbon oxidation and nitrification typically take place during the aerobic stage, while denitrification takes place during the anoxic stage. A carbon source to support denitrification is needed in the anoxic stage, thereby positioning the anoxic stage after the fill stage ensures the availability of a carbon source.

FS-PFBR1 was operated and examined using two different operational settings to determine which setting was optimum for effluent quality and energy usage (Table 3.8). The main difference between the two studies (Study 3 and Study 4) was the increased aeration time (360 minutes as opposed to 275 minutes) and the reduced anoxic time (134 minutes as opposed to 60 minutes).

Table 3.8 – Operational stages of FS-PFBR1

PFBR stage	Study 3 duration (minutes)	Study 4 duration (minutes)
Fill (t_1)	4	6
Anoxic (t_2)	134	60
Aerobic (t_3)	275	360
Settle (t_4)	14	30
Draw (t_5)	4	6
Total cycle time	431	462
No. of aerobic cycles	5	8

The details of the operating conditions for Study 3 and 4 are summarised in Table 3.9.

Table 3.9 – Operational conditions of FS-PFBR1

Parameter	Study 3	Study 4
PE	150	120
Average daily flow	29.2 m^3/d	24.8 m^3/d
Average volume cycle	8.74 m^3/cycle	7.95 m^3/cycle

3.5.3 Wastewater Characteristics

The influent, which was pumped from the nearby Tuam WWTP, comprised a municipal wastewater, and two different wastewaters of varying strengths were used as influents for Study 3 and Study 4. The Tuam WWTP also received leachate from a nearby municipal landfill. It should be noted there was little influent and effluent data available over a long period of time.

There was extensive monitoring equipment, such as DO and pH probes, and flow and energy meters, installed in the FS-PFBR1 allowing detailed analysis of set parameters to be carried out. All monitoring and control equipment were combined in one programmable logic controller (PLC) with a human machine interface (HMI), allowing ease of access to both the plant operation and logged data either on-site or through remote interrogation capabilities.

Throughout the studies, daily wastewater samples were taken at the beginning and end of a treatment cycle from R1 and R2 using refrigerated automatic samplers and tested in the Environmental Engineering Laboratories at NUI Galway. The samples were analysed in accordance with the standard procedures (APHA et al. 2005) (Table 3.3) for the following parameters COD_f, NH_4-N and NO_3-N.

In FS-PFBR1 there was average influent and effluent wastewater data available over 32 days for Study 3 and 30 days for Study 4. There was 20 influent samples and 26 effluent samples taken in Study 3. There was 33 influent and effluent samples taken in Study 4. There were four phase studies conducted during Study 3 and three phase studies conducted during Study 4, where samples were taken at frequent intervals during the individual treatment cycles. In Study 3 there was phase studies conducted for DO, COD_f, NH_4-N and NO_3-N. In Study 4 there were phase studies conducted for DO, NH_4-N and NO_3-N. The details of the wastewaters characteristics and the operating conditions for Study 3 and 4 are summarised in Table 3.10.

Table 3.10 – Typical average influent and effluent concentrations for Study 3 and Study 4. Standard deviations shown in ().

	Study 3	**Study 3**	**Study 4**	**Study 4**
Parameters	Average influent concentrations (mg/l)	Average effluent concentrations (mg/l)	Average influent concentrations (mg/l)	Average effluent concentrations (mg/l)
COD_f	187 (48)	66 (13)	144 (41)	33 (10)
NH_4-N	34 (10)	26 (5)	32 (7)	12 (6)
NO_3-N	(not measured)	0.95 (0.5)	0.03 (0.12)	1 (1)

3.6 FIELD-SCALE PFBR – MONEYGALL (FS-PFBR2)

3.6.1 System Overview

The FS-PFBR2 is located at Moneygall, Co. Offaly. The facility was designed and constructed by Molloy Environmental Systems (Tullamore, Co Offaly) in conjunction with NUI Galway, Offaly County Council and Enterprise Ireland (Figure 3.9).

Moneygall is a small village on the border of counties Offaly and Tipperary, with a population of approximately 400 people. The village has no industrial and very little commercial activity. There is a substantial surface water input due to the location of the village at the foot of a large hill.

Moneygall PFBR was designed to treat wastewater for a population equivalent of 750. The average daily flow to the FS-PFBR2 was 115 m^3/d. The influent wastewater comprised a municipal wastewater with combined storm and sewer.

Figure 3.9 – FS-PFBR2 located at Moneygall, Co. Offaly

The complete FS-PFBR2 installation was comprised of preliminary screening, a primary settlement tank, a balance system and a two-stream PFBR system. Each PFBR stream is made up of three chambers – two reactor chambers (Reactor 1 and Reactor 2) and a clarification chamber. The PFBR system was installed in a single *in situ* concrete tank, containing a total of six chambers, or three chambers per stream, as per Figure 3.10.

Each reactor chamber of the PFBR system has a working volume of 42.2 m^3. Stationary plastic biofilm modules installed in each reaction chamber constitute vertical trapezoidal tubes with a specific surface area of 230 m^2/m^3, giving a total surface area of 15,130 m^2 (including internal tank wall surfaces) per stream. At any one time, no more than one reactor volume of water was in the two-tank system and was cycled between the reactors using gravity and hydraulic pumps (O'Reilly, Rodgers & Clifford, 2011). Thus, the biofilm in each reactor was alternatively exposed to wastewater and atmospheric air.

The PFBR was controlled by a PLC unit. This device allows the user to vary control parameters, such as water levels, rest periods and aeration cycle counts. All process information was displayed on a human machine interface (HMI) (Clifford, 2013).

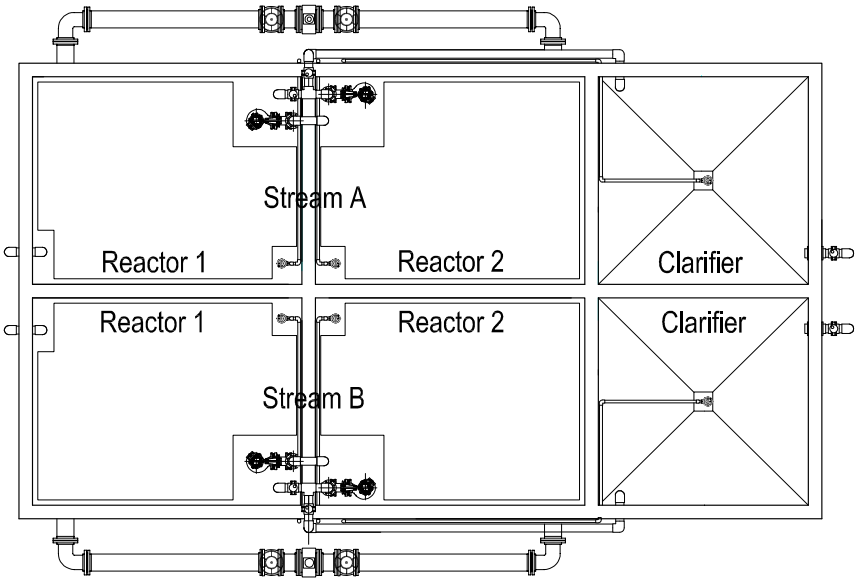

Figure 3.10 – Schematic of Two-Stream PFBR system housed in a single unit (Clifford, 2013)

3.6.2 FS-PFBR2 operating conditions

The FS-PFBR2 operated under one cycle regime (Study 5), with typical phases including fill/draw, anoxic, aerobic and settle, as outlined in Table 3.11. These phases were combined with rest periods to allow organic carbon, suspended solids and nitrogen removal.

Table 3.11 – Operational stages of FS-PFBR2

PFBR Stage	Duration (minutes)
Fill (t_1)	7
Anoxic (t_2)	30
Aerobic (t_3)	280
Settle (t_4)	13
Draw (t_5)	7
Total cycle time	337

3.6.3 Wastewater Characteristics

It should be noted there was minimal detailed influent/effluent data available over a significant period of time. Details of the influent and effluent wastewater characteristics

sampled over a period of seven months are summarised in Table 3.12. There was no phase study data available. At the FS-PFBR2, daily composite influent and effluent samples were taken using refrigerated automatic samplers. Influent samples were taken from the balance tank at the beginning of the Stream A treatment cycle. Effluent samples were removed from the clarifier chamber of Stream A prior to discharge. Influent flows were measured using an ultrasonic sensor and a flume.

Table 3.12 – Typical average influent and effluent concentrations. Standard deviations shown in ()

	Study 5	**Study 5**
Parameter	Average influent concentrations (mg/l)	Average effluent concentrations (mg/l)
COD_t	143 (68.3)	24 (8.4)
NH_4-N	10.3 (2.5)	3.0 (1.2)
NO_3-N	(not measured)	5.1 (1.5)

There was no alkalinity data available for LS-PFBR, FS-PFBR1 or FS-PFBR2. However in all model studies the alkalinity was kept above 7 mole/m^3 in order to prevent alkalinity impacting or limiting nitrification.

3.7 STATISTICAL ANALYSIS

A statistical analysis was carried out in Excel using an ANOVA analysis F-test to determine the difference between modelled and measured sets of data in the field scale and laboratory scale PFBR (Section 4.3 and Section 5.3). An ANOVA analysis F-test was used as opposed to a typical t-test as the t-test is usually used to examine the differences between the means of two sets of data whereas the F-test allows comparisons to be made between more than two sets of data

3.8 SUMMARY

This chapter describes the design, construction and operation of three PFBR systems that were modelled as part of this thesis: the laboratory-scale PFBR located in NUI Galway and the two field-scale PFBRs located in Tuam, Co. Galway, and Moneygall, Co. Offaly. Table 3.13 outlines the models discussed in the following chapters.

Table 3.13 – Details of the modelling software and PFBR systems

System Tested	Modelling Software	Chapter
LS-PFBR (Study 1 and 2)	GPS-X	4
FS-PFBR1 (Study 3 and 4)	GPS-X	5
FS-PFBR1 (Study 3 and 4)	AQUASIM	6
FS-PFBR2 (Study 5)	GPS-X and AQUASIM	7

4 MODELLING THE LABORATORY SCALE PFBR (LS-PFBR) USING GPS-X

4.1 INTRODUCTION

This chapter investigates the potential for (1) modelling a laboratory scale PFBR (an example of a batch biofilm PAS) using activated sludge-based models and (2) predicting effluent results and contaminant concentration changes during individual treatment cycles. The PFBR was modelled and calibrated using laboratory-scale experimental data (O'Reilly, 2005). It was decided to initially model a laboratory system as it was subject to less variability in influent constituents when compared to site systems.

The model of the laboratory-scale PFBR system was initially calibrated using the results from a high-strength synthetic wastewater (Study 1) and then validated against a study investigating the treatment of low-strength synthetic wastewater (Study 2).

4.2 MODEL DEVELOPMENT

4.2.1 Model Description

A generic modelling development approach, which included the five main steps of (i) project definition, (ii) data collection, (iii) plant model set-up, (iv) data collection from the model, and (v) simulation and results interpretation, was implemented for developing all of the models discussed in this thesis.

The approach to this model development was adapted from numerous model studies, such as Petersen et al., 2000; Boltz et al., 2013; and Brockmann et al., 2013 and from experience gained while modelling the PFBR. This approach was used in the development of all models in both GPS-X and AQUASIM. The overall goal was to summarize the approach to model development by following a series of generic steps (Figure 4.1).

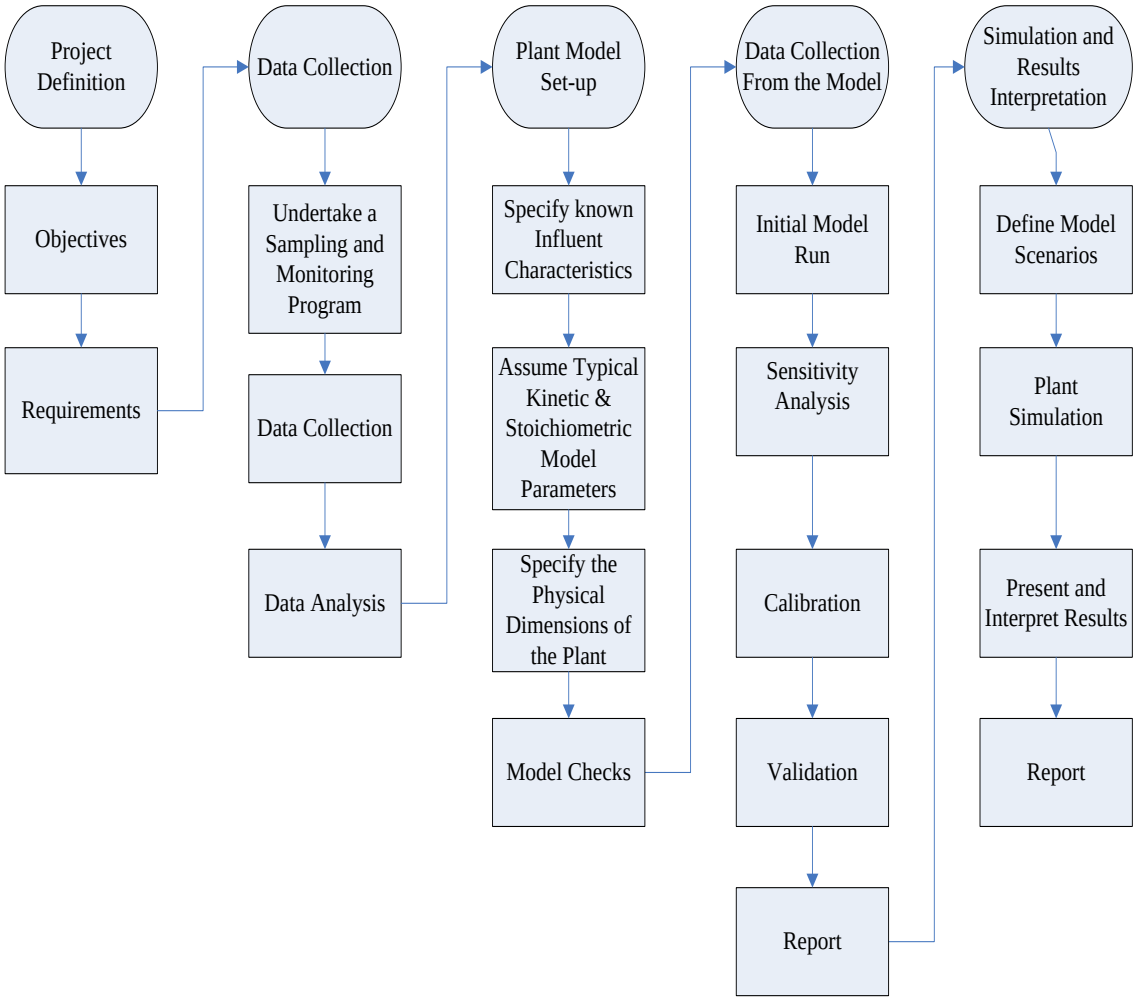

Figure 4.1 – Model development and calibration steps

Initial work in this chapter focused on developing a model that could accurately represent the physical operation of the LS-PFBR (notably the cyclic variation in reactor levels due to the alternate pumping of wastewater between the two connected reactors in the system). The objects considered for modelling the LS-PFBR in GPS-X included trickling filters, rotating biological contactors and submerged biological contactors. However, an initial investigation showed that two linked SBR objects most accurately and efficiently simulated the physical operation of the LS-PFBR. Each SBR object could incorporate typical PFBR stages, comprising fill, anoxic, aeration, settle and draw.

The three SBR objects available in GPS-X were considered namely; (i) the simple SBR object, (ii) the advanced SBR object and (iii) the manual SBR object. All three objects have the same functionality, appearance and choice of biological models but they differ in the manner in which the user specifies the operation of the SBR unit.

The simple and advanced SBR objects require the specification of the timing and flow rates to define the phases. The manual SBR object requires that the entire operation cycle be defined by the user by having the liquid flows, air flows, and mixing as file inputs.

Suitable layouts for representing the hydraulic characteristics of the LS-PFBR were developed using each of the three SBR objects available in GPS-X. Some results from the initial investigations using the advanced SBR object, the simple SBR object, the RBC and the trickling filter are shown in Appendix C. Table 4.1 shows a number of plant layouts and different process objects trialled in GPSX in order to model the PFBR. It is important to note that this is just a small sample of the layouts trialled to model the PFBR, the rest are shown in Appendix C.

Table 4.1 – GPS-X layouts trialled to model the PFBR

GPS-X object	GPS-X layout	Comments
Simple SBR	The layout involved using 4 SBR objects and 1 modelling toolbox. One SBR object was used for each process of the PFBR i.e. SBR 1 – Fill SBR 2 – Anoxic SBR 3 – Aerobic SBR 4 – Settle	The hydraulics were modelled successfully using this layout; however, it took the model nearly 60 minutes to simulate a 5 day hydraulic model so it was not practical to use. Also, between every SBR object, a splitter was required before the model could be built. Hydromantis was informed of this problem and are working on a solution.
Simple SBR	The layout involved using 3 SBR objects and a 4 way splitter. One SBR object was used for each of the following processes. SBR 1 – Fill SBR 2 – Anoxic, Aerobic SBR 3 – Aerobic, Settle The 4 way splitter controlled the influent and the recycle flow.	The hydraulics could be modelled using this layout; however, the 4 way splitter did not accurately divide the influent and the recycle flow in every cycle. Hydromantis were informed of this problem and they said they would work on a solution.

GPS-X object	GPS-X layout	Comments
Simple SBR	The layout involved using 2 SBR objects however this layout required 5 modelling toolboxs modelling the on/off flows and was extremely complicated to set up.	The flows were initially modelled correctly however after one cycle the 5th modelling toolbox which controlled the recycle on/off flow did not read correctly so the hydraulics couldn't be modelled after the first cycle. Hydromantis were informed of this problem and they said they would work on a solution.
Advanced SBR	This layout included 2 SBR objects, 4 splitters and 5 modelling toolboxes.	The hydraulics and the DO were modelled successfully using this layout. However the model was slow to run due to the 5 modelling toolboxes.
Advanced SBR	This layout included 2 SBR objects, 3 splitters and 3 modelling toolboxes.	The hydraulics and the DO were modelled successfully using this layout.
Rotating biological contactor	The RBC was trialled as an object to model the PFBR. It was proposed to fill the RBC with wastewater and move the biofilm in and out of the tank in order to expose it the atmosphere and mimic the aerobic and anoxic stages of the PFBR. The option of moving the wastewater in and out of the RBC was also examined.	The submerged fraction of biofilm in an RBC cannot be changed during a simulation. It was also not possible to move the wastewater in and out of the biofilm as initially thought. RBC based layouts took about 30 minutes to simulate 1 operating day.
Rotating biological contactor	Layout 1: This layout included one RBC and involved changing the K_La value to turn on and off the oxygen throughout a cycle.	This layout did not work and also took about 15 minutes for the plant to start running.

GPS-X object	GPS-X layout	Comments
Rotating biological contactor	Layout 2: This layout included 2 RBC objects to mimic the 2 reactors in the PFBR.	It was not possible to transfer wastewater between the two RBCs.
Submerged biological contactor	The SBC was examined as an object to model the PFBR.	The same problems as the RBC arose.
Trickling Filter	The trickling filter was trialled in GPS-X as it provided biofilm biological treatment.	The limitations of the object to model the PFBR concerned the hydraulics. It was not possible to circulate wastewater between two trickling filters.

Table 4.2 shows the general layout of the three SBR objects in GPS-X.

Table 4.2 – Layout of SBR object in GPS-X

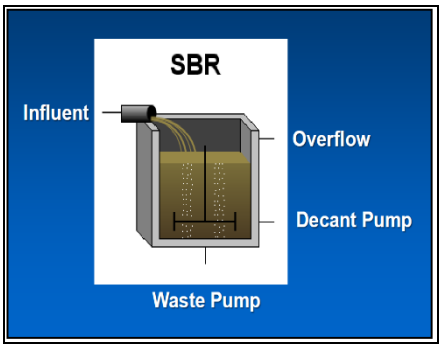

Influent: connection point where the wastewater is filling from.
Overflow: connection point where wastewater can overflow. However, if the model system is set up correctly, the overflow should be zero throughout the cycle.
Decant pump: connection point for decanting. The pump always decants from the upper layer.
Waste Pump: connection point from where the wastewater is discharged.

The manual SBR object was chosen to model the LS-PFBR as it enabled maximum user flexibility in defining key parameters, such as wastewater flow rates, mixing and air flow rates. The manual SBR object enables the entire operational cycle to be defined by the user, either by directly defining cycle parameters or via file inputs.

The final plant model for the LS-PFBR comprised two manual SBR objects, an influent object, two flow combiners and a flow splitter (Figure 4.2). The two SBR units were used to model the different stages of the treatment cycle, i.e.

- SBR1 – fill, anoxic and aerobic stage
- SBR2 – aerobic, settle and draw stage

This is an exact replication of what happens in the LS-PFBR. The fill and discharge from the system typically takes place in R1 and R2 respectively. The anoxic stage takes place in R1 and the aerobic stage takes place in both R1 and R2.

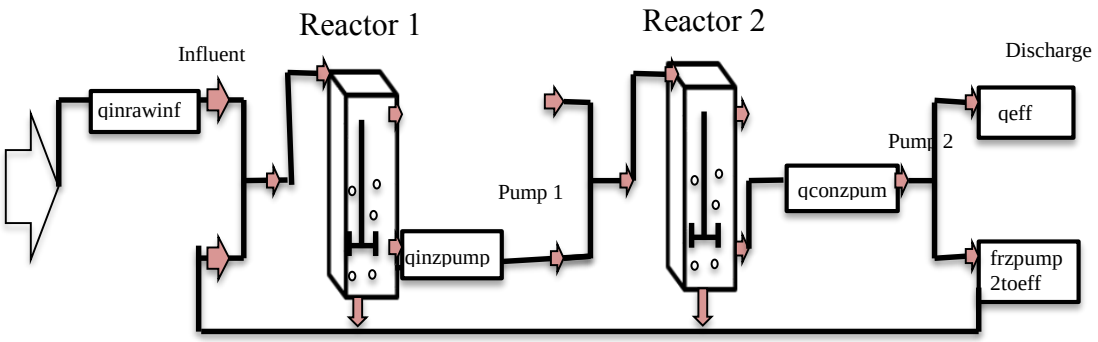

Figure 4.2 – GPS-X layout of the LS-PFBR model using two manual SBR objects

Table 4.3 shows the physical dimensions of the SBR reactors used in the laboratory and the model.

Table 4.3 – Physical design parameters (measured and modelled)

Physical dimensions	Size
Surface area of tanks	0.0576 m^2
Maximum water level height	0.4 m

The LS-PFBR was operated under two cycle regimes (Study 1 and Study 2). The treatment cycle comprised anoxic, aerobic and settle stages of varying lengths (as described in *Section 3.4.2*) and summarised in Table 4.4.

Table 4.4 – Operational cycle of LS- PFBR (Study 1 and 2)

PFBR Stage	Duration (minutes)
Fill (t_1)	8
Anoxic (t_2)	150
Aerobic (t_3)	106
Settle (t_4)	60
Draw (t_5)	5

ASM1 was chosen to calibrate the LS-PFBR model as the model was mainly concerned with predicting COD and N removal concentrations both in the effluent but also during individual treatment cycles within the PFBR. The model calibration process was initiated with all the ASM1 values set to default.

4.2.2 System characteristics and hydraulics

The next step in the model development involved simulating system hydraulics as closely as possible. The first step in developing the hydraulics for the plant model involved creating input control files that described (i) input flows, (ii) output flows, (iii) the recycle flows between R1 and R2, (iv) the flow splitter positions and (v) the aeration times. Input control files are specifically used in the manual SBR so that the user can define the entire operational cycle of the SBR on an Excel sheet. These control files are then read by GPS-X during each cycle.

The labels used in creating eight input files were then input into 'flow control forms' (the flow control forms used are shown in Appendix D). An operational cycle was then defined using the input control files to mimic the LS-PFBR operation. The input control files used are shown in Tables 4.5 and 4.6.

Table 4.5 – Input Control Files

File Input	Unit	Input file column descriptions
qinrawinf	l/min	Controls the influent object's flow rate
mixconzover1		Sets whether mixing or settling occurs within SBR1
klaconzover1	d^{-1}	Controls the oxygen mass transfer rate in SBR 1
mixconzover2		Sets whether mixing or settling is occurring within SBR2
qinzpump1	l/min	Controls the flow rate from SBR1 to SBR2
klaconzover2	d^{-1}	Controls the oxygen mass transfer rate for SBR 2
qconzpump2	l/min	Controls decanting in SBR 2
frzpump2toeff		The fraction of flow from SBR 2 pumped to the effluent rather than back to SBR 1 (For example, if this variable is set at 0, all flow returns to SBR 1, and if it is set at 1, all flow is discharged as effluent)

Table 4.6 – Input control files and times for one complete cycle in Studies 1 and 2

			Influent	Mixing on/off R1	K_La R1	Mixing on/off R2	Pump 1	K_La R2	Pump2	Discharge
		t	qinrawinf	mixconzover1	klaconzover1	mixconzover2	qinzpump1	klaconzover2	qconzpump2	frzpump2toeff
		min	l/min	-	d^{-1}	-	l/min	d^{-1}	l/min	-
Fill		1 - 8	* 0.625	** 1	0	0	0	0	0	0
Anoxic		9 - 158	0	0	0	0	0	0	0	0
Aerobic	**Transfer to R2**	159	0	0	0	1	****12	122	0	0
	Aerobic R2	160 - 162	0	0	0	0	0	122	0	0
	Transfer to R1	163	0	1	***122	0	0	0	12	0
	Aerobic R1	164 - 166	0	0	122	0	0	0	0	0
	Transfer to R2	167	0	0	0	1	12	122	0	0
	Aerobic R2	168 - 170	0	0	0	0	0	122	0	0
	Transfer to R1	171	0	1	122	0	0	0	12	0
	Aerobic R1	172 - 174	0	0	122	0	0	0	0	0
			The aerobic sequence and recycling between R1 and R2 continued for 264 minutes							
Settle		267 - 325	0	0	0	0	0	0	0	0
Draw		325 -329	0	0	0	0	0	0	12	***** 0.42

* The average volume/cycle for Study 1 and Study 2 was 12 l. At the start of a cycle, there was 7 l in R1 so 5 l was required to fill the tank. A flow of 0.625 l/min for 8 minutes, which equates to 5 l, was used to fill the tank to 12 l.

** The number 1 was used as this turned on the mixing in R1.

*** This is the K_La value used.

**** This is the total volume of wastewater in the reactors, 12 l.

***** At the end of each cycle, 7 l of wastewater is decanted and 5 l is recycled back to R1 in preparation for the next treatment cycle. 0.42 is the percentage of wastewater recycled back to R1.

The input excel files in the model were saved as .dat files. When running the model, the communication interval, i.e. the average integration step size, was set to one minute (the communication interval must be equal to or less than the size of the time steps in all the input files, which is one minute). The input file shown in Table 4.6 was read by GPS-X during each cycle.

The average volume/cycle for Study 1 and Study 2 was 12 l, and the operating regime for the LS-PFBR was similar for Study 1 and Study 2 (as described in *Section 3.4*). During a typical cycle in Study 1 and Study 2, influent wastewater flowed into R1 over an eight-minute period (R1 contained treated wastewater from a previous cycle and R2 is empty at this stage). The wastewater then settled in R1 for 150 minutes (which equated to an anoxic period). After the anoxic period, wastewater was circulated between R1 and R2 for 106 minutes (aerobic period). Pumps 1 and 2 operated in sequence to transfer wastewater between R1 and R2 during the aeration cycle (Figure 4.3). A rest period of 60 minutes followed in R2 (R1 is empty at this stage). Finally, 42% of the total volume was decanted from R2 while 58% was recycled back to R1 in preparation for the next treatment cycle. In general a reduction of discharge volume, where other factors such as carbon are not limiting, can enhance nitrogen removal. However, this will be at the expense of decreased wastewater throughput.

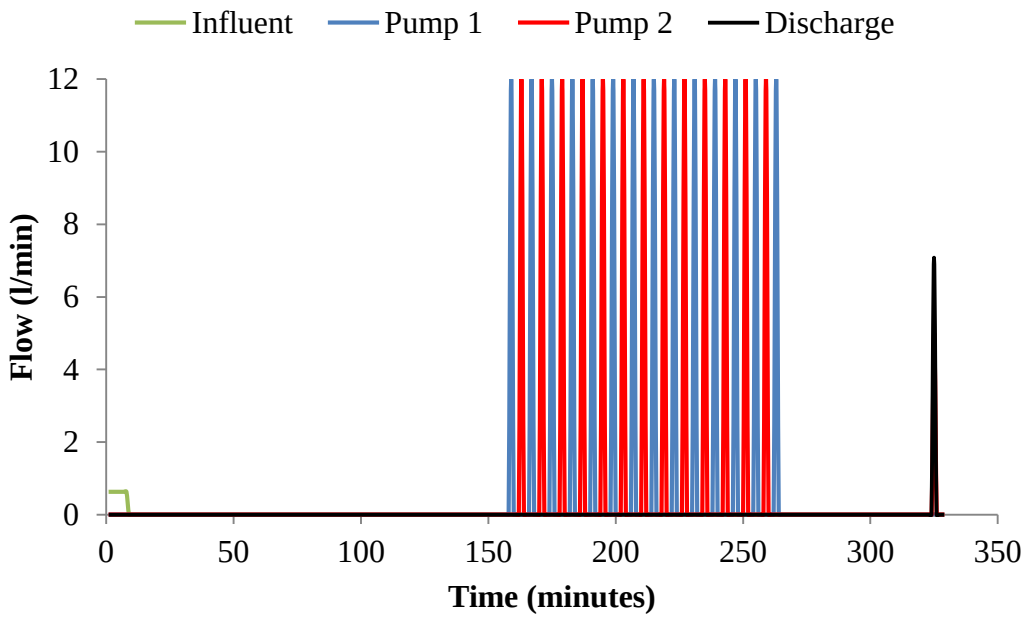

Figure 4.3 – Influent and discharge profiles and transfer flow profiles between R1 and R2 during a typical treatment cycle

4.2.3 Wastewater Characteristics

The influent characteristics for this model were based on the laboratory data described in Chapter 3.4.3. Using 'Influent Advisor' (an influent modelling tool associated with GPS-X), a detailed overview of the influent was developed (Table 4.7) (only non-zero components are shown, the full influent advisor is shown in Appendix E). As phosphorous removal was not considered in this model, it was omitted from the influent model. Influent characteristics were quite consistent over time, and thus the system was modelled in steady-state mode (i.e. using average influent concentrations during the experimental period).

It is important to note that in the measured data there was no breakdown of soluble biodegradable COD, soluble un-biodegradable COD, slowly biodegradable COD or particulate un-biodegradable COD. There was also no breakdown of nitrogenous material. However from carry out initial model runs it was evident what the inert fractions of COD and nitrogen were. The known mathematical description of the influent wastewater from the PFBR was fed into the Influent Advisor in GPS-X and a series of calculations were undertaken by GPS-X to ensure that the influent data entered by the user was partitioned correctly and an influent profile generated. It is impossible to know if this partitioning was 100% accurate or not. As a means of double checking to ensure that the influent partitioning was satisfactory the influent figures used in the influent advisor were compared to typical characteristics of domestic wastewater figures used by Henze et al. (2000). There was limited influent data available however by utilising the influent advisor in GPS-X and having an idea of the inert fractions this allowed an influent wastewater profile to be generated.

The wastewater composition is an important issue in the calibration of the PFBR and it is important that the wastewater data is entered correctly. This is discussed in more detail in Chapter 8.

Table 4.7 – Influent composition modelled using influent advisor in GPS-X

Parameters	Units	Study 1		Study 2	
Biological Model: asm1		Measured	Modelled	Measured	Modelled
Influent Composition					
total COD	g COD/m^3	1021	1020	346	346
total nitrogen	g N/m^3	97	96	33	32
Nitrogen Compounds					
free and ionized ammonia	g N/m^3	62	63.36	18	18.9
Alkalinity					
alkalinity	mole/m^3		7		7
Influent Fractions					
XCOD/VSS ratio	g COD/g VSS		1.8		1.8
$BOD_5/BOD_{ultimate}$ ratio	-		0.66		0.66
TSS & COD Model Coefficients					
inert fraction of soluble COD	-		0.2		0.2
substrate fraction of particulate COD	-		0.82		0.82
heterotrophic fraction of particulate COD	-		0		0
ammonium/TKN ratio	-		0.66		0.59
particulate organic N/total organic N ratio	-		0.9		0.9
VSS/TSS ratio	g VSS/g TSS		0.75		0.75
ASM1 Nutrient Fractions					
N content of active biomass	g N/g COD		0.086		0.086
N content of endogenous/inert mass	g N/g COD		0.06		0.06

4.3 RESULTS AND DISCUSSION

4.3.1 Dissolved Oxygen

For both studies, the passive aeration process in the PFBR was modelled by using diffused air and entering a K_La (mass transfer coefficient) value. A K_La value of 122 d^{-1} had previously been calculated from a laboratory-scale PFBR study (O'Reilly, 2005), and this figure was used in the model calibration. The option of using mechanical surface aeration to model the passive aeration process was also examined in GPS-X. However the 'diffused air' option was chosen as this most resembled the passive aeration process in the PFBR. Figure 4.4 gives a typical DO profile graph produced from the GPS-X model for R1 and R2. The wastewater was transferred between the reactors eleven times during the aerobic period for Study 1 and Study 2.

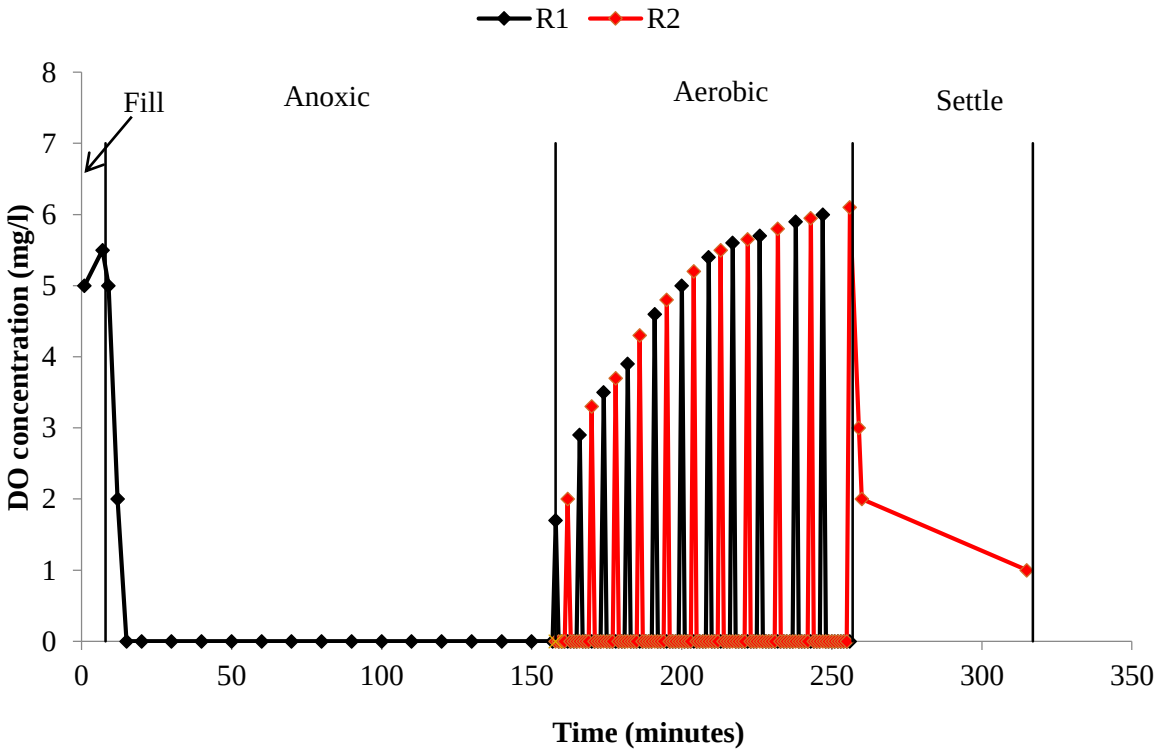

Figure 4.4 – GPS-X model data for a typical DO phase study

The models were run to ensure that oxygen profiles from measured and modelled data correlated well. Similar profiles were obtained for modelled and measured results for Study 1 (Figure 4.5). There was no DO phase study data available for Study 2. Modelling the passive aeration process and the uncertainties surrounding it is discussed in more detail in Chapter 8

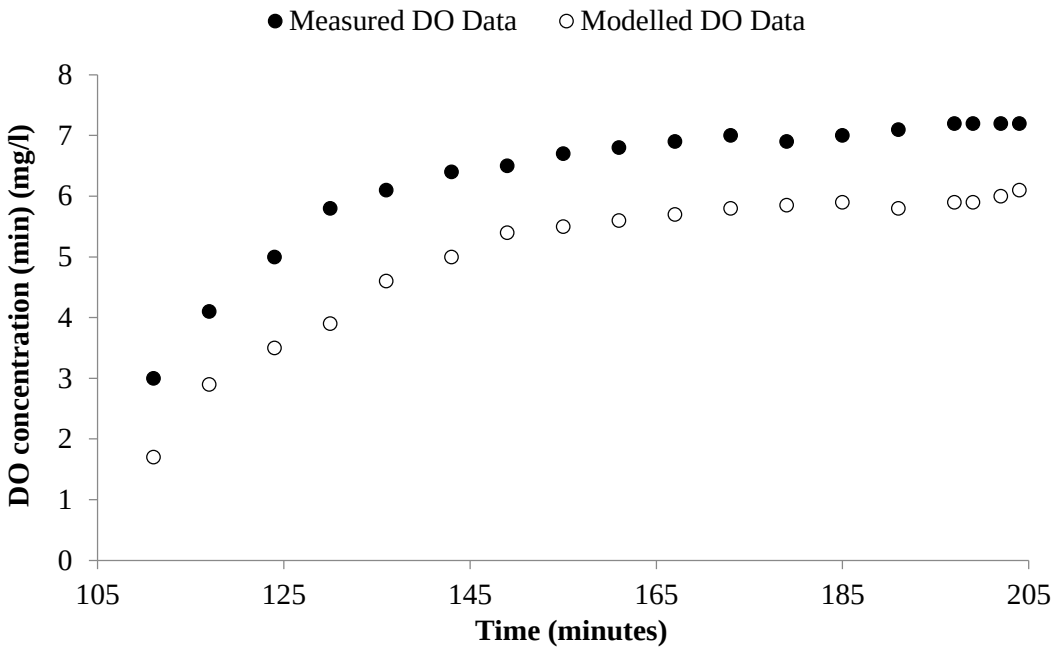

Figure 4.5 – Modelled and measured DO for one aerobic cycle during Study 1

Further attempts were made to gather oxygen data in the PFBR while undertaking during this study. A new product called the 'RedEye Oxygen Sensor Patch' was used to monitor DO concentrations within the PFBR. The RedEye patch is an oxygen sensing product designed specifically to measure oxygen in packaging. The patch uses proprietary coatings that can detect dissolved oxygen in liquids down to 20ppb. A patch was glued to the inside of the reactor wall (which acted as a substratum for biofilm development). The patch was then monitored through the Perspex tank wall using an associated oxygen sensor probe. The premise was that once biofilm developed on the patch DO concentrations could be measured at the base of the biofilm and used in conjunction with bulk fluid measurements to provide more insight into DO characteristics within the PFBR. Dissolved oxygen readings were obtained for a two month period and are shown in Appendix F. The DO readings from the RedEye Patches were not used in the calibration of the model as it was considered that the DO results from the DO probe were more accurate at the time of testing as the DO probe was recently calibrated and different results were obtained between the probe and the patches. A comparison of DO probe results and red eye patch results are shown in Appendix F. The dissolved oxygen measurements were carried out in-situ at the media surface over two months using the

'RedEye Oxygen Sensor Patch' which gave DO concentration data at the biofilm base during anoxic and aerobic phases.

4.3.2 Sensitivity Analysis

Following initial model development the most relevant parameters to be estimated during calibration were determined by completing a sensitivity analyses. GPS-X software contains a sensitivity analyses tool which can be used to study the sensitivity to any relevant parameters. Using the default values for ASM1, a sensitivity analyses was carried out and the default values were adjusted to calibrate the model.

The sensitivity analysis was carried out on Study 1 and the results validated against Study 2. Experimental phase studies for nitrogen were undertaken during Study 2 where wastewater samples were taken at regular intervals from both R1 and R2 and analysed for NH_4-N and NO_3-N. This data was used to further verify the model.

For Study 1 model, four plots, 'Sensitivity COD_t', 'Sensitivity TN_t', 'Sensitivity NO_3-N' and 'Sensitivity NH_4-N', were used to describe the sensitivity of the variables COD_t, TN_t, NH_4-N and NO_3-N with respect to the six model parameters listed in Table 4.8 (all stoichiometric, kinetic and operation parameters in GPS-X were tested in the sensitivity analysis but the six listed in Table 4.8 were the most important/sensitive in terms of calibration).

The upper and lower boundaries for each parameter during calibration were taken from reported literature values (see Table 4.15). The results of the full sensitivity analysis carried out are included in Appendix G.

Table 4.8 – Key parameters for sensitivity analysis

Parameter	Description	Range used for sensitivity analysis
μ_A	Autotrophic growth rate	0.1 d^{-1} to 1 d^{-1}
μ_H	Heterotrophic growth rate	1 d^{-1} to 12 d^{-1}
Y_A	Yield of autotrophs	0.07-0.28 g COD/g N
Y_H	Yield of heterotrophs	0.38-0.75 g COD/g COD
b_A	Autotrophic decay rate	0.01 d^{-1} to 0.2 d^{-1}
b_H	Heterotrophic decay rate	0.05 d^{-1} to 1.6 d^{-1}

Typical results from the sensitivity analyses for Study 1 are shown in Figure 4.6. The negative sign indicates that the variable increases with decreasing parameter values (and vice versa for a positive sign). The positive and negative figure indicates the magnitude of change of that value. For example, as shown in Figure 4.6, as μ_H increased from 1 d^{-1} to 12 d^{-1}, effluent COD_t concentrations predicted by the model decreased by 91%.

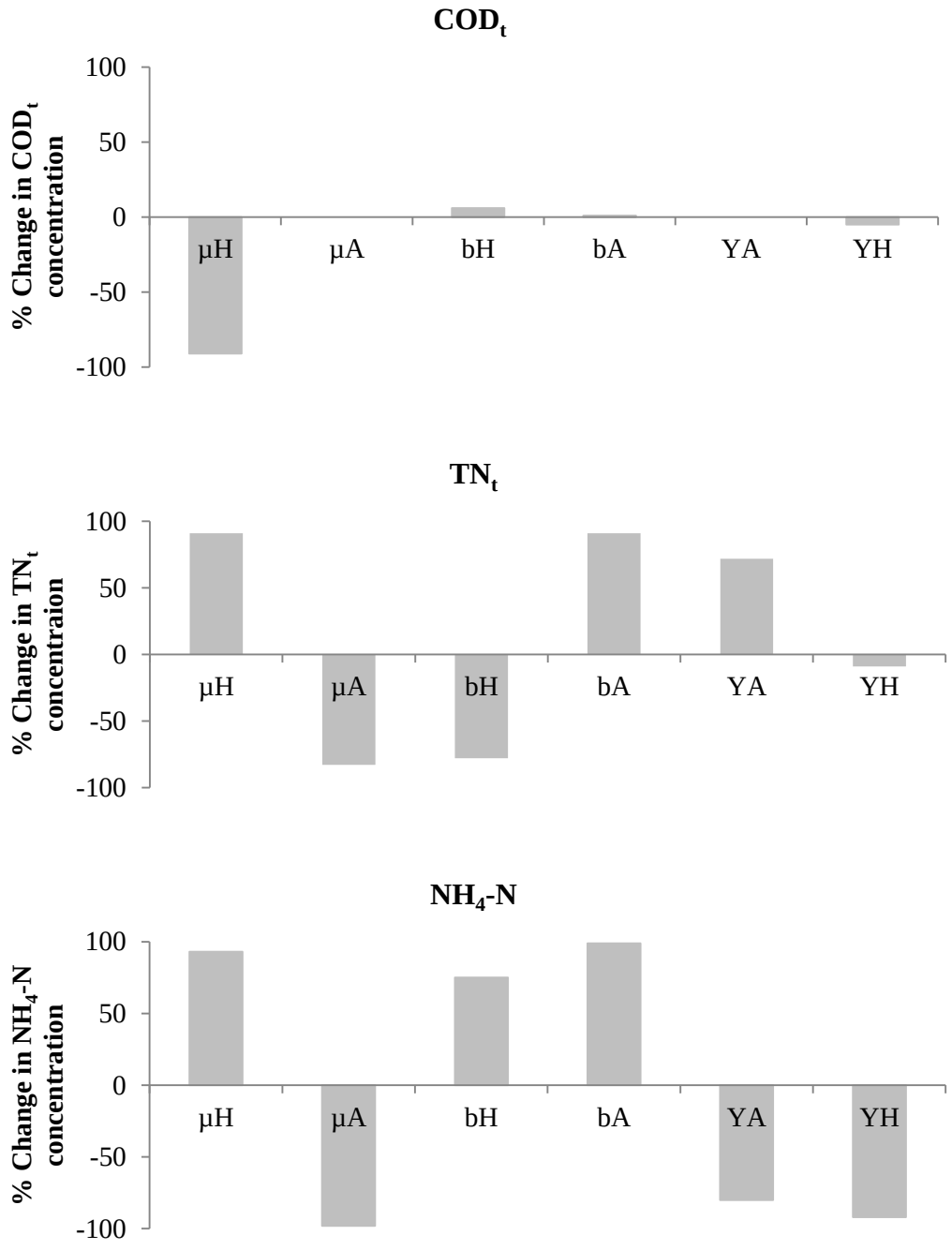

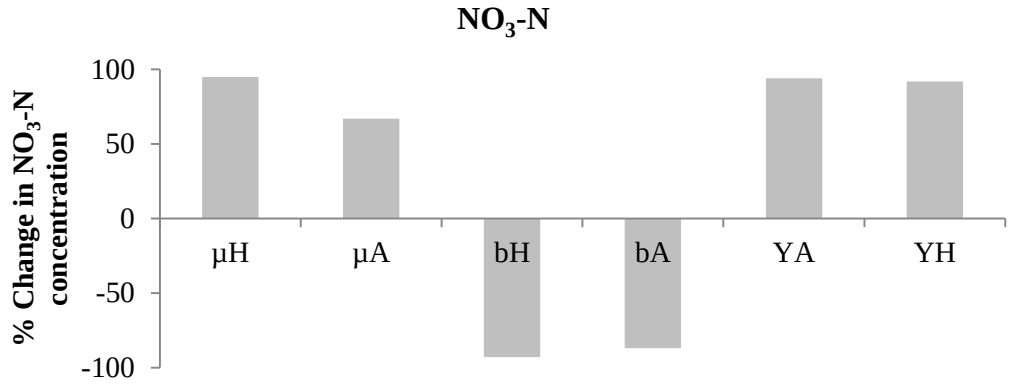

Figure 4.6 – Sensitivity analysis on modelled effluent COD_t, TN_t, NH_4-N, NO_3-N

Effluent COD_t concentrations were most sensitive to changes in μ_H; TN_t, NH_4-N, and NO_3-N were most sensitive to changes in Y_A, μ_A and b_A.

There was an 83% decrease in effluent TN_t concentrations as μ_A increased from 0.1 d^{-1} to 1 d^{-1}. There was a 91% increase in effluent TN_t concentrations as b_A increased from 0.01 d^{-1} to 0.2 d^{-1}. As μ_A increased from 0.1 d^{-1} to 1 d^{-1}, the modelled effluent NH_4-N concentration decreased by 98%. As b_A increased from 0.01 d^{-1} to 0.2 d^{-1}, effluent concentrations increased by 99%. Effluent NO_3-N concentrations were most sensitive to changes in Y_A. As Y_A increased from 0.07-0.28 g COD/g N, effluent NO_3-N concentrations increased by 94%. Tables 4.9 to 4.14 show the variation in COD_t, TN_t, NH_4-N, NO_3-N, Ss and Si effluent concentrations with the change in each stoichiometric/kinetic parameter. It is important to note that only one parameter was changed at a time and the other parameters were kept at the default values for example while μ_H was changed to 2 d^{-1} μ_A remained at the default value of 0.8 d^{-1}. The full list of default values are shown in Table 4.15.

As part of the sensitivity analysis two of the influent fractions in the influent advisor were adjusted in order to determine the impact that these fractions had on effluent concentrations. The influent fractions chosen were the XCOD/VSS fraction which is the ratio of particulate COD (XCOD) to volatile suspended solids (VSS) and the ammonium/TKN ratio. The XCOD/VSS fraction was selected in order to decipher what effect it had on effluent Si, SS, Xs and Xi. The ammonium/TKN fraction was selected in order to determine the impact that it had on effluent S_{NH}, S_{NO}, S_{ND}, X_{ND}. These two fractions were selected to be adjusted in the simulations as in the influent advisor by

adjusting these parameters led to the greatest changes in the state variables. Five simulations were carried out which involved adjusting the XCOD/VSS fraction in increments from 1.8 to 2.5. The results showed that this fraction had little or no impact on the effluent COD state variables. It also had no impact on effluent NH_4-N or NO_3-N. The second influent fraction analysed was the ammonium/TKN ratio. This faction was adjusted in 5 increments from 0.5 to 0.9 and a simulation carried out for each one. The results showed that adjusting this faction had no impact on the effluent nitrogen compounds i.e. free and ionized ammonia, soluble biodegradable organic matter, particulate biodegradable organic matter and nitrate (Table 4.13 and 4.14).

Table 4.9 – Sensitivity analysis results for modelled COD_t effluent concentrations

Sensitivity ranges (μ_H)	COD_t (mg/l)	Sensitivity ranges (μ_A)	COD_t (mg/l)	Sensitivity ranges (Y_H)	COD_t (mg/l)	Sensitivity ranges (Y_A)	COD_t (mg/l)	Sensitivity ranges (b_A)	COD_t (mg/l)	Sensitivity ranges (b_H)	COD_t (mg/l)
2	891	**0.2**	80	**0.38**	85	**0.07**	79	**0.01**	80	**0.05**	78
4	309	**0.4**	80	**0.5**	80	**0.1**	80	**0.05**	80	**0.1**	78
6	119	**0.6**	80	**0.6**	79	**0.15**	80	**0.1**	80	**0.5**	80
10	103	**0.8**	80	**0.7**	80	**0.2**	81	**0.15**	80	**1**	81
12	81	**1**	80	**0.75**	81	**0.28**	79	**0.2**	81	**1.6**	83

Table 4.10 – Sensitivity analysis results for modelled TN_t effluent concentrations

Sensitivity ranges (μ_H)	TN_t (mg/l)	Sensitivity ranges (μ_A)	TN_t (mg/l)	Sensitivity ranges (Y_H)	TN_t (mg/l)	Sensitivity ranges (Y_A)	TN_t (mg/l)	Sensitivity ranges (b_A)	TN_t (mg/l)	Sensitivity ranges (b_H)	TN_t (mg/l)
2	1	**0.2**	54	**0.38**	11	**0.07**	3	**0.01**	6	**0.05**	18
4	2	**0.4**	32	**0.5**	10	**0.1**	7	**0.05**	11	**0.1**	17
6	4	**0.6**	18	**0.6**	9	**0.15**	8	**0.1**	33	**0.5**	12
10	7	**0.8**	11	**0.7**	9	**0.2**	9	**0.15**	52	**1**	5
12	11	**1**	9	**0.75**	10	**0.28**	12	**0.2**	65	**1.6**	4

Table 4.11 – Sensitivity analysis results for modelled NH_4–N effluent concentrations

Sensitivity ranges (μ_H)	NH_4–N (mg/l)	Sensitivity ranges (μ_A)	NH_4–N (mg/l)	Sensitivity ranges (Y_H)	NH_4–N (mg/l)	Sensitivity ranges (Y_A)	NH_4–N (mg/l)	Sensitivity ranges (b_A)	NH_4–N (mg/l)	Sensitivity ranges (b_H)	NH_4–N (mg/l)
2	0.2	**0.2**	50	**0.38**	12	**0.07**	1.13	**0.01**	0.6	**0.05**	0.1
4	0.3	**0.4**	28	**0.5**	10	**0.1**	0.75	**0.05**	5	**0.1**	0.4
6	0.8	**0.6**	10	**0.6**	5	**0.15**	0.66	**0.1**	29	**0.5**	0.3
10	2	**0.8**	4	**0.7**	2	**0.2**	0.41	**0.15**	48	**1**	0.2
12	3	**1**	1	**0.75**	1	**0.28**	0.2	**0.2**	60	**1.6**	0.4

Table 4.12 – Sensitivity analysis results for modelled NO_3–N effluent concentrations

Sensitivity ranges (μ_H)	NO_3–N (mg/l)	Sensitivity ranges (μ_A)	NO_3–N (mg/l)	Sensitivity ranges (Y_H)	NO_3–N (mg/l)	Sensitivity ranges (Y_A)	NO_3–N (mg/l)	Sensitivity ranges (b_A)	NO_3–N (mg/l)	Sensitivity ranges (b_H)	NO_3–N (mg/l)
2	0.02	**0.2**	1.4	**0.38**	0.5	**0.07**	0.2	**0.01**	4.85	**0.05**	16
4	0.11	**0.4**	2.7	**0.5**	1.6	**0.1**	1.7	**0.05**	3.87	**0.1**	14
6	1	**0.6**	3.8	**0.6**	1.9	**0.15**	4.1	**0.1**	2.7	**0.5**	4
10	2.2	**0.8**	4.0	**0.7**	5.0	**0.2**	4.8	**0.15**	1.48	**1**	3
12	4.1	**1**	4.3	**0.75**	6.5	**0.28**	5.3	**0.2**	0.6	**1.6**	1

Table 4.13 – Sensitivity analysis results for influent fraction XCOD/VSS

XCOD/VSS	Si (mg/l)	Ss (mg/l)	Xi (mg/l)	Xs (mg/l)	S_{NH} (mg/l)	S_{ND} (mg/l)	X_{ND} (mg/l)	S_{NO} (mg/l)
1.8	81	0.9	0	0.43	0.07	4.33	0.09	28.4
2.0	81	0.4	0	0.43	0.11	3.96	0.05	28.4
2.2	81	0.6	0	0.43	0.11	3.96	0.05	28.4
2.5	81	0.8	0	0.43	0.11	3.96	0.05	28.4

Table 4.14 – Sensitivity analysis results for influent fraction Ammonium/TKN

Ammonium/TKN	Si (mg/l)	Ss (mg/l)	Xi (mg/l)	Xs (mg/l)	S_{NH} (mg/l)	S_{ND} (mg/l)	X_{ND} (mg/l)	S_{NO} (mg/l)
0.5	81	0.2	0	0.43	0.11	3.96	0.05	28.4
0.6	81	0.2	0	0.43	0.11	3.96	0.05	28.4
0.7	81	0.2	0	0.43	0.11	3.96	0.05	28.4
0.8	81	0.2	0	0.43	0.11	3.96	0.05	28.4
0.9	81	0.2	0	0.43	0.11	3.96	0.05	28.4

4.3.3 Kinetic and Stoichiometry Results

The main goal of the calibration process was to develop a model that accurately predicted plant performance. The calibration of the model involved adjusting certain key model parameters to minimize the error between the measured and predicted data. During calibration, the concentration of each substance modelled was compared to the equivalent concentration from the experimental data. Two alternative calibration approaches are commonly used for adjusting the model variables in GPS-X; (i) model independent variables can be adjusted automatically by GPS-X when performing a sensitivity analysis (ii) a manual analysis which involves adjusting one parameter at a time and then making a visual inspection of the graphical simulation results.

In the calibration of the PFBR the manual analysis option was chosen because before calibration was carried out the results were good. The calibration approach used involved adjusting the stoichiometric and kinetic parameters in GPS-X one at a time in the model and then making a visual inspection of the simulation results for COD_t, NH_4-N and NO_3-N. The main aim was to get a good match between measured and modelled COD_f, NH_4-N and NO_3-N. Numerous permutations were used in order to calibrate the model. It should be noted that there was probably over 1000 different variations modelled using the stoichiometric and kinetic parameters in GPS-X in order to get a reasonable match for the effluents COD_t, NH_4-N and NO_3-N. Some of these parameters were not overly sensitive to calibration but they were still tested in the manual calibration of the model.

The results of the sensitivity analyses indicated that the parameters most significant for calibration were μ_H, Y_A, μ_A, b_A, Y_H and b_H. A comparison between calibrated parameters and typical literature ranges are presented in Table 4.15.

Table 4.15 – Estimated and typical literature values for kinetic and stoichiometry coefficients (Mulas, 2005)

	Parameters (units)	Starting default in GPS-X	Literature ranges	Calibrated values
	Kinetic			
	Active Heterotrophic Biomass			
μ_H	heterotrophic maximum specific growth rate (d^{-1})	6	0.6-13.2	12
K_S	readily biodegradable substrate half saturation coefficient (mg COD/L)	20	5-225	20
K_{OH}	oxygen half saturation coefficient (mg O_2/L)	0.2	0.01-0.20	0.2
K_{NO}	nitrate half saturation coefficient (mg N/L)	0.5	0.1-0.5	0.5
η_g	anoxic growth factor	0.8	0.8	0.8
b_H	heterotrophic decay rate (d^{-1})	0.62	0.05-1.6	0.62
	Active Autotrophic Biomass			
μ_A	autotrophic maximum specific growth rate (d^{-1})	0.8	0.2-1.0	0.8
K_{NH}	ammonia half saturation coefficient for autotrophs growth (mg N/L)	1	1	1
b_A	autotrophic decay rate (d^{-1})	0.04	0.01-0.2	0.04
K_{OA}	oxygen half saturation coefficient for autotrophs growth (mg O_2/L)	0.4	0.4-2.0	0.4
	Hydrolysis			
k_h	maximum specific hydrolysis rate (d^{-1})	3	3	3
K_X	slowly biodegradable substrate half saturation coefficient (g COD/g COD)	0.03	0.03	0.03
η_h	anoxic hydrolysis factor	0.4	0.4	0.4
	Ammonification			
k_a	ammonification rate m^3/g COD/d	0.08	0.08	0.08
	Model Stoichiometry			
fp	fraction of biomass leading to particulate products (g COD/g COD)	0.08	0.08	0.08
Y_H	heterotrophic yield (g COD/g COD)	0.666	0.38-0.75	0.666
Y_A	autotrophic yield (g COD/g N)	0.24	0.07-0.28	0.25

4.3.4 Measured and Modelled Results

The results shown in Table 4.16 show that there is strong agreement between measured and modelled results both for the calibrated model (Study 1) and for Study 2 (which was

used to validate the model). The average measured removal efficiency for COD_t was 93% and 86% for Study 1 and Study 2 respectively. This compared well with a modelled removal efficiency of 92% and 90% for Study 1 and Study 2 respectively. The removal efficiency for TN_t was 74% and modelled 78% for Study 1 and measured was 58% and modelled 61% for Study 2. Similarly good agreement between measured and predicted waste treatment efficiency was observed for NH_4-N (84% and 87% for measured and predicted removal efficiency in Study 1, and 98% and 95% for measured and predicted removal efficiency in Study 2). It is important to note that the soluble results from GPS-X are compared to the filtered results from measured analysis. This is acceptable as the soluble components are a close approximation of what would be obtained from a filtered sample (Snowling, 2014). There are no standard deviation results presented for the model results, this applies to the thesis as a whole.

Table 4.16 – Measured and modelled results for Study 1 and Study 2. Standard deviations shown in ()

	Study 1				**Study 2**			
	Measured (average of a 100-day study)		Model		Measured (average of a 100-day study)		Model	
(mg/l)	Effluent	Removal efficiency (%)	Effluent	Removal efficiency (%)	Effluent	Removal efficiency (%)	Effluent	Removal efficiency (%)
COD_t	76 (20)	93	85	92	40 (32)	86	34	90
TSS	10 (6)	-	16	-	3 (3)	-	1	-
TN_t	25 (7)	74	21	78	14 (6)	58	13	61
NH_4-N	10 (8)	84	8	87	0.4 (1)	98	0.5	95
NO_3-N	12 (5)	-	11	-	13 (3)	-	9	-

Figures 4.7 to 4.14 show the relationships between the modelled daily, measured daily, model average and measured average COD_t, TSS, TN_t, NH_4-N and NO_3-N concentrations for Study 1 and 2. In all cases, the modelled profiles were close to the measured data for both Study 1 and 2. The results shown in Table 4.16 and Figures 4.7 to 4.14 indicate that the model could be used to predict effluent concentrations using different wastewater strengths in a laboratory environment. A full set of model results for Study 1 and Study 2 are given in Appendix H.

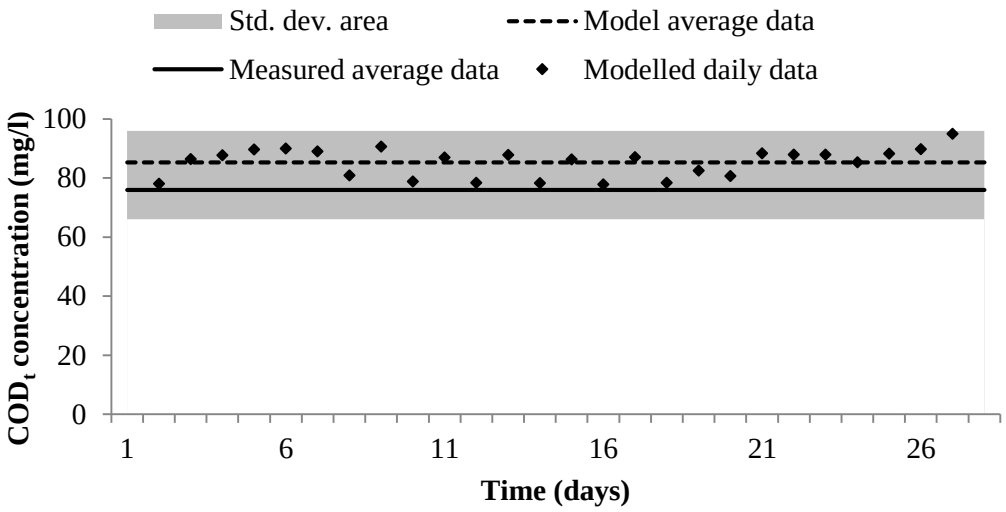

Figure 4.7 – Study 1 modelled and measured effluent COD_t. The area shaded grey indicates the upper and lower bounds of the measured standard deviation.

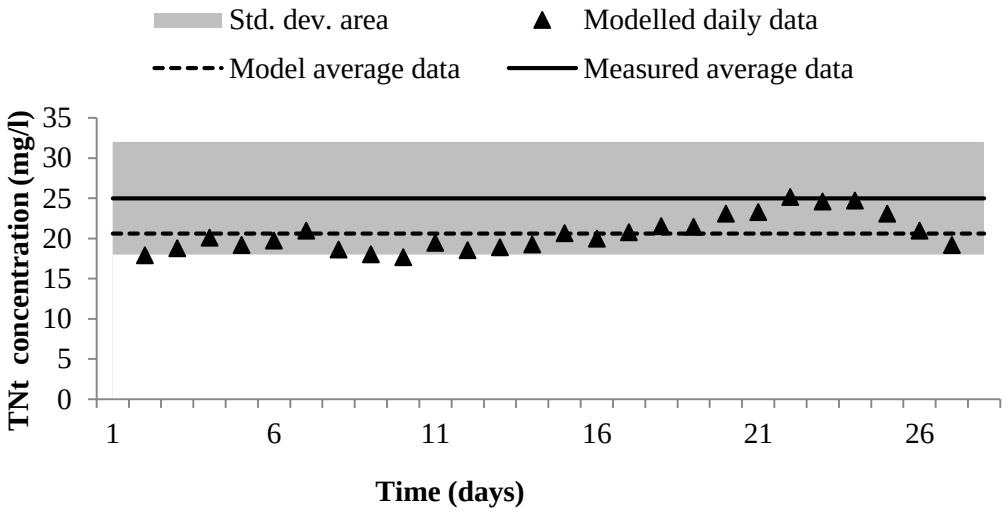

Figure 4.8 – Study 1 modelled and measured effluent TN_t

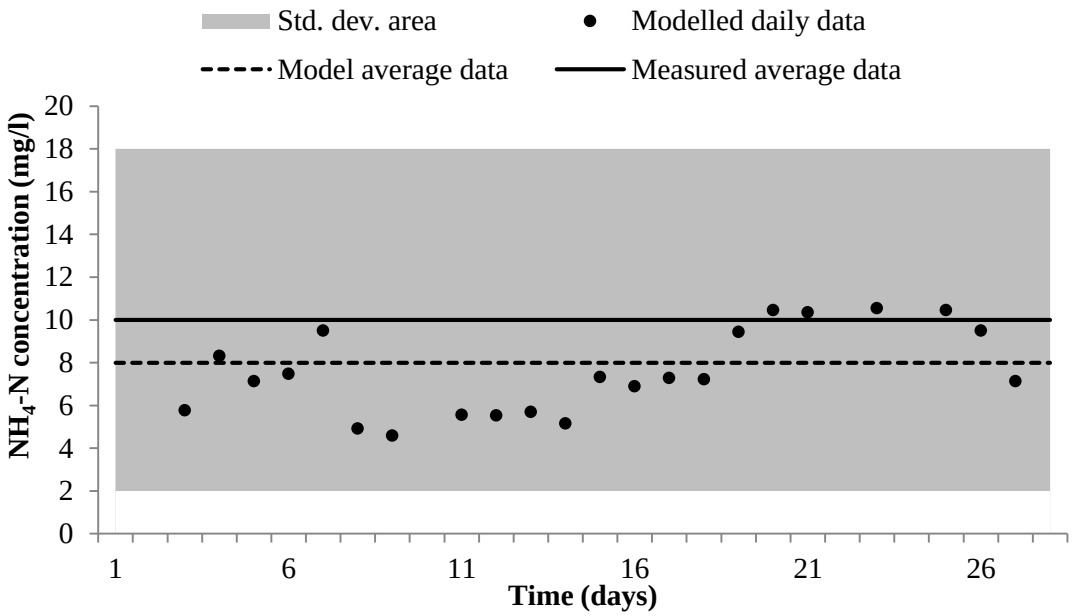

Figure 4.9 – Study 1 modelled and measured effluent NH_4-N

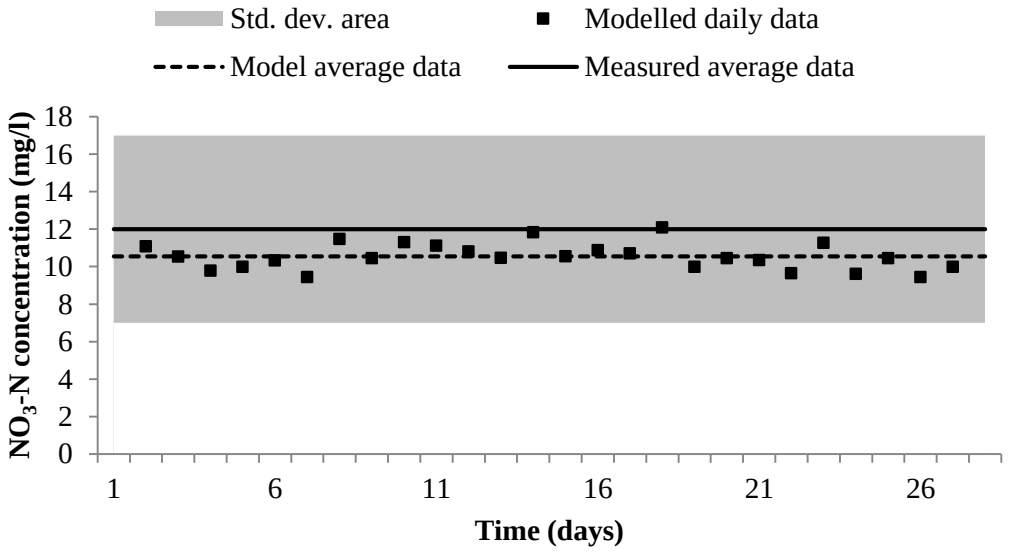

Figure 4.10 – Study 1 modelled and measured effluent NO_3-N

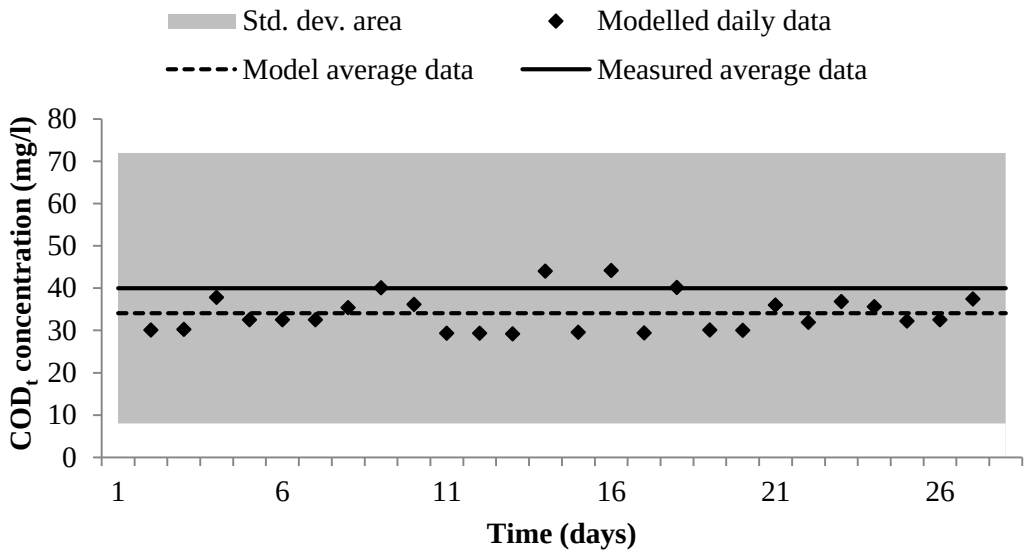

Figure 4.11 – Study 2 modelled and measured effluent COD_t

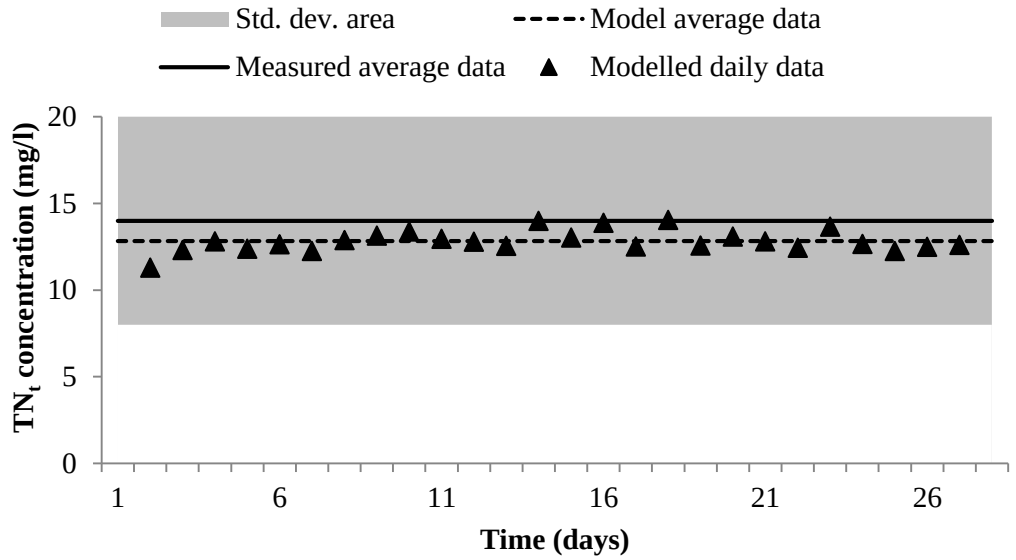

Figure 4.12 – Study 2 modelled and measured effluent TN_t

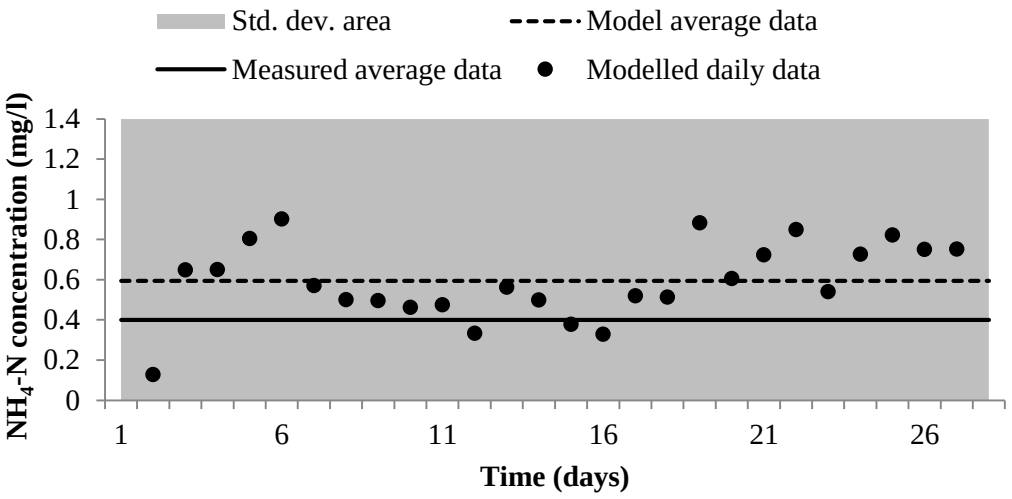

Figure 4.13 – Study 2 modelled and measured effluent NH_4-N

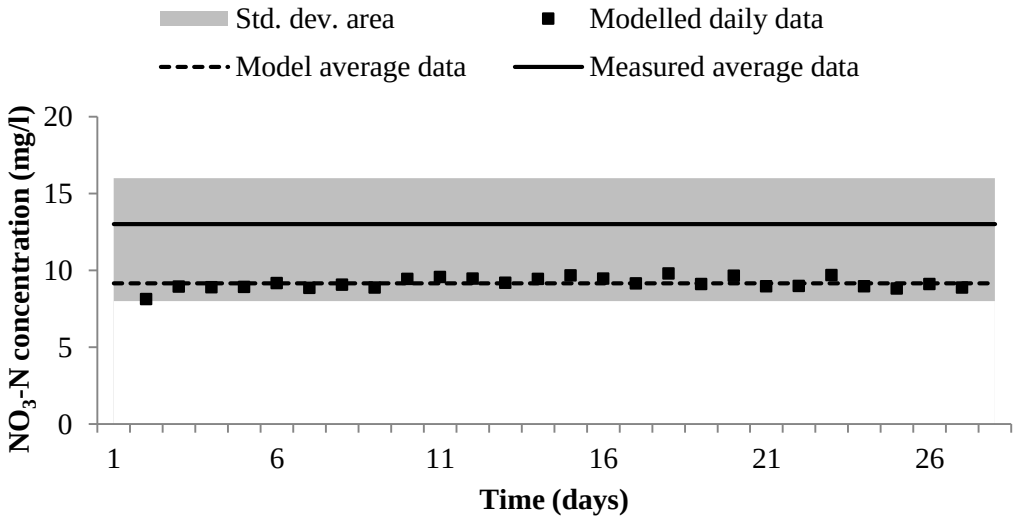

Figure 4.14 – Study 2 modelled and measured effluent NO_3-N

A statistical analysis was carried out on Study 1 between modelled and measured effluent results for COD_t, TN_t, NH_4-N and NO_3-N. An 'Anova analysis F-Test' was used to compare the removal efficiency of the modelled and measured results with a confidence interval of 95 %. COD_t comparisons gave an F ratio of 0.06 and an F critical value of 0.45 at α =0.05. TN_t comparisons gave an F ratio of 0.09 and an F critical value of 0.45 at α =0.05. NH_4-N comparisons gave an F ratio of 0.07 and an F critical value of 0.45 at α =0.05. NO_3-N comparisons gave an F ratio of 0.02 and an F critical value of 0.45 at α

=0.05. As F < F critical, there is no evidence of significant difference between the variances of two populations.

Experimental phase studies for nitrogen were undertaken during Study 2 and this data was used to further validate the model. There was no carbon or nitrogen phase study data available for Study 1 or carbon or DO phase study data for Study 2.

The steady state nitrogen profile results for Study 2 are shown in Figure 4.15, which shows the concentrations from equivalent times during the phase study and the model. During the anoxic phase, as expected, NH_4-N concentrations remained relatively constant. Denitrification was most likely observed as evidence in both experimental and modelled results by reducing NO_3-N concentrations during the anoxic phase. Ideally total nitrogen and organic carbon (alongside dissolved oxygen, pH and nitrous oxide emissions) could be measured to confirm this, however this data was not available. NH_4-N concentrations rapidly decreased during the aerobic phase, which was due to the supply of oxygen (Figure 4.16) that allowed the nitrifying bacteria to oxidise the NH_4-N to NO_3-N. The NH_4-N and NO_3-N modelled profiles were close to the experimental data.

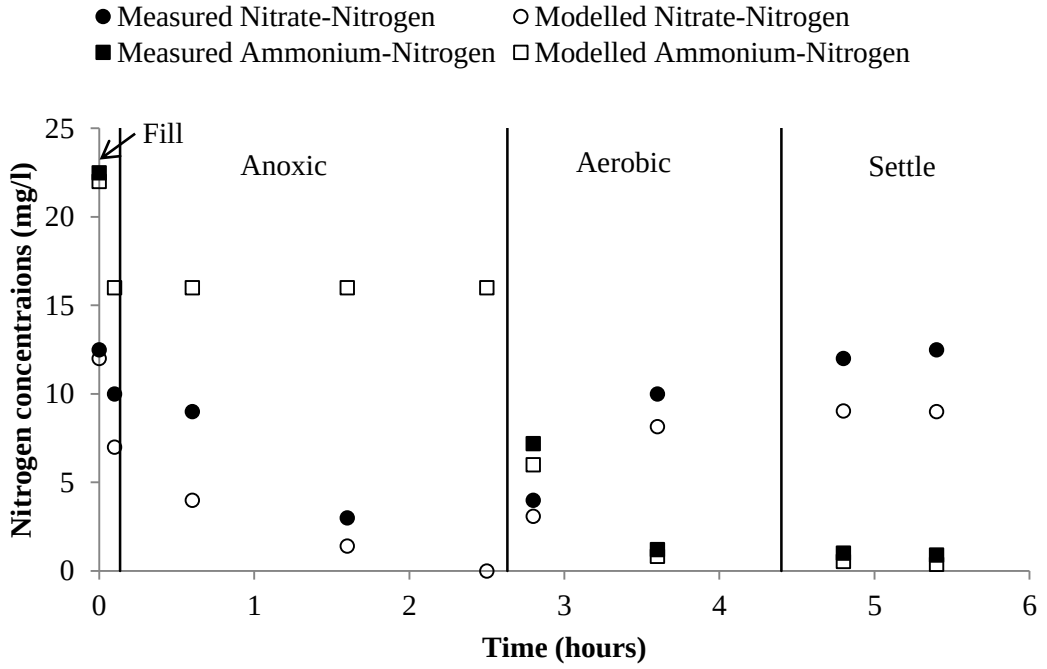

Figure 4.15 – Nitrogen profiles for Phase Study 2 during a typical treatment cycle. There was no data available for NH_4-N concentrations during the anoxic phase.

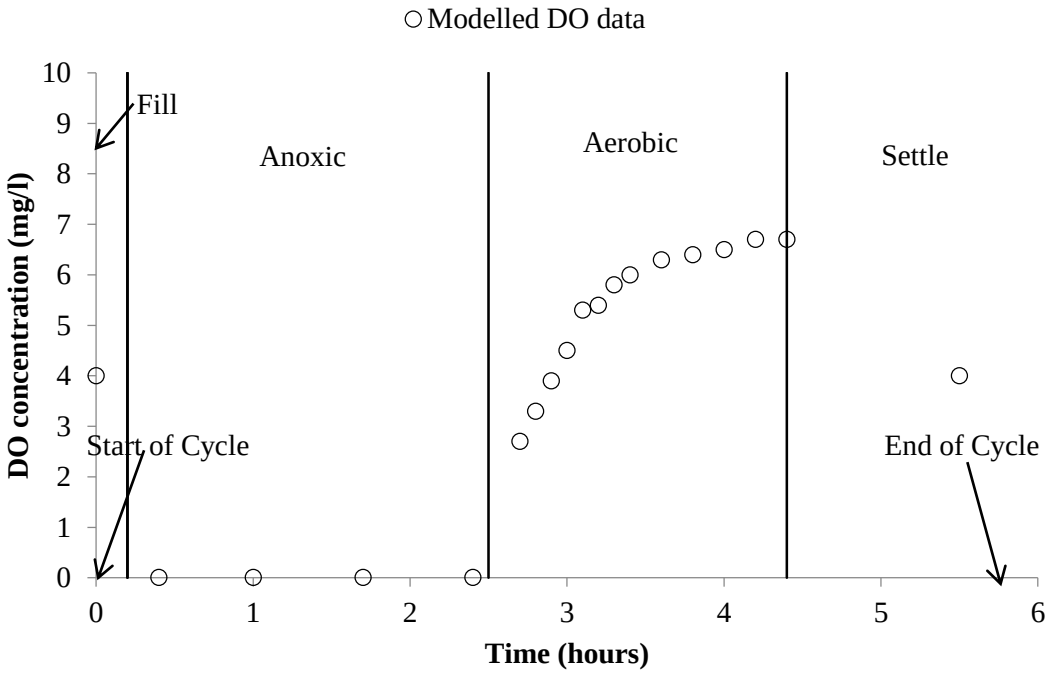

Figure 4.16 – Modelled DO data for one aerobic cycle during Study 2

As mentioned previously there were no phase study data for carbon in either Study 1 or 2. However COD_t would likely have been predicted correctly had there been phase study data as there was very good predictions from the model for the average effluent COD_t concentrations in both Study 1 and Study 2.

The results shown in Table 4.16 and Figure 4.15 indicate that the model could be used to predict both cycle performance and effluent concentrations using different wastewater strengths in a laboratory environment.

4.4 CONCLUSIONS

It was difficult to model the PFBR in GPS-X as a number of process objects and models were built and tested in order to try to calibrate the LS-PFBR. It was very time consuming and problematic to set up the hydraulics of the PFBR in the model. It was also challenging to get the passive aeration process working. However, once the PBFR model was built, it was quick and easy to calibrate and validate the model.

In this chapter, a model for the LS-PFBR was developed using GPS-X. The model was calibrated and validated using experimental data from a laboratory-based PFBR. The

model was initially calibrated from experimental data, where a high strength synthetic wastewater was treated by the PFBR unit. It was then validated against an independent study using a low strength synthetic wastewater. The main conclusions of the study are as follows:

1. A model of the laboratory scale batch biofilm passive aeration process – the PFBR – was successfully calibrated using a surrogate-activated sludge process object in GPS-X to model the PFBR. The model was calibrated using experimental data and then validated using independent experimental data from the PFBR.
2. The model successfully predicted
   (i) effluent characteristics for carbon and nitrogen;
   (ii) individual treatment cycles for nitrogen.

5 MODELLING THE FIELD-SCALE PFBR (FS-PFBR1) USING GPS-X

5.1 INTRODUCTION

This chapter investigates the potential for (i) modelling FS-PFBR1 using the activated sludge model developed in Chapter 4, (ii) predicting effluent results and contaminant concentration changes during individual treatment cycles, and (iii) using the calibrated model to predict the optimal operational regimes, i.e. meeting regulatory requirements while minimising energy costs.

A major challenge often encountered when modelling on-site systems can be the lack of sufficient operation and performance data from such systems. In Chapter 4 the calibration of the LS-PFBR was carried out using data from specific and well-controlled experiments at laboratory scale assuming constant operating conditions. The values obtained in such a way may not be totally reliable as it is difficult to configure and operate a small-scale plant in exactly the same way as a full-scale plant (Jeppsson, 1996). There were significant differences between the operating conditions and plant configurations of LS-PFBR and FS-PRBR, including: (i) influent wastewater composition, (ii) DO and (iii) the correct measurement or prediction of the K_La value for the field-scale models.

The FS-PFBR1 model was developed and calibrated using data from a field study with two cycle regimes, Study 3 and Study 4.

5.2 MODEL DEVELOPMENT

5.2.1 Modelling Description

The methodology used and applied to the development of a model for FS-PFBR1 was based on the series of generic steps shown in Figure 4.1 and as described in *Section 4.2.1*.

FS-PFBR1 operated under two cycle regimes (Study 3 and 4). In each study, a typical treatment cycle comprised fill, anoxic, aerobic and settle stages of varying lengths (as described in *Section 3.3.3*). Table 5.1 describes the models that were built and calibrated in this study.

Table 5.1 – Model descriptions

	Study 3	Study 3	Study 4	Study 4
PFBR operation	Steady-state system operation (average of 48 days)	Phase study 432 minutes (1 PFBR cycle)	Steady state system operation (average of 34 days)	Phase study 452 minutes (1 PFBR cycle)
Model Name	Study 3AS	Study 3PS	Study 4AS	Study 4PS

A model was initially developed and calibrated for Study 3AS and then applied to Study 4AS. In order to validate the model, the phase study data from Study 3PS and Study 4PS were applied to it. ASM1 was chosen to calibrate the FS-PFBR1 as the model was concerned with COD and N removal only.

FS-PFBR1 was operated under two cycle regimes (Study 3 and Study 4). The treatment cycle comprised anoxic, aerobic and settle stages of varying lengths (as described in *Section 3.5.2*) (Table 5.2).

Table 5.2 – Operational stages of FS-PFBR1

PFBR stage	Study 3 duration (minutes)	Study 4 duration (minutes)
Fill (t_1)	4	6
Anoxic (t_2)	134	60
Aerobic (t_3)	275	360
Settle (t_4)	14	30
Draw (t_5)	4	6
Total cycle time	431	462
No. of aerobic cycles	5	8

5.2.2 System characteristics and hydraulics

Similar to the laboratory-scale model, the initial work focused on developing a model that could accurately represent the hydraulic characteristics of FS-PFBR1. The layout of FS-PFBR1 in GPS-X was the same as the LS-PFBR (as described in *Chapter 4*); however, the eight input control files were adjusted to simulate the operational conditions of FS-PFBR1. The input control files used for Study 3 and Study 4 are shown in Tables 5.3 and 5.4.

Table 5.3 – Input control files and times for one complete cycle in Study 3

			Influent	Mixing on/off R1	K_La R1	Mixing on/off R2	Pump 1	K_La R2	Pump2	Discharge
		t	qinrawinf	mixconzover1	klaconzover1	mixconzover2	qinzpump1	klaconzover2	qconzpump2	frzpump2toeff
		min	m^3/min		d^{-1}		m^3/min	d^{-1}	m^3/min	
Fill		1-4	*1.5	**1	0	0	0	0	0	0
Anoxic		5-138	0	0	0	0	0	0	0	0
Aerobic	**Transfer to R2**	139	0	0	0	1	****8	122	0	0
	Aerobic R2	140-166	0	0	0	0	0	122	0	0
	Transfer to R1	167	0	1	***122	0	0	0	8	0
	Aerobic R1	168-194	0	0	122	0	0	0	0	0
	Transfer to R2	195	0	0	0	1	8	122	0	0
	Aerobic R2	196-222	0	0	0	0	0	122	0	0
	Transfer to R1	223	0	1	122	0	0	0	8	0
	Aerobic R1	224-250	0	0	122	0	0	0	0	0
			The aerobic sequence and recycling between R1 and R2 continued for 275 minutes							
Settle		413	0	0	0	0	0	0	0	0
Draw		431	0	0	0	0	0	0	8	0.75

* The average volume/cycle for Study 3 was 8 m^3. At the start of a cycle, there was 2 m^3 in R1 so 6 m^3 was required to fill the tank. A flow of 1.5 m^3/min for 4 minutes, which equates to 6 m^3, was used to fill the tank to 8 m^3.

** The number 1 was used as this turned on the mixing in R1.

*** This is the K_La value used.

**** This is the total volume of wastewater in the reactors, 8 m^3.

***** At the end of each cycle, 6 m^3 of wastewater was decanted and 2 m^3 was recycled back to R1 in preparation for the next treatment cycle. 0.75 is the percentage of wastewater recycled back to R1.

Table 5.4 – Input control files and times for one complete cycle in Study 4

			Influent	Mixing on/off R1	K_La R1	Mixing on/off R2	Pump 1	K_La R2	Pump2	Discharge
		t	qinrawinf	mixconzover1	klaconzover1	mixconzover2	qinzpump1	klaconzover2	qconzpump2	frzpump2toeff
		min	m^3/min		d^{-1}		m^3/min	d^{-1}	m^3/min	
Fill		1-6	*0.75	**1	0	0	0	0	0	0
Anoxic		7-66	0	0	0	0	0	0	0	0
Aerobic	**Transfer to R2**	67	0	0	0	1	****8	122	0	0
	Aerobic R2	68-88	0	0	0	0	0	122	0	0
	Transfer to R1	89	0	1	***122	0	0	0	8	0
	Aerobic R1	90-110	0	0	122	0	0	0	0	0
	Transfer to R2	111	0	0	0	1	8	122	0	0
	Aerobic R2	112-132	0	0	0	0	0	122	0	0
	Transfer to R1	133	0	1	122	0	0	0	8	0
	Aerobic R1	134-154	0	0	122	0	0	0	0	0
			The aerobic sequence and recycling between R1 and R2 continued for 360 minutes							
Settle		430	0	0	0	0	0	0	0	0
Draw		462	0	0	0	0	0	0	8	0.75

* The average volume/cycle for Study 4 was 8 m^3. At the start of a cycle, there was 2 m^3 in R1 so 6 m^3 was required to fill the tank. A flow of 0.75 m^3/min for 8 minutes, which equates to 6 m^3, was used to fill the tank to 8 m^3.

** The number 1 was used as this turned on the mixing in R1.

*** This is the K_La value used.

**** This is the total volume of wastewater in the reactors, 8 m^3.

***** At the end of each cycle, 6 m^3 of wastewater was decanted and 2 m^3 was recycled back to R1 in preparation for the next treatment cycle. 0.75 is the percentage of wastewater recycled back to R1.

Table 5.5 shows the physical dimensions of the SBR reactors used in FS-PFBR1.

Table 5.5 – Physical design parameters (measured and modelled)

Physical dimensions	Size
Surface area of tanks	6 m^2
Maximum water level height	3.4 m

The average volume of wastewater treated per cycle for each of Study 3 and Study 4 was 8 m^3. The influent and discharge profiles and transfer flow profiles between R1 and R2 during a typical treatment cycle for Study 3 and Study 4 are shown in Figure 5.1 and 5.2 respectively.

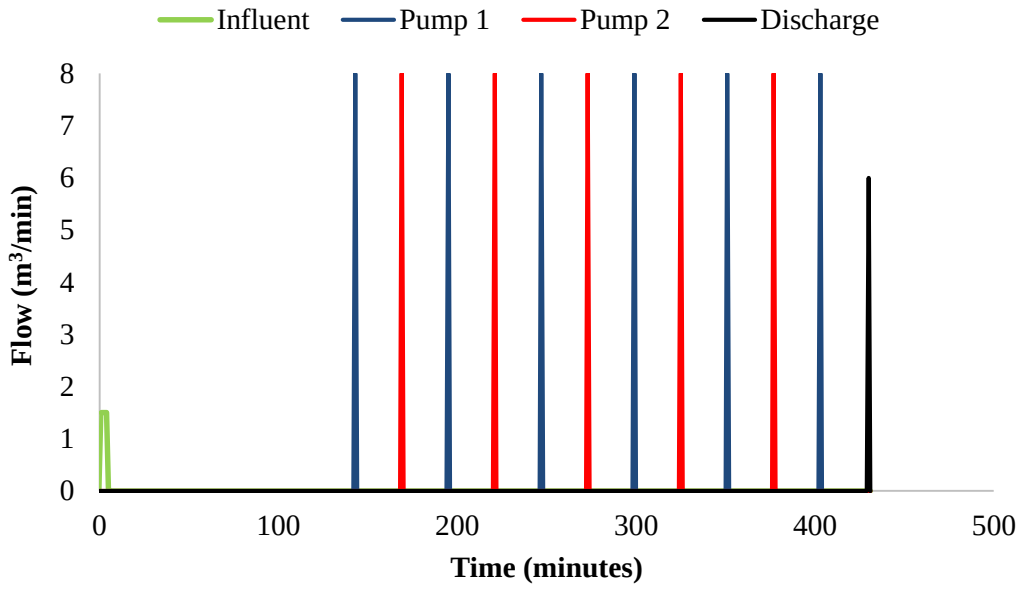

Figure 5.1 – Influent and discharge profiles and transfer flow profiles between R1 and R2 during a typical treatment cycle for Study 3

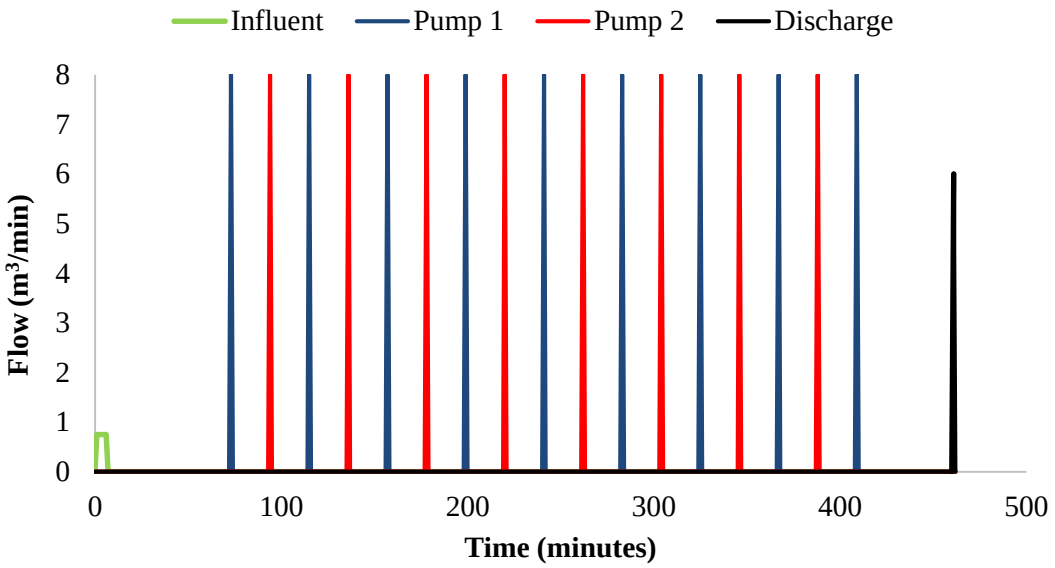

Figure 5.2 – Influent and discharge profiles and transfer flow profiles between R1 and R2 during a typical treatment cycle for Study 4

5.2.3 Wastewater Characteristics

The influent wastewater for both Study 3 and Study 4 comprised municipal wastewater (described in *Section 3.3.4*). Influent characteristics were reasonably consistent, and thus the system was modelled in steady-state mode (i.e. using average influent concentrations during the experimental period). Using Influent Advisor in GPS-X and the measured influent characteristics, a detailed overview of the influent was developed for the model (Table 5.6) (only non-zero components are shown). The full influent composition developed in influent advisor is shown in Appendix E).

Table 5.6 – Influent composition modelled using influent advisor in GPS-X

Parameters	Units	Study 3		Study 4	
Biological Model: ASM1		Measured	Modelled	Measured	Modelled
Influent Composition					
filtered COD	g COD/m^3	187	186	144	146
particulate COD	g COD/m^3		76		164
total suspended solids	g/m^3		90		73
total nitrogen	g N/m^3		40		40
Nitrogen Compounds					
free and ionized ammonia	g N/m^3	34	34	32	32
Alkalinity					
alkalinity	mole/m^3		7		7
Influent Fractions					
XCOD/VSS ratio	g COD/g VSS		1.4		2.25
$BOD_5/BOD_{ultimate}$ ratio	-		0.66		0.66
TSSCOD Model Coefficients					
inert fraction of soluble COD	-		0.3		0.2
substrate fraction of particulate COD	-		0.82		0.82
heterotrophic fraction of particulate COD	-		0		0
ammonium/TKN ratio	-		0.85		0.8
particulate organic N/total organic N ratio	-		0.15		0.9
VSS/TSS ratio	g VSS/g TSS		0.6		1
ASM1 Nutrient Fractions					
N content of active biomass	g N/g COD		0.086		0.086
N content of endogenous/inert mass	g N/g COD		0.06		0.06

5.3 RESULTS AND DISCUSSION

5.3.1 Dissolved Oxygen

In the model, the K_La value of 122 d^{-1} was used for the laboratory and field-scale models; according to Garcia-Ochoa & Gomez (2009) and Ouellette (2011), scale up in bioreactors is often performed on the basis of keeping the K_La constant. A K_La value of 122 d^{-1} was used to model FS-PFBR1. Figure 5.3 shows the modelled and measured DO data for one aerobic cycle during Study 4.

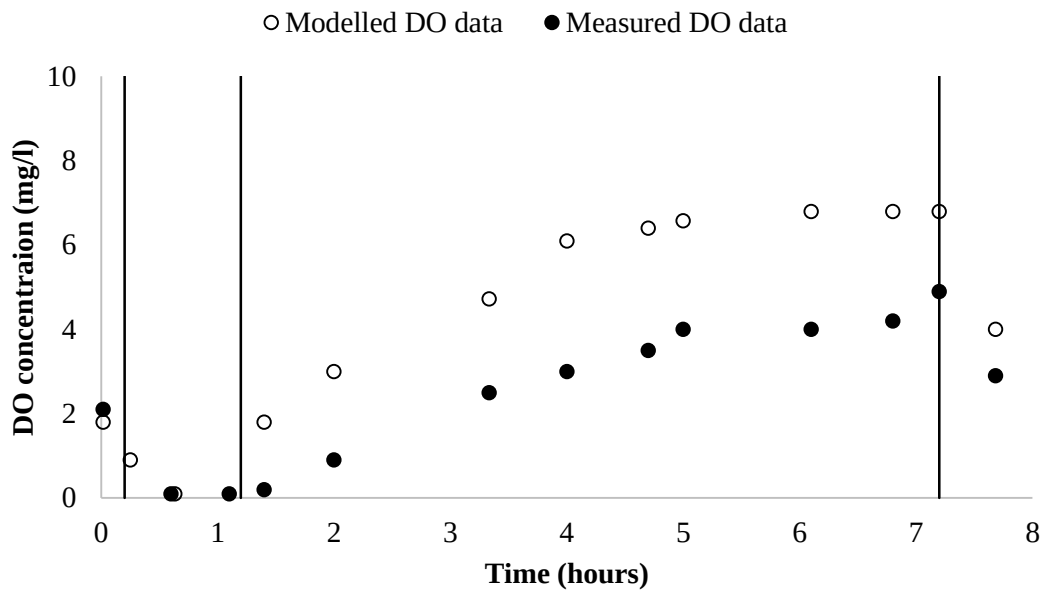

Figure 5.3 – Modelled and measured DO data for one aerobic cycle during Study 4

The model was run to ensure that oxygen profiles from experimental and modelled data correlated well however it is evident from Figure 5.3 that there was not an exact match between the modelled and measured DO concentrations when using a K_La value of 122 d^{-1}. Hence a number of simulations were run in the model to determine the effect that the K_La value had on effluent concentrations.

Five model simulations were carried out on Study 4 that compared K_La values (10 d^{-1}, 50 d^{-1}, 100 d^{-1}, 122 d^{-1} and 200 d^{-1}) against the measured effluent COD_f, NH_4-N and NO_3-N concentrations. It is interesting to note that while the K_La value had an impact on the DO concentrations (Figure 8.3) in the model, it did not have a huge bearing on the effluent parameter concentrations once K_La value was above 50d^{-1} and once calibration was carried out and the stoichiometric and kinetic parameters were adjusted to meet the

measured effluent data (Table 8.1). It is important to note that the previously calibrated values for LS-PFBR were adjusted to calibrate FS-PFBR1. These simulations are discussed in detail in Chapter 8. For the purpose of this study, the K_La value remained at the measured value of 122 d^{-1} in the model as it was found not to have a significant bearing on effluent concentrations once calibration was carried out correctly. Also there was no site data available to characterise this.

5.3.2 Kinetic and Stoichiometry Results

Initially the calibrated kinetic and stoichiometric parameters from LS-PFBR (as described in *Section 4.3.1*) were applied to this model FS-PFBR1. However, the modelled effluent data did not accurately match the measured effluent data from the field-scale studies.

The initial model run showed that COD_f was over estimated. In order to increase the accuracy of the model Y_H and μ_H were increased which in turn led to an increase in heterotrophic biomass and therefore an increase in COD_f removal.

The NH_4-N was also over estimated in the model and therefore further work was necessary to refine the model. The autotrophic growth rate adjusted from 0.8 d^{-1} to 1 d^{-1}. This increase in μA led to an increase in autotrophic biomass and therefore an increase in ammonium removal.

The kinetic and stoichiometric parameters that were most significant for calibration of the LS-PFBR were adjusted manually, and the modelled results were checked in terms of how close they were to the measured values. The parameters were adjusted until the measured and modelled data correlated well. Minimal adjustments to the model parameters were required to calibrate the model. The most important parameters for the calibration of the FS-PFBR1 were the heterotopic and autotrophic growth rates and the heterotrophic yield. In order to calibrate the FS-PFBR1 model, the following adjustments to the kinetic and stoichiometric parameters were necessary (Table 5.7).

Table 5.7 – Differences in stoichiometric and kinetic model parameters between LS-PFBR and FS-PFBR1

Parameters(units)	LS-PFBR	FS-PFBR1
Heterotrophic maximum specific growth rate (d^{-1})	12	13.2
Autotrophic maximum specific growth rate (d^{-1})	0.8	1.0
Heterotrophic yield (g COD/g COD)	0.666	0.75

The comparison between calibrated parameters and typical literature ranges are presented in Table 5.8.

Table 5.8 – Estimated and typical literature values for kinetic and stoichiometry coefficients (Mulas, 2005)

Symbol	Parameters (units)	Starting defaults in GPS-X	Literature ranges	Calibrated values
	Kinetic			
	Active Heterotrophic Biomass			
μ_H	heterotrophic maximum specific growth rate (d^{-1})	6	0.6-13.2	13.2
K_S	readily biodegradable substrate half saturation coefficient (mg COD/L)	20	5-225	20
K_{OH}	oxygen half saturation coefficient (mg O_2/L)	0.2	0.01-0.20	0.2
K_{NO}	nitrate half saturation coefficient (mg N/L)	0.5	0.1-0.5	0.5
η_g	anoxic growth factor	0.8	0.8	0.8
b_H	heterotrophic decay rate (d^{-1})	0.62	0.05-1.6	0.62
	Active Autotrophic Biomass			
μ_A	autotrophic maximum specific growth rate (d^{-1})	0.8	0.2-1.0	1.0
K_{NH}	ammonia half saturation coefficient for autotrophs growth (mg N/L)	1	1	1
b_A	autotrophic decay rate (d^{-1})	0.04	0.01-0.2	0.02
K_{OA}	oxygen half saturation coefficient for autotrophs growth (mg O_2/L)	0.4	0.4-2.0	0.4
	Hydrolysis			
k_h	maximum specific hydrolysis rate (d^{-1})	3	3	3
K_X	slowly biodegradable substrate half saturation coefficient (g COD/g COD)	0.03	0.03	0.03
η_h	anoxic hydrolysis factor	0.4	0.4	0.4
	Ammonification			
k_a	ammonification rate (m^3/g COD/d)	0.08	0.08	0.08
	Model Stoichiometry			
fp	fraction of biomass leading to particulate products (g COD/g COD)	0.08	0.08	0.08
Y_H	Heterotrophic yield (g COD/g COD)	0.666	0.38-0.75	0.75
Y_A	Autotrophic yield (g COD/g N)	0.24	0.07-0.28	0.24

The calibration of the FS-PFBR1 corresponded with the literature ranges as only a number of key parameters needed to be changed to ensure model calibration (Hauduc et al., 2011).

5.3.3 Experimental and Modelled Results

5.3.3.1 Study 3AS and Study 4AS

A model was initially developed and calibrated for Study 3AS and then applied to Study 4AS. In order to validate the model, the phase study data from Study 3PS and Study 4PS were applied to it. A full set of model results are shown in Appendix I and key results are described below.

There is trade off in calibration between accuracy and changing parameters. It is important to try to not 'over fit' measured and modelled data results. It is preferable to fit most of the measured variables reasonably rather than fitting them perfectly to one selected component concentration and poorly to the others. One also needs to identify the key parameters you want to model. It is not necessary to exactly match modelled and measured data, this is because standard deviation allows for deviation in model results. The standard deviation for the measured data is included in Table 5.9 and shown in the shaded grey area in Figures 5.5 to 5.10.

Table 5.9 summarises the measured and modelled results for Study 3AS and Study 4AS. The average measured removal efficiency for COD_f was 65% and 77% for Study 3AS and 4AS respectively. This compared well with a modelled removal efficiency of 69% and 78% for Study 3AS and 4AS. Similarly, acceptable agreement between measured and predicted wastewater treatment efficiency was observed for NH_4-N.

Table 5.9 – Measured and modelled results for Study 3 and Study 4. Standard deviations shown in ()

	Study 3AS				Study 4AS			
	Measured steady state system operation (average of 48 days)		Modelled		Measured steady state system operation (average of 34 days)		Modelled	
(mg/l)	Effluent	Removal efficiency (%)	Effluent	Removal efficiency (%)	Effluent	Removal efficiency (%)	Effluent	Removal efficiency (%)
COD_f	66 (13)	65	58	69	33 (10)	77	31	78
NH_4-N	26 (5)	24	26	24	12 (6)	63	10	65
NO_3-N	0.95 (0.5)	-	0.4	-	1 (1)	-	1.3	-

During Study 3AS the average measured DO concentrations remained lower throughout the treatment cycle than in Study 4AS with an average of 2.5 mg/l in the bulk fluid by the end of the treatment cycle compared to 3.9mg/l in Study 4AS (Figure 5.4). The increase in DO in Study 4AS can be attributed to additional aeration time and the fact that the bulk fluid was transferred between the reactors 8 times in Study 4AS compared to 5 times in Study 3AS (Table 5.2).

In Study 4AS, the additional DO resulted in an increase in nitrification efficiency. Limited NO_3-N was evident in the effluent during Study 3AS, where average DO concentrations were lower during the aeration stage than in Study 4AS.

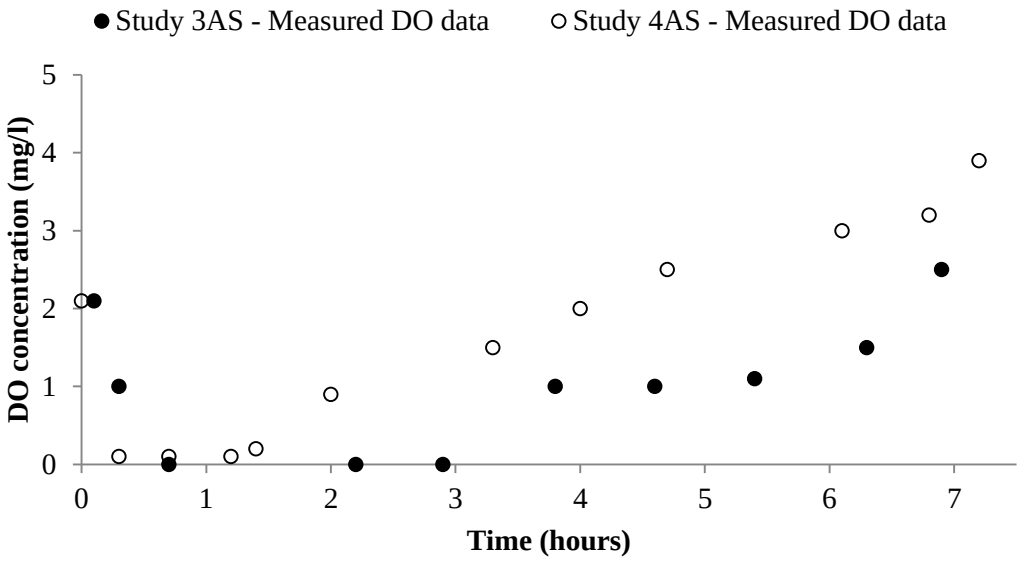

Figure 5.4 –Measured DO data for one aerobic cycle during Study 3 and Study 4

Efficient NH_4-N removal was achieved in Study 4AS, with an average removal efficiency of 65% gained. The modelled results are close to experimental data for the three parameters tested. It was difficult to determine whether denitrification occurred or not as there was no total nitrogen data available. However, it might be reasonable to assume that some denitrification did occur due to the high NH_4-N removal rates and the relatively low NO_3-N concentrations in the effluent.

Figures 5.5 to 5.10 show the relationship between the modelled daily data, measured daily data, model average data and measured average data for COD_f, NH_4-N and NO_3-N for Study's 3AS and Study 4AS.

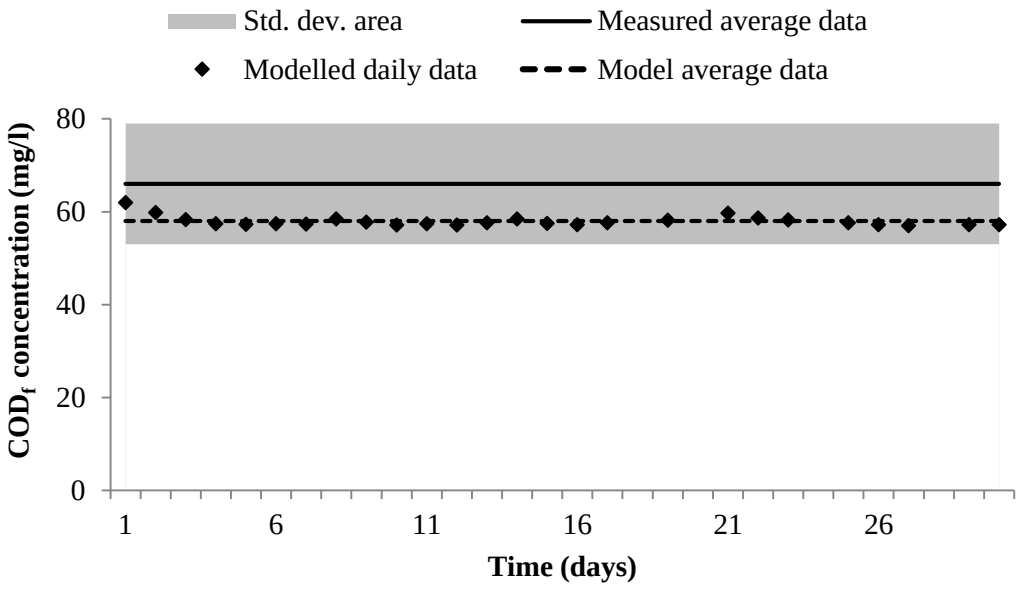

Figure 5.5 – Study 3AS modelled and measured effluent COD_f. The area shaded grey indicates the upper and lower bounds of the measured standard deviation.

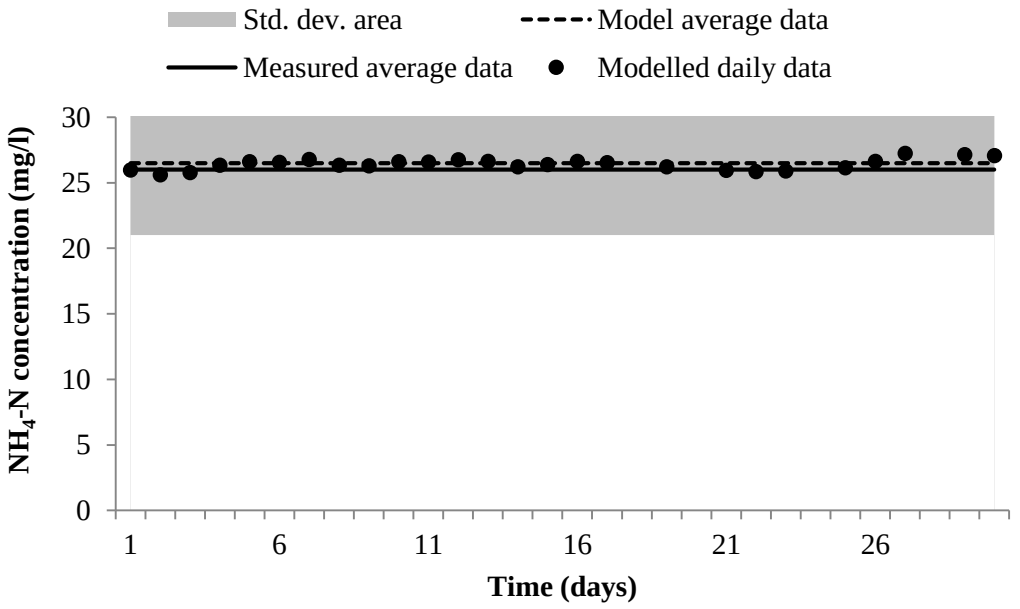

Figure 5.6 – Study 3AS modelled and measured effluent NH_4-N

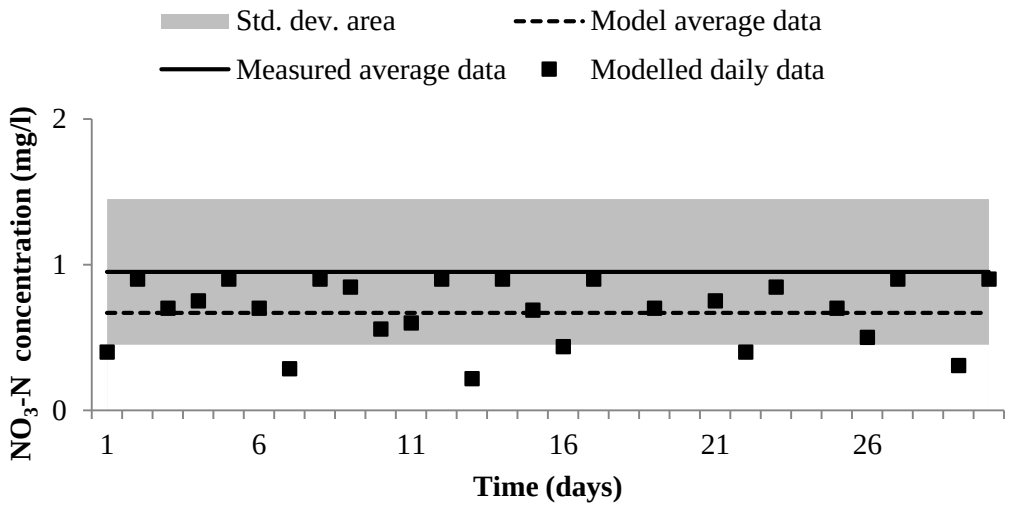

Figure 5.7 – Study 3AS modelled and measured effluent NO_3-N

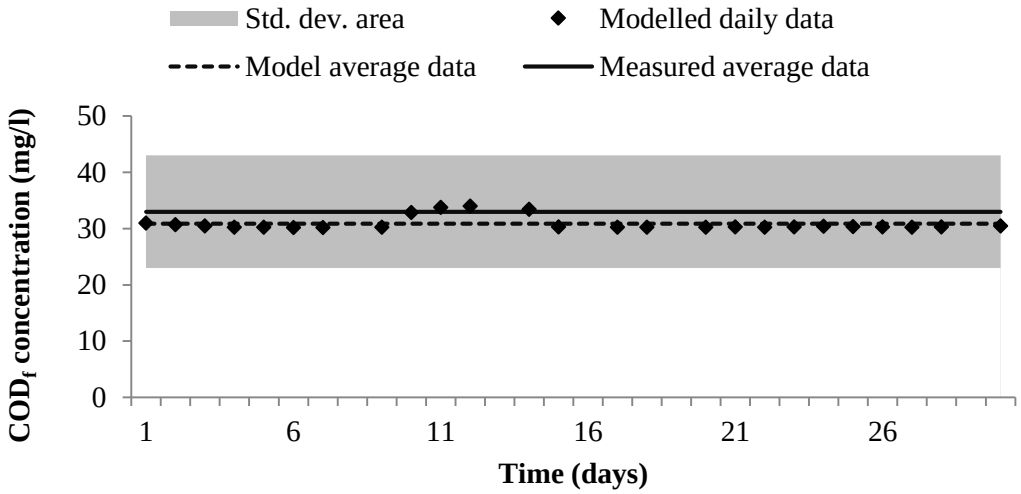

Figure 5.8 – Study 4AS modelled and measured effluent COD_f

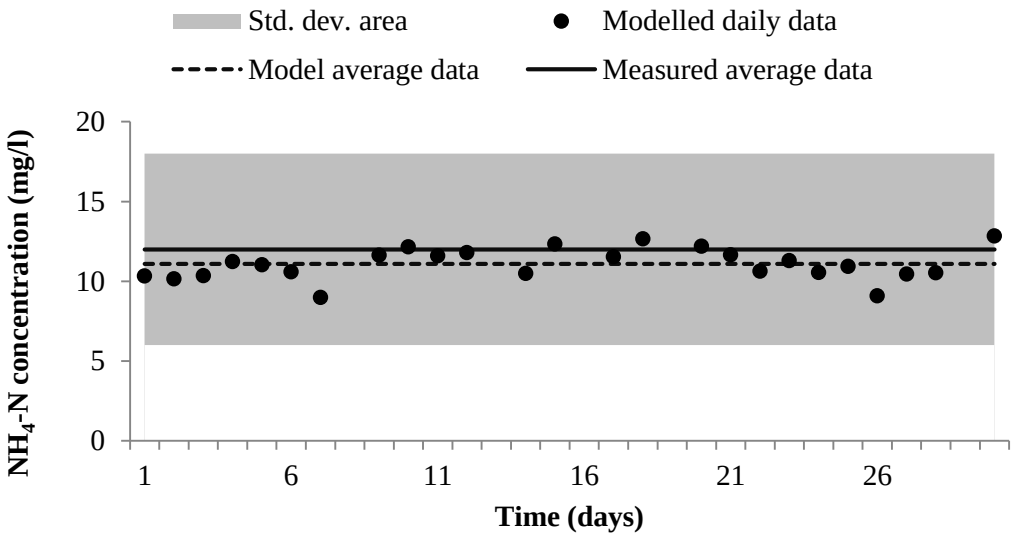

Figure 5.9 – Study 4AS modelled and measured effluent NH_4–N

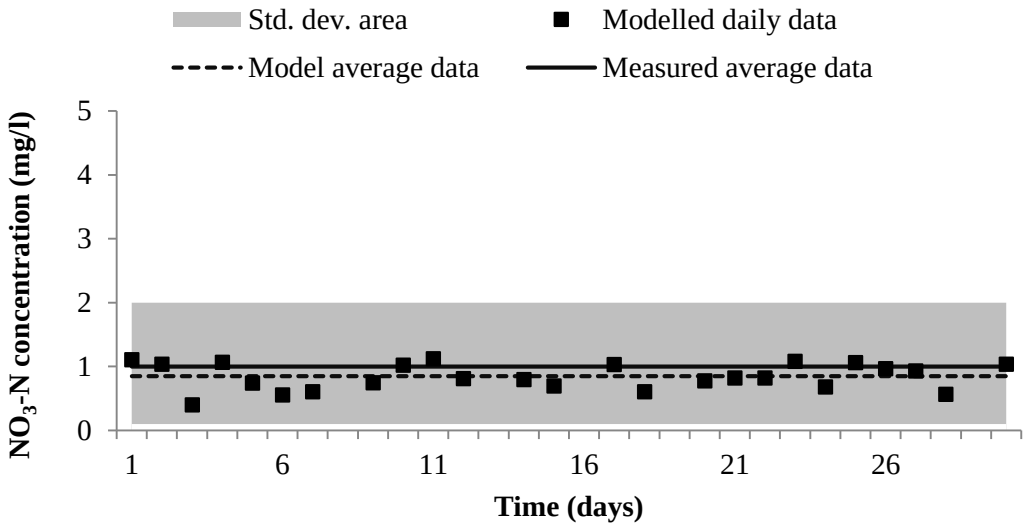

Figure 5.10 – Study 4AS modelled and measured effluent NO_3–N

A single factor Anova analysis F-Test of COD_f, NH_4-N and NO_3-N was carried out on Study 3 and Study 4 between modelled and measured results. In Study 3 COD_t gave an F ratio of 0.007 and an F critical value of 0.51 at α =0.05; NH_4-N gave an F ratio of 0.02 and an F critical value of 0.51 at α =0.05 and NO_3-N gave an F ratio of 0.16 and an F critical value of 0.51 at α =0.05. As F < F critical, there is no evidence of significant difference between the variances of two populations. In Study 4 COD_t comparisons gave an F ratio of 0.01 and an F critical value of 0.47 at α=0.05; NH_4-N comparisons gave an

F ratio of 0.1 and an F critical value of 0.47 at α=0.05; NO_3-N comparisons gave an F ratio of 0.06 and an F critical value of 0.47 at α=0.05. As F < F critical, there is no evidence of significant difference between the variances of two populations.

As shown in the calibration plots above, the model was able to predict the FS-PFBR1 plant data well considering the variability typically associated with wastewater measurements and the fact that there was minimal data available. The plots of measured COD_f, NH_4-N and NO_3-N and equivalent modelled data suggest that the fit is quite good as the majority of the data points are within the standard deviation area. Modelling the COD_f, NH_4-N and NO_3-N concentrations in the FS-PFBR1 worked very well, and only minor changes were required between LS-PFBR and FS-PFBR1 in the influent kinetic and stoichiometry parameters to correct any discrepancies during calibration. This show the model is relatively robust as they are two completely different scenarios.

5.3.3.2 Study 3PS and Study 4PS

Experimental phase studies were undertaken during Study's 3 and 4, where wastewater samples were taken at regular intervals from both R1 and R2 and analysed for COD_f, NH_4-N and NO_3-N (as described in *Section 3.5).* In order to validate the model, the phase study data from Study 3PS and Study 4PS were applied to the model. The plots of the validation process for COD_f and nitrogen are shown in Figures 5.11, 5.13 and 5.14. The stoichiometric parameter, Y_A, used in Study 3 and 4 had to be 'fine-tuned' to match the measured ammonia nitrogen during the phase study.

Study 3PS and Study 4PS – COD_f

Modelled COD_f profiles for Study 3PS showed a similar trend to experimental measurements (Figure 5.11). Limited COD_f was removed during the anoxic stage while the bulk fluid in R1 remained quiescent. As the bulk fluid from both R1 and R2 was mixed and DO concentrations increased as shown in Figure 5.4, a reduction in COD_f was recorded during the aerobic stage. There was a similar trend between the measured and modelled data.

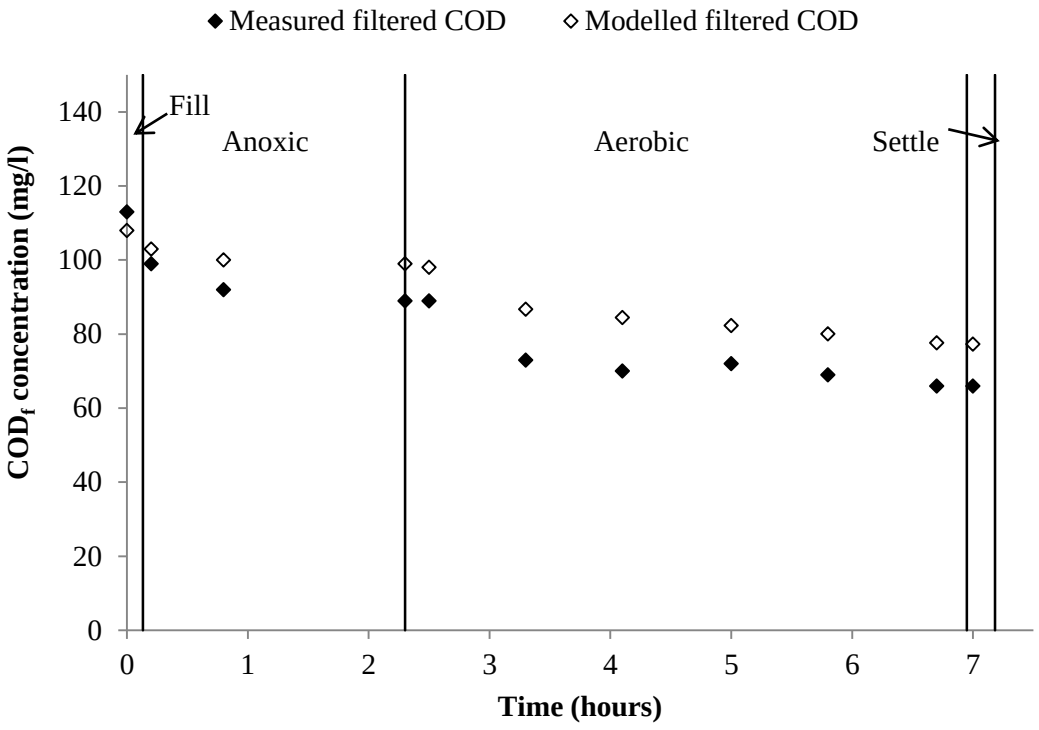

Figure 5.11 – COD$_f$ profile for Study 3PS during a typical treatment cycle

There was no COD$_f$ data available for Study 4PS as it was not measured on-site during the corresponding phase-studies. It would, however, be expected that COD$_f$ concentrations would decrease during the fill stage due to the dilution factor and then decrease rapidly during the aerobic stage as the COD$_f$ would be consumed by heterotrophic bacteria, as predicted in the model (Figure 5.12).

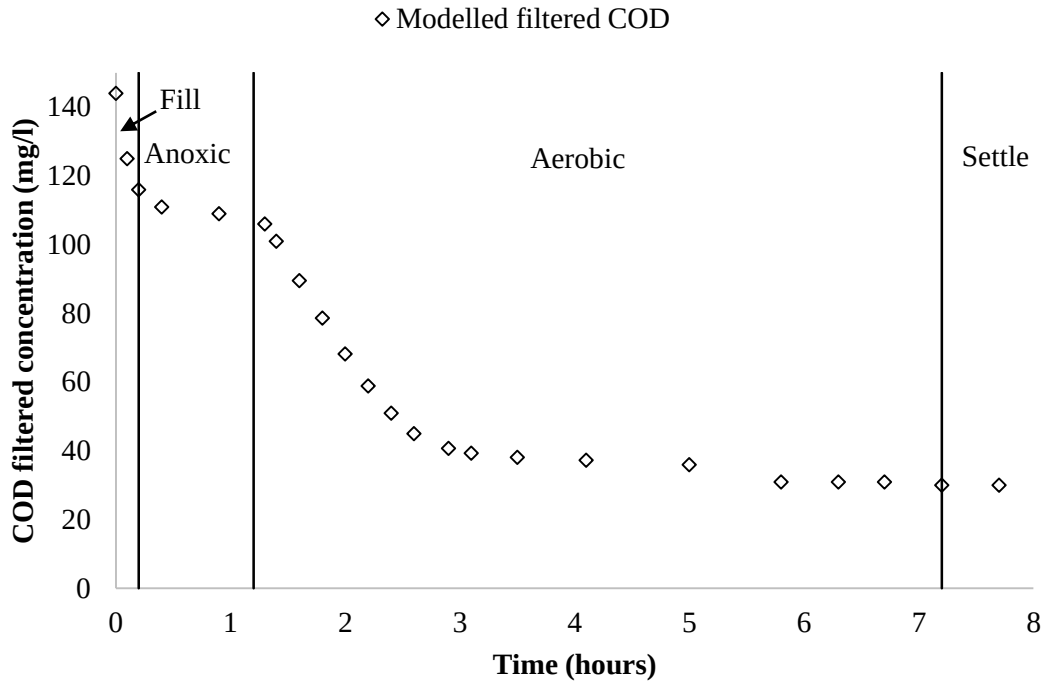

Figure 5.12 – Modelled COD_f profile for Study 4PS during a typical treatment cycle

Study 3PS and Study 4PS – Nitrogen

Figures 5.13 and 5.14 show nitrogen phase study results for Study 3PS and Study 4PS respectively. NH_4-N removal was more effect during Study 4PS, where the final NH_4-N concentration at the end of the treatment cycle was 7 mg/l compared to 15 mg/l for Study 3PS. This was due to the additional DO in Study 4PS as shown in Figure 5.3.

In both cases modelled NH_4-N and NO_3-N profiles are close to the experimental data. It can be seen that the reduction in NH_4-N concentrations did not give an equivalent increase in NO_3-N during the aerobic phase. This may be due to ammonium removal due to carbon oxidation in the initial stages of the aerobic phase though it may be possible that simultaneous nitrification and denitrification (SND) was occurring.

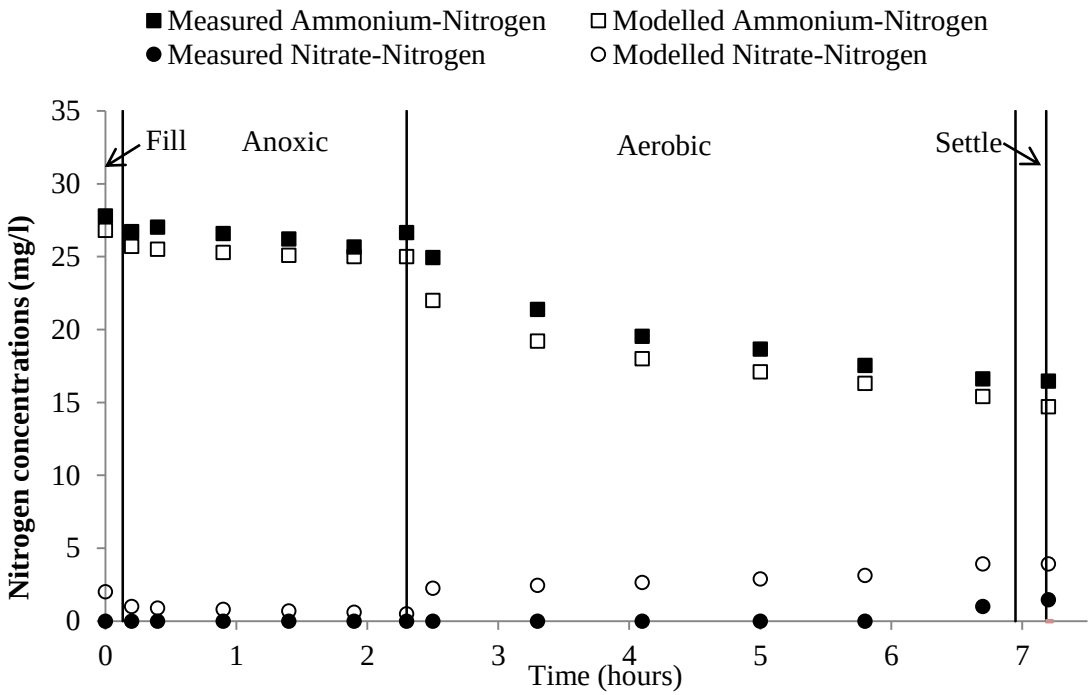

Figure 5.13 – Nitrogen profiles for Study 3PS during a typical treatment cycle

The NH_4-N removal rate levels off at the end of the cycle in Figure 5.13. There are a number of possible explanations for this, such as (i) there might be inhibitors in the landfill leachate, (ii) the autotrophs spent so much time in the anoxic zone some of them might have died by time the aerobic period starts.

Figure 5.14 shows the nitrogen profiles for Study 4PS during a typical treatment cycle during steady state operation. The modelled NH_4-N and NO_3-N profiles are close to the measured data.

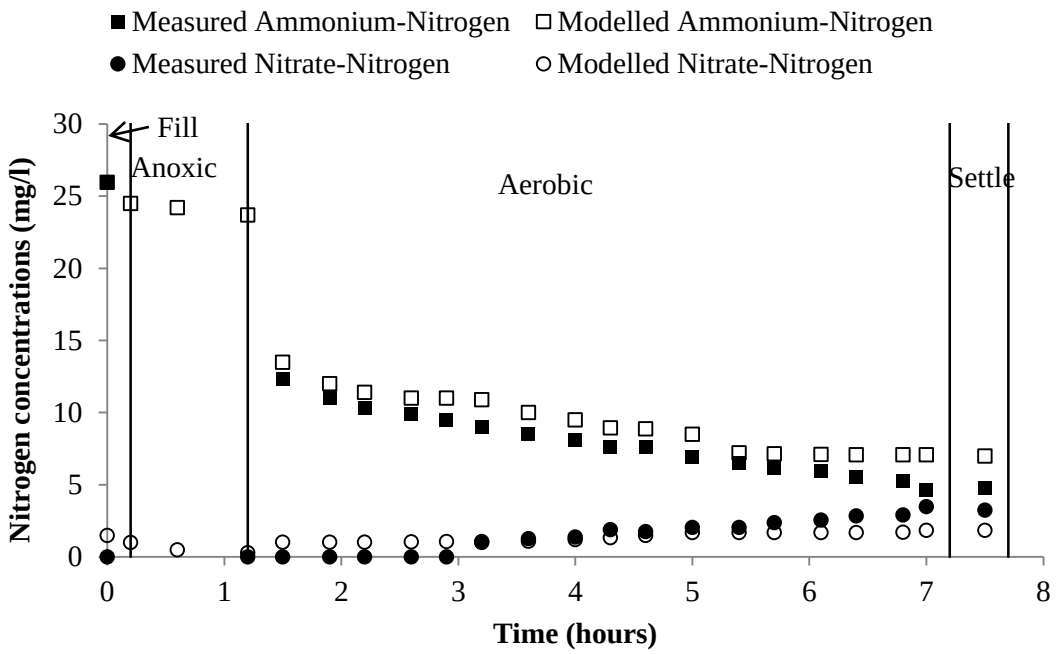

Figure 5.14 – Nitrogen profiles for Study 4PS during a typical treatment cycle

In the calibration of the FS-PFBR1, there was minimal detailed influent/effluent data available over a significant period of time. Figures 5.11, 5.13 and 5.14 show good calibration was still achieved based on this minimum data. The model resulted in good predictions of effluent results and contaminant concentration changes (nitrogen and organic carbon) during the individual phase studies. Thus, the model was able to simulate effluent contaminant concentrations within the FS-PFBR1 during the individual phase studies under a variety of operating conditions, such as different aeration times, different cycle conditions and different loading rates. The model predicted the general trends in the phase study data, indicating that the model was able to track overall plant performance.

5.3.4 Energy Consumption and Modelling Scenarios for Study 4

Based on the calibration and verification results, it was concluded that the model could adequately predict plant performance and was suitable for analysing plant operation and performing various simulations. In this exercise, a number of different scenarios were simulated for the FS-PFBR1 to determine the most energy efficient and cost efficient operational regime. The simulations focused on the potential to minimise energy costs while maintaining effluent concentrations within regulatory discharge licence

requirements.

One of the main differences between Study 3 and Study 4 was the shorter anoxic period and the longer aerobic period (as described in *Section 3.5.2*). As NH_4-N discharge concentrations were lower in Study 4 (Table 5.9), this experimental setting was selected as the base study for running four scenarios (Scenarios I to IV).

The operating characteristics (e.g. hydraulic head, pump efficiency) of the circulation pumps were put into the model and the effects of the changing cycle duration, anoxic time, aerobic time and the number of aerobic cycles were simulated. The influent characteristics were maintained for each scenario as per Study 4. The results were used to determine potential optimisations that could be carried out in the operation of the FS-PFBR1 (Table 5.10).

5.3.4.1 Wastewater Removal Efficiencies

The influence of the anoxic and aerobic cycle length (Scenario I, III and IV) and the number of aerobic cycles (Scenario I, II) were evaluated as summarised in Table 5.10.

Table 5.10 – Modelling scenarios and steady state simulation results

	Modelling Scenarios				**COD_f**		**NH_4-N**		**NO_3-N**
	Total cycle time	Anoxic time	Aerobic time	No. of aerobic cycles	(mg/l)	Removal efficiency (%)	(mg/l)	Removal efficiency (%)	(mg/l)
Study 4	462	60	360	8	32	78	15	53	1
S I	462	10	410	8	30	79	12	77	4
S II	462	10	410	17	30	79	6	92	5
S III	462	30	390	17	30	79	8	91	2
S IV	462	60	360	17	30	79	11	87	1

The DO profiles for Scenarios I, II, III and IV are shown in Figure 5.15. The DO concentrations were the lowest in SI and the highest in SII with an average of 7.39 mg/l and 9.11 mg/l respectively in the bulk fluid by the end of the treatment cycle. The highest DO in SII can be attributed to additional aeration time of 410 minutes and the fact that the bulk fluid was transferred between the reactors 17 times compared to 8 times in SI.

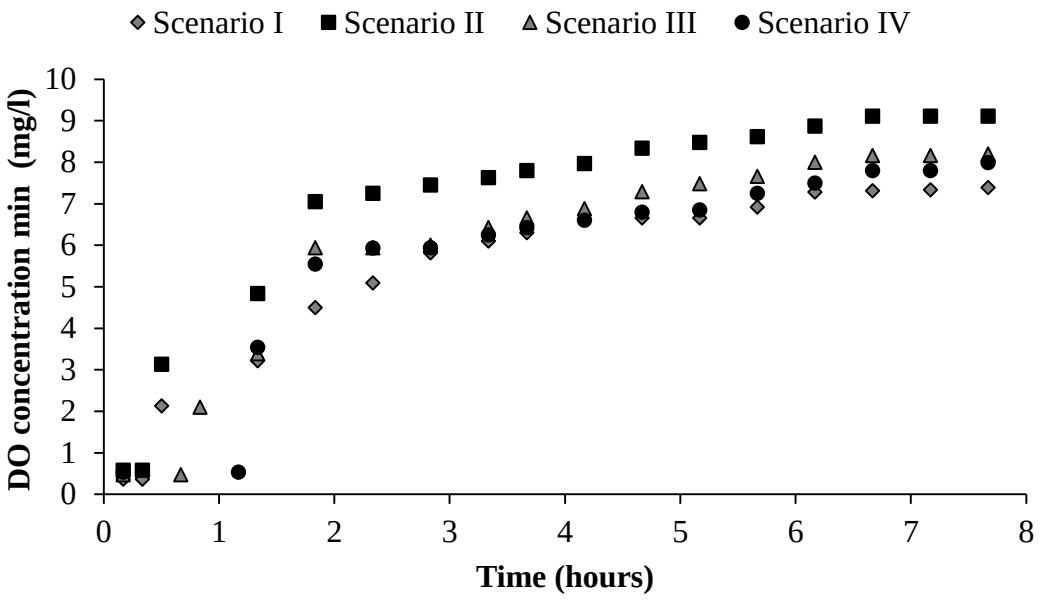

Figure 5.15 – DO profiles during Scenarios I, II, III and IV

Scenario I – In Scenario I, the additional aeration time provided when compared to Study 4 resulted in an increase in nitrification efficiency from 53% to 77%. The decrease in anoxic time coincided with an increase in effluent NO_3-N concentrations (Figure 5.16). During the anoxic period NO_3-N was reduced from 2 mg/l to 0.13 mg/l.

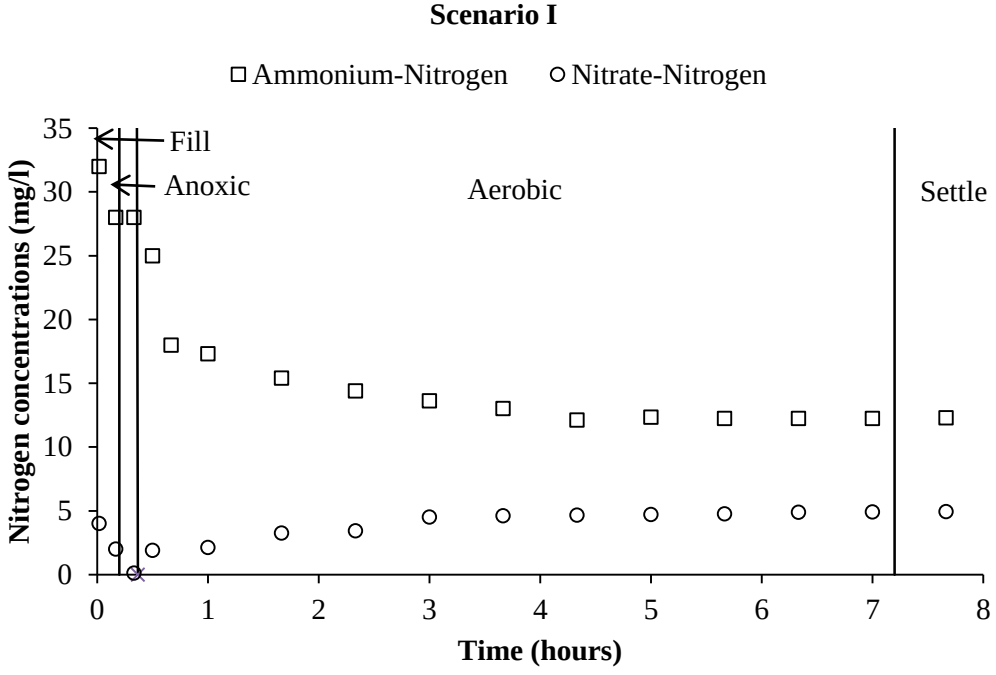

Figure 5.16 – NH_4-N and NO_3-N profiles for a typical cycle in Scenario I

Scenario II – In Scenario II, the anoxic and aeration time remained the same as Scenario I but the number of cycles increased to 17. A clear improvement in NH_4-N removal was evident from the previous scenario. Effluent NO_3-N concentrations averaged 5 mg/l, an increase when compared to Scenario I (Table 5.10). The increased supply of DO from the increase in the number of aerobic cycles was probably a key factor in the increase in nitrification efficiency (as measured by effluent NH_4-N concentrations) (Figure 5.17). The autotrophic biomass concentration for each scenario is shown in Figure 5.18. As DO increased the autotrophic biomass was also seen to increase and this in turn led to an increase in nitrification efficiency. During the anoxic period NO_3-N was reduced from 3 mg/l to 0.55 mg/l.

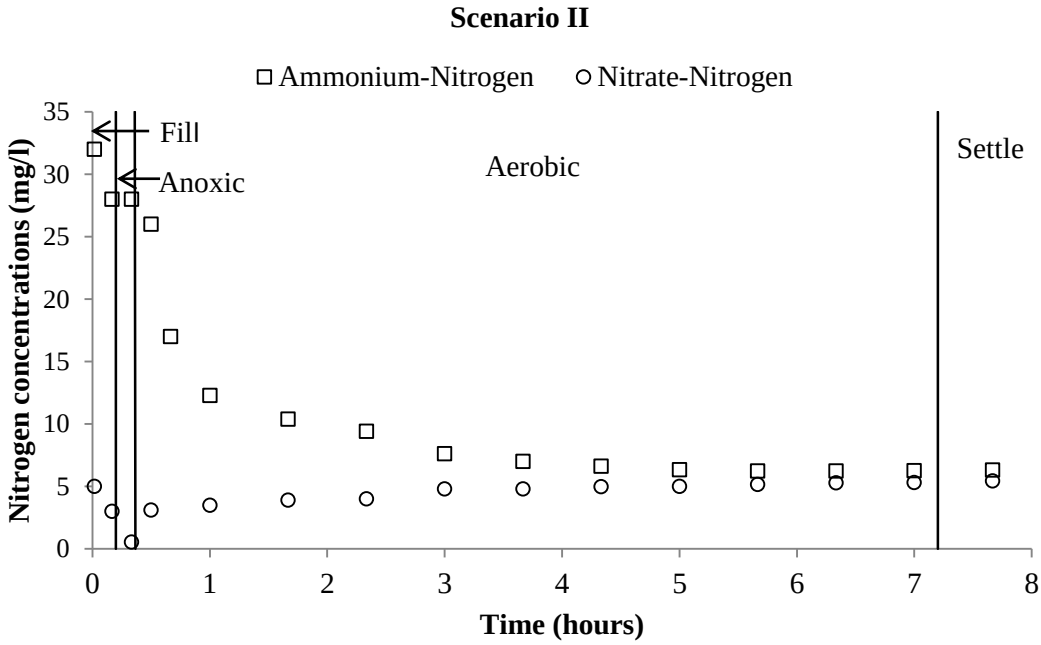

Figure 5.17 – NH_4-N and NO_3-N profiles for a typical cycle in Scenario II

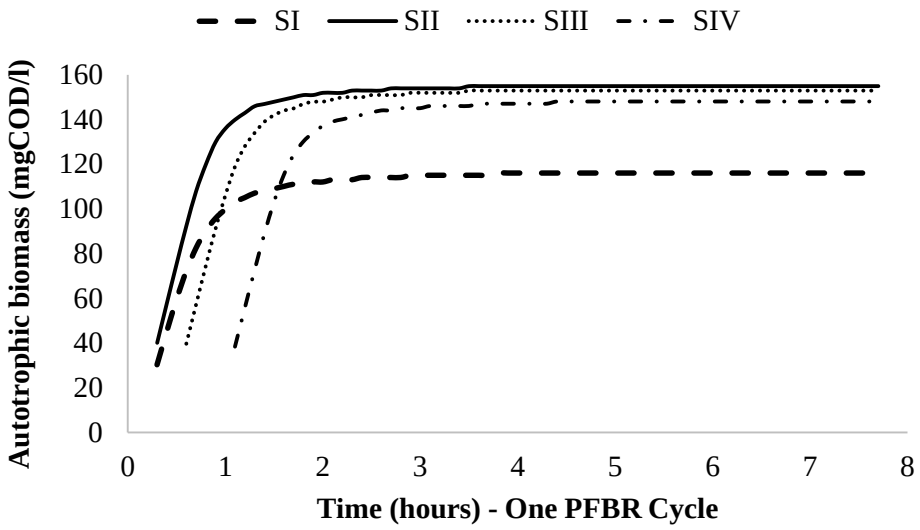

Figure 5.18 – Autotrophic biomass concentration in SI, SII, SIII and SIV

Scenario II, III and IV – The purpose of Scenarios II, III and IV was to steadily increase the anoxic time and steadily decrease the aerobic time in each scenario to determine the impact on the effluent parameters. The number of cycles remained the same at 17. As shown in Table 5.10, increasing the anoxic time and decreasing the aerobic time led to a decrease in the nitrification efficiency because there was less DO available for the nitrifying autotrophs to oxidise the NH_4-N. Figure 5.19 shows the relationship between anoxic time/aerobic times and the NH_4-N removal efficiency for each scenario. Scenario II with an anoxic time/aerobic time ratio of 0.02 had the highest nitrification efficiency at 92%.

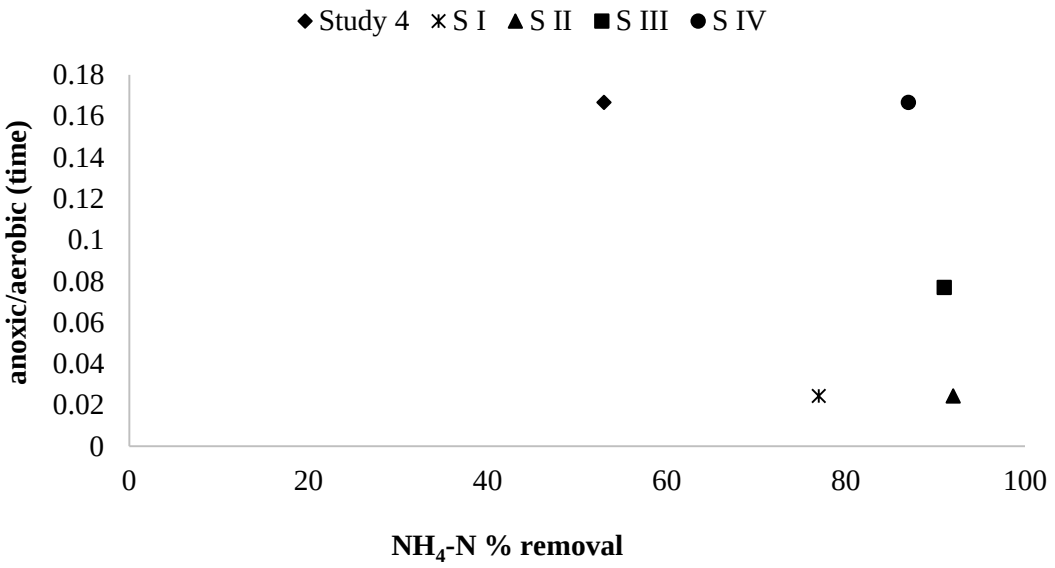

Figure 5.19 – The impact of the ratio of anoxic time to aerobic time ratio on NH_4-N removal efficiency in the aerobic stage

The anoxic time increased from 10 to 60 minutes and the aerobic time decreased from 410 to 360 minutes. This led to the removal efficiency of NH_4-N decreasing from 92% to 87%. Effluent NO_3-N concentrations were lower in Scenario IV when compared to Scenario II possibly due to the longer anoxic period. Figure 5.20 shows the relationship between anoxic time/aerobic times and the denitrification rate for each scenario.

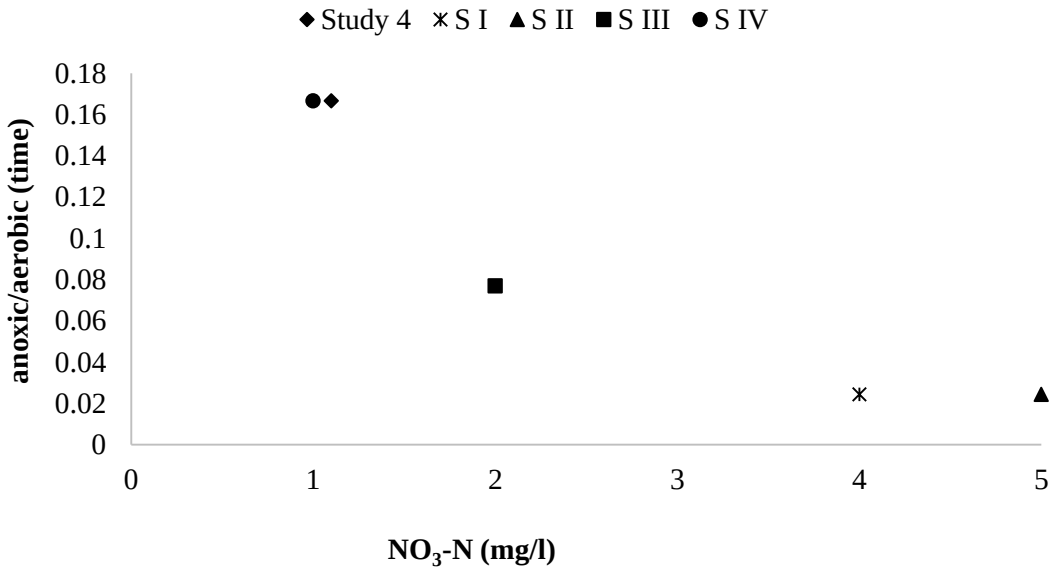

Figure 5.20 – The impact of the ratio of anoxic time to aerobic time ratio on NO_3-N removal in the anoxic stage

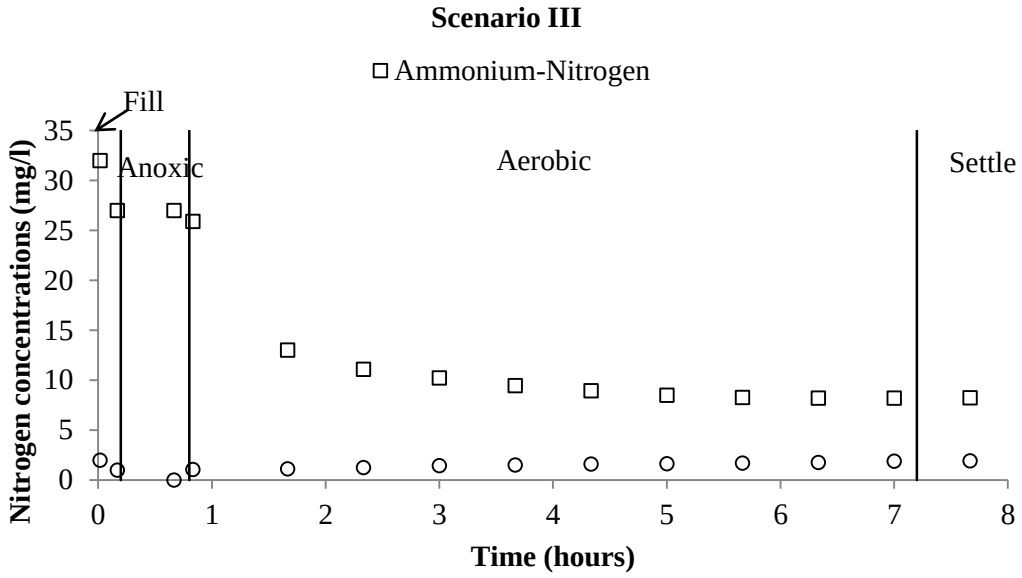

Figure 5.21 – NH_4-N and NO_3-N profiles for a typical cycle in Scenario III

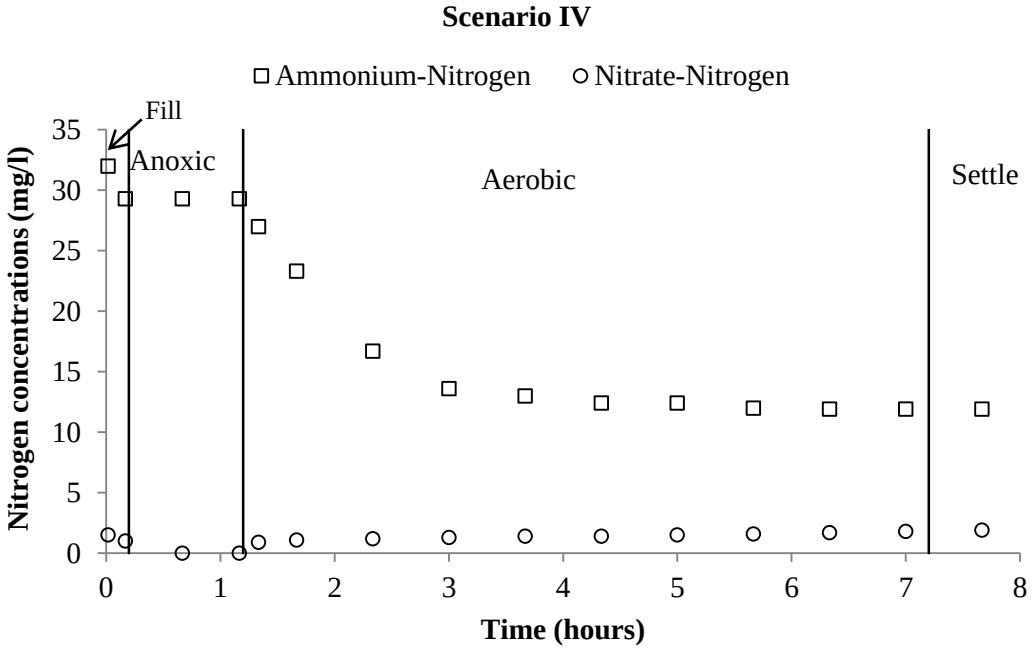

Figure 5.22 – NH_4-N and NO_3-N profiles for a typical cycle in Scenario IV

In all scenarios the NH_4-N removal rate levels off at the end of the cycle (Figure 5.16, 5.17, 5.21 and 5.22). There are a number of possible explanations for this, such as the initial drop in NH_4-N was due to carbon being removed. As a means of checking this the

model was checked during simulation and it was apparent from the model that limited numbers of autotrophs were present at the end of the cycle indicating that nitrification was no longer taking place.

By modelling the four different scenarios, it was possible to estimate the optimal operating cycle in terms of wastewater removal efficiency and cost. As might be expected, Scenario II, during which dissolved oxygen concentrations were simulated to rise most rapidly, showed the most effective scenario for achieving nitrification. In all scenarios, dissolved oxygen concentrations were above 5 mg/L after about three hours in the cycle (Figure 5.15). The anoxic period caused a reduction in NO_3-N in all scenarios which is due to denitrification.

As expected, limited additional COD_f removal was observed during the four scenarios. This was due to the concentration of soluble inert organic material in the influent being 29.2 mg/l; therefore, it would not be possible to biologically oxidise additional COD. Furthermore in all cases COD removal occurred quite rapidly during the aerobic phase and thus shortening this phase would have limited impact on effluent COD concentrations. The heterotrophic biomass concentration for each scenario is shown in Figure 5.23. As DO increased the heterotrophic biomass was also seen to increase however this did not lead to an increase in COD_f removal.

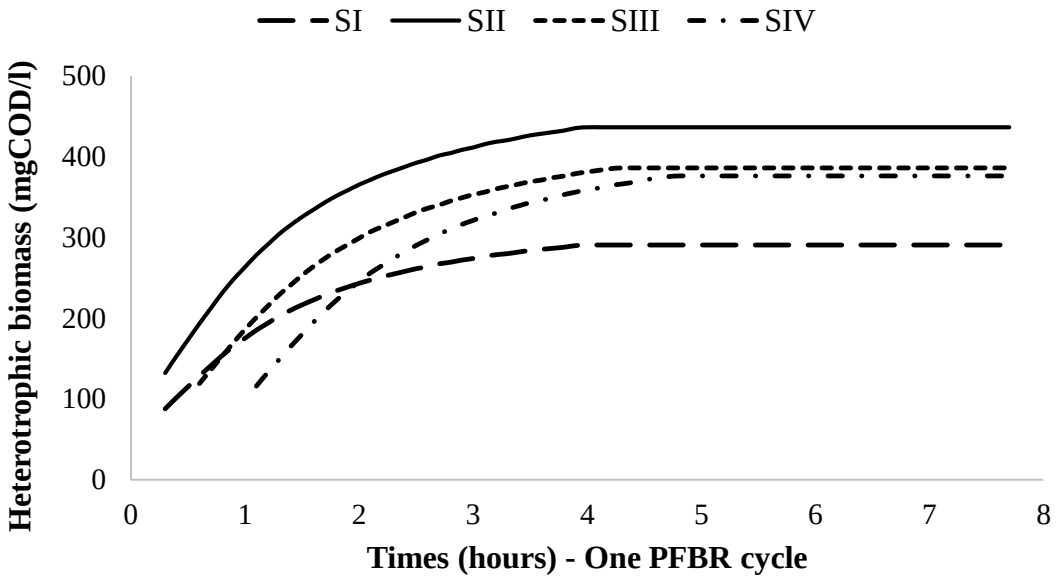

Figure 5.23 – Heterotrophic biomass concentration in SI, SII, SIII and SIV

5.3.4.2 Energy Consumption

Study 4 was simulated to be the most cost efficient but conversely (and perhaps as expected) had the lowest NH_4-N removal rates, whereas Scenario II may have the highest running costs but also had the highest NH_4-N removal rates (Table 5.11). It was not possible to achieve high NH_4-N removal rates in Scenario II with the low running costs of Study 4.

Table 5.11 – Modelling scenarios and energy usage results

	kWh/m^3 treated	**kWh/kg NH_4-N removed**	**kWh/kg COD_f removed**	**Effluent NH_4-N (mg/l)**
Study 4	0.59	34	5.2	15
Scenario I	0.61	30	5.3	12
Scenario II	1.07	41	9.3	6
Scenario III	1.05	43	9.2	8
Scenario IV	1.04	49	9.1	11

The energy required to remove NH_4-N as shown in Table 5.11 was calculated as follows (Study 4 used in the example). The same approach was used to calculate the energy used to remove COD_f.

Step 1	Flowrate	24.8 m^3/d (1033 l/hr)
Step 2	Total NH_4-N removed	Influent NH_4-N = 32 mg/l Effluent NH_4-N = 15 mg/l Removed NH_4-N = 17 mg/l 17 mg/l x 1033 l/hr = 17566 mg/hr = 0.0175 kg NH_4-N removed per hour
Step 3	Energy Usage	0.59 kWhr/m^3 treated 0.59*1.033 l/hr = 0.61 kWhr
Step 4		0.61 kWhr/0.0175 kg NH_4-N removed per hour = 34 kWhr/kg Ammonium removed

Figure 5.24 shows the energy costs per cycle (462 minutes) for the four different scenarios. The energy costs were estimated from the average cost per kWhr for electricity consumers in May 2014 which were €0.18 day time rate and €0.09 night time rate, which averaged €0.135 over 24 hours.

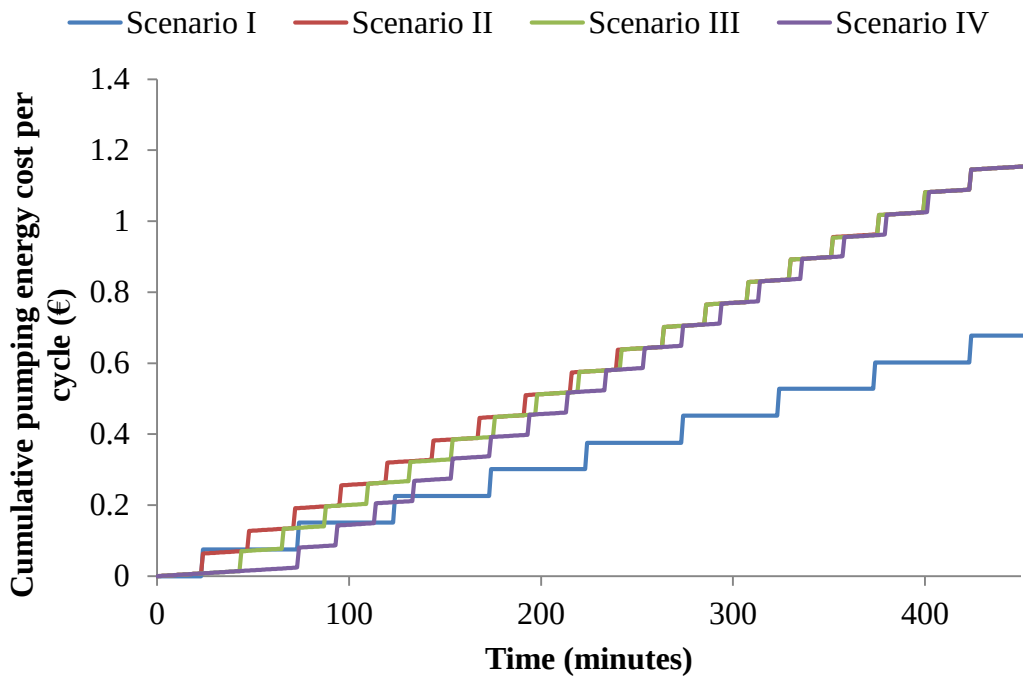

Figure 5.24 – Simulated operating costs for each scenario

Figure 5.25 shows a comparison of the energy usage per kg of COD_f removed and the energy usage per kg of ammonium removed. An average flow rate of 24.8 m^3/day (1033 l/hr) for Study 4 was used in these calculations (as described in *Section 3.5.2*).

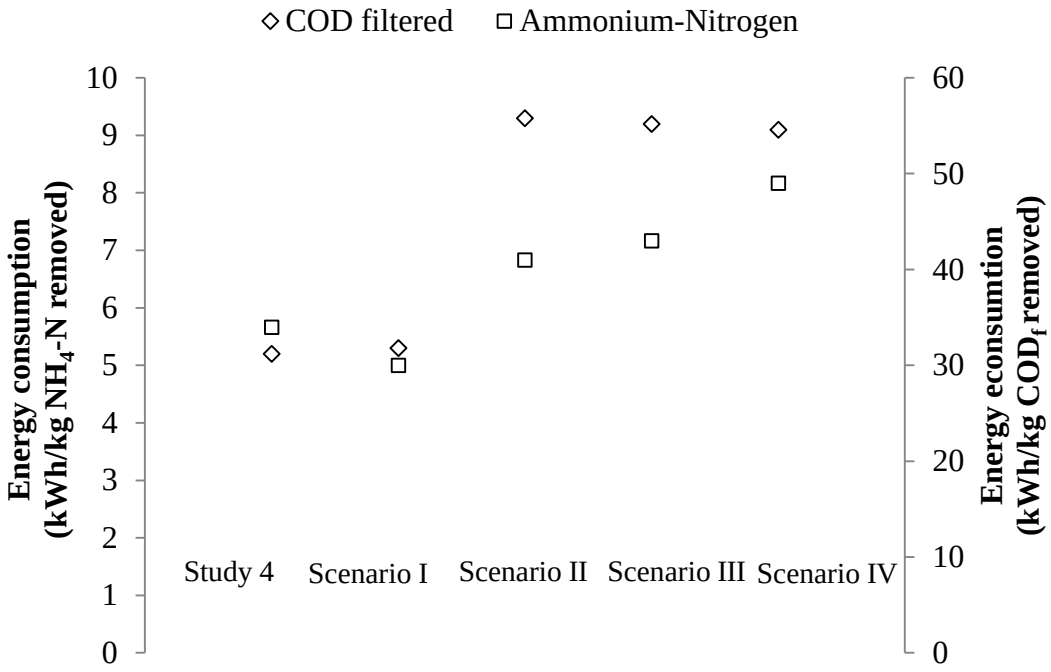

Figure 5.25 – Simulated energy consumption for COD_f and NH_4-N removal

5.4 CONCLUSION

In this study, a passively aerated batch biofilm system was successfully modelled using an activated sludge unit process (an SBR) in GPS-X. At steady state, effluent results from field-scale systems were accurately modelled as were carbon and nitrogen concentrations during individual treatment cycles. The main conclusions of the study are as follows:

1. A model of a batch biofilm passively aerated process – the FS-PFBR1 – was successfully calibrated using an activated sludge process object in GPS-X.
2. The model successfully predicted
    - effluent characteristics for carbon and nitrogen;
    - individual treatment cycles for carbon and nitrogen.
3. Such models, while not providing in-depth analysis of biofilm characteristics, can be used to enhance reactor operation and inform future studies without the need to develop a bespoke model.
4. Good calibration was achieved based on minimal influent data. With this in mind, it appears that for the calibration of the FS-PFBR1, extremely detailed influent/effluent breakdown data is not critical.
5. The model was used to simulate various scenarios for optimising the operation of the field-scale system.

While this approach has limitations, it can offer a method of rapidly developing and calibrating models for new technologies without the need to develop bespoke unit processes for existing software. The approach of using ‘surrogate’ unit processes, as described in this case-study, could allow accurate simulation of existing or new technologies not readily modelled with commercial software while minimising the time and cost necessary to develop new objects in such software.

6 MODELLING THE FIELD-SCALE PRBR (FS-PFBR1) USING AQUASIM SOFTWARE

6.1 INTRODUCTION

A key limitation of the previous models is that activated sludge processes were used to model a biofilm system. While accurate simulations of effluent concentrations and cycle performance were achieved such models cannot simulate (i) biofilm characteristics within biofilm processes, or (ii) how process changes can impact on biofilm development and thickness. For this chapter, a model of the FS-PFBR1 was built and calibrated using the modelling software AQUASIM in order to study the PFBR at a micro-scale level.

The objectives of this study were to (i) develop a unique biofilm model for FS-PFBR1, (ii) calibrate the effluent characteristics and the cycle performance of the FS-PFBR1, (iii) simulate the biofilm composition and the impact process changes have on this, and (iv) predict the impact that biofilm thickness has on COD_f and NH_4-N removal using the calibrated model.

The model was developed and calibrated using data from FS-PBBR1 (Study 3 and Study 4). A particular focus was placed on modelling individual treatment cycles as this can help optimise both technology design and operation. This work can inform model development for novel passive aeration systems, and it investigates the potential of modelling individual treatment cycles, which can lead to more robust models and process optimisation (even where process data is limited).

6.2 MODEL DEVELOPMENT

6.2.1 Modelling Description

The methodology used and applied to the development of a model for FS-PFBR1 was based on the series of generic steps shown in Figure 4.1 and as described in *Section 4.2.1*.

Tables 6.1 and 6.2 describe the models that were built and calibrated in this study. As with Chapter 5, a model was initially developed and calibrated for Study 3AS and then applied to Study 4AS. In order to validate the model, the phase study data from Study 3PS and Study 4PS were applied to it.

Table 6.1 – Model descriptions

	Study 3	Study 3	Study 4	Study 4
PFBR operation	Steady-state system operation (average of 48 days)	Phase study 432 minutes (1 PFBR cycle)	Steady state system operation (average of 34 days)	Phase study 452 minutes (1 PFBR cycle)
Model Name	Study 3AS	Study 3PS	Study 4AS	Study 4PS

Table 6.2 – Operational stages of FS-PFBR1

PFBR stage	Study 3 duration (minutes)	Study 4 duration (minutes)
Fill (t_1)	4	6
Anoxic (t_2)	134	60
Aerobic (t_3)	275	360
Settle (t_4)	14	8
Draw (t_5)	4	6
Total cycle time	431	462
No. of aerobic cycles	5	8

6.2.2 Activated Sludge Models used in Development of Model for the PFBR

As in Chapter 5, ASM1 was used to calibrate this model. In the AQUASIM model, the endogenous respiration processes from ASM3 were used instead of the decay processes in ASM1. In the PFBR the repeated and prolonged food limited environments (due to low organic carbon concentrations) created during the aeration phase may explain the enhanced endogenous respiration observed. In addition the lack of sloughing and low sludge yields may be enhanced by biofilm adhering more strongly to vertically aligned surfaces of the vertically stacked media in order to resist gravity and the shear forces applied by rising and falling water levels in the reactors (Fox, 2014). ASM3 was also extended for two-step nitrification and two-step denitrification process in order to better describe nitrite dynamics during the treatment of wastewater (Kaelin, et al. 2009). The two step nitrification process in ASM3 was not used in this project due to the lack of nitrite data. There appears to be a consensus that using endogenous respiration processes is better than using decay processes when modelling biofilms (Brockmann, 2013; Friedrich et al., 2013). It is not uncommon to couple different model families for successful model calibration (Lopez-Vazquez et al., 2013). The following processes were simulated in the biofilm model:

- aeration
- aerobic growth of heterotrophs (ASM1)
- aerobic growth autotrophs (ASM1)
- anoxic growth heterotrophs (ASM1)
- aerobic endogenous respiration of autotrophs (ASM3)
- aerobic endogenous respiration of heterotrophs (ASM3)
- anoxic endogenous respiration of autotrophs (ASM3)
- anoxic endogenous respiration of heterotrophs (ASM3)
- hydrolysis (ASM1)

Unlike GPS-X in AQUASIM, the ASM equations for the nine processes mentioned could be manually inputted into the model.

Tables 6.3 to 6.7 detail the information used in developing the model for Study 3AS. Table 6.3 summarizes the state variables. Tables 6.4 and 6.5 outline the biofilm parameters and diffusion coefficients and the process rate equations used for ASM1 and ASM3. Tables 6.6 and 6.7 show the stoichiometric matrix used for ASM1 and the stoichiometric matrix used for ASM3.

Table 6.3 – State variables

Symbol	Description	Unit
Dissolved components		
S_S	Readily biodegradable organic matter	g $CODm^3$
S_I	Soluble inert organic matter	g $CODm^3$
S_{N2}	Dinitrogen	g Nm^3
S_{NH4}	Ammonium	g Nm^3
S_{NO3}	Nitrate	g Nm^3
S_{O2}	Dissolved oxygen	g $CODm^3$
S_{ALK}	Alkalinity	moleHCO_3/L
Particulate components		
X_H	Heterotrophic organisms	g $CODm^3$
X_I	Inert particulate organic matter	g $CODm^3$
X_S	Slowly biodegradable organic matter	g $CODm^3$
X_A	Nitrifying organisms	g $CODm^3$
X_{TSS}	Total suspended solids	g $CODm^3$

Table 6.4 – Biofilm parameters and diffusion coefficients (Henze et al., 2000)

Symbol	Description	Value	Unit
Diffusion coefficients in water			
D_S	Readily biodegradable organic matter	0.0001	m^2d^{-1}
D_{O2}	Oxygen	0.00021	m^2d^{-1}
D_{NH4}	Ammonium	0.00017	m^2d^{-1}
D_{NO3}	Nitrate	0.00016	m^2d^{-1}
D_{N2}	Dinitrogen	0.00021	m^2d^{-1}
D_{ALK}	Alkalinity	0.0001	m^2d^{-1}
D_{SI}	Soluble inert matter	0.0001	m^2d^{-1}
D_{XS}	Slowly biodegradable organic matter	6e-005	m^2d^{-1}
Biofilm Parameters			
D_F/D	Ratio of diffusion in biofilm to diffusion in water	0.8	
$L_{F,tot}$	Biofilm thickness	200	μm
L_L	Boundary layer thickness	100	μm

The values listed above are default values from Henze et al. (2000), except for $L_{F,tot}$ and L_L, which are calibrated values.

Table 6.5 – Process rate equations (Henze et al., 2000)

Process	ASM	Process Rate Equation
Aerobic Growth of Heterotrophs	ASM1	$\mu_H \left(\frac{S_S}{K_S + S_S} \right) \left(\frac{S_O}{K_{OH} + S_O} \right) X_{BH}$
Anoxic Growth Heterotrophs	ASM1	$\mu_H \left(\frac{S_S}{K_S + S_S} \right) \left(\frac{K_{OH}}{K_{OH} + S_O} \right) \left(\frac{S_{NO}}{K_{NO} + S_{NO}} \right) \eta_g X_{BH}$
Aerobic Growth Autotrophs	ASM1	$\mu_A \left(\frac{S_{NH}}{K_{NH} + S_{NH}} \right) \left(\frac{S_O}{K_{OA} + S_O} \right) X_{BA}$
Aerobic endogenous respiration of heterotrophic organisms, aerobic and denitrifying activity	ASM3	$b_{H,O2} \left(\frac{S_{O2}}{K_{H,O2} + S_{O2}} \right) X_H$
Aerobic endogenous respiration of autotrophic organisms, nitrifying activity	ASM3	$b_{A,O2} \left(\frac{S_{O2}}{K_{A,O2} + S_{O2}} \right) X_A$
Anoxic endogenous respiration of heterotrophic organisms, aerobic and denitrifying activity	ASM3	$b_{H,NOX} \left(\frac{K_{O2}}{K_{O2} + S_{O2}} \right) \left(\frac{S_{NOX}}{K_{NOX} + S_{NOX}} \right) X_H$
Anoxic endogenous respiration of autotrophic organisms, nitrifying activity	ASM3	$b_{A,NOX} \left(\frac{K_{O2}}{K_{O2} + S_{O2}} \right) \left(\frac{S_{NOX}}{K_{NOX} + S_{NOX}} \right) X_A$
Hydrolysis	ASM3	$k_H \left(\frac{X_S / X_H}{K_X + X_S / X_H} \right) X_H$

Table 6.6 – Stoichiometric matrix ASM1 (Henze et al., 2000)

Process	S_S	X_{BH}	X_{BA}	S_O	S_{NO}	S_{NH}	S_{ALK}
Aerobic Growth of Heterotrophs	$-\frac{1}{Y_H}$	1		$-\frac{1-Y_H}{Y_H}$		$-i_{XB}$	$-\frac{i_{XB}}{14}$
Anoxic Growth of Heterotrophs	$-\frac{1}{Y_H}$	1			$-\left(\frac{1-Y_H}{2.86Y_H}\right)$	$-i_{XB}$	$\left(\frac{1-Y_H}{14*2.86Y_H}\right)-\left(\frac{i_{XB}}{14}\right)$
Aerobic Growth of Autotrophs			1	$-\left(\frac{4.57-Y_A}{Y_A}\right)$	$\frac{1}{Y_A}$	$(-i_{XB})-\left(\frac{i}{Y_A}\right)$	$\left(\frac{i_{XB}}{14}\right)-\left(\frac{1}{7Y_A}\right)$

Table 6.7 – Stoichiometric matrix ASM3 (Henze et al., 2000)

Process	S_{O2}	S_I	S_S	S_{NH4}	S_{N2}	S_{NOX}	S_{ALK}	X_I	X_S	X_H	X_A
Aerobic endogenous respiration of heterotrophic organisms, aerobic and denitrifying activity	$-(1-f_{XI})$			$i_{NBM}-i_{NXI}*f_{XI}$			$\left(\frac{i_{NMB}-i_{NXI}*f_{XI}}{14}\right)$	f_{XI}		-1	
Aerobic endogenous respiration of autotrophic organisms, nitrifying activity	$-(1-f_{XI})$			$i_{NBM}-i_{NXI}*f_{XI}$			$\left(\frac{i_{NMB}-i_{NXI}*f_{XI}}{14}\right)$	f_{XI}			-1
Anoxic endogenous respiration of heterotrophic organisms, aerobic and denitrifying activity				$i_{NBM}-i_{NXI}*f_{XI}$	$\left(\frac{1-f_{XI}}{2.86}\right)$	$-\left(\frac{1-f_{XI}}{2.86}\right)$	$\frac{\left(i_{NMB}-i_{NXI}+f_{XI}+\frac{(1-f_{XI})}{2.86}\right)}{14}$	f_{XI}		-1	
Anoxic endogenous respiration of autotrophic organisms, nitrifying activity				$i_{NBM}-i_{NXI}*f_{XI}$	$\left(\frac{1-f_{XI}}{2.86}\right)$	$-\left(\frac{1-f_{XI}}{2.86}\right)$	$\frac{\left(i_{NMB}-i_{NXI}+f_{XI}+\frac{(1-f_{XI})}{2.86}\right)}{14}$	f_{XI}			-1
Hydrolysis of slowly biodegradable substrates		f_{SI}	$1-f_{SI}$				$\left(\frac{i_{NXS}-f_{SI}*i_{NSI}-(1-f_{SI})*i_{NSS}}{14}\right)$		-1		

6.2.3 Temperature effects

ASM1 and ASM3 do not account for the impacts of temperature on reaction kinetics. Thus, modified Arrhenius equations were applied to the seven temperature-dependent parameters in the model developed for the PFBR (Table 6.8).

Table 6.8 – Thermal dependent parameters and thermal factor values (Brockmann, 2013)

Thermal dependent model parameters	Symbol	Unit	10ºC	20ºC	Thermal Factor
Hydrolysis rate	k_h	g COD/ g COD	2	3	$\frac{\ln\left(\frac{kH\_20}{kH\_10}\right)}{20-10}$
Autotrophic maximum specific growth rate	μ_A	d^{-1}	0.35	1	$\frac{\ln\left(\frac{mue\_A\_20}{mue\_A\_10}\right)}{20-10}$
Heterotrophic maximum specific growth rate	μ_H	d^{-1}	3	6	$\frac{\ln\left(\frac{mue\_H\_20}{mue\_H\_10}\right)}{20-10}$
Anoxic endogenous respiration rate of autotrophs	$b_{A,NO}$	d^{-1}	0.02	0.05	$\frac{\ln\left(\frac{bA\_NO\_20}{bA\_NO\_10}\right)}{20-10}$
Aerobic endogenous respiration rate of autotrophs	$b_{A,O2}$	d^{-1}	0.05	0.15	$\frac{\ln\left(\frac{bA\_O2\_20}{bA\_O2\_10}\right)}{20-10}$
Anoxic endogenous respiration rate of heterotrophs	$b_{H,NO}$	d^{-1}	0.05	0.1	$\frac{\ln\left(\frac{bH\_NO\_20}{bH\_NO\_10}\right)}{20-10}$
Aerobic endogenous respiration rate of heterotrophs	$b_{H,O2}$	d^{-1}	0.1	0.2	$\frac{\ln\left(\frac{bH\_O2\_20}{bH\_O2\_10}\right)}{20-10}$

6.2.4 Hydraulics

In the AQUASIM system, a single biofilm reactor compartment (BRC) was used to model the PFBR. Only one reactor was used as the BRC is a constant volume reactor and does not allow water to be transferred in and out of the reactor (as described in *Section 2.10.3*). The mixed reactor compartment in AQUASIM was also considered for modelling the FS-PFBR1 however as it would not allow simulation of growth and population dynamics of biofilms the BRC was the preferred option. The possibility of using three reactors to model the PFBR was also examined in AQUASIM. The layout involved a mixed compartment (circulation compartment) with a variable reactor volume and two linked

biofilm reactors. Biological process only took place in Reactors 1 and 2, while there were no biological reactions in the circulation compartment, this only acted as a circulation reactor. The cycle time of the PFBR was controlled by setting the durations of the anoxic and aerobic phase. This option was not used as using as running one PFBR cycle took nearly 10 minutes.

Although conceptually simple in operation, the hydraulics of the PFBR can be complicated. Using the BRC, the initial work focused on developing a model that could accurately represent the hydraulics and the anoxic and aerobic conditions of the PFBR. In the PFBR, water is transferred over and back between the two reactors (R1 and R2) to allow aerobic conditions to develop. There was no transference of water in or out of the BRC as AQUASIM does not allow for this. Instead, oxygen was switched on and off to simulate the different stages of the PFBR.

In the model, the influent and effluent flows were denoted as Qinf and Qeff respectively, and were multiplied by the terms t_inon and t_outon as described in Table 6.9.

Table 6.9 – Some of the terms used in the AQUASIM model

Term	Description
Qinf	Influent flow
Qeff	Effluent flow
t_airon	Aeration switch
t_inon	Turn on and off Qinf
t_outon	Turn on and off Qeff

Figure 6.1 shows the general layout of the modelled system.

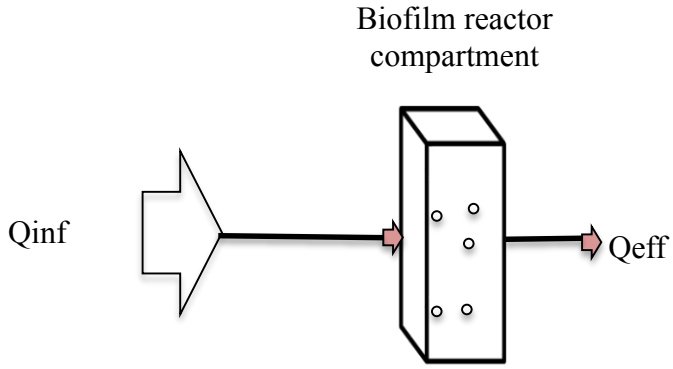

Figure 6.1 – Schematic diagram of the reactor compartments in AQUASIM

The influent flow was modelled by turning Qinf on for 4 and 6 minutes respectively for Study 3 and Study 4 at the beginning of the cycle and then switching it off for the remainder of the cycle. Then at 427 minutes and 434 minutes respectively for Study 3 and Study 4, Qeff was switched on for 4 and 6 minutes respectively and then turned off. The times to turn on and off Qinf was controlled by the parameter t_inon. The times to turn on and off Qeff was controlled by the parameter t_outon. This process was repeated for each cycle, which allowed the wastewater to enter and leave the reactor. The anoxic and aerobic period was replicated by switching on and off the dissolved oxygen parameter (t_airon). The input control times used for Study 3 and Study 4 are shown in Tables 6.10 and 6.11.

Table 6.10 – Input control times for one complete cycle in Study 3

Qinf on/off		**Qeff on/off**		**DO on/off R1**	
t_inon	**on (1) off (0)**	**t_outon**	**on (1) off (0)**	**t_airon**	**on (1) off (0)**
time (days)		time (days)		time (days)	
0	0	0	0	0	0
0.001	1	0.001	0	0.098	0
0.006	1	0.292	0	0.099	1
0.007	0	0.293	1	0.289	1
0.3	0	0.299	1	0.29	0
		0.3	0	0.3	0

Table 6.11 – Input control times for one complete cycle in Study 4

Qinf on/off		**Qeff on/off**		**DO on/off R1**	
t_inon	**on (1) off (0)**	**t_outon**	**on (1) off (0)**	**t_airon**	**on (1) off (0)**
time (days)		time (days)		time (days)	
0	0	0	0	0	0
0.001	1	0.001	0	0.04	0
0.009	1	0.309	0	0.05	1
0.01	0	0.31	1	0.297	1
0.32	0	0.319	1	0.298	0
		0.32	0	0.32	0

The influent and effluent flow patterns simulated using AQUASIM are shown in Figure 6.2 for one cycle in Study 3. The average volume/cycle for Study 3 and Study 4 was 8 m^3.

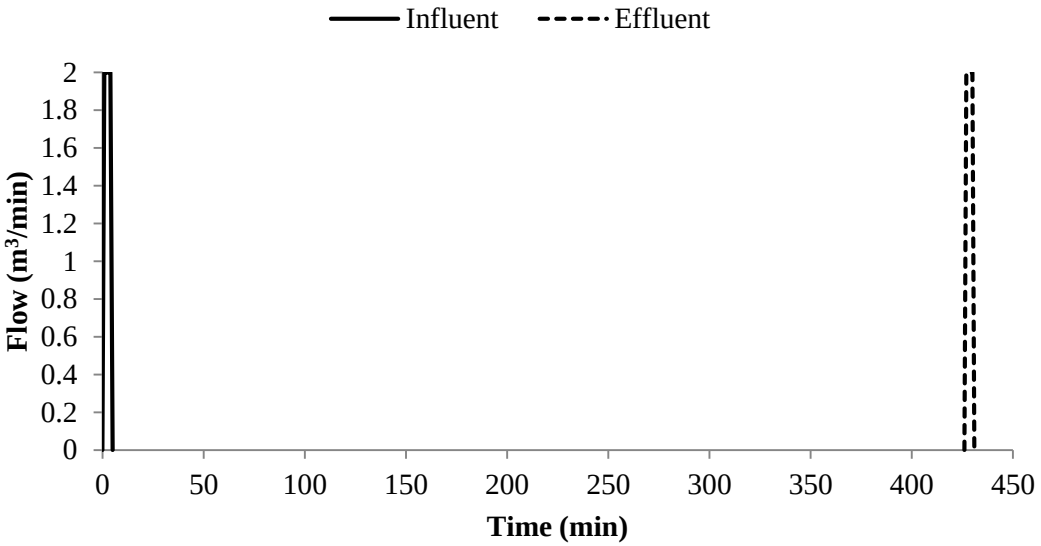

Figure 6.2 – Influent and effluent flow pattern for a typical cycle in Study 3

6.2.5 Wastewater Characteristics

In the FS-PFBR1, the influent was comprised of municipal wastewater (as described in *Section 3.5.3*).

Table 6.12 – Typical average influent and effluent concentrations in the municipal wastewater. Standard deviations shown in ()

	Study 3	**Study 3**	**Study 4**	**Study 4**
Parameters	Influent wastewater (mg/l)	Effluent wastewater (mg/l)	Influent wastewater (mg/l)	Effluent wastewater (mg/l)
COD_f	187 (48)	66 (13)	144 (41)	33 (10)
NH_4-N	34 (10)	26 (5)	32 (7)	12 (6)
NO_3-N	-	0.95 (0.5)	0.03 (0.12)	1 (1)

6.3 RESULTS AND DISCUSSION

6.3.1 Dissolved Oxygen

In the AQUSIM model, since only a single BRC was used, the aerobic period was replicated by switching on a dissolved oxygen parameter (t_airon), while the anoxic period was replicated by switching off this dissolved oxygen parameter.

The passive aeration process in the PFBR was modelled by entering an oxygen mass transfer coefficient (K_La). A K_La value of 122 d^{-1} had previously been calculated for the laboratory scale PFBR study (O'Reilly, 2005). However, when the K_La value was set at 122 d^{-1}, it was not possible to calibrate the model and get a reasonable match between modelled and measured effluent COD_f, NH_4-N and NO_3-N data thus for the purposes of this model, the K_La value was adjusted to 35 d^{-1} in order to achieve good calibration. This figure was arrived at by carrying out a manual sensitivity analysis. This is discussed in more detail in Chapter 8.

As mentioned previously, wastewater was alternately pumped between R1 and R2 for the duration of the aerobic period, and thus an aeration switch was designed in the model to turn on and off aeration in order to mimic the aeration pattern in the FS-PFBR1. The pattern of the aeration switch is shown in Figure 6.3 for a full PFBR cycle.

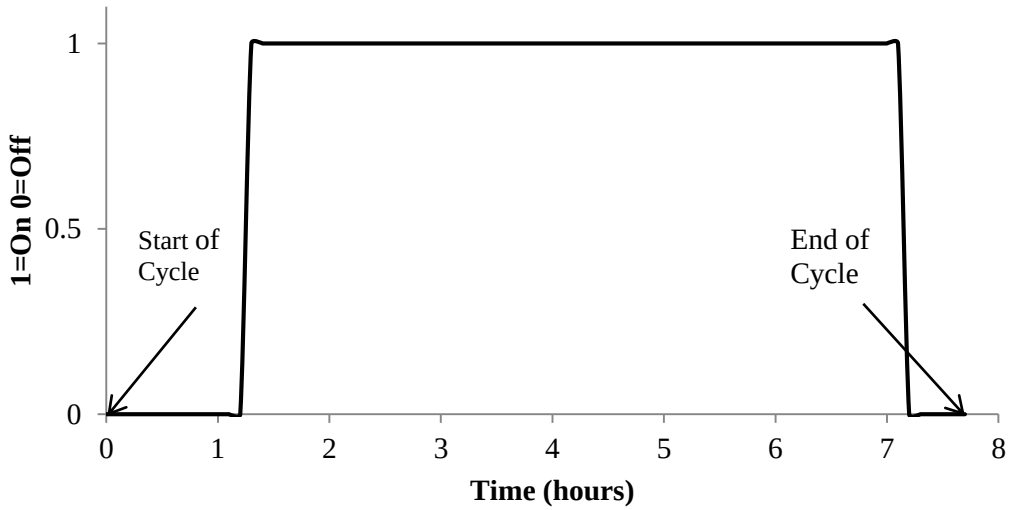

Figure 6.3 – Aeration switch

Due to limitations with AQUASIM software, it was not possible to imitate the dual tank configuration. The aerobic period modelled in AQUASIM did not allow for transfer of

water between R1 and R2. To replicate the conditions present in the configuration, it was decided to control the oxygen levels in the AQUASIM object instead. For the duration for the aerobic period of the cycle, the aeration switch was turned on. For the anoxic period, the aeration switch was turned off. The main purpose of cycling the water between the two tanks was to ensure the wastewater was fully aerated, keeping the aeration switch on ensured that the oxygen conditions were replicated from the PFBR set up to AQUASIM. Numerous other methods of replicating the oxygen conditions were trialled, however, none were as effective as using the aeration switch. Transferring water between two tanks was not possible within the confines of the software, and although would be more representative of the PFBR, replicating the oxygen conditions was sufficient to imitate the water characteristics as it went through the treatment cycle.

Figure 6.4 shows a comparison between modelled and measured DO data for a full PFBR cycle. There was not an exact match between measured and modelled DO. Six simulations were carried out on Study 4 that compared K_La values against measured effluent results. These simulations are discussed in detail in Chapter 8.

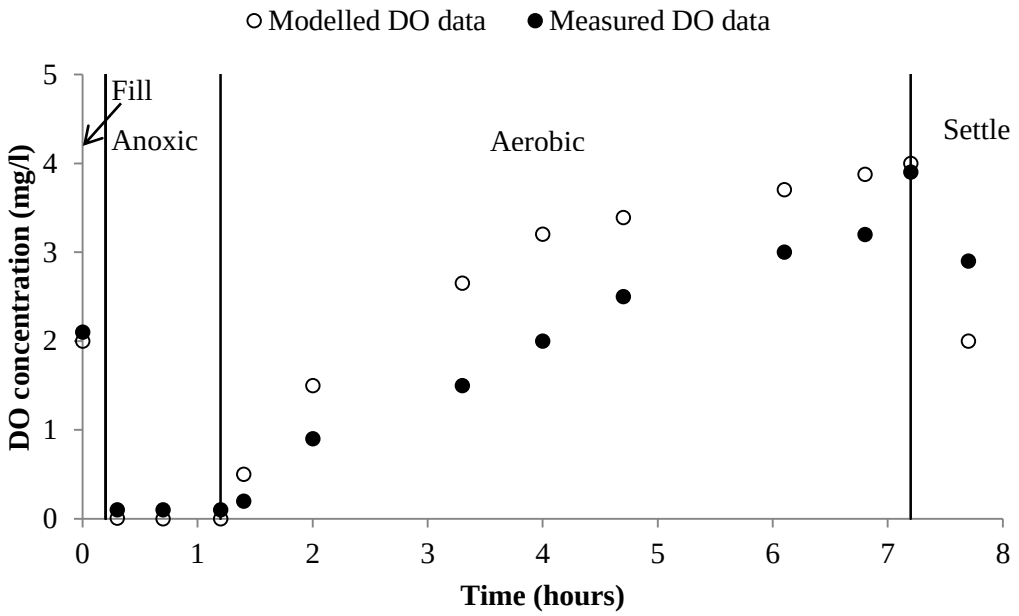

Figure 6.4 – Modelled and measured DO data

6.3.2 Sensitivity Analyses and Model Calibration

The calibration of the model was based on experimental field study data (effluent concentrations). To arrive at apparent steady-state values, the model was run until steady-state conditions were reached after approximately 10 days of a simulated operation.

The sensitivity functions of the variables COD_f, NH_4-N and NO_3-N with respect to the 17 model parameters listed in Table 6.13 were determined. The upper and lower boundaries for each parameter during calibration were taken from reported literature values. With regard to the sensitivity analysis, some or all of the parameters listed in Table 6.13 were expected to impact on the calibration of the model. The results of the full sensitivity analysis are included in Appendix J.

Table 6.13 – Parameters used in sensitivity analysis (Henze et al., 2000)

Parameters tested in the sensitivity analysis	Description	Sensitivity ranges
$K_{O2,A}$	Saturation coefficient for oxygen for nitrifying organisms	0.1 to 1
$K_{O2,H}$	Saturation inhibition coefficient for oxygen for heterotrophic organisms	0.1 to 1
$K_{NO3,A}$	Saturation/inhibition coefficient for nitrate for nitrifying organisms	0.1 to 1
$K_{NO3,H}$	Saturation/inhibition coefficient for nitrate for heterotrophic organisms	0.1 to 1
$K_{NH4,A}$	Saturation coefficient for ammonium for nitrifying organisms	0.1 to 1
$K_{NH4,H}$	Saturation coefficient for ammonium for heterotrophic organisms	0.1 to 1
$K_{HCO3,A}$	Bicarbonate saturation constant of autotrophs	0.1 to 1
$K_{HCO3,H}$	Bicarbonate saturation constant of heterotrophs	0.1 to 1
μ_A	Maximum growth rate of Nitrifying organisms	0.1 d^{-1} to 1 d^{-1}
μ_H	Maximum growth rate of Heterotrophic organisms	1 d^{-1} to 12 d^{-1}
K_S	Substrate half saturation coefficient for heterotrophic biomass	5 to 225
K_X	Hydrolysis saturation constant	0.01 to 1
Y_A	Yield of autotrophs	0.07-0.28 g COD/g N
$Y_{H,O2}$	Yield of heterotrophs using oxygen	0.1g to 0.9 g COD/g COD
$Y_{H,NO}$	Yield of heterotrophs using nitrate	0.38-0.75 g COD/g COD
$L_{F,tot}$	Biofilm thickness	0.0002 - 0.002 m
L_L	Boundary layer thickness	0.0001 - 0.001 m

Figure 6.5 presents the results from the sensitivity analyses carried out. The negative sign indicates that the variable increases with decreasing parameter values (and vice versa for a positive sign). The positive and negative figure indicates the magnitude of change of that value in the ranges shown in Table 6.13. For example, as shown in Figure 6.5, as μ_H increases from 1 d^{-1} to 12 d^{-1}, effluent COD_f concentrations predicted by the model decreased by 60%.

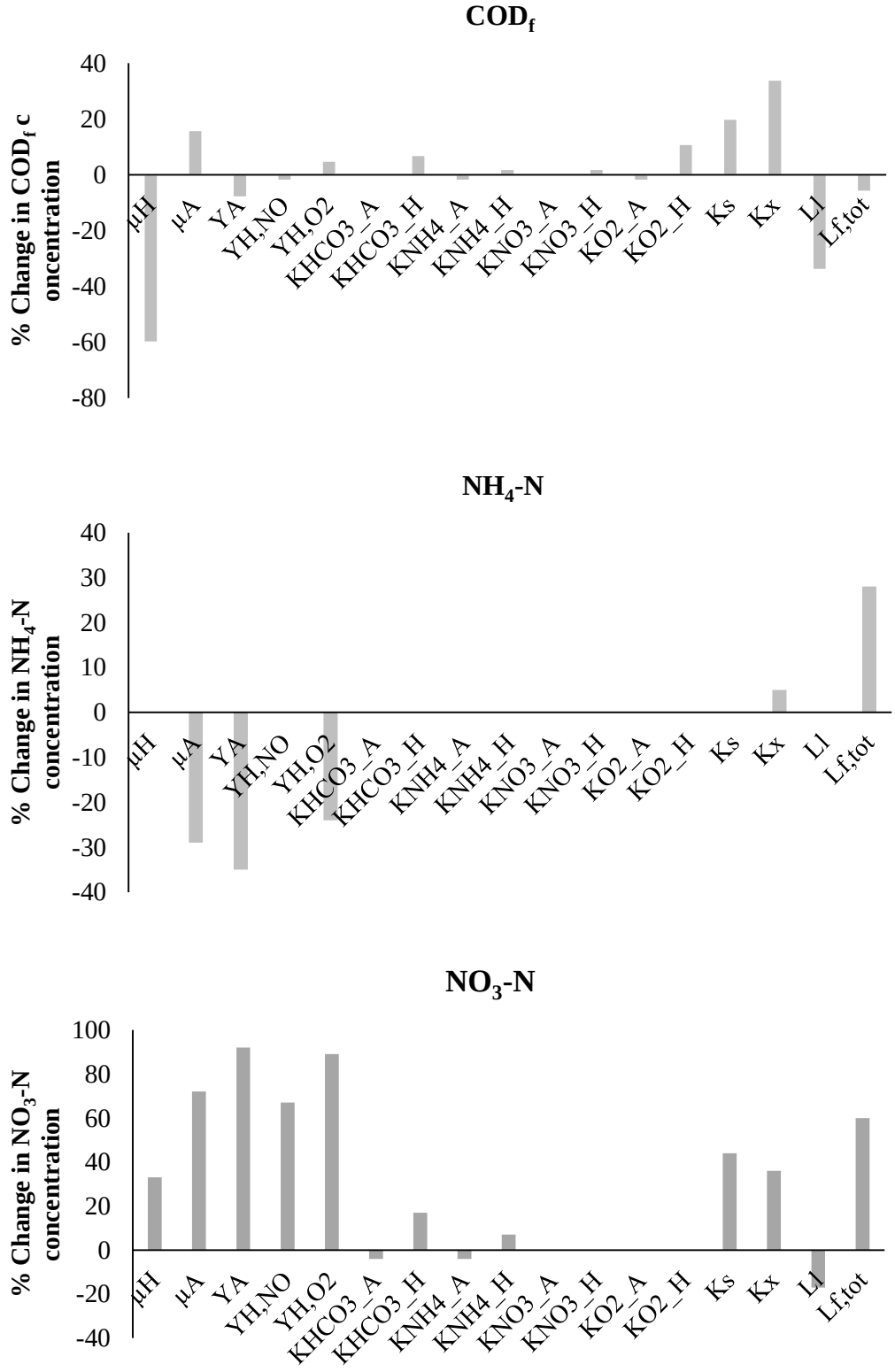

Figure 6.5 – Sensitivity analyses on modelled effluent COD_f, NH_4-N and NO_3-N

Effluent COD_f concentrations were most sensitive to changes in μ_H; whereas NH_4-N, and NO_3-N were most sensitive to changes in Y_A and μ_A. There was a 29% decrease in effluent NH_4-N concentrations as μ_A increased from 0.1 d^{-1} to 1 d^{-1} and a 35% decrease as Y_A

increased from 0.07 to 0.28 g COD/g N. Effluent NO_3-N concentrations were most sensitive to changes in μA and Y_A; as Y_A increased from 0.07-0.28 g COD/g N, effluent NO_3-N concentrations increased by 92%. There was a 72% increase in effluent NO_3-N concentrations as μA increased from 0.1 d^{-1} to 1 d^{-1}. Figure 6.5 shows the variation in COD_f, NH_4-N and NO_3-N concentrations with the change in each stoichiometric/kinetic parameter. The coefficients $K_{O2,A}$, $K_{O2,H}$, $K_{NO3,A}$, $K_{NO3,H}$, $K_{NH4,A}$, $K_{NH4,H}$, $K_{HCO3,A}$ and $K_{HCO3,H}$ had little impact on simulated COD_f, NH_4-N or NO_3-N concentrations. The analyses indicated that the kinetic parameters most significant for calibration were μ_H, μ_A and Y_A.

The sensitivity analyses in AQUASIM and GPS-X compared well, with COD_f most dependent on the parameter μ_H, and NH_4-N and NO_3-N most sensitive to changes in μ_A and Y_A in both modelling packages.

6.3.3 Kinetic and Stoichiometry Results

The calibration approach used involved adjusting each of the parameters listed in Table 6.13 in turn and then making a visual inspection of the simulation results for DO, COD_f, NH_4-N and NO_3-N. Numerous permutations were used in order to calibrate the model, some of which are shown in Table 6.14. It should be noted that there was probably over 1000 different variations modelled using the variables μ_A, μ_H, Y_A, $Y_{H,O2}$, $Y_{H,NO}$, $K_{O2,A}$, $K_{O2,H}$, $K_{NO3,A}$, $K_{NO3,H}$, $K_{NH4,A}$, $K_{NH4,H}$, $K_{HCO3,A}$, $K_{HCO3,H}$, K_S, K_X, $L_{F,tot}$, L_L and K_{LA} in order to get a good match for DO and the effluents COD_f, NH_4-N and NO_3-N. Some of these parameters listed in Table 6.14 were not overly sensitive to calibration but they were still tested in the manual calibration of the model. A more detailed description of the calibration approach is outlined in Chapter 8.

Table 6.14 – Example of the manual calibration approach used

Parameters adjusted in the model			Effluent concentrations				
K_{LA} d^{-1}	uA d^{-1}	uH d^{-1}	O_2 mg/l	NH_4-N mg/l	NO_3-N mg/l	COD_t mg/l	COD_f mg/l
1	1	1	*0.08*	*26*	*0.1*	*264*	*190*
10	1	1	*2.6*	*22*	*0.8*	*194*	*134*
20	1	2		*22*	*0.1*		
20	1	4	*7*	*21*	*0.39*	*114*	*60*
20	1	6		*20*	*0.3*	*113*	*60*
20	1	8		*16*	*0.9*	*113*	*60*
20	1	10	*3.9*	*10*	*2*	*113*	*60*
20	2	1	*1.9*	*6*	*11*	*190*	*129*
20	4	1	*1.1*	*2*	*13*	*195*	*132*
30	1	1	*6*	*13*	*7*	*181*	*120*
30	1	2	*8*	*22*	*0.3*	*131*	*66*
30	1	4		*22*	*0.1*		
30	1	6	*9*	*19*	*0.4*	*114*	*60*
40	1	1	*7.5*	*9*	*11*	*183*	*123*
40	1	2	*9*	*22*	*0.2*	*120*	*67*
40	1	4	*9*	*20*	*0.2*	*115*	*60*
40	1	6	*9*	*18*	*0.5*	*115*	*60*
40	1	8	*10*	*20*	*0.2*	*113*	*60*
20	2	2	*3*	*11*	*3*	*122*	*70*
20	2	4	*3.5*	*10*	*2.4*	*113*	*60*
20	2	6	*2.8*	*8*	*2.8*	*112*	*59*
20	2	8	*2*	*7*	*3*	*112*	*59*
30	2	2	*4.5*	*4*	*8*	*120*	*66*
30	2	4	*5*	*2*	*6*	*114*	*60*
30	2	6	*5*	*1*	*5*	*115*	*60*
30	2	8	*6*	*0*	*5*	*115*	*60*
40	2	2	*9*	*20*	*9*	*120*	*60*
40	2	4	*7*	*1*	*8*	*115*	*61*
40	2	6	*7*	*1*	*6*	*115*	*61*
40	2	8	*9*	*1*	*7*	*115*	*61*
100	2	2	*9*	*1*	*15*	*122*	*67*
100	2	6	*10*	*0*	*8*	*122*	*67*
100	2	10	*11*	*0*	*8*	*122*	*67*
100	4	10	*11*	*0*	*8*	*122*	*67*
100	1	10	*10*	*0*	*10*	*122*	*67*
100	1	8	*9*	*0*	*10*	*122*	*67*

The aim of the calibration process involved trying to match the modelled effluent data to between 5% and 20% of the actual measured effluent data. The model was deemed calibrated when this was achieved. It is important to add that this was not achieved in the case where the values were low, this is discussed in Chapter 8. The stoichiometric

parameter values and the kinetic parameter values were adjusted within the ranges provided by the literature to calibrate the FS-PFBR1 model (Tables 6.15 and 6.16).

Table 6.15 – Stoichiometric parameter values (Henze, 2000)

Symbol	Description	Value	Unit
Conversion factors			
Nitrogen:			
Soluble Material			
i_{NSI}	Nitrogen content of inert soluble COD, S_I	0.01	g COD/g N
i_{NSS}	Nitrogen content of readily biodegradable organic matter, S_S	0.03	g COD/g N
Particulate Material			
i_{NXI}	Nitrogen content of inert particulate COD, X_I	0.02	g COD/g N
i_{NXS}	Nitrogen content of slowly biodegradable organic matter, X_S	0.04	g COD/g N
i_{NBM}	Nitrogen content of biomass, X_H, X_A	0.07	g COD/g N
Total Suspended Solids			
i_{TSSXI}	TSS to COD ratio for X_I	0.75	g TSS/g COD
i_{TSSXS}	TSS to COD ratio for X_S	0.75	g TSS/g COD
i_{TSSBM}	TSS to COD ratio for biomass, X_H, X_A	0.9	g TSS/g COD
Stoichiometric parameters			
Hydrolysis			
f_{SI}	Production of S_I in hydrolysis	0.1	g COD/g COD
Heterotrophic biomass			
$Y_{H,O2}$	Yield of heterotrophs using oxygen	0.63	g COD/g COD
$Y_{H,NO}$	Yield of heterotrophs using nitrate	0.54	g COD/g COD
f_{XI}	Production of X_I in endogenous respiration	0.2	g COD/g COD
Autotrophic biomass			
Y_A	Yield of autotrophs	0.09	g COD/g COD
f_{XI}	Production of X_I in endogenous respiration	0.2	g COD/g COD

Table 6.16 – Kinetic parameter values (Henze, 2000)

Symbol	Description	Value	Unit
Hydrolysis of particulate substrates: X_S			
k_h	Hydrolysis rate constant	3	d^{-1}
K_X	Hydrolysis saturation constant	1	g COD/g COD
Heterotrophic organisms: X_H			
μ_H	Maximum growth rate on substrate	5.00	d^{-1}
$b_{H,O2}$	Aerobic endogenous respiration rate of X_H	0.20	d^{-1}
$b_{H,NO}$	Anoxic endogenous respiration rate of X_H	0.10	d^{-1}
$K_{O2,H}$	Saturation/inhibition coefficient for oxygen	0.2	g O_2 / m^3
K_S	Saturation coefficient for growth on S_S	10	g COD / m^3
$K_{NO3,H}$	Saturation/inhibition coefficient for nitrate	0.5	g N / m^3
$K_{NH4,H}$	Saturation coefficient for ammonium (nutrient)	0.01	g N / m^3
Nitrifying (autotrophic) organisms: X_A			
μ_A	Maximum growth rate of X_A	1.00	d^{-1}
$b_{A,O2}$	Aerobic endogenous respiration rate of X_A	0.15	d^{-1}
$b_{A,NO}$	Anoxic endogenous respiration rate of X_A	0.05	d^{-1}
$K_{O2,A}$	Saturation coefficient for oxygen	0.4	g O_2 / m^3
$K_{NH4,A}$	Saturation coefficient for ammonium (substrate)	1	g N/ m^3
$K_{NO3,A}$	Saturation/inhibition coefficient for nitrate	0.5	g N / m^3

6.3.4 Experimental and Modelled Results

6.3.4.1 Study 3AS and 4AS

A model was initially built and calibrated using data from Study 3AS and 4AS. In order to validate the model, independent data from Study 3PS and Study 4PS was then simulated. The results for Study 3AS and Study 4AS are shown in Table 6.17. They show good agreement between measured and modelled effluent results for COD_f, NH_4-N and NO_3-N. A full set of model results are shown in Appendix K.

Table 6.17 – Measured and modelled effluent results for Study 3AS and Study 4AS. Standard deviation shown in ().

	Study 3AS				**Study 4AS**			
	Measured steady state system operation (average of 48 days)		Modelled		Measured steady state system operation (average of 34 days)		Modelled	
	Effluent (mg/l)	Removal efficiency (%)	Effluent (mg/l)	Removal efficiency (%)	Effluent (mg/l)	Removal efficiency (%)	Effluent (mg/l)	Removal efficiency (%)
COD_f	66 (13)	65	70	63	33 (10)	77	45	69
NH_4-N	26 (5)	24	25	26	12 (6)	62	11	65
NO_3-N	0.95 (0.5)	-	1.6	-	1 (1)	-	1.8	-

In Study 4AS, the additional aeration time of 85 minutes resulted in increased ammonium removal rates; 65% removal for Study 3AS and 77% removal for Study 4AS. There was less NO_3-N in the effluent during Study 3 than Study 4. This could be due to DO concentrations being lower during the aeration phase in Study 3 than in Study 4. It was difficult to determine whether denitrification occurred or not as there was no total nitrogen data available. However, it might be reasonable to assume that denitrification did occur due to the high NH_4-N removal rates and the relatively low NO_3-N concentrations in the effluent. The model showed denitrification during the phase studies which are discussed below.

In Study 4AS, there was also an improved performance in the average COD_f removal, with a 77% removal rate achieved in 4AS compared with a 65% removal rate in Study

3AS. There was a difference in measured influent and effluent COD_f between Study 3 and Study 4 (Table 6.12). The improved performance in the COD_f removal during Study 4 could be attributed to the quantity of leachate processed by the FS-PFBR1 being reduced during Study 4. It is important to note that in the measured data, the COD was not partitioned into biodegradable or non-biodegradable sections. One of the reasons for the error between the measured and modelled data could be that the partitioning of biodegradable and non-biodegradable differed in each case. However, the modelled results are close to experimental data for the three parameters tested.

6.3.4.2 Study 3PS and Study 4PS

Study 3PS – COD_f

Modelled COD_f profiles for Study 3PS showed a similar trend to experimental measurements (Figure 6.6). Modelled COD_f concentrations decreased similarly to those measured on site, with most of the COD_f removal occurring in the first hour of the aeration period. No COD_f profiles were measured during Study 4PS and thus it cannot be compared to the modelled profiles.

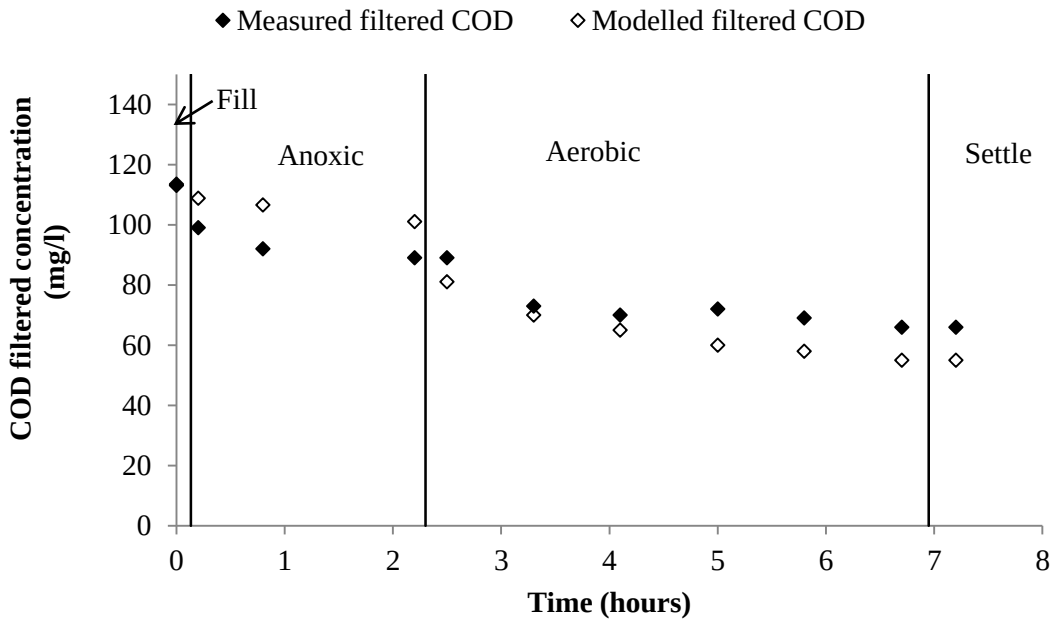

Figure 6.6 – Modelled and measured COD_f results for Study 3PS

Study 3PS and Study 4PS – Nitrogen

Figure 6.7 shows steady-state Nitrogen profile results for Study 3PS. The NH_4-N and NO_3-N modelled profiles almost match the experimental data and the final effluent figure is the same for both the modelled and measured results. NO_3-N trends corresponded well to the measured data. During the anoxic period NO_3-N was reduced from 1mg/l to 0 mg/l which indicates that denitrification took place. The modelled NO_3-N concentrations were slightly higher than the experimental profiles during the aerobic period but the final effluent concentration was almost equal. A possible explanation for the difference between the modelled and measured NO_3-N could be that the DO oxygen conditions were not the same in the model as they were on site. There may have been partial nitrification during periods where oxygen concentrations were lower. However, nitrite was not measured on site and thus this could not be verified. The modelled nitrogen profiles showed a similar trend to the experimental measurements.

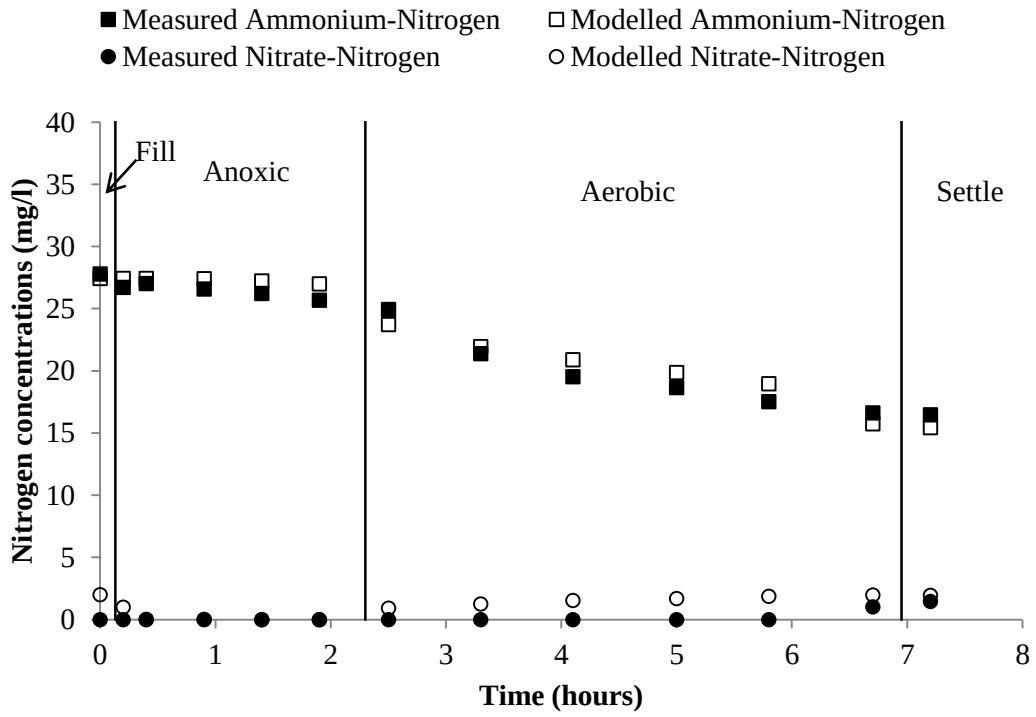

Figure 6.7 – Modelled and measured nitrogen profiles for Study 3PS

Figure 6.8 modelled NH_4-N and NO_3-N concentration profiles for Study 4PS. The nitrogen profiles showed a good fit the between measured and modelled data. As with Study 3PS, modelled NH_4-N removal rates were slightly slower than the experimental

results. NO_3-N trends corresponded well during both the anoxic and aerobic periods and were close to the measured data. During the anoxic period NO_3-N was reduced from 2mg/l to 0.6 mg/l which indicates that denitrification took place. The model appears to be more accurate for Study 4PS. This may be because the modelled DO conditions were closer to Study 4PS than Study 3PS.

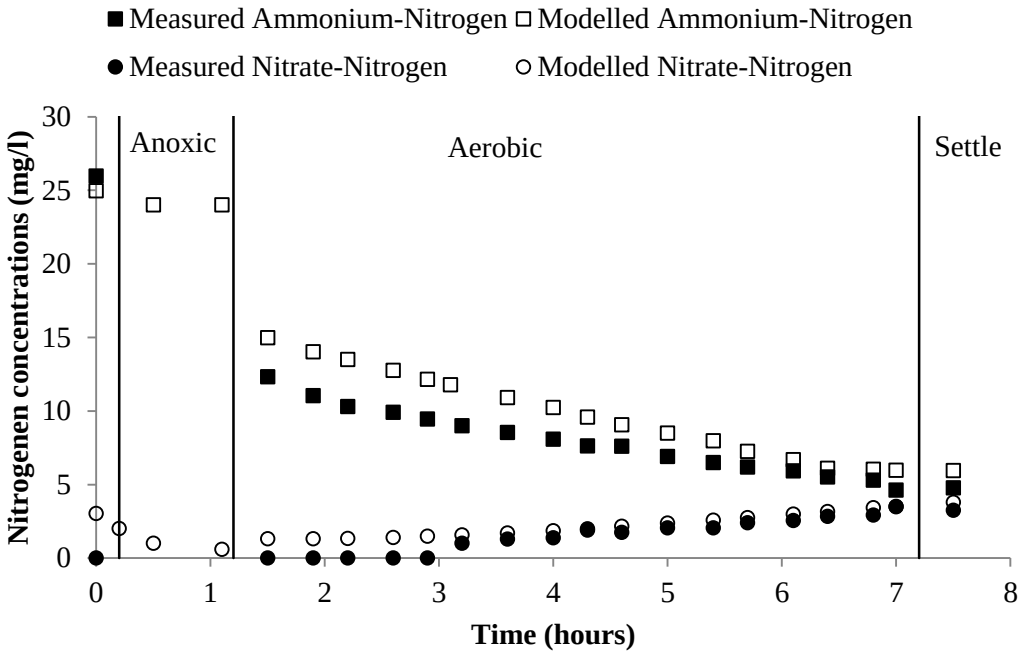

Figure 6.8 – Modelled and measured nitrogen profiles for Study 4PS

A clear improvement in NH_4-N removal was evident between the two phase studies. This can be attributed to three factors: (i) the increase in aeration time from 275 minutes to 360 minutes, (ii) the modelled DO profile shown in Figure 6.4 matching the DO profile in Study 4 more accurately than Study 3, and (iii) the quantity of leachate in the influent being reduced during Study 4 (the presence of landfill leachate in the influent wastewater may have inhibited the growth of nitrifying bacteria).

Denitrification was determined during the two phase studies in the model. There was a disparity however between the measured NH_4-N decrease and the NO_3-N produced. It may be possible that simultaneous nitrification and denitrification (SND) was occurring in the biofilm. However, with no total nitrogen data, it is difficult to know if this was the case.

The results from Study 3PS and Study 4PS show that there is a good fit between the modelled and measured data, and they show similar trends for COD_f, NH_4-N and NO_3-N. The results indicate that the model could be used to predict the PFBR performance under a variety of operating conditions, such as different influent and effluent flow rates, and different aeration times, cycle conditions and wastewater loadings.

6.3.5 Biomass Thickness and Composition

The PFBR model was designed to track the growth of two different types of biomass, autotrophic and heterotrophic bacteria. In the model, the biofilm thickness was assumed to be constant at 200µm (detachment rate equal to biofilm growth velocity uF) in all model studies. The biofilm thickness of 200µm was chosen as previous experimental work carried out estimated the biofilm thickness in Reactor 1 to range from 120µm to 720µm and in Reactor 2, from 50µm to 220µm (Zhan et al, 2006). The process of assuming a constant biofilm thickness in order to calibrate is quite common as such data can be difficult to measure (Bilyk et al., 2008 and Boltz, 2010). Biofilm thickness and its effect on nitrogen concentrations in the PFBR is discussed in Section 6.3.5.1.

In order to check the impacts on model accuracy of a static or dynamic biofilm thickness, an additional model was developed which represented an 'unconfined reactor type', where the biofilm thickness varied over time. In order to calibrate this model, the growth, attachment and detachment rates were adjusted. In order to calibrate the model for the unconfined reactor the following adjustments to the kinetic parameters were necessary (Table 6.18).

Table 6.18 – Differences in kinetic model parameters between confined reactor and unconfined reactor

Parameter (Units)	Confined Reactor	Unconfined Reactor
Heterotrophic specific growth rate (d^{-1})	5	13
Autotrophic specific growth rate (d^{-1})	1	1

Once the model was calibrated, some similar effluent results to the 'confined rector type' were achieved (Table 6.19) (the results in Table 6.19 are average daily results). The biofilm thickness in the unconfined reactor varied from 100µm to 500µm over the 50-day simulation (Figure 6.9). The results are shown in Appendix L. In AQUASIM, it is

possible to put in an upper biofilm thickness in the model to stop the growth of the biofilm when using an unconfined reactor.

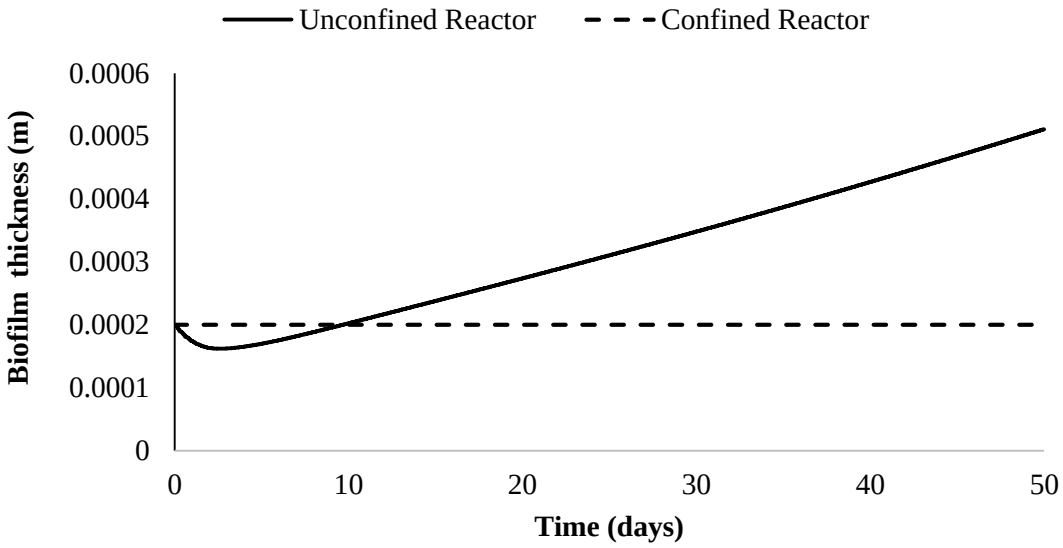

Figure 6.9 – Biofilm thickness in confined and unconfined reactor types

Table 6.19 – Confined vs unconfined reactor modelling results for Study 4AS

Parameters	**Confined Reactor**		**Unconfined Reactor**	
(mg/l)	Effluent	Removal efficiency (%)	Effluent	Removal efficiency (%)
COD_f	45	68	44	69
NH_4-N	11	65	13	59
NO_3-N	1.8	-	0.8	-

The 'confined reactor type' model was the model chosen to perform further studies, as having a constant biofilm thickness is more commonly used in modelling biofilm systems and also because the FS-PFBR1 was assumed to be at steady state.

Figures 6.10 and 6.11 show that the average heterotrophic and autotrophic concentrations follow the same trend in both the bulk fluid and the biofilm. The average autotrophic concentrations in the bulk fluid reached steady state at 10 g/m^3. The average heterotrophic bacteria concentrations reached steady state at 48 g/m^3 for both Study 3 and 4 (Figure 6.10). In the biofilm, the heterotrophs reached a steady state of approximately 1.9 g

COD/m^2 for both Study 3 and 4. The autotrophs reached a steady state of 0.03 g COD/m^2 at 10 days (Figure 6.11).

The PFBR reactors had a working volume of 20.9 m^3. There was approximately 11.5 m^3 of stationary biofilm media modules with a specific surface area of 180 m^2/m^3. In order to calculate the total heterotrophic and autotrophic biomass concentration in the bulk volume in the reactor the heterotrophic concentration of 48 g/m^3 was multiplied by the total volume of wastewater in the reactor (20.9 m^3) and the autotrophic biomass concentration of 10 g/m^3 was also multiplied by the volume of wastewater in the reactor. This gives a total heterotrophic mass of 1003 g and a total autotrophic mass of 209 g in the in the bulk fluid in the reactor.

When the approximate surface area of the biofilm in the reactor (2,070 m^2) was multiplied by the modelled concentrations of heterotrophs and autotrophs (1.9 g/m^2 of heterotrophs and 0.03 g/m^2 of autotrophs) it could be estimated that the heterotrophic biofilm mass was about 3933 g and the autotrophic biofilm mass was 62 g. There was more bacteria in the biofilm than the bulk water which was expected.

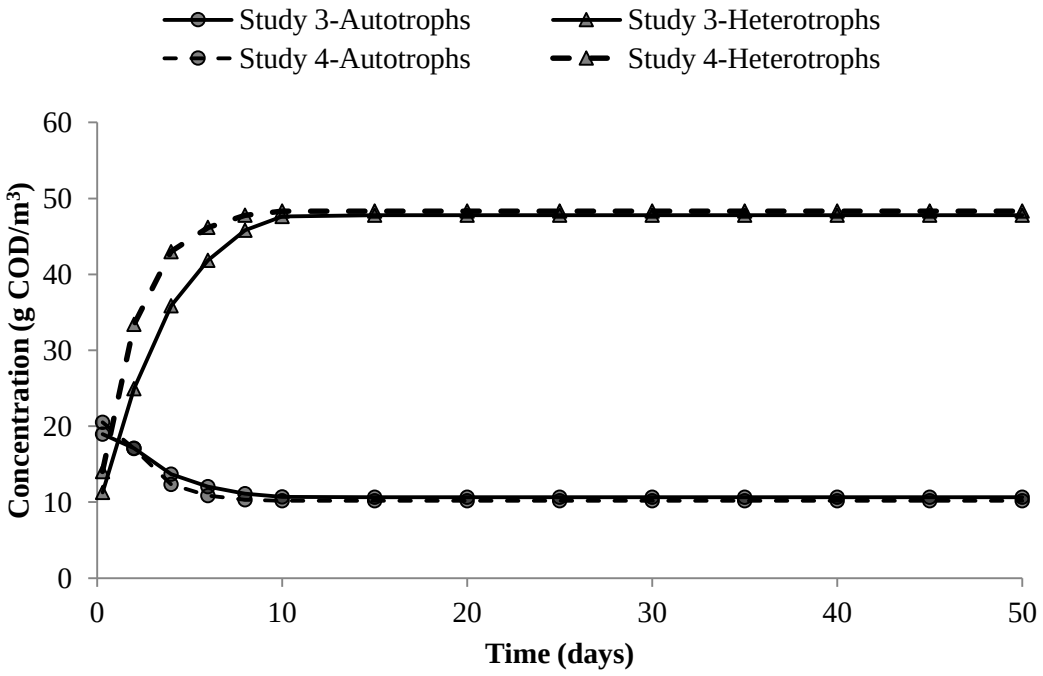

Figure 6.10 – Biomass concentrations in the bulk volume (confined reactor)

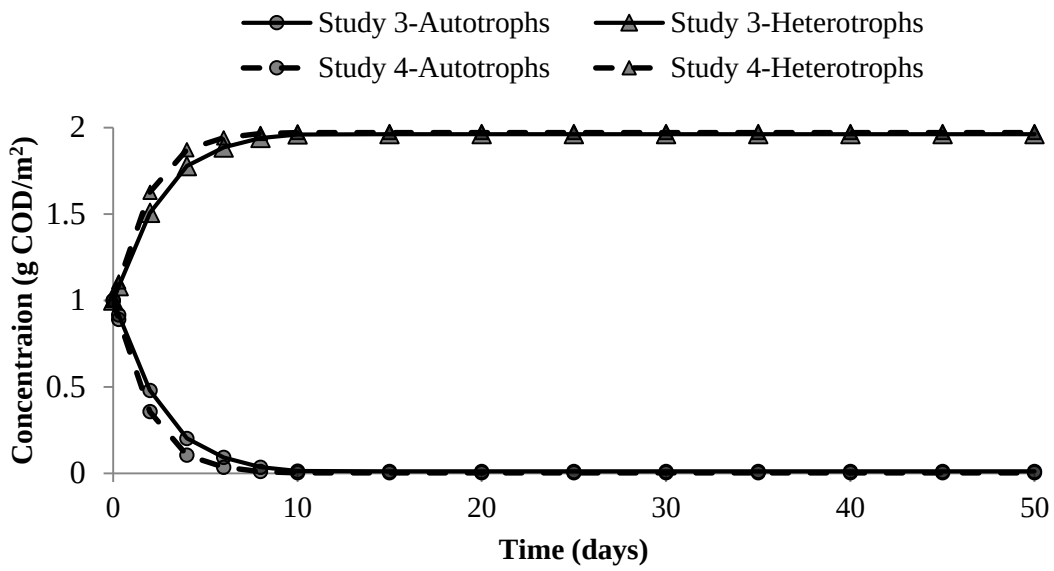

Figure 6.11 – Biomass concentrations per unit biofilm surface area (confined reactor)

In Figures 6.10 and Figure 6.11, the results show that both studies have more or less the same similar concentrations of autotrophs. This was not expected as there was more nitrification in Study 4 than Study 3. The NH_4-N removal efficiency in Study 3AS was 26% compared to 65% in Study 4AS. A possible explanation for this might be the autotrophs are more efficient in Study 4 as there was more DO available. Also, in Study 4 the quantity of landfill leachate in the influent was reduced. The presence of landfill leachate in the influent wastewater may have affected the performance of nitrifying bacteria in Study 3.

6.3.5.1 Effect of biofilm thickness for Study 4

In this exercise, a number of different scenarios were simulated for the PFBR to show the impacts of biofilm thickness on effluent concentrations. One of the main differences between Study 3 and Study 4 was the shorter anoxic period and the longer aerobic period (as described in *Section 3.5.2*). As the NH_4-N discharge concentrations were lower in Study 4 (Table 6.17), this experimental setting was selected as the base study for running different scenarios where only the biofilm thickness that was changed.

Figure 6.12 shows that effluent COD_f concentrations were 45 mg/l with a biofilm thickness under 100 µm. However, when the biofilm thickness was increased to over 100 µm, effluent COD_f concentrations were 40 mg/l. These results show that a thin biofilm can be used effectively for COD_f removal.

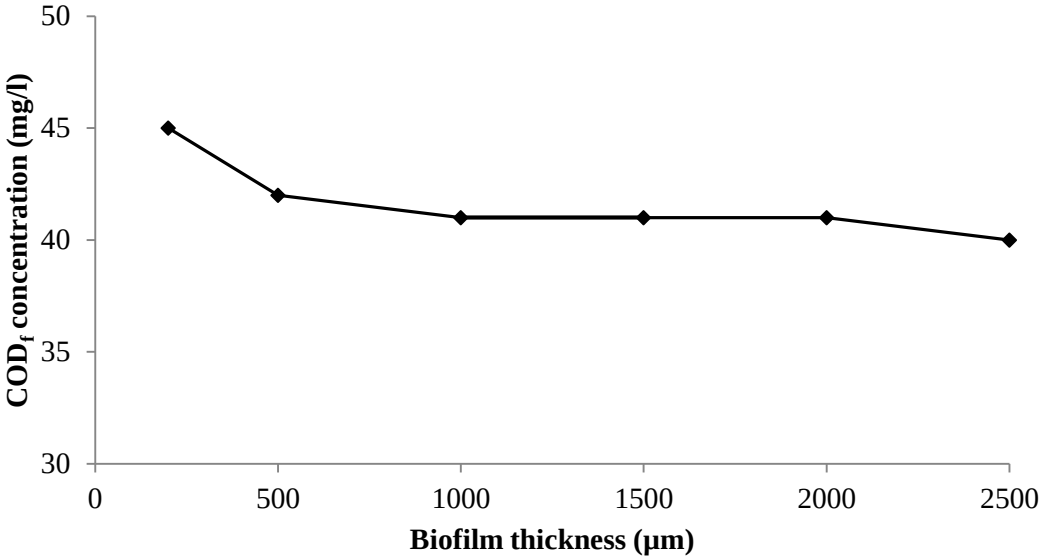

Figure 6.12 – Effect of biofilm thickness on effluent COD_f

The trend for nitrogen removal was quite different to that for COD_f. In the model, it took the biofilm approximately five days before it was capable of nitrifying a significant amount of ammonium and oxidizing it to nitrate. Figure 6.13 presents the impact of varying biofilm thickness on effluent concentrations in the simulations carried out. The overall NH_4-N concentration decreased and the NO_3-N increased as the biofilm thickness was increased. The modelled effluent NH_4-N concentrations were below 4 mg/l when the biofilm thickness was increased to 2500 µm. The modelled effluent NO_3-N concentrations increased from 1.3 mg/l to 6 mg/l, with the biofilm thickness being in the range of 250–2500 µm. These results seem to suggest that a thicker biofilm helped nitrification due to the more autotrophs present.

The total biomass of the two microbial communities at various biofilm thicknesses are given in Table 6.20. With increasing biofilm thickness, the autotroph and heterotroph biomass increased in the reactor. At 200µm, the total nitrifier biomass was very low. However, it increased with increasing biofilm thickness. The heterotroph biomass

followed a similar pattern. The heterotroph/autotroph ratio is also shown in Table 6.20. At a biofilm thickness of 200 µm there is a heterotroph/autotroph ratio of 1:1900. As the biofilm thickness increases to 2500 µm the heterotroph/autotroph ratio changes to 1:3. The thicker the biofilm the more autotrophs present and the more autotrophs present in relation to heterotrophs.

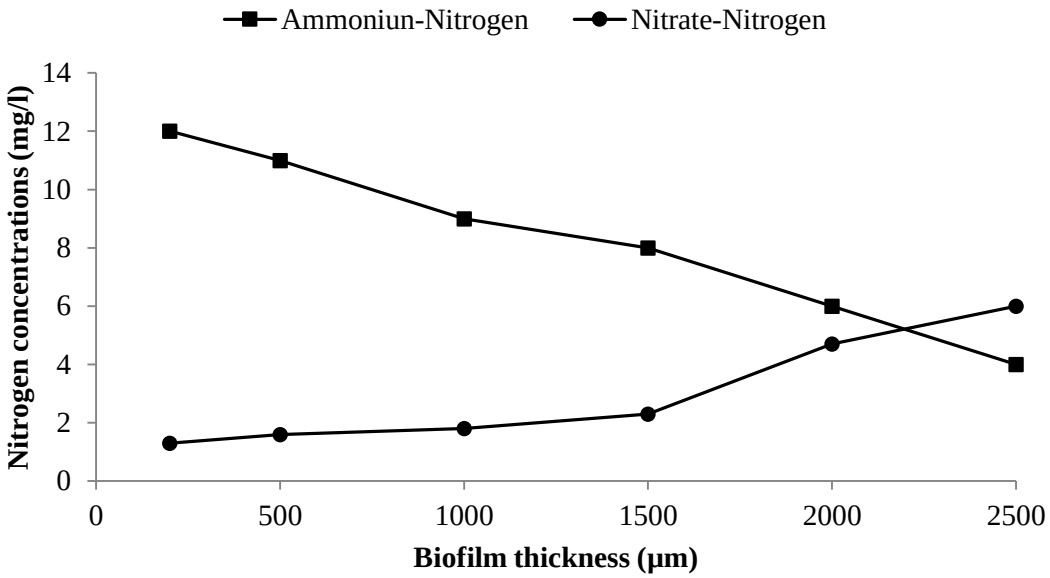

Figure 6.13 – Effect of biofilm thickness on effluent nitrogen concentrations

Table 6.20 – Microbial community concentrations in the reactor for various biofilm thicknesses (Study 4AS)

Biofilm Thickness (µm)	Autotrophs ($gCOD/m^2$)	Heterotrophs ($gCOD/m^2$)	Heterotroph/Autotroph ratio
0	0	0	0
200	0.001	1.9	1900
500	0.003	2	667
1000	1.3	8.5	7
2000	4.93	15	3
2500	6.7	18	3

The results of the model show that the optimum biofilm thickness in the PFBR for nitrification was 2500µm and anything above 100µm for COD_f removal. However, in the case of modelling the PFBR, the biofilm had grown sufficiently after five days to achieve good COD_f removal and good nitrification. For the purpose of modelling the PFBR, a

biofilm thickness of 200μm was chosen as this figure is more realistic to what actually happened in the experimental PFBR.

6.4 CONCLUSIONS

Using the modelling package AQUASIM, the PFBR was modelled in this chapter in order enable the study of cycle performance, biofilm thickness and biofilm composition. The main conclusions from this chapter are:

- The AQUASIM model was successfully used to simulate PFBR performance under a variety of operating conditions, such as different influent and effluent loadings, aeration conditions and cycle conditions.
- Carbon and nitrogen transformations can be simultaneously predicted using the biofilm compartment model.
- It was necessary to model the PFBR by switching off and on air supply in lieu of pumping between two reactors as is the case on-site. This however offered the advantage of a relatively rapid simulation that could be easily adapted to changing input parameters.
- The simulation was used to demonstrate the potential impacts of biofilm thickness on nitrogen concentrations.

7 ADAPTING THE GPS-X AND AQUASIM MODELS FROM FS-PFBR1 TO FS-PFBR2

7.1 INTRODUCTION

In this chapter the GPS-X and AQUASIM models, originally developed for the PFBR plant in Tuam, Co. Galway (FS-PFBR1), were adapted and applied to a full scale PFBR plant in Moneygall, Co. Offaly (FS-PFBR2).

The chapter investigates the potential for (i) using the previously developed simple activated sludge-based model developed in Chapters 4 and 5 and applying it to the FS-PFBR2, and (ii) using the previously developed biofilm based model, as discussed in Chapter 6, and applying it to the FS-PFBR2. The benefits of adapting an existing model rather than creating a new model are:

- there is less chance of error due to the rigorous testing already conducted on the model.
- the calibration process is much simpler and ultimately more reliable.
- it is more cost effective to adapt a generic model.
- the adaptable predictive model may be used as the basis for commercial design software.
- it demonstrates the robustness of the existing model as it can be easily applied to a new scenario.

The steps applied in building and calibrating the FS-PFBR1 models in Chapters 5 and 6 and are applied to FS-PFBR2 to investigate if the models work effectively and efficiently when applied to a different PFBR installation; thus making each model more applicable for further site installations.

7.2 MODEL DEVELOPMENT

7.2.1 Modelling Description

The methodology used and applied to the development of a new model for FS-PFBR2 was based on lessons learned in the previous chapters and on the series of generic steps described in *Section 4.2.1*.

FS-PFBR2 operated under one cycle regime (Study 5). In each study, a typical treatment cycle comprised fill, anoxic, aerobic and settle stages of varying lengths (as described in *Section 3.6.2*) (Table 7.1).

Table 7.1 – Operational stages of FS-PFBR2

PFBR Stage	Duration (minutes)
Fill (t_1)	7
Anoxic (t_2)	30
Aeration (t_3)	280
Settle(t_4)	13
Draw (t_5)	7
Total cycle time	337

Table 7.2 shows the physical dimensions of the SBR reactors used in the FS-PFBR2 model and on site. Each reactor chamber of FS-PFBR2 had a working volume of 42.2 m^3.

Table 7.2 – Physical design parameters (measured and modelled)

Physical Dimensions	Size
Surface area of tanks	12 m^2
Maximum water level height	3.5 m

7.3 MODELLING FS-PFBR2 USING GPS-X

ASM1 was chosen to calibrate FS-PFBR2 as the model was only concerned with COD and N removal. The model calibration process was initiated with all the ASM1 values set to the values that were used for the calibration of FS-PFBR1 (as described in *Section 5.3.2 and Section 6.3.2*).

The following steps were employed for the calibration of FS-PRBR2:

1. The operation of the FS-PFBR2 was examined to select a period of relatively stable operation, i.e. steady-state operation.
2. The GPS-X simulator was configured and set up in accordance with the design parameters of the FS-PFBR1 models.
3. The operation of the FS-PFBR2 was examined to prepare preliminary input variables and to prepare a preliminary calibration of the model parameters.
4. The model was run for FS-PFBR2 to examine how accurately the predicted results matched the plant performance in terms of treated effluent quality predictions.

5. The model's inputs and model calibration were refined as required to improve its accuracy in relation to the plant's predictive output data.

7.3.1 System characteristics and hydraulics

The layout of the FS-PFBR2 model was similar to FS-PFBR1 model; however, the eight input control files were adjusted as required to simulate operating conditions in FS-PFBR2 (Table 7.3).

Table 7.3 – Input control files and times for one complete cycle in Study 5

			Influent	Mixing on/off R1	K_La R1	Mixing on/off R2	Pump 1	K_La R2	Pump2	Discharge
		t	qinrawinf	mixconzover1	klaconzover1	mixconzover2	qinzpump1	klaconzover2	qconzpump2	frzpump2toeff
		min	m^3/min		d^{-1}		m^3/min	d^{-1}	m^3/min	
Fill		1-7	*4.5	**1	0	0	0	0	0	0
Anoxic		8-38	0	0	0	0	0	0	0	0
Aerobic	**Transfer to R2**	39	0	0	0	1	****42	122	0	0
	Aerobic R2	40-79	0	0	0	0	0	122	0	0
	Transfer to R1	80	0	1	***122	0	0	0	42	0
	Aerobic R1	81-119	0	0	122	0	0	0	0	0
	Transfer to R2	120	0	0	0	1	42	122	0	0
	Aerobic R2	121-159	0	0	0	0	0	122	0	0
	Transfer to R1	160	0	1	122	0	0	0	42	0
	Aerobic R1	161-199	0	0	122	0	0	0	0	0
			The aerobic sequence and recycling between R1 and R2 continued for 280 minutes							
Settle		320	0	0	0	0	0	0	0	0
Draw		337	0	0	0	0	0	0	42	0.75

* The average volume/cycle for Study 5 was 42 m^3. At the start of a cycle, there was 10 m^3 in R1 so 32 m^3 was required to fill the tank. A flow of 4.5 m^3/min for 7 minutes, which equates to 32 m^3, was used to fill the tank to 42 m^3.

** The number 1 was used as this turned on the mixing in R1.

*** This is the K_La value used.

**** This is the total volume of wastewater in the reactors, 42 m^3.

***** At the end of each cycle, 32 m^3 of wastewater was decanted and 10 m^3 was recycled back to R1 in preparation for the next treatment cycle. 0.75 is the percentage of wastewater recycled back to R1.

Figure 7.1 shows the wastewater sequence for one complete cycle in FS-PFBR2.

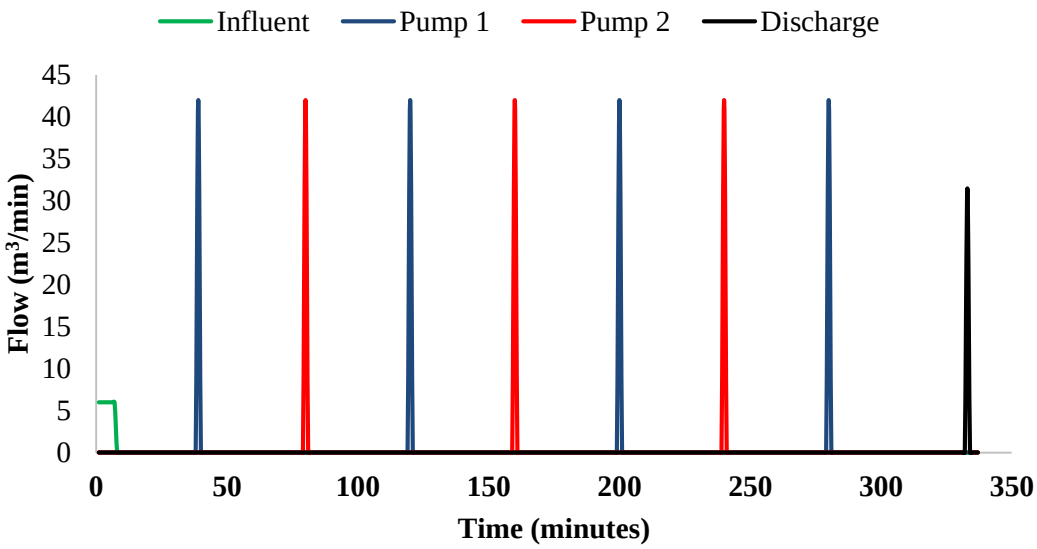

Figure 7.1 – Wastewater flows in FS-PFBR2

7.3.2 Wastewater Characteristics

The influent wastewater comprised both storm water and municipal wastewater (as described in *Section 3.6.3*). The system was modelled in steady-state mode (i.e. using average influent concentrations during the experimental period). The influent characteristics of the modelled wastewater were estimated using this measured data. Using Influent Advisor in GPS-X, a detailed overview of the influent was developed for the model (Table 7.4) (only non-zero components are shown. The full Influent Advisor is shown in Appendix E).

Table 7.4 – Influent composition modelled using influent advisor in GPS-X

Parameters	Units	Measured	Modelled
Biological Model: ASM1			
Influent Composition			
total COD	g COD/m^3	143	143
total nitrogen	g N/m^3		15.2
Nitrogen Compounds			
free and ionized ammonia	g N/m^3	10.3	10.6
Alkalinity			
alkalinity	mole/m^3		7
Influent Fractions			
XCOD/VSS ratio	g COD/g VSS		1.8
BOD_5/BODultimate ratio	-		0.66
TSSCOD Model Coefficients			
inert fraction of soluble COD	-		0.2
substrate fraction of particulate COD	-		0.82
heterotrophic fraction of particulate COD	-		0
ammonium/TKN ratio	-		0.7
particulate organic N/total organic N ratio	-		0.15
VSS/TSS ratio	g VSS/g TSS		0.6
ASM1 Nutrient Fractions			
N content of active biomass	g N/g COD		0.086
N content of endogenous/inert mass	g N/g COD		0.06

7.4 RESULTS AND DISCUSSION

7.4.1 Dissolved Oxygen

The model was checked to ensure the modelled oxygen data matched the measured oxygen data. The dissolved oxygen concentrations were modelled by using diffused air and entering a K_La value of 122 d^{-1} (this was the same K_La value used in FS-PFBR1). The models were initially run to ensure that the oxygen profiles from the experimental and modelled data correlated well.

Figure 7.2 shows a comparison between the modelled and measured DO data for a full PFBR cycle in FS-PFBR2. The DO concentrations were over estimated by the model but showed a similar pattern. As previously discussed in Chapter 5 the K_La did not have a huge bearing on the effluent parameter concentrations once there was enough DO in the system and the stoichiometric and kinetic parameters were adjusted to meet the measured effluent data. This is discussed in detail in Chapter 8. For the purpose of this study, the K_La value remained at the measured value of 122 d^{-1} in the model as it was found not to

have a significant bearing on effluent concentrations once calibration was carried out correctly. Also there was no site data available to characterise this. The main aim was to get a good match between the measured and modelled COD_t, NH_4-N and NO_3-N rather than having a perfect match for the DO.

It was necessary to make assumptions relating to the K_La value in FS-PFBR2 that could not be supported by experimental data in order to model oxygen profiles.

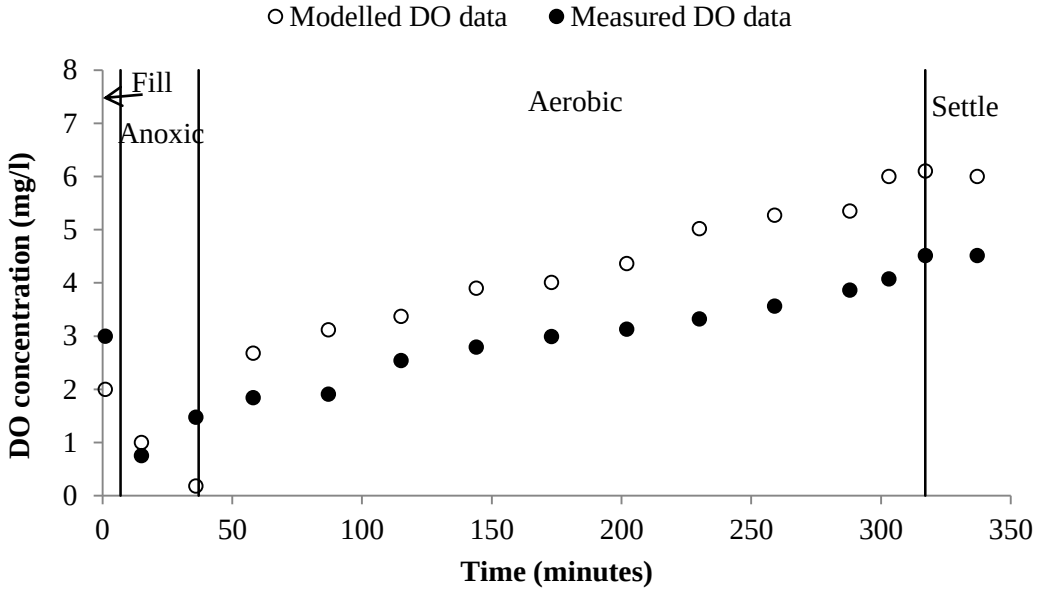

Figure 7.2 – Modelled and measured DO data for FS-PFBR2

7.4.2 Kinetic and Stoichiometry Results

Initially the calibrated kinetic and stoichiometric parameters from FS-PFBR1 (as described in *Section 5.3.2*) were applied to this model FS-PFBR2.

The initial model was initially run for 50 days to check whether modelled COD and ammonium removal was satisfactorily accurate when compared to experimental results. After this initial run further model calibration was required and the following parameters were chosen to be adjusted as these were the parameters that were most sensitive to model calibration in the previous chapters (as described in *Section 4.3.2 and Section 6.3.2*); namely:

- heterotrophic growth rate (μH)
- heterotrophic yield (Y_H)
- autotrophic growth rate (μ_A)

- autotrophic yield (Y_A)

The initial model run showed that COD_t removal was under estimated. In order to increase the accuracy of the model, Y_H was adjusted gradually from 0.666 g COD/g COD to 0.75 g COD/g COD. At an Y_H of 0.666 g COD/g COD the effluent COD_t was 28.1 g COD/g COD however this decreased to 24.8 g COD/g COD when Y_H was adjusted upwards to 0.75 g COD/g COD (Figure 7.3). The lower Y_H led to a decrease in heterotrophic biomass and therefore a decrease in COD_t removal. When Y_H was adjusted, the effluent COD_t calibrated immediately. The heterotrophic growth rate (μH) was not adjusted as this parameter was already at the upper end of the accepted literature range.

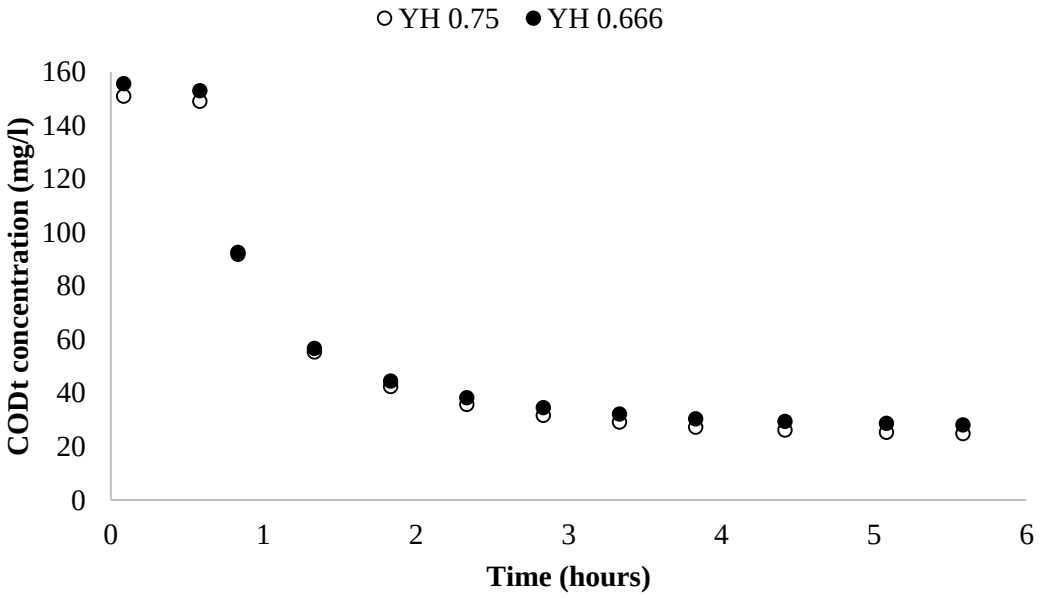

Figure 7.3 – Effluent COD_t at Y_H 0.75 g COD/g COD and at Y_H 0.666 g COD/g COD

The next step in the calibration of the model was to compare modelled NH_4-N removals with experimental NH_4-N removals. The initial model configuration predicted a lower rate of ammonium removal than that observed experimentally. Therefore, further work was necessary to refine the model. The autotrophic yield (Y_A) was adjusted to 0.25 g COD/g N. This increase in Y_A led to an increase in autotrophic biomass and therefore an increase in ammonium removal. This figure was still within the literature range of 0.07 g COD/g N to 0.28 g COD/g N for autotrophic yield. μA was not adjusted as this parameter was already at the upper end of the accepted literature range. In order to calibrate the

model for FS-PFBR2, the following adjustments to the kinetic and stoichiometric parameters were necessary (Table 7.5).

Table 7.5 – Differences in stoichiometric and kinetic model parameters between FS-PFBR1 and FS-PFBR2

Parameter (Units)	FS-PFBR1	FS-PFBR2
Heterotrophic maximum specific growth rate (d^{-1})	13.2	13.2
Autotrophic maximum specific growth rate (d^{-1})	1.0	1.0
Heterotrophic yield (g COD/g COD)	0.666	0.75

The calibration of FS-PFBR2 corresponded with previous literature as only a number of key parameters needed to be changed to ensure model calibration (Hauduc et al., 2011).

7.4.3 Experimental and Modelled Results

Table 7.6 summarises the measured and modelled results for Study 5. The average measured removal efficiency for COD_t was 83%, which compared well with a modelled removal efficiency of 82%. Similarly, an acceptable agreement between the measured and predicted waste treatment efficiency was observed for NH_4-N and NO_3-N. There was no phase study data available for Study 5.

Table 7.6 – Measured and modelled results for FS-PFBR2. Standard deviations in ()

Parameters	Measured Data			Modelled Data		
(mg/l)	Influent	Effluent	% removal	Influent	Effluent	% removal
COD_t	143 (68.3)	24 (8.4)	83	143	25	82
NH_4-N	10.3 (2.5)	3.0 (1.2)	71	10	4.4	59
NO_3-N	-	5.1 (1.5)	-	-	3.3	-

The results from a two day simulation on COD_t effluent concentration are shown in Figure 7.4. The dynamic simulation compared well with what would be expected from measured data.

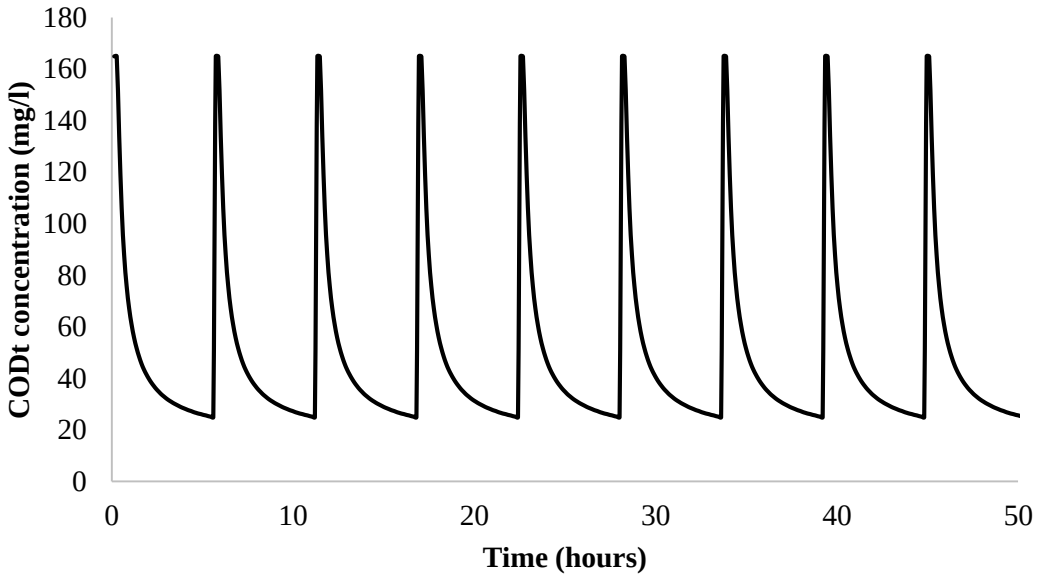

Figure 7.4 – Modelled dynamic simulation for COD_t

7.5 MODELLING FS-PFBR2 USING AQUASIM

Similarly to FS-PFBR1, the FS-PFBR2 was modelled using ASM1 and the endogenous respiration processes from ASM3 (as described in *Section 6.3.2*). The model calibration process was initiated with all the ASM values set to the values that were used for the calibration of FS-PFBR1 (as described in *Section 6.3.2*).

7.5.1 Hydraulics

The model was implemented as one single biofilm reactor. In the model, the influent and effluent flows were denoted as Qinf and Qeff respectively, and were multiplied by the terms t_inon and t_outon as described in Table 6.9 in Chapter 6. The influent flow was modelled by turning Qinf on for 7 minutes at the beginning of the cycle and then switching it off for the remainder of the cycle. Then at 330 minutes Qeff was switched on for 7 minutes and then turned off. The times to turn on and off Qinf was controlled by the parameter t_inon. The times to turn on and off Qeff was controlled by the parameter t_outon. This process was repeated for each cycle, which allowed the wastewater to enter and leave the reactor. The anoxic and aerobic period was replicated by switching on and off the dissolved oxygen parameter (t_airon). The input control times used for Study 5 are shown in Table 7.7.

Table 7.7 – Input control times for one complete cycle in Study 3

Qinf on/off		Qeff on/off		DO on/off R1	
t_inon	on (1) off (0)	t_outon	on (1) off (0)	t_airon	on (1) off (0)
time (days)		time (days)		time (days)	
0	0	0	0	0	0
0.001	1	0.001	0	0.025	0
0.005	1	0.228	0	0.026	1
0.006	0	0.229	1	0.22	1
0.234	0	0.233	1	0.221	0
		0.234	0	0.234	0

The inflow into FS-PFBR2 was 42m^3 per cycle. The influent and effluent flow patterns simulated using AQUASIM for one cycle are shown in Figure 7.5.

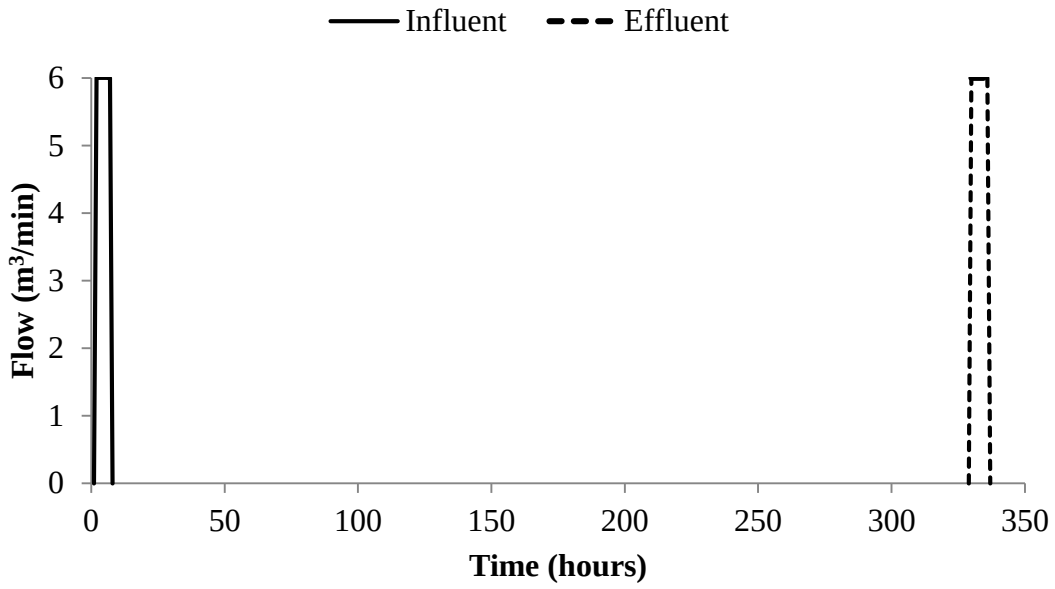

Figure 7.5 – Influent and effluent flow pattern for a cycle in FS-PFBR2

7.5.2 Wastewater Characteristics

The data on the known influent characteristics (COD and nitrogen) for Study 5 were specified in the AQUASIM model. The main carbonaceous and nitrogenous influent characteristics for this study are given previously in Section 7.3.2.

7.6 RESULTS AND DISCUSSION

7.6.1 Dissolved Oxygen

A K_La value of 35 d^{-1} was used as this is what was used in FS-PFBR1. The DO was modelled the same way as FS-PFBR1 (as described in *Section 6.3.1*). The aeration period for a full PFBR cycle in FS-PFBR2 shows the aeration switching on at 37 minutes and switching off again at 317 minutes (Figure 7.6).

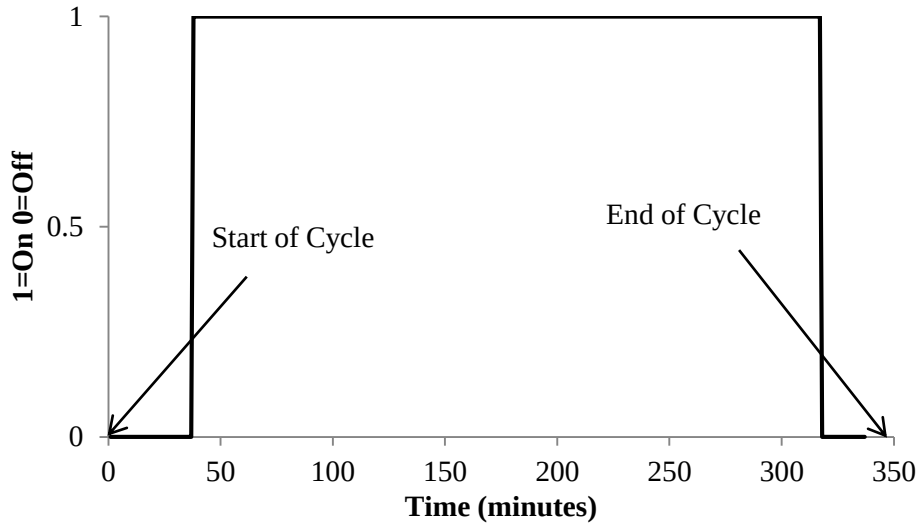

Figure 7.6 – Aeration Switch

Figure 7.7 shows a comparison between modelled and measured DO data for a full cycle in FS-PFBR2. A more accurate DO profile was achieved in AQUASIM than in GPS-X, which might explain the improved modelled effluent results achieved in AQUASIM (Table 7.9). A number of simulations were carried out in AQUASIM to examine the sensitivity of oxygen in relation to the effluent results. These simulations are discussed in detail in Chapter 8.

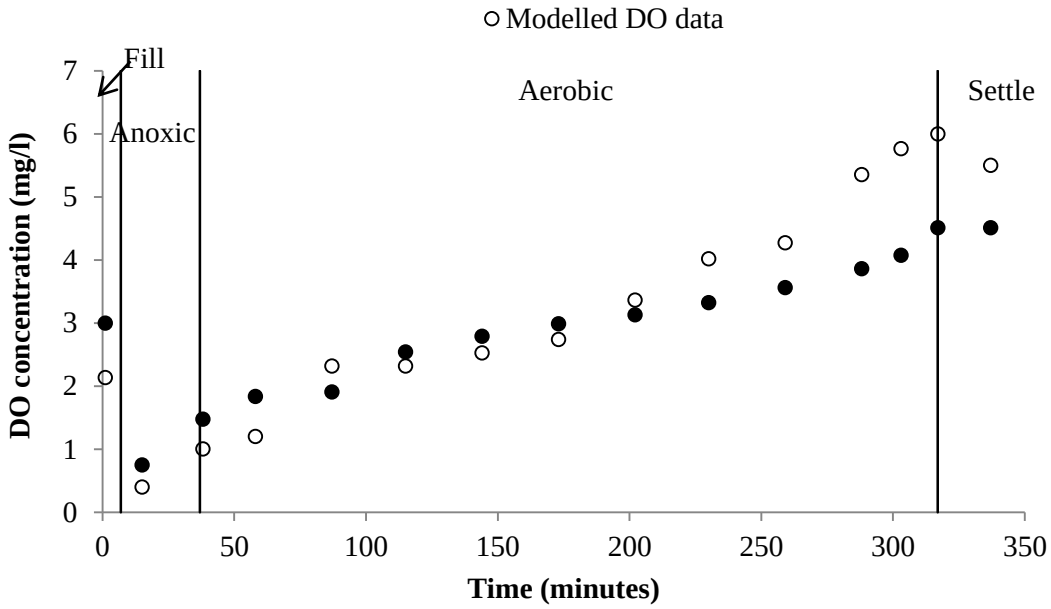

Figure 7.7 – Modelled and Measured DO data

7.6.2 Kinetic and Stoichiometry Results

The initial model run in FS-PFBR2 showed that COD removal was satisfactorily achieved. The μH figure used to calibrate the model was 5 d^{-1} (this figure is within the literature range of 0.6 – 13.2 d^{-1} for a heterotrophic growth rate).

Initially the model did not accurately predict the ammonium removal performance of the PFBR. The initial model configuration predicted a lower rate of ammonium removal than what was observed experimentally. Therefore Y_A was adjusted gradually from 0.09 g COD/g N to 0.19 g COD/g N until a match between measured and modelled results was achieved in order to increase the amount of ammonium removal. This final figure was within the literature range of 0.07 g COD/g N to 0.28 g COD/g N for autotrophic yield.

7.6.3 Biofilm Thickness and Composition

The geometric data for the FS-PFBR2 and the biofilm were specified in the model, as per Table 7.8.

Table 7.8 – FS-PFBR2 physical dimension data of the PFBR and the biofilm characteristics

Term	Description	Value	Units
V_CNitri	Reactor liquid volume	42	m^3
Af_CNitri	Biofilm surface area	15130	m^2
Lf_Tot	Biofilm thickness	0.0002	m
Ll	Boundary layer thickness	0.0001	m
	Reactor Volume	42	m^3

In the model, the biofilm thickness was assumed to be constant at 200 µm (i.e. the cell detachment rate is equal to biofilm growth velocity, uF; therefore, the net growth of microorganisms is zero).

The results should be reviewed to ensure that this was the case. If not the case, then the rate constants (growth rate, decay rate and hydrolysis rate) should be reviewed. Additionally, the time variable (t) should be reviewed to ensure the rate constants all had the same units (days). Where the biofilm thickness was constant, there was zero accumulation of biomass and the system was in steady-state operation.

As for FS-PFBR1 the PFBR model was designed to track the growth of two different types of biomass, autotrophic and heterotrophic bacteria. Figures 7.8 and 7.9 show that the heterotrophic and autotrophic concentrations follow the same trend in both the bulk fluid and the biofilm.

In the model, the autotrophic concentrations in the bulk fluid drop quite quickly early in the simulation, but recover after about 11 days and reach a steady state at 11 g COD/m^3. Simultaneously, there is immediate growth in the heterotrophic bacteria, and it reaches a steady state of 63 g COD/m^3 (Figure 7.8). In the biofilm, the heterotrophs reached a steady state of approximately 1.8 g COD/m^2 and the autotrophs reached a steady state of 0.03 g COD/m^2 at 10 days (Figure 7.9).

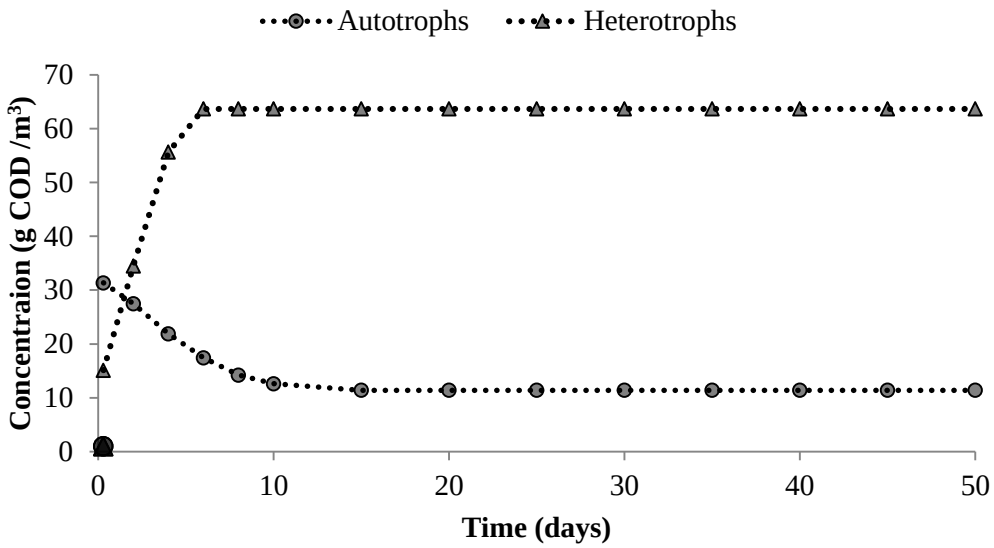

Figure 7.8 – Biomass concentrations in the bulk (confined reactor)

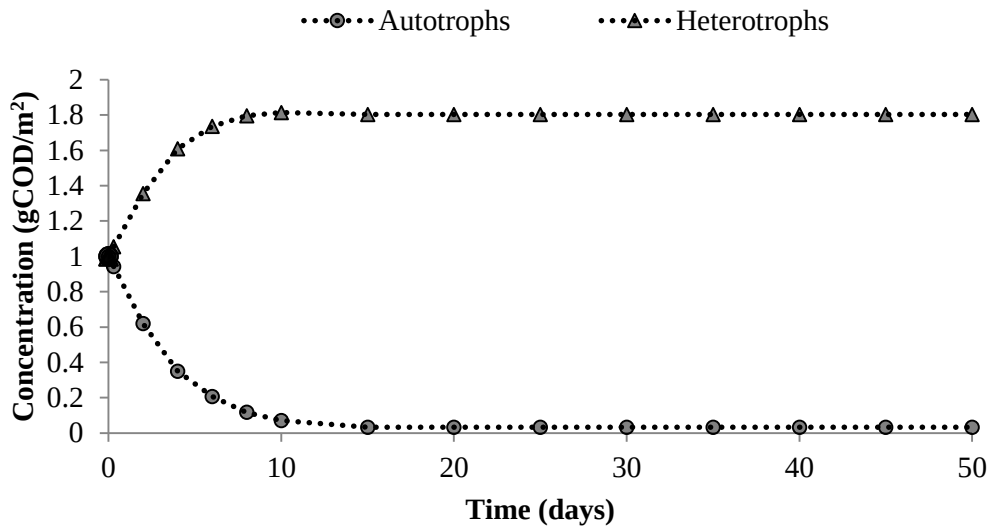

Figure 7.9 – Biomass concentrations in the biofilm (confined reactor)

7.6.4 Experimental and Modelled Results

The results in Table 7.9 show that there is good agreement between the measured and modelled results for the calibrated model. The average measured removal for COD_t was 83%, which compared well with a modelled removal of 79%. The experimental removal efficiency for NH_4-N was 71% and the modelled result was 69%. Similarly, an acceptable agreement between measured and modelled results was observed for NO_3-N.

Table 7.9 – Measured and modelled results for FS-PFBR2

	Measured Data			Modelled Data		
(mg/l)	Influent	Effluent	% removal	Influent	Effluent	% removal
COD_t	143 (68.3)	24 (8.4)	83	143	29	79
NH_4-N	10.3 (2.5)	3.0 (1.2)	71	10.3	3.2	69
NO_3-N	-	5.1 (1.5)	-	-	3.3	-

The AQUASIM model appears to be more accurate for NH_4-N removal than GPS-X. This could be due to the modelled DO conditions being closer in AQUASIM than in GPS-X.

7.7 COMPARISON OF MODEL PARAMETERS IN GPS-X AND AQUASIM

The differences between the stoichiometric and kinetic model parameters in GPS-X and AQUASIM are shown in Table 7.10. The greatest variance was between the heterotrophic growth rates, 13.2 d^{-1} in GPS-X and 5 d^{-1} in AQUASIM. The default for the heterotrophic growth rate in GPS-X was 6 d^{-1}; however, this had to be increased to 13.2 d^{-1} in GPS-X in order to achieve good calibration. It is important to note that all the kinetic and stoichiometric parameters were kept within the literature ranges. It is not clear why there is a difference between the two sets of figures, but it is probably due to two different pieces of modelling software being used.

Table 7.10 – Differences in stoichiometric and kinetic model parameters between GPS-X and AQUASIM

Parameter (Units)	GPS-X	AQUASIM
Heterotrophic maximum specific growth rate (d^{-1})	13.2	5
Autotrophic maximum specific growth rate (d^{-1})	1.0	1.0
Heterotrophic yield (g COD/g COD)	0.75	0.54
Autotrophic yield (g COD/g N)	0.25	0.19
Heterotrophic decay rate (d^{-1})	0.62	0.1
Autotrophic decay rate (d^{-1})	0.04	0.05

The heterotrophic maximum specific growth rate was higher in GPS-X than in AQUASIM. The explanation for this could possibly be the fact that in GPS-X the PFBR was modelled as an activated sludge unit whereas in AQUASIM the PFBR was modelled as a biofilm unit.

The heterotrophic yield in GPS-X was adjusted as the heterotrophic growth rate was already at the upper end of the accepted literature range. In GPS-X the heterotrophic yield

was high at 0.75 g COD/g COD. The high heterotrophic yield could be due to the fact that other organisms could have contributed to the carbon removal, such as phosphorus accumulating organisms (PAOs) and these were modelled as heterotrophs and therefore led to a high heterotrophic yield (Gray, 2004). In the model only heterotrophs and autotrophs were modelled and no other type of microorganism, this is not the case in the PFBR or indeed any other type of wastewater treatment plant as other microorganisms would also be present.

7.8 CONCLUSION

This study examined the application of the existing FS-PFBR1 AQUASIM and GPS-X models to a PFBR system installed at Moneygall, County Offaly. The objective of the study was to assess the ability of the models to predict the treated effluent quality of the Moneygall PFBR by adapting existing models. By carrying out this process, it was hoped to achieve a more universal PFBR model that can be used in commercial applications, end user design products and licensing in the future.

This chapter investigated the possibility of (1) using the previously developed simple activated sludge-based model developed in Chapter 5 and adapting it to FS-PFBR2, and (2) using the previously developed biofilm-based model discussed in Chapter 6 and adapting it to FS-PFBR2.

The main conclusions are:

- This work shows that it is possible to apply a GPS-X model originally designed for a specific plant (FS-PFBR1) to a similar PFBR plant (FS-PFBR2) by following a sequence of steps to modify, calibrate and validate the original model against new experimental data. The new model was then applied to accurately predict the treated effluent quality of the new plant.
- The existing GPS-X model developed for FS-PFBR1 was successfully adapted to predict the treated effluent quality of FS-PFBR2.
- The existing AQUASIM model developed for FS-PFBR1 was successfully adapted to predict the treated effluent quality of FS-PFBR2.
- These models could be applied to future experimental and pilot scale units for design purposes.

- The models could be used to run different scenarios to predict the optimal scenario, i.e. contaminants removed using the minimum of inputs (cost of energy).
- The models could be used to enhance and improve reactor operation and inform future studies.
- It is recommended that further experimental work be carried out estimating the exact K_La of FS-PFBR2.

The ability of the models were assessed based on the two software programs used to predict the treated effluent quality of FS-PFBR2 and the results show that once a PFBR model is built and calibrated correctly, it can be easily adapted and applied to other PFBR plants. This demonstrates that the model presented in this study is sufficiently adaptable, making the technology more accessible and attractive to stakeholders in the wastewater treatment sector.

A generic model has now been developed for the PFBR that is more cost effective than initiating a new model for every new WWTP. Further work will focus on improving model results by modelling the experimental measurements of biofilm mass and applying the model to a wider range of field scale systems.

8 UNCERTAINTIES ENCOUNTERED IN WWTP MODELLING

8.1 INTRODUCTION

This Chapter investigates some of the modelling uncertainties that were encountered while undertaking this research.

The five main causes of uncertainty identified during this thesis were:

1. modelling the hydraulics of new technologies
2. modelling the passive aeration process in new technologies
3. modelling new technologies with minimal performance datasets
4. accurate undertaking/execution of the calibration process
5. scaling up laboratory-scale data to full-scale models

This chapter describes the method used to model process hydraulics and the passive aeration process and discusses the accuracy and uncertainty surrounding these parameters. This chapter also discusses different types of calibration required in modelling and also the importance of influent characterisation. The issue of scaling up laboratory-scale data to full-scale models was also addressed. Finally the PFBR was modelled using both GPS-X and AQAUSIM and a comparison of these modelling packages is presented.

8.2 MODELLING THE HYDRAULICS OF NEW TECHNOLOGIES

At the beginning of this project it was anticipated a challenging aspect of developing a model for the PFBR, and many new emerging technologies, would be to accurately represent the hydraulics of the process. The GPS-X models used two linked SBR objects to simulate the hydraulics of the PFBR accurately; however this was only possible using an activated sludge model.

In the AQUASIM system, a single biofilm reactor compartment (BRC) was used to model the PFBR. Only one reactor was used as the BRC is a constant volume reactor and does not allow water to be transferred in and out of the reactor therefore a single biofilm reactor compartment was employed. There was no transference of water in or out of the reactor as the AQUASIM does not allow for this, instead oxygen was switched on and off to simulate the different stages of the PFBR.

The hydraulics of the PFBR for both GPS-X and AQAUSIM are shown in Figure 8.1 and 8.2.

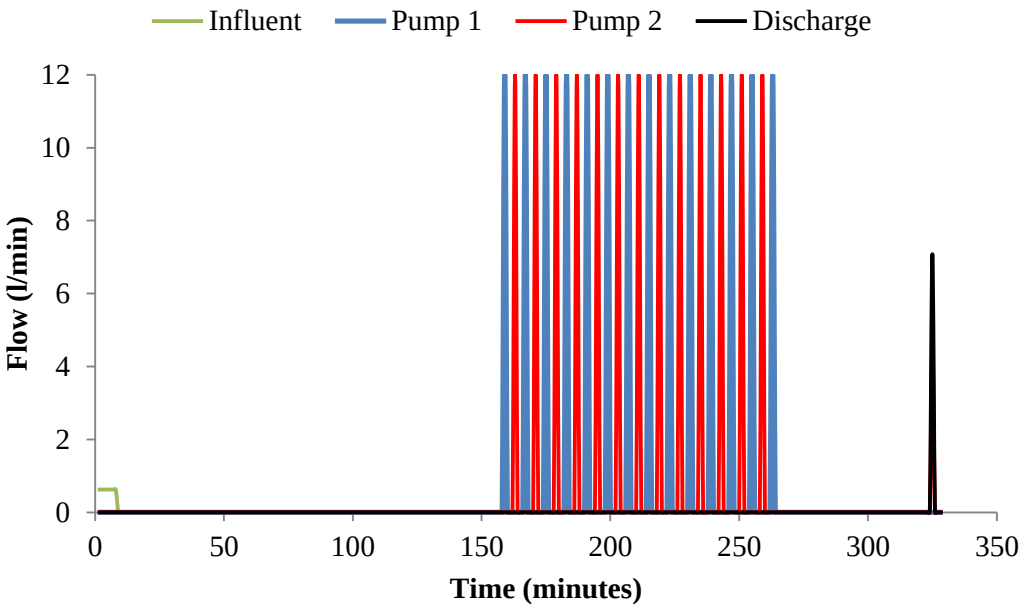

Figure 8.1 - Wastewater flows in GPS-X for LS-PFBR1

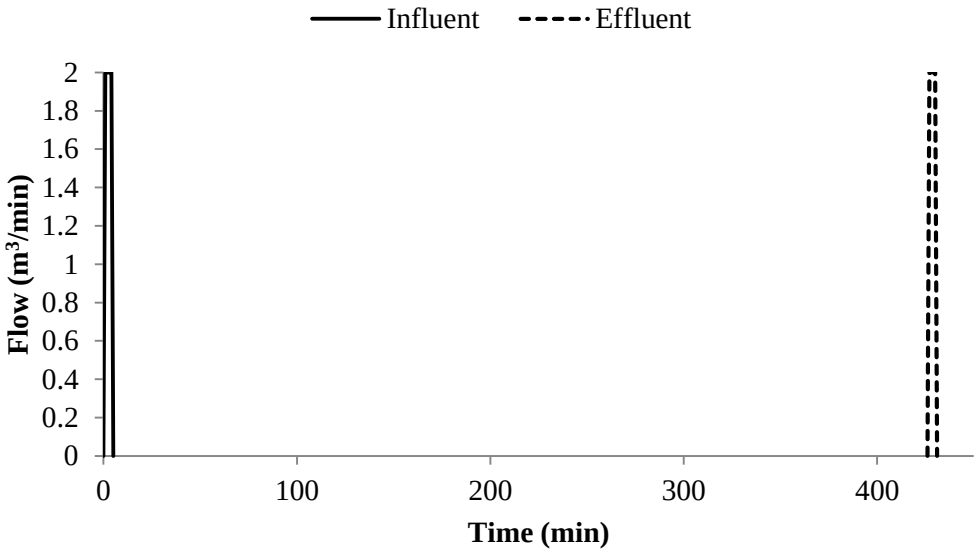

Figure 8.2 – Wastewater flows in AQUASIM for FS-PFBR1

While it was good/useful to have the hydraulics working correctly for the GPS-X model, it was shown in the AQUASIM model that having the hydraulics working correctly was not critical to successful model calibration. The hydraulic layout of the GPS-X and AQAUSIM models were different, however good effluent results were achieved for both

models. In each model the cycle time, anoxic period, aerobic period and settle period and daily influent and effluent volumes were sufficient to ensure accurately calibrated models.

8.3 MODELLING THE PASSIVE AERATION PROCESS IN NEW TECHNOLOGIES

The passive aeration process in the PFBR is central feature of the technology. Due to the nature of passive aeration systems it can be challenging to experimentally determine oxygen transfer rates. In this study experimental data on oxygen transfer was limited and thus a number of assumptions had to be made on oxygen transfer rates. This section discusses the impact of this on model calibration.

8.3.1 GPS-X Model

In the GPS-X model, a K_La value of 122 d^{-1} was used for both the laboratory and field scale models. The models were run to ensure that oxygen profiles from experimental and modelled data correlated well for both the laboratory and field scale study however there was not an exact match between the modelled and measured DO data for the field scale model when using a K_La value of 122 d^{-1} as described in *Section 5.3.1*.

To determine if accurately simulating oxygen concentrations would impact on model accuracy or calibration a number of simulations were run in the model to determine the effect that the K_La value had on effluent concentrations. Six simulations were carried using the data from Study 4 in FS-PFBR1. In these simulations K_La values of 10 d^{-1}, 35 d^{-1}, 50 d^{-1}, 100 d^{-1}, 122 d^{-1} and 200 d^{-1} were in turn applied to the model and the impacts on modelled effluent COD_f, NH_4-N and NO_3-N concentrations analysed. As expected increasing K_La values increased overall DO concentrations (Figure 8.3) in the model, however these increases did not have a major bearing on the effluent parameter concentrations once K_La value was above 50d^{-1} and once calibration was carried out.

Figure 8.3 shows the relationship between the K_La values of 10 d^{-1}, 35 d^{-1}, 50 d^{-1}, 100 d^{-1}, 122 d^{-1} and 200 d^{-1} and the measured DO data. The K_La value of 35 d^{-1} was the most applicable in terms of measured DO. Table 8.1 shows the impact of the K_La in the model on the effluent parameters (a full set of K_La model results is displayed in Appendix M).

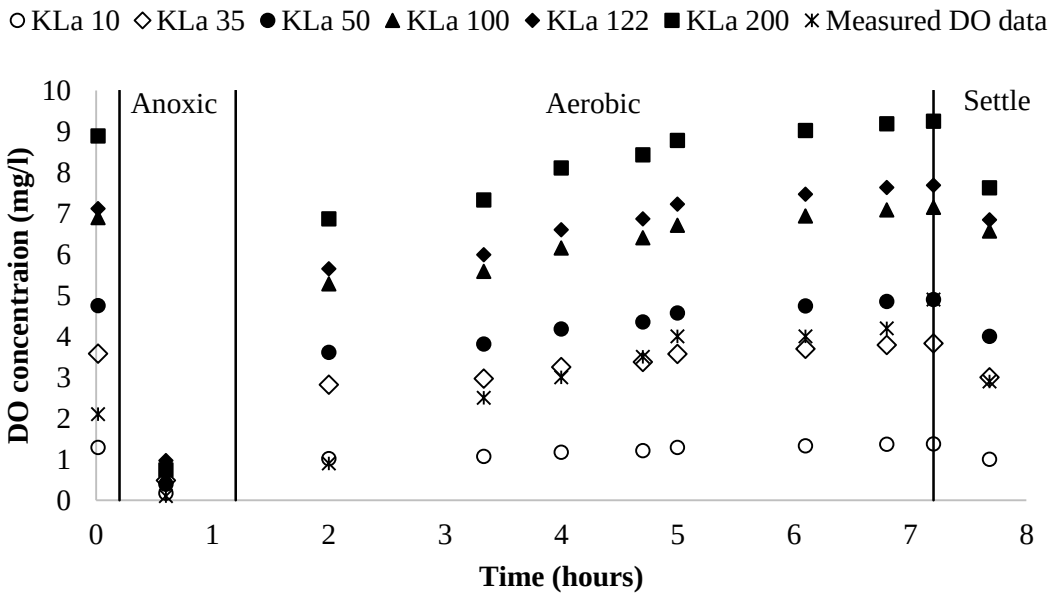

Figure 8.3 – Impact of K_La values on DO

Table 8.1 – Impact of K_La in model on effluent parameters (average Day 30)

	COD_f (mg/l)	**NH_4–N (mg/l)**	**NO_3–N (mg/l)**
Measured effluent	33 (10)	12 (6)	1 (1)
K_La Value			
10	98	27	0.03
35	56	22	1
50	30	13	1.3
100	31	11	1.3
122	31	10	1.3
200	31	10	1.3

In the model the K_La was found not to have a significant bearing on effluent concentrations once it was above 50 d^{-1} as shown in Table 8.1 This may be a result of DO concentrations being relatively high for all K_La values above 50 d^{-1} – it was observed that above this value maximum DO concentrations for most of the aerobic phase were above 2 or 3 mg/l; thereafter additional dissolved oxygen was unlikely to result in further process efficiency.

The influence of K_La on COD_f removal was evaluated as shown in Figure 8.4 (the graph only shows K_La 10 d^{-1}, K_La 35 d^{-1} and K_La 122 d^{-1} as the results from K_La 50 d^{-1}, 100 d^{-1}

and 200 d^{-1} were almost the same as 122 d^{-1} and could not be seen clearly). As expected, limited COD_f removal was observed during the anoxic period for all six K_La values. For K_La 122 d^{-1} COD_f removal occurred more rapidly than K_La 10 d^{-1} and K_La 35 d^{-1} during the aerobic phase where the final COD_f concentration at the end of the treatment cycle was 31 mg/l compared to 56 mg/l for K_La 35 d^{-1} and 98 mg/l for K_La 10 d^{-1}. This was due to the additional DO in K_La 122 d^{-1}.

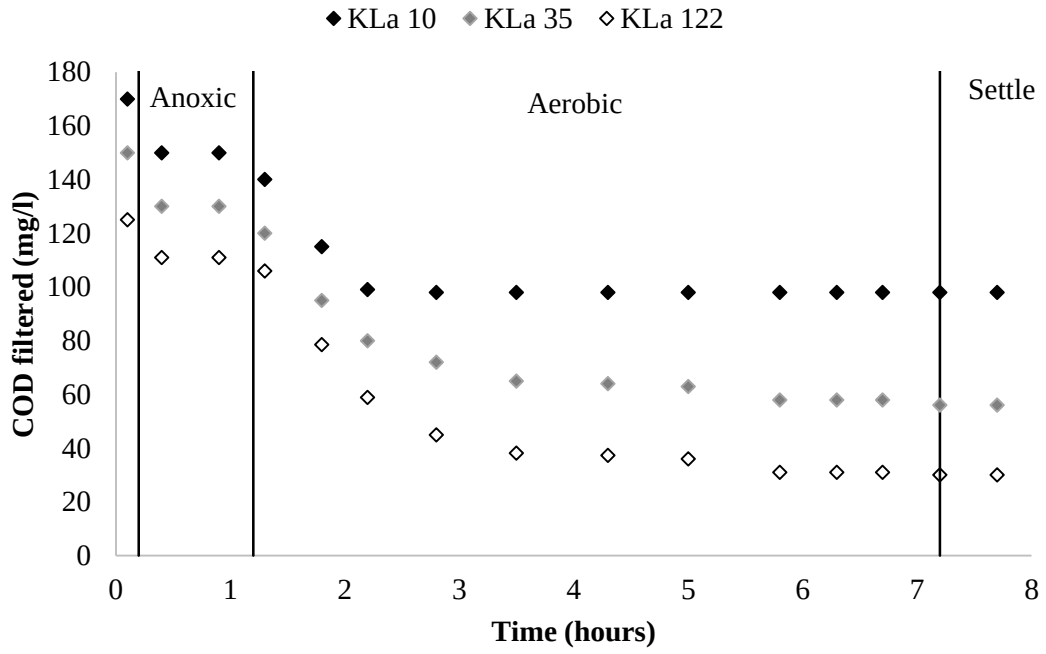

Figure 8.4 – Impact of K_La on COD_f removal

8.3.2 AQUASIM Model

In the AQUASIM model the passive aeration process in the PFBR was also modelled using K_La value. The correct measurement or prediction of the K_La value was a crucial step in modelling the PFBR biofilm system in AQUASIM. A K_La value of 122 d^{-1} was initially used to calibrate the PFBR, however, for successful model calibration, the K_La value had to be adjusted to 35 d^{-1} in order to achieve good calibration.

Similarly to the GPS-X model the impact of K_La on simulation accuracy was determined. Six simulations were carried out on Study 4 in FS-PFBR1 that compared K_La values 10 d^{-1}, 35 d^{-1}, 50 d^{-1}, 100 d^{-1}, 122 d^{-1} and 200 d^{-1} against the measured effluent COD_f, NH_4-N and NO_3-N concentrations. As might be expected K_La values had an impact on the DO

concentrations in the model, however, it also had a significant impact on simulated ammonium removal rates (and carbon removals) for K_La values below 50 d^{-1} (Table 8.2).

Table 8.2 – Impact of K_La in model on effluent parameters (average Day 30)

	COD_f (mg/l)	**NH_4–N (mg/l)**	**NO_3–N (mg/l)**
Measured effluent	33 (10)	12 (6)	1 (1)
K_La Value			
10	115	24	0.3
35	45	11	1.8
50	38	0.06	6.5
100	38	0.06	12
122	38	0.06	14
200	38	0.06	19

As the K_La increased from 10 d^{-1} to 200 d^{-1} dissolved oxygen concentrations increased from 0.03 mg/l to 10 mg/l in the bulk fluid by the end of the treatment cycle. In parallel simulated effluent NH_4-N concentrations decreased from 24 mg/l to 0.06 mg/l and NO_3-N concentrations increased from 0.03 mg/l to 19 mg/l. The influence of K_La on NH_4-N removal is shown in Figure 8.5. The K_La value of 35 d^{-1} led to the most accurate NH_4-N effluent concentrations where the final concentration at the end of the treatment cycle was 11 mg/l compared to 12 mg/l for the measured data.

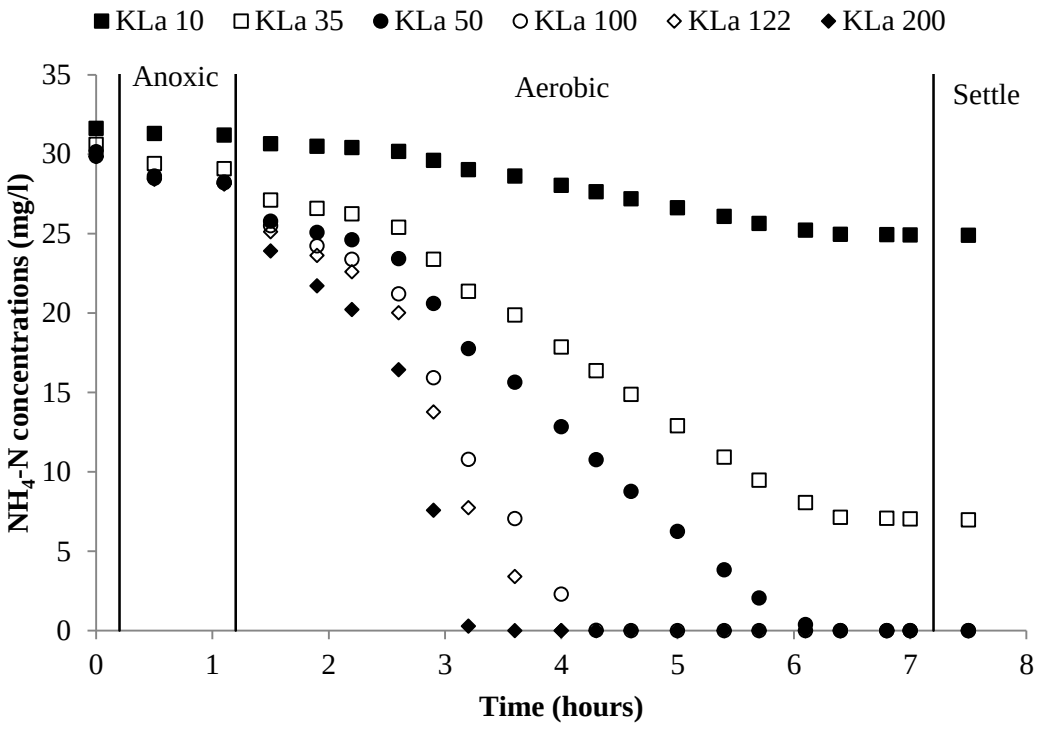

Figure 8.5 – Impact of K_La on NH_4-N removal

The K_La value of 35 d^{-1} led to the most accurate DO and effluent concentrations. It appears that the K_La and dissolved oxygen was a more significant factor in AQUASIM than in GPS-X particularly in relation to effluent ammonium-nitrogen concentrations. For example an increase in K_La from 10 d^{-1} to 50 d^{-1} resulted in simulated effluent ammonium concentrations reducing from 24 to 0.6 mg N/l; in GPS-X a similar increase in K_La values reduced simulated ammonium concentrations from 27 to 13 mg N/l. This could be due to the fact that the PFBR was modelled in AQUASIM using a biofilm model and thus was more sensitive to K_La values (it should be remembered that for each laboratory and site study DO concentrations, where measured, were only measured in the bulk fluid). An increase in K_La in the bulk fluid would ensure greater oxygen transfer into the biofilm and thus increase process efficiency significantly. A full set of K_La model results is displayed in Appendix M.

8.4 MODELLING NEW TECHNOLOGIES WITH MINIMAL PERFORMANCE DATASETS

Wastewater influent/effluent characteristics have a significant impact on wastewater treatment modelling. One of the main limitations in wastewater treatment plant modelling can often be minimal datasets; particularly influent monitoring. It has generally been accepted reasonably detailed influent wastewater characteristics datasets were necessary to ensure good model calibration. However, the collection of influent/effluent data can be a costly undertaking and frequently proves prohibitively expensive; this in turn can limit the use of modelling in process optimisation. Furthermore, in many cases, unless required for regulatory reasons, frequent monitoring may not be considered at many wastewater treatment plants (particularly small scale or decentralised systems).

8.4.1 Utilising minimal datasets

In this study there was minimal influent and effluent data available. The available influent data included COD_t, COD_f, TN_t, NH_4-N and NO_3-N. There was no breakdown of soluble biodegradable COD, soluble un-biodegradable COD, slowly biodegradable COD or particulate un-biodegradable COD. There was also no breakdown of nitrogenous material. However using representative basic datasets and user experience, in combination with previous literature, it was possible to predict with significant accuracy the composition of the wastewater. While there are assumptions made with this data and it is always better to have more data – experienced users can utilise tools such as influent advisor to ensure they optimise the value of existing data. The known values of the influent wastewater from the PFBR was fed into the Influent Advisor in GPS-X and a series of calculations were undertaken to ensure that the data was partitioned correctly, and an influent profile generated. A crucial aspect of the study was that there was detailed phase study data available. By utilising the phase study data it was possible to ensure a robust model was calibrated (discussed further in *Section 8.5*). As a result, where there are limitations in collecting more comprehensive data sets in batch type reactors, investment in basic analysis of cycle performance may be more efficient than completing additional analysis of influent parameters. As a means of double checking to ensure that the influent partitioning was satisfactory the influent figures used in the influent advisor were compared to typical characteristics of domestic wastewater figures used by Henze et al.

(2000). The partitioned figures generated from the influent advisor in GPS-X were used in AQAUSIM.

The model was initially built and calibrated using the average influent data and the results showed good agreement between measured and modelled results. However when the model was verified using the phase study data the model results from the initial calibration were not totally accurate so the stoichiometric and kinetic parameters had to be readjusted and tweaked for correct calibration.

This shows that while the model influent and effluent data may be correct in the model, what happens in between in each phase study cycle may not necessarily be correct. This demonstrated that detailed phase study data proved more important in calibrating the model than the influent and effluent data. It is also cheaper to gather phase study data than influent and effluent data over a long period of time. This idea would prove beneficial in the development of new technologies as it is time consuming, difficult and expensive to gather extensive influent and effluent data for every new emerging technology.

In this case study there was minimal detailed influent/effluent data available over a significant period of time, however very good calibration was still achieved due to the detailed phase study data available. The detailed phase study data enabled the users to ensure that each individual cycle was calibrated correctly. If the model was just calibrated for the influent and effluent average data then the model would not be very robust. However because the model was calibrated for phase study data, which varies over time, this show the model is robust as it was calibrated and verified using two completely different scenarios.

It appears that extremely detailed influent/effluent breakdown data is not necessary if good phase study data is available. For the calibration of the PFBR, and perhaps other emerging technologies phase study data could be more important than detailed influent/effluent breakdown data. It is important to remember that the quality of the data used to calibrate the model has a direct impact on the reliability of the predictions made when using the final calibrated model.

8.5 ACCURATE UNDERTAKING/EXECUTION OF THE CALIBRATION PROCESS

Over the past three decades numerous calibration protocols have been developed however the calibration process still represents the main obstacle to modelling. Various model calibration approaches and optimisation techniques (e.g. Petersen (2003); Sin (2005); Mannina (2011); Boltz (2012); Brockmann (2012); Boltz (2013) were considered as part of this study in order to try and adapt a technique to calibrate the PFBR; however there was no one calibration protocol suitable for the calibration of the PFBR.

In this study the technology being modelled was a key influencer in the choice of calibration approach. The model calibration approach used in the calibration of the PFBR is outlined in Figure 8.6.

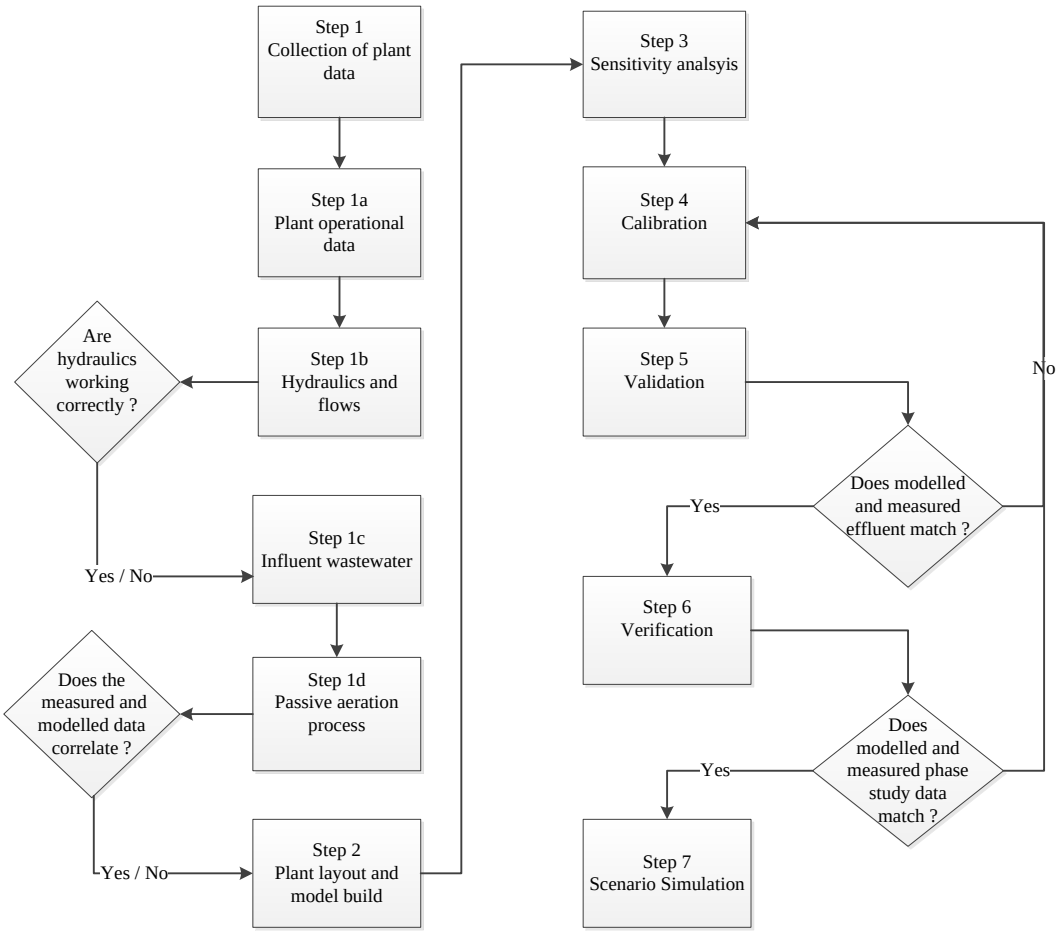

Figure 8.6 - Schematic/general overview of the PFBR calibration protocol

The PFBR calibration protocol was comprised of 7 main steps (1) collection of plant data (2) plant layout and model build, (3) sensitivity analysis, (4) calibration, (5) validation, (6) verification, and (7) scenario simulation.

Step 1 – Collection of Plant data

The first step of the calibration protocol requires a comprehensive plant survey to be carried out in order to identify the plant operation data, hydraulics and flow data, influent and effluent wastewater and the passive aeration process.

Step 1a – Plant operational data

The operational plant data needs to be detailed in this step. This includes the operating temperature and cycle data for batch processes. The process library to model the plant is chosen (this option is available in GPS-X only, not AQUASIM). In the case of the PFBR the Carbon-Nitrogen (cnlib) library was chosen. The biological model also needs to be chosen in this step. The ASM1 model was the biological model used in GPS-X and both a combination of ASM1 and ASM3 was used in AQUASIM.

Step 1b – Hydraulics and flows

In this step, information concerning the different flows in the plant need to be quantified, collected and inputted into the model, i.e. influent, effluent, waste and internal recirculation flows. The hydraulic model can then be calibrated. As shown in *Section 8.2* having the hydraulics working correctly is not critical to successful model calibration so proceed even if hydraulics aren't accurate.

Step 1c – Influent wastewater

This step involves the collection of influent wastewater data (full-scale and laboratory-scale) and transferring the influent characterisation data into the ASM model parameters. The influent chemical oxygen demand (COD) fractions, i.e. soluble biodegradable COD, soluble un-biodegradable COD, slowly biodegradable COD and particulate un-biodegradable COD and the influent nitrogen fractions are used to construct the influent loading data for the treatment plant model.

Step 1d – Passive aeration process

The aeration characteristics and the dissolved oxygen process needs to be detailed and calibrated in this step. The ultimate goal is to obtain a good fit between measured and modelled oxygen. In the case of the PFBR this step involved entering a K_La value and checking to ensure modelled and measured DO concentrations match. An exact DO correlation was not essential (*as described in Section 8.3*) so proceed to Step 2.

Step 2 – Plant layout and model build

In the second step of the protocol the plant configuration and model structure is defined. This comprises the collection of physical plant data such the physical dimensions of the reactors and the layout of the plant components.

Step 3 – Sensitivity Analysis

This step involved undertaken a sensitivity analyses to identify the parameters to be adjusted during calibration.

Step 4 – Calibration

The effluent wastewater data and profile data need to be gathered in this step and then the model can be calibrated. At this stage, the protocol advises to perform an initial calibration and compare the simulation results with the plant data. If there is a considerable discrepancy between the model and measurements the protocol advises to check the data quality is Step 1 and then calibrate the model again. After correcting the model if appropriate a detailed calibration can be performed.

The protocol provides a manual calibration procedure in which parameters of different biological processes are calibrated one at a time until a good fit is obtained to the plant data. In order to get a good match between measured and modelled data the following three steps should be undertaken.

1. Check whether COD removal is achieved correctly. If not the parameters that COD are sensitive to (identified during the sensitivity analyses) need to be adjusted.
2. Check the nitrification performance. Adjust the appropriate kinetic and stoichiometric parameters that nitrification and denitrification are sensitive to (identified during sensitivity analysis).

3. In the AQUASIM model only, the biofilm thickness was fixed to be constant at 200 µm in all model studies. The calibration was performed manually. This approach involved adjusting the stoichiometric and kinetic parameters one at a time in the model and then making a visual inspection of the simulation results for COD_t, NH_4-N and NO_3-N.

Step 5 – Validation

After calibration was completed, the model should be validated using effluent plant data from a period different than the period used in the calibration. If the modelled and measured data match proceed to Step 6, if not return to Step 4 and recalibrate the model.

Step 6 – Verification

After the model has been validated it can be verified using phase study data. If the modelled and measured data match proceed to Step 7, if not return to Step 4 and recalibrate the model.

Step 7 – Scenario Simulation

After the model has successfully passed the validation and verification stage, it can finally be used for its ultimate purpose. The calibrated and validated model can be used to simulate different scenarios defined according to the objectives of the study.

There is currently no agreed approach towards calibration of activated sludge models or biofilm reactor models. These short comings need to be addressed as researchers, modellers and engineers would benefit from guidance on calibration of biofilm models. In conclusion the calibration step is the most difficult and time consuming step and is considered as an obstacle for widespread model use. As part of this thesis model calibration was one of the main areas that introuduced uncertainites to model predictions.

8.6 SCALING UP LABORATORY-SCALE DATA TO FULL-SCALE MODELS

Developing and testing new technologies at laboratory scale is a key step in the development of new technologies. Laboratory scale units can be used to test and optimise a technology at a manageable scale before a field scale unit is constructed, while minimising the use of resources. However, the transferability and representability of results obtained from laboratory-scale experiments to full-scale models needs to be

considered and used carefully (Chudoba et al., 1992; Novak et al., 1994; Grady et al., 1996).

The calibration of the LS-PFBR model was carried out using data from specific and well-controlled experiments at laboratory scale at relatively constant operating conditions (e.g. loading rates and temperature). The development of the PFBR laboratory scale unit offered an efficient way of getting to know the system and also a steady data set to work with. Though there were challenges due to the differences in influent wastewater and in particular whether the oxygen transfer characteristics were similar for laboratory scale and field scale units. The results of calibration from laboratory scale units may not be totally reliable as it can difficult to configure and operate a small-scale plant in exactly the same way as a full-scale plant (Jeppsson, 1996).

In this study there were significant differences between the operating conditions and plant configurations of LS-PFBR and FS-PRBR, including: (i) influent wastewater composition, (ii) DO, (iii) system operation and cycle times and (iv) the correct measurement or prediction of the K_La value for the field-scale models.

The wastewater composition was identified to be an important issue in the calibration of the PFBR as discussed in *Section 4.2.3 and Section 8.4*. The LS-PFBR was operated using a synthetic wastewater while the influent in both the FS-PFBR1 and FS-PFBR 2 was municipal wastewater from their respective sites. The difference in the LS-PFBR influent and the FS-PFBR influents challenged the transferability of the LS-PFBR model to the full-scale FS-PFBR model due to the different influent profiles required. The difficulty of scaling up the K_La value and prediction of DO is previously discussed in *Section 8.3*.

8.7 COMPARISON OF GPS-X AND AQUASIM

8.7.1 Modelling Software

The modelling software GPS-X and AQUASIM were compared to ascertain the relative advantages and disadvantages of using each package. GPS-X and similar modelling packages generally include user friendly interfaces. In GPS-X the user can choose from four influent models (ASM1, ASM2, ASM3, Mantis); these can be modified if necessary though this process is not necessarily straightforward. In AQUASIM the user must enter all the ASM equations into the model and while more time consuming it provides considerable flexibility to the user. In terms of model run-time it took 72 minutes for

GPS-X to run a 50 day simulation for FS-PRBR1. It took 20 minutes for AQUASIM to run a 50 day simulation for FS-PRBR1 and thus the model runtime was less on AQUASIM, possibly due to the nature of the model implemented.

8.7.2 Modelling Results

The percentage error for the GPS-X and AQUASIM models are summarised in Tables 8.3 and 8.4. It is important to note that the calibrated parameters e.g. growth rates, decay rates and yields in GPS-X and AQAUSIM were different (*as described in Section 7.7*).

Table 8.3 – Comparison of GPS-X and AQUASIM percentage error for Study 3AS

Study 3AS						
	GPS-X			AQUASIM		
(mg/l)	Measured Effluent	Modelled Effluent	% Error	Measured Effluent	Modelled Effluent	% Error
COD_f	66	58	12	66	70	6
NH_4-N	26	26	0	26	25	4
NO_3-N	0.95	0.4	58	0.95	1.6	68

Table 8.4 - Comparison of GPS-X and AQUASIM percentage error for Study 4AS

Study 4AS						
	GPS-X			AQUASIM		
(mg/l)	Measured Effluent	Modelled Effluent	% Error	Measured Effluent	Modelled Effluent	% Error
COD_f	33	31	6	33	45	36
NH_4-N	12	15	25	12	11	8
NO_3-N	1	1.3	30	1	1.8	80

Some of the percentage errors in Table 8.3 and Table 8.4 appear high for example the 80% error for NO_3-N in AQUASIM. However it should be noted that the percentage error appears high due to the low concentration of NO_3-N and in both cases the models were deemed to be sufficiently accurate. Overall the percentage errors were lower in GPS-X than in AQUASIM.

Modelled COD_f profiles for Study 3PS showed a similar trend to experimental measurements in both GPS-X and AQUASIM (Figure 8.7). Limited COD_f was removed during the anoxic stage in both GPS-X and AQUASIM while the bulk fluid in R1 remained quiescent. As the bulk fluid from both R1 and R2 was mixed and DO

concentrations increased a reduction in COD_f was recorded during the aerobic stage in both packages. The final effluent concentration was overestimated in GPS-X and underestimated in AQUASIM.

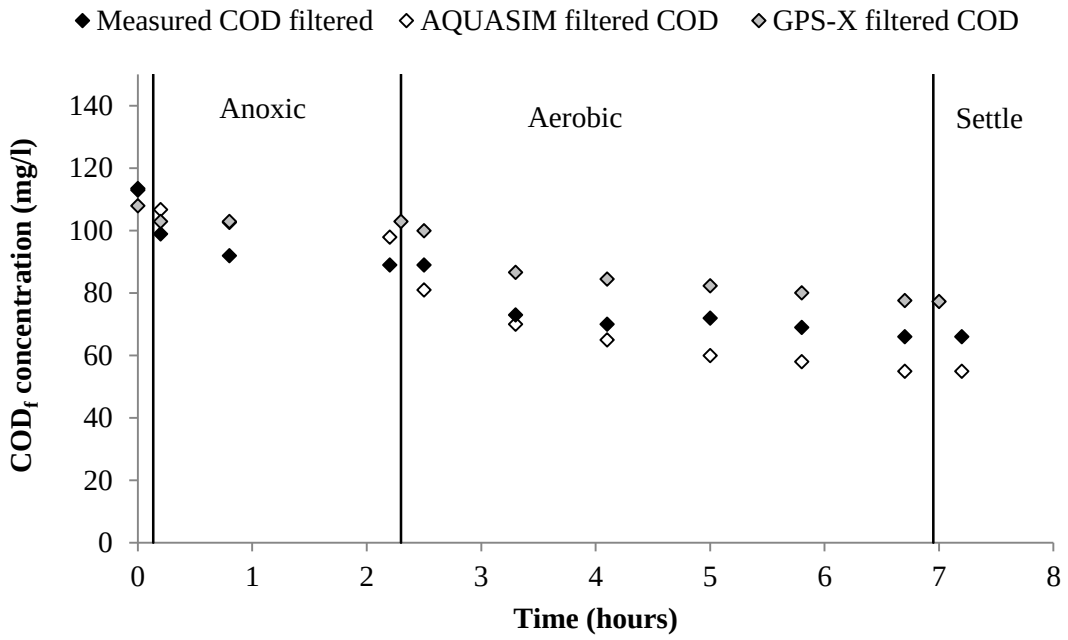

Figure 8.7 – Modelled and measured COD_f results for Study 3PS

Figure 8.8 show the nitrogen profiles for Study 4PS during a typical treatment cycle during steady state operation. The modelled NH_4-N and NO_3-N profiles in both GPS-X and AQUASIM were close to the measured data.

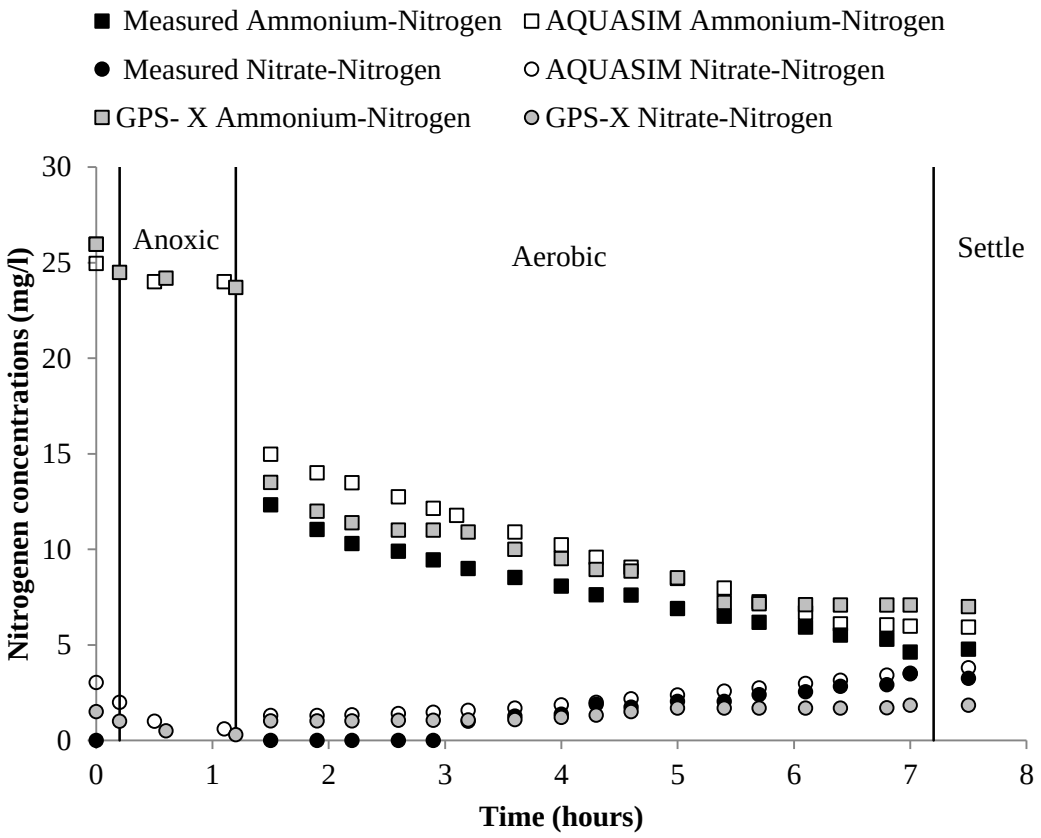

Figure 8.8 – Modelled and measured nitrogen profiles for Study 4PS

The results shown in Table 8.3 and 8.4 and in Figure 8.7 and 8.8 would indicate that the models developed in GPS-X and AQUASIM are relatively robust as they were both calibrated and verified using different scenarios and a good fit between measured and modelled data was achieved in both models.

8.8 CONCLUSION

This chapter investigated some of the uncertainties associated with modelling new technologies. The main conclusions of the study are as follows:

1. The hydraulic layout of the GPS-X and AQAUSIM models were different, however good effluent results were achieved for both models. While it was good to have the hydraulics working correctly for the GPS-X model, it was shown in the AQUASIM model that having the hydraulics working correctly was not critical to successful model calibration.

2. It appears that, for the calibration of the PFBR and perhaps other emerging technologies, the correct measurement or prediction of the K_La value may not be critical if simulating oxygen concentrations is not an objective of the model.
3. It appears that extremely detailed influent/effluent breakdown data is not necessary if good phase study data is available.
4. The model calibration process is one of main obstacles to modelling. The recently introduced calibration protocols have attempted to tackle the calibration issue but it still remains a problem. The PFBR is a unique and novel plant and did not 'fit in' to a typical WWTP that could easily be calibrated therefore a new and unique calibration procedure was developed in order to calibrate the PFBR.
5. For the calibration of the PFBR, and perhaps other batch-type technologies (e.g. sequencing batch reactors or sequencing batch biofilm reactors) phase study data can play a significant role in ensuring robust model calibration.
6. Laboratory-scale data is an important additional source of information to the calibration of full-scale model however the scaling up problem of the laboratory-scale results is a significant issue. It is important that the modeller should check the assumptions made if using laboratory data to simulate the performance of site-scale reactors.

The ultimate goal of this discussion was to generate transparent and objective methods to evaluate the reliability of model results, before they are implemented in an engineering decision-making context.

9 CONCLUSION

9.1 INTRODUCTION

During this research study the possibility of modelling the pumped flow biofilm reactor (PFBR) at laboratory scale and field scale, using the modelling software packages GPS-X and AQUASIM, was investigated. Modelling the PFBR offered a unique challenge as it is a new technology that was not easily built and calibrated using existing commercial modelling software.

The main objectives of this study were (i) to determine if it was possible to model a new technology using an activated sludge processes in existing software (GPS-X), (ii) to develop a unique biofilm-based model for the PFBR, using the modelling package AQUASIM, (iii) to inform new approaches for rapidly developing and calibrating models without the need for developing bespoke unit processes.

The first part of this research involved building and calibrating a model for the laboratory and field scale PFBRs using an activated sludge unit process in GPS-X in order to predict effluent results and contaminant concentration changes (nitrogen and organic carbon) during individual treatment cycles. These models were then used to inform optimal system operation, (e.g. maximising contaminant removal per unit energy input) and compare various treatment scenarios from an economic and effluent quality point of view.

The second part of this research was to develop a biofilm-based model for the PFBR, using the modelling package AQUASIM, that (i) predicted the effluent characteristics, (ii) the cycle performance of the PFBR and (iii) simulate biofilm composition.

Then finally some of the modelling uncertainties that were encountered while undertaking this research were investigated.

9.2 CONCLUSIONS

9.2.1 GPS-X modelling

The main conclusions of these studies are:

1. Models of the laboratory scale and field scale units (LS-PFBR, FS-PFBR1 and FS-PFBR2) were successfully built and calibrated using a surrogate activated sludge process object in GPS-X. The model successfully predicted (i) effluent

characteristics for carbon (chemical oxygen demand) and nitrogen (ammonium-nitrogen and nitrate-nitrogen) and (ii) individual treatment cycles for carbon and nitrogen (ammonium-nitrogen and nitrate-nitrogen).

2. The passive aeration process was modelled by entering a K_La (mass transfer coefficient) value of 122 d^{-1} which had previously been calculated from a laboratory-scale PFBR study. In the laboratory and field scale models the oxygen profiles from experimental and modelled data correlated well however there was not an exact match between the modelled and measured DO data for the field scale model when using a K_La value of 122 d^{-1}. A number of simulations were run in the model to determine the effect that K_La had on effluent concentrations. K_La was found not to have a significant bearing on effluent COD_f, NH_4–N and NO_3–N concentrations once the K_La value remained above 50 d^{-1}.
3. Sensitivity analyses showed that effluent COD_t concentrations were most sensitive to changes in μ_H; while effluent TN_t, NH_4-N, and NO_3-N concentrations were most sensitive to changes in Y_A, μ_A and b_A.
4. There was minimal detailed influent and effluent data available for all units modelled however there was detailed phase study data available. FS-PFBR1 model was initially built and calibrated using the average influent data and the results showed good agreement between measured and modelled results. However when the model was validated using the phase study data the model results from the initial calibration were not totally accurate. This showed that while the model influent and effluent data may be correct in the model, the contaminant changes during reaction cycles may not be well modelled. This demonstrated that detailed phase study data proved important in ensuring calibration was robust. It may also be efficient to gather phase study data alongside influent and effluent data and could potentially reduce the length of data gathering exercises required for modelling.
5. It was necessary to adapt existing calibration protocols in order to calibrate the PFBR system as indeed it may be for most systems.
6. A number of different scenarios were simulated for the FS-PFBR1 to determine the most energy efficient and cost efficient operational regime. Four different scenarios were modelling which examined the influence of the anoxic and aerobic cycle length and the number of aerobic cycles on the model. Scenario II, during

which dissolved oxygen concentrations were simulated to rise most rapidly, showed the most effective scenario for achieving nitrification. The increase in anoxic period in Scenario IV caused the greatest reduction in NO_3-N which was due to denitrification. Scenario II had the highest running costs but also the highest NH_4-N removal rates. The best option in terms of nutrient removal was to increase the number of cycles however this was the most expensive option to operate.

7. The models developed using GPS-X, while not providing in depth analysis of biofilm characteristics can be used to enhance reactor operation and inform future studies without the need to develop a bespoke model. These models could be applied to future experimental and pilot scale units for design purposes.

9.2.2 AQUASIM modelling conclusions

The main conclusions of these studies are:

1. A unique biofilm model of the FS-PFBR1 and FS-PFBR2 was successfully modelled and calibrated using the biofilm reactor compartment in AQUASIM. The model was used to predict PFBR performance (effluent carbon and nitrogen concentrations and changes in these parameters during individual cycles) under a variety of operating conditions, such as different influent and effluent flow rates, aeration conditions, cycle conditions and different loadings.
2. The modelled hydraulics were not similar to those in situ however this proved not to be critical as good model calibration was still achieved. The biofilm reactor compartment (BRC) in AQUASIM was used to model the field scale PFBRs. AQUASIM does not allow the transference of water in or out of the BRC thus oxygen was switched on and off to simulate the different stages of the PFBR.
3. A K_La value of 122 d^{-1} was initially used to calibrate the PFBR, however, for successful model calibration, the K_La value had to be adjusted to 35 d^{-1} in order to achieve good calibration. The impact of K_La on simulation accuracy was determined by running six simulations to determine the effect that K_La had on effluent concentrations. K_La was found not to have a significant bearing on effluent COD_f, NH_4–N and NO_3–N concentrations once the K_La value remained above 50 d^{-1}. A K_La value of 35 d^{-1} led to the most accurate NH_4-N effluent

concentrations. This could be due to the fact that the PFBR was modelled in AQUASIM using a biofilm model and thus was more sensitive to K_La values.

4. Sensitivity analyses showed that effluent COD_f concentrations were most sensitive to changes in μ_H; whereas effluent NH_4-N, and NO_3-N concentrations were most sensitive to changes in Y_A and μ_A. This was similar to the results from the GPS-X models.
5. Good calibration was achieved based on minimal influent data. This may help to promote the use of modelling in smaller treatment facilities where detailed datasets are not available. It was possible to develop a single set of parameters that were calibrated to describe the results for Study 3 and then applied to predict the results for Study 4. All calibrated parameters were within reported ASM1 and ASM3 literature values.
6. It was possible to track the growth of two different types of biomass, autotrophic and heterotrophic bacteria in the model (though it should be noted this could not be compared to experimental data). The average autotrophic concentrations in the bulk fluid reached steady state at 10 g/m^3. The average heterotrophic bacteria concentrations reached steady state at 48 g/m^3 for both Study 3 and 4. In the biofilm, the heterotrophs reached a steady state of approximately 1.9 g COD/m^2 for both Study 3 and 4. The autotrophs reached a steady state of 0.03 g COD/m^2 at 10 days.
7. The simulated model showed the effect of biofilm thickness on COD_f and NH_4-N removal. The results showed that with a biofilm thickness under 100 µm the effluent COD_f concentrations were 45 mg/l. However, when the biofilm thickness was increased to over 100 µm, effluent COD_f concentrations decreased to 40 mg/l. The overall NH_4-N concentrations decreased and the NO_3-N concentrations increased as the biofilm thickness was increased. The modelled effluent NH_4-N concentrations were below 4 mg/l when the biofilm thickness was increased to 2500 µm. The modelled effluent NO_3-N concentrations increased from 1.3 mg/l to 6 mg/l, with the biofilm thickness being in the range of 250–2500 µm. These results seem to suggest that a thicker biofilm helped nitrification potentially as relative autotroph populations were observed to increase in thicker biofilms.
8. An additional model was developed which represented an ‘unconfined reactor type’, where the biofilm thickness varied over time. The biofilm thickness in the

unconfined reactor varied from 100µm to 500µm over a 50-day simulation. There was little difference between the effluent concentrations between the confined and unconfined reactor.

9.2.3 Overall Modelling Conclusions

1. It was shown in the AQUASIM model that having the hydraulics working correctly was not critical to successful model calibration.
2. The K_La value and dissolved oxygen concentrations was more a significant factor in AQUASIM than in GPS-X particularly in relation to effluent ammonium-nitrogen concentrations. This could be due to the fact that the PFBR was modelled in AQUASIM using a biofilm model and thus was more sensitive to K_La values; particularly at lower values.
3. Accurate models of wastewater facilities can be developed with limited influent/effluent data if good cycle analysis data is available.
4. The calibration protocols studied as part of this thesis were not applicable for the PFBR and were very much technology specific. Every WWTP is different and every model needs to be calibrated to ensure correct and reliable application. The choice of calibration approach can depend on the WWTP being modelled.
5. The transferability of results, such as K_La, obtained from laboratory-scale experiments to full-scale models needs to be considered and used carefully.

9.3 FURTHER RESEARCH AND RECOMMENDATIONS

A number of areas that may require further research are suggested below. The PFBR may offer further research opportunities in both wastewater treatment modelling and related areas.

1. This study indicates that even with limited data relatively accurate models of wastewater facilities can be developed. It is recommended that such work be carried out to inform process optimisation in smaller plants. A particular focus could be placed on obtaining data on changes in parameter concentrations during individual cycles for batch reactors.

2. There are specific challenges in determining oxygen transfer in biofilm reactors and specifically systems such as the PFBR (or RBC) where biofilm is alternately exposed to air and water. This study investigated the role new oxygen sensors could play in this area and past work has focused on using microsensors however this is an area that should be further explored; particularly for site scale reactors.
3. There has been a focus recently on developing generic calibration methodologies for wastewater treatment systems. This study suggests a focus could be put on developing technology specific calibration methodologies which may be more beneficial to practitioners.
4. The developed models could be applied to future experimental and pilot scale units for design purposes. The model can be used to enhance and improve reactor operation and inform future studies.
5. The development of a unique PFBR object in either AQUASIM or GPS-X should be investigated.
6. It is recommend that experimental studies be carried out to enable modelling of phosphorus removal processes.

9.4 SIGNIFICANCE OF WORK

The work done in this study has demonstrated that it is possible to model a novel wastewater technology using 'surrogate' processes in existing software. This has the potential to provide substantial cost benefits as means of rapidly modelling new technoloiges which in turn can lead to cost savings during technology development and on-site operation. The calibrated model will enhance the understanding of the PFBR technology and thus lead to better design and more cost-effective wastewater treatment systems.

GLOSSARY OF TERMS

Term / Abbreviation	Definition
ASM	Activated Sludge Model
ASP	Activated sludge process
$b_{H,O2}$	Aerobic endogenous respiration rate of X_H
$b_{H,NO}$	Anoxic endogenous respiration rate of XH
$b_{A,O2}$	Aerobic endogenous respiration rate of X_A
$b_{A,NO}$	Anoxic endogenous respiration rate of X_A
BOD_5	5-day biochemical oxygen demand
C	Carbon
COD	Chemical Oxygen Demand
COD_t	Filtered COD
COD_f	Total COD
DO	Dissolved Oxygen
eff	effluent
EPA	Environmental Protection Agency
F/M	Food to mass ration (gCOD/gTS.day)
f_{SI}	Production of SI in hydrolysis
f_{XI}	Production of XI in endogenous respiration
HRT	Hydraulic Retention Time
inf	influent
i_{NSI}	Nitrogen content of inert soluble COD, S_I
i_{NSS}	Nitrogen content of readily biodegradable organic matter, S_S
i_{NXI}	Nitrogen content of inert particulate COD, X_I
i_{NXS}	Nitrogen content of slowly biodegradable organic matter, X_S
i_{NBM}	Nitrogen content of biomass, X_H, X_A
i_{TSSXI}	TSS to COD ratio for X_I
i_{TSSXS}	TSS to COD ratio for X_S
i_{TSSBM}	TSS to COD ratio for biomass, X_H, X_A
k_h	Hydrolysis rate constant
K_X	Hydrolysis saturation constant
$K_{O2,H}$	Saturation/inhibition coefficient for oxygen
K_S	Saturation coefficient for growth on S_S
$K_{NO3,H}$	Saturation/inhibition coefficient for nitrate
$K_{NH4,H}$	Saturation coefficient for ammonium (nutrient)
$K_{O2,A}$	Saturation coefficient for oxygen
$K_{NH4,A}$	Saturation coefficient for ammonium (substrate)
$K_{NO3,A}$	Saturation/inhibition coefficient for nitrate
$L_{F,tot}$	Biofilm thickness
L_L	Boundary layer thickness
MWTP	Municipal wastewater treatment plant
N	Nitrogen
NH_3-N	Ammonia nitrogen
NH_4-N	Ammonium-nitrogen
NO_2-N	Nitrite nitrogen
NO_3-N	Nitrate-nitrogen
NOx	Oxidised Nitrogen
P	Phosphorous
PE	Population Equivalent

PFBR	Pumped Flow Biofilm Reactor
Q	Daily influent flow-rate (l/day)
SBR	Sequencing batch reactor
S_S	Readily biodegradable organic matter
S_I	Soluble inert organic matter
S_{N2}	Dinitrogen,
S_{NH4}	Ammonium
S_{NO3}	Nitrate
S_{O2}	Dissolved oxygen
S_{ALK}	Alkalinity
TN_t	Total Nitrogen
TN_f	Filtered Nitrogen
TSS	Total suspended solids
TKN	Total Kjehldahl nitrogen
TN	Total nitrogen
TOC	Total organic carbon
TON	Total oxidised nitrogen
UWWTD	Urban Wastewater Treatment Directive
μ_A	Maximum growth rate of autotrophs
μ_H	Maximum growth rate of heterotrophs
WFD	Water Framework Directive
X_H	Heterotrophic organisms
X_I	Inert particulate organic matter
X_S	Slowly biodegradable organic organic matter
X_A	Nitrifying organisms
X_{TSS}	Total suspended solids
$Y_{H,O2}$	Yield of heterotrophs using oxygen
$Y_{H,NO}$	Yield of heterotrophs using nitrate
Y_A	Yield of autotrophs

BIBLIOGRAPHY

Abbassi, B., Dullstein, S. & Räbiger, N., 2000. Minimization of excess sludge production by increase of oxygen concentration in activated sludge flocs; experimental and theoretical approach. Water Research, **34**(1), pp.139–146.

Akunna, J.C., Jefferies, C. (2000) Performance of family-size sequencing batch reactor and rotating biological contactor units treating sewage at various operating conditions Water Sci. Technol., **41** (1) (2000), pp. 97–104

Andreottola, G., Foladori, P., Ragazzi, M., 2000. Upgrading of a small wastewater treatment plant in a cold climate region using a moving-bed biofilm reactor (MBBR) system. Water Science and Technology **41** (1), 177–185.

APHA, AWWA and WEF (2005). Standard methods for the examination of water and wastewater (M. A. N. Franson, ed.) Port City Press, Baltimore, USA

Barker P.S and Dold P.L. (1997) General model for biological nutrient removal activated-sludge systems: model presentation. Wat. Env. Res **69**(5): 969-985

Batstone D.J., Keller, J., Angelidaki, I., Kalyuzhnyi, S.V., Pavlostathis, S.G., Rozzi, A., Sanders, W.T.M., Siegrist, H., Vavilin, V.A. (2002) Anaerobic Digestion Model No. 1 Scientific and Technical Report, No. 13IWA Publishing, London

Beck, M. B. 1986 Identification, estimation and control of biological wastewater treatment processes. Proc. Inst. Elec. Eng. **133**, 254-264

Beck, M. B. 1987 Water quality modelling: A review of the analysis of uncertainty. Wat. Resour. Res. **23**(8), 1393-1442

Beck, M. B. 1991 Principals of modelling. Wat. Sci. Tech. 24(6), 1-8

Beijerinck MW, Minkman DCJ (1910) Bildung und Verbrauch von Stikoxydul durch bacterien. Zentralbl Bakteriol Parasitenk, Abt II **25**:30-63

Belia, E., Amerlinck, Y., Benedetti, L., Johnson, B., Sin, G., Vanrolleghem, P. a, Villez, K. (2009). Wastewater treatment modelling: dealing with uncertainties. Water Science and Technology : A Journal of the International Association on Water Pollution Research, **60**(8), 1929–41. doi:10.2166/wst.2009.225

Bilyk, K., Takács, I., Rohrbacher, J., Pitt, P., Latimer, R., and Dold, P. (2008). Full-scale testing advances fundamental understanding of denitrification filtres. Proceedings of the

81st Annual Water Environment Federation Technical Exhibition and Conference (WEFTEC). Chicago, Illinois, USA.

Boltz, J. P., Morgenroth, E., & Sen, D. (2010). Mathematical modelling of biofilms and biofilm reactors for engineering design. Water Science and Technology : A Journal of the International Association on Water Pollution Research, **62**(8), 1821–36. doi:10.2166/wst.2010.076

Boltz, J., Morgenroth, E., Brockmann, D., GT, D., Henze, M., Rittmann, B., van Lossdrecht, M. (2012). Framework for biofilm reactor model calibration. In WWTmod 2012, 3rd IWA/WEF Wastewater Treatment Modelling Seminar. Mont-Sainte-Anne, Quebec, Canada.

Boltz, J., Morgenroth, E., Brockmann, D., GT, D., Henze, M., Rittmann, B., van Lossdrecht, M. (2013). A biofilm reactor model calibration framework. In 9th International Conference on Biofilm Reactors. Paris, France.

Borkar, R. P., Gulhane, M. L., & Kotangale, A. J. (2013). Moving Bed Biofilm Reactor – A New Perspective in Wastewater Treatment, **6**(6), 15–21.

Brockmann, D., Boltz, J. P., Morgenroth, E., Daigger, G. T., & Henze, M. (2012). Applying a framework for calibrating a biofilm-reactor model : a full-scale moving-bed biofilm reactor active in nitrification. In WWTmod 2012, 3rd IWA/WEF Wastewater Treatment Modelling Seminar. Mont-Sainte-Anne, Quebec, Canada.

Brockmann, D., 2013. Personal communication.

Chaudhry, MAS., Beg, SA., (1998) A review on the mathematical modelling of biofilm processes: advances in fundamentals of biofilm modelling. Chem Eng Technol **21**: 701-710

Chimney, M. J., Wenkert, L., & Pietro, K. C. (2006) Patterns of vertical stratification in a subtropical constructed wetland in south Florida (USA). Ecological Engineering **27**(4), 322-330

Chudoba, P., Capdeville, B., Chudoba, J. (1992) Explanation of biological meaning of the S0/X0 ratio in batch cultivation. Water Sci. Technol., 26 (3 – 4) (1992), pp. 743 – 75

Clifford, E. (2009) Horizontal Flow Biofilm Reactors for Domestic Wastewater Treatment. Ph.D Thesis. National University of Ireland, Galway.

Clifford, E., Kennelly, C., Walsh, R. Gerrity, S., O' Reilly, E., Collins, G. (2012) Optimisation of a horizontal flow biofilm reactor for the removal of methane at low temperatures. Journal of the Air and Waste Management Association. **62**(10):1154-1161.

Clifford, E., Fox, S., Cahill, M., O'Reilly, E., (2013) Decentralised wastewater treatment using 'Pumped Flow Biofilm Reactor' (PFBR) technology. The 11th IWA conference on Small Water & Wastewater Systems and Sludge Management.

Council Direction 91/271/EEC concerning urban wastewater treatment (OJ L 135, 30.5.1991)

Coen, F., Vanderhaegen, B., Boonen, I., Vanrolleghem, P.A. and Van Meenen, P. (1997) Improved design and control of industrial and municipal nutrient removal plants using dynamic models. Water Science and Technology **35**(10), 53-61

Cortez, S., Teixeira, P., Oliveira, R., & Mota, M. (2008). Rotating biological contactors: a review on main factors affecting performance. Reviews in Environmental Science and Bio/Technology, **7**(2), 155–172.

Daigger, G. (2011). A practitioner's perspective on the uses and future developments for wastewater treatment modelling. Water Science and Technology. **63**(3):516-26

Devisscher, M., Ciacci, G., Fé, L., Benedetti, L., Bixio, D., Thoeye, C., Vanrolleghem, P. a. (2006). Estimating costs and benefits of advanced control for wastewater treatment plants – the MAgIC methodology. Water Science & Technology, **53**(4-5), 215.

Dudley, J., Chambers B., (1995). Dynamic modelling of wastewater treatment processes using STOAT. WaPUG Meeting, Blackpool

Dupont, R. and Sinkjaer, O., (1994) Optimisation of wastewater treatment plants by means of computer models. Water Science and Technology **25** (6) (1994), 181–190

Eberl, H., Morgenroth, E., Noguera, D., Picioreanu, C., Rittmann, B., & Loosdrecht, M. Van. (n.d.). Mathematical Modeling of Biofilms IWA Task Group on Biofilm Modeling : 2006, (18).

EC. (2013). Seventh Report on the Implementaion of the Urban Waste Water Treatment Directive (91/271/EEC). Brussels.

EPA (1997) Wastewater Treatment Manuals Primary, Secondary and Tertiary Treatment. EPA, Wexford. Ireland

EPA (1999) Wastewater treatment manuals; treatment systems for small communities, business, leisure centres and hotels. EPA, Wexford. Ireland

EPA (2010) Wastewater discharge licence, Tuam wastewater treatment plant, Galway County Council. Licence registration no. D0031-01

EPA. (2012a). Focus on Urban Waste Water Discharges in Ireland. Wexford.

EPA. (2012b). Ireland's Environment An Assessment 2012.

Environmental Technology Centre (ETC) (2013) Environmental Guide to Pollution Control Technologies, University of Nottingham

Environmental Technology Centre (ETC) (2014) Environmental Guide to Pollution Control Technologies. The University of Nottingham

Ferrai, M., Guglielmi, G., & Andreottola, G. (2010). Modelling respirometric tests for the assessment of kinetic and stoichiometric parameters on MBBR biofilm for municipal wastewater treatment. Environmental Modelling & Software, **25**(5), 626–632.

Fox, S., Cahill, F., O'Reilly, E., Clifford, E., (2015) Decentralised wastewater treatment using 'Pumped Flow Biofilm Reactor (PFBR) technology'. Civil engineering, College of Engineering & Informatics, NUI Galway, Ireland

Fu, B., Liao, X.Y, Ding, L. L., Ren, H. Q. (2010) Characterisation of microbial community in an aerobic oving bed biofilm reactor applied for simultaneous nitrification and denitrification'. World Journal of Microbiological and Biotechnology, **26**, 1981-1990

Funamizu, N. and Takakuwa, T. (1994) Simulation of the operating conditions of the municipal wastewater treatment plant at low temperatures using a model that includes the IAWPRC activated sludge model. Water Science and Technology **30**(4),150-113

Gabaldon, C., Ferrer, J., Seco, A., Marzal, P. (1998). A software for the integrated design of wastewater treatment plants. Environmental Modelling and Software, **13**, pp. 31–44

Garcia-Ochoa, F., & Gomez, E. (2009). Bioreactor scale-up and oxygen transfer rate in microbial processes: an overview. Biotechnology Advances, **27**(2), 153–76.

Gernaey, K. V, van Loosdrecht, M. C. ., Henze, M., Lind, M., & Jørgensen, S. B. (2004). Activated sludge wastewater treatment plant modelling and simulation: state of the art. Environmental Modelling & Software, **19**(9), 763–783.

Grady, C.P.L. (1983) Modelling of fixed films—A state of the art review Fixed Film Biological Processes for Wastewater Treatment, Noyes Data Corp, Park Ridge, NJ, pp. 75–134

Grady Jr. C.P.L., Smets, B.F., Barbeau, D.S. (1996) Variability in kinetic parameter estimates: a review of possible causes and a proposed terminology. Water Res., 30 (1996), pp. 742 – 748

Gray, N.F. (1999) Water Technology: An introduction for Environmental Scientists and Engineers. John Wiley & Sons, New York, USA.

Gray, N.F. (2004) Biology of wastewater treatment. 2nd Ed. Imperial College Press, London UK

Griffin, P., Findlay, G.E., (2000) Process and engineering improvements to rotating biological contactor design Water Sci. Technol., **41** (1) (2000), pp. 137–144

Haimi, H., Mulas, M., Sahlstedt, K., & Vahala, R. (2009). Advanced Operation and Control Methods of Municipal Wastewater Treatment Processes in Finland. Helsinki University of Technology Water and Wastewater Engineering.

Hank Andres, Zhi-Rong Hu, Spencer Snowling, Oliver Schraa (2006) Model-Based Optimum Design of Sequencing Batch Reactors for COD and Nitrogen Removal from a Slaughterhouse Wastewater, Water Environment Foundation.

Hauduc, H., Rieger, L., Ohtsuki, T., Shaw, A., Takács, I., Winkler, S., Gillot, S. (2011). Activated sludge modelling: development and potential use of a practical applications database. Water Science & Technology, **63**(10), 2164.

Hellstedt, Cajsa (2005) Calibration of a dynamic model for the activated sludge process at Henriksdal wastewater treatment plant. Department of Information Technology, Uppsala University

Henry, L.G., (2013) – Comparison of Intermittently Aerated Sequencing Batch Reactors (IASBRs) and Conventional Sequencing Batch Reactors (cSBRs) in Wastewater Treatment. PhD Thesis, NUI Galway

Henze M., Grady C.P.L. Jr., Gujer W., Marais G.v.R. and Matsuo T. (1987) Activated Sludge Model No. 1. IAWQ Scientific and Technical Report No. 1, London, UK.

Henze, M. (1988) Constants in mathematical models. IAWPRC Technology Transfer Seminar on Mathematical Modeling of Biological Wastewater Treatment Processes, 4-6 May, Rome, Italy, pp.1-13

Henze M., (1992) Characterization of wastewater for modelling of activated sludge process. Water Science and Technology. **25**(6), 1 – 15.

Henze M., Gujer W., Mino T. and van Loosdrecht M.C.M. (2000) Activated Sludge Models ASM1, ASM2, ASM2d and ASM3. IWA Scientific and Technical Report 9 IWA. London.

Henze, Mogens, Gujer, Willi, Mino, Takashi, van Loosdrecht, M. (2000). Activated Sludge Models ASM1, ASM2, ASM2D and ASM3 - IWA Task Group on Mathematical Modelling for Design and Operation of Biological Wastewater Treatment.

Henze, M., Harremoes, P., La Cour Jansen, J and Arvin, E. (2002) Wastewater Treatment: Biological and Chemical Processes. Springer – Verlag; 3rd Edition

Hydromantis (2006) GPS-X Technical Reference Version 5.0

Hydromantis (2010) GPS-X User's Guide Version 6.0

IWA Scientific and Technical report on Activated Sludge Model No. 2 (Henze et al, 1995)

Jeppsson, U. (1996). Modelling aspects of wastewater treatment processes. Lund Institute of Technology.

Jones, N., Clifford, E. (2014) Modelling a Novel Batch Biofilm Passive Aeration Technology Using AQUASIM. Volume 68 of International Proceedings of Chemical, Biological & Environmental Engineering. Volume **68**. 50-5

Kaelin, D., Manser, R.,Rieger, L., Eugster, J., Rottermann, K., Siegrist, H., (2009) Extension of ASM3 for two-step nitrification and denitrification and its calibration and validation with batch tests and pilot scale data. Water Res. **43**(6):1680-92

Kennelly, C., Clifford, E., Gerrity, S., Walsh, R., Rodgers, M,. Collins, G., (2012) A horizontal flow biofilm reactor (HFBR) technology for the removal of methane and hydrogen sulphide at low temperatures. Water Sci Technol. **66**(9):1997-2006

Kim, H., & Hao, O. J. (2001). pH and Oxidation-Reduction Potential Control Strategy for Optimization of Nitrogen Removal in an Alternating Aerobic-Anoxic System All use

subject to JSTOR Terms and Conditions pH and Control Nitrogen Strategy Removal Potential of for Optimization in an A. Water Environment Research, **73**(1), 95–102.

Kloc, J. (2012). The Study of Biological Wastewater Treatment through Biofilm Development on Synthetic Material vs. Membranes. Worcester Polytechnic Institute

Kluyver AJ, Donker HJK (1926) Die Einheit in der Biochemie. Chem Zelle u Gewebe **13**:134-190

Kristensen, H.G., la Cour Janssen, J. and Jorgensen, E. (1998) Batch test procedures as tools for calibration of the activated sludge model – A pilot scale demonstration. Water Science and Technology **37**(4-5), 235-242

Lazarova, V., & Manem, J. (1995). Biofilm characterization and activity analysis in water and wastewater treatment. Water Research, **29**(10), 2227–2245.

Lesouef, A., Payraudeau, M., Rogalla, F. and Kleiber, B. (1992) Optimizing nitrogen removal reactor configurations by on-site calibration of the IAWPRC activated sludge model. Water Science and Technology **25**(6)105-123

Levenspiel, O (1980) The Monod equation: A revisit and a generalization to product inhibition situations. Biotechnology and Bioengineering **22**, 1671–1687

Liu, Y. & Tay, J.H., 2001. Strategy for minimization of excess sludge production from the activated sludge process. Biotechnology advances, **19**, pp.97–107.

Low, E.W. & Chase, H. a., 1999. Reducing production of excess biomass during wastewater treatment. Water Research, **33**(5), pp.1119–1132.

Mannina, G., Cosenza, A., Vanrolleghem, P. a., & Viviani, G. (2011). A practical protocol for calibration of nutrient removal wastewater treatment models. Journal of Hydroinformatics, **13**(4), 575.

Melcer, H. (2003). Methods for Wastewater Characterisation in Activated Sludge Modelling. IWA Publishing and Water Environment Federation.

Merkey, B. V., Rittmann, B.E.,Chopp, D. (2009) Modeling how soluble microbial products (SMP) support heterotrophic bacteria in autotroph-based biofilms. Journal of Theoretical Biology **259**(4):670-83

Metcalf and Eddy, Inc. (2003) Wastewater engineering: treatment and reuse. Fourth Edition, McGraw-Hill

Njenga, M., (2014) Simulation of batch operated experimental wetland mesocosms in AQUASIM biofilm reactor compartment. Journal of Environmental Management 134: 100-108

Noguera, D.R., Okabe, S., Picioreanu, C. (1999). Biofilm modelling: present status and future direction. Water Science and Technology **39**: 273-278

Norton, D., (2009) – Nitrogen Removal from Slaughterhouse Wastewater by Simultaneous Nitrification and Denitrification using a Pilot-Scale Sequencing Batch Reactor MEngSc Thesis, NUI Galway

Novák, L., Larrea, L., Wanner, J. (1994) Estimation of maximum specific growth rate of heterotrophic and autotrophic biomass: a combined technique of mathematical modelling and batch cultivations. Water Sci. Technol., 30 (11) (1994), pp. 171 – 180

Nowak, O., (2000) Upgrading of wastewater treatment plants equipped with rotating biological contactors to nitrification and P removal Water Sci. Technol., **41** (1) (2000), pp. 145–15

Odegaard, H. & Rusten, B. (1980) Nitrogen removal in rotating biological contactors without the use of external carbon source. In proceedings: 1st symposium/workshop on rotating biological contactors, Champion, P.A. 4-6th February 1980. University of Pittsburgh, PA, USA

Ødegaard, H., Melin, E., Helness, H., Kenakkala, T., (2004). High-rate wastewater treatment based on moving bed biofilm reactors, polymer coagulation and flotation. In: Hahn, H.H., Hoffmann, E., Ødegaard, H. (Eds.), Chemical Water and Wastewater Treatment VIII. IWA Publishing.

Ødegaard, H., (2006). Innovations in wastewater treatment: the moving bed biofilm process. Water Science and Technology **53** (9), 17–33.

O'Reilly E., (2005) – Biological Wastewater Treatment using an Alternating Pumped Sequencing Batch Biofilm Reactor (APSBBR) MEngSc Thesis, NUI Galway

O'Reilly, E., Rodgers, M., & Zhan, X.-M. (2008). Pumped flow biofilm reactors (PFBR) for treating municipal wastewater. Water Science and Technology : A Journal of the International Association on Water Pollution Research, **57**(12), 1857–65.

O'Reilly, E., Clifford, E. and Rodgers, M. (2011) Municipal Wastewater Treatment using a Full-Scale Pumped Flow Biofilm Reactor (PFBR) Water Science and Technology **64** 1218-1225

O'Reilly E., (2011) – Removal of Organic Carbon, Nitrogen and Phosphorus from Wastewater using a Novel Biofilm Reactor PhD Thesis, NUI Galway

O'Reilly, E., Rodgers, M. & Clifford, E., 2011. Operation of a full-scale pumped flow biofilm reactor (PFBR) under two aeration regimes. Water Science & Technology, **64**(6), p.1218.

Ouellette, G. D. (2009). Oxygen Mass Transfer Coefficient (Kla) consideration for Scale-Up Fermentation Systems. Biotechnology Advances **27** 153–176

Pedersen, J. and Sinkjaer, O. (1992) Test of the activated sludge models capabilities as a prognostic tool on a pilot scale wastewater treatment plant. Water Science and Technology **25**(6)185-194

Pena-Tijerina, A.J., and Chiang, W. (2007). What does it take to model a wastewater treatment plant? In Proceedings: Texas Water, Fort Worth Convention Centre, Texas, USA.

Petersen, B., Gernaey, K., Henze, M., & Vanrolleghem, P. A. (2000). Calibration of Activated Sludge Models: A Critical Review of Experimental Designts (pp. 1–80). Ghent University.

Petersen B., Gernaey, K., Henze, M. & Vanrolleghem (2003) Calibration of Activated Sludge Models: A Critical Review of Experimental Designs. Biotechnology for the Environment: Wastewater Treatment and Modelling, Waste Gas Handling. Focus on Biotechnology Volume **3C**, 2003, pp 101-186

Picioreanu, C., Van Loosdrecth MCM., Heijnen, J.J. (1999) Discrete-differential modelling of biofilm structure. Water Science and Technology **39**: 115-122

Picioreanu, C. Xavier, J. B., Van Loosdrecth MCM. (2004) Advances in mathematical modelling of biofilm structures. Biofilms **1**: 337-349

Pylnik, S. V., & Dueck, I. G. (2012). Startup simulation for a rotating biological contactor. Theoretical Foundations of Chemical Engineering, **46**(1), 72–79.

Reichert, P. (1995). Design techniques of a computer program for the identification of processes and the simulation of water quality in aquatic systems, (**3**), 199–210.

Reichert, P. (1998). AQUASIM 2.0 - User Manual. Computer Program for the Identi cation and Simulation of Aquatic Systems. Swiss Federal Institute for Environmental Science and Technology (EAWAG).

Rodgers, M., Zhan, X.-M. (2003) Moving-medium biofilm reactors. Reviews of Environmental Science and Biotechnology, **2**, 213-224

Roeleveld, P.J., van Loosdrecht MC. (2002) Experience with guidelines for wastewater characterisation in The Netherlands. Water Sci Technol.**45**(6):77-87.

Siegrist, H. and Tschui, M. (1992) Interpretation of experimental data with regards to the activated sludge model no.1 and calibration of the model for municipal wastewater treatment plants. Water Science and Technology **25**(6)167-183

Sin, G. (2004). Systematic Calibration of Activated Sludge Models. Gent University

Sin, G., Van Hulle, S. W. H., De Pauw, D. J. W., van Griensven, A., & Vanrolleghem, P. a. (2005). A critical comparison of systematic calibration protocols for activated sludge models: a SWOT analysis. Water Research, **39**(12), 2459–74.

Sincero, A., Sincero, G. (2003) Physical-Chemical Treatment of Water and Wastewater. IWA publishing

Snowling, S., 2014. Personal communication.

Stokes, L., Takacs, I., Watson, B. and Watts J.B. (1993) Dynamic modelling of an A.S.P. sewage works – A case study. Water Science and Technology **28**(11-12),151-161

Suescun, J., Rivas, A., Ayesa, E., Larrea, L. (1994) A new simulation program oriented to the design of complex biological processes for wastewater treatment. P. Zanetti (Ed.), Computer Techniques in Environmental Studies V, Computational Mechanics Publications, Southampton, Boston pp. 209–215

US EPA (2000) Wastewater Technology factsheet Sequence Batch Reactors. Washington, DC.

US EPA (2000) Wastewater Technology factsheet Trickling Filters. Washington, DC.

US EPA. (2010). Evaluation of Energy Conservation Measures. Washington, DC.

Van Loosdrecht, M. C. M., Heijnen, J. J., Eberl, H., Kreft, J., & Picioreanu, C. (2002). Mathematical modelling of biofilm structures. Antonie van Leeuwenhoek, **81**(1-4), 245–56.

Vanrolleghem, P.A., Jeppsson, U., Carstensen, J., Carlsson, B., Olsson, G. (1996) Integration of wastewater treatment plant design and operation – A systematic approach using cost functions. Water Science and Technology **34** (3–4) (1996), pp. 159–17

Vesilind, P. Aarne (2003) Wastewater Treatment Plant Design

Wanner O. (1996) Modelling of Biofilm. Biofouling **10**: 31-41

Wanner, O., & Morgenroth, E. (2004). Biofilm modeling with AQUASIM. Water Science and Technology : A Journal of the International Association on Water Pollution Research, **49**(11-12), 137–44.

Weiss, J. S., Alvarez, M., Tang, C., Horvath, R. W., & Stahl, J. F. (2005). Evaluation of Moving Bed Biofilm Reactor Technology, 2085–2102.

Wilderer, P. A., McSwain, B. S., (2004) The SBR and its biofilm application potentials. Water Science and Technology, **50**, 1-10

Winogradsky S (1890) Recherches sur les organismes de la nitrification. Ann Inst Pastuer 4:213-231

Wolf, G., Picioreanu, C., van Loosdrecht MCM, (2007) Kinetic modelling of phototrophic biofilms: the PHOBIA model. Biotecnology Bioeng 97:1064-1079

Xu, S. and Hultman, B. (1996) Experiences in wastewater characteristics and model calibration for the activated sludge process. Water Science and Technology **33**(12), 89-98

Zhan, X.-M., Rodgers, M., & O'Reilly, E. (2006). Biofilm growth and characteristics in an alternating pumped sequencing batch biofilm reactor (APSBBR). Water Research, **40**(4), 817–25.

Zhang, L. Q., Wei, C. H., Zhang, K. F., Zhang, C. S., Fang, Q., Li, S. G. (2009) Effects of temperature on simultaneous nitrification and denitrification via nitrate in a sequencing batch biofilm reactor. Bioprocess and Biosystem Engineering, **32**, 175-182

APPENDICES

APPENDIX A

Conference papers

Development and Calibration of a new model for Designing and Optimising a new Passive Aeration System for the Treatment of Municipal Wastewater

Noelle Jones[1,*], Edmond O' Reilly[1,2], Eoghan Clifford[1,2]
[1] Civil Engineering, College of Engineering & Informatics, NUI Galway, Galway
(Email: *n.jones2@nuigalway.ie, eoghan.clifford@nuiglaway.ie)*

Abstract: Biofilm-based passive aeration systems (PAS) have attracted recent attention as alternative energy efficient and low maintenance technologies for the treatment of municipal wastewater. However the modelling of biofilm-based PAS offers unique challenges for modellers particularly where new technologies are not easily modelled using existing commercial modelling software. However, if the modeller is concerned only with modelling the effluent from the system it may be possible to model these technologies using "surrogate" unit process systems (e.g. using an activated sludge process to model a biofilm process). The pumped flow biofilm reactor (PFBR); a batch biofilm technology, is one such example of a passive aeration system. The PFBR is a two reactor technology that employs a unique hydraulic regime and enables aerobic, anoxic and anaerobic conditions to be sequenced. Biofilm, growing on plastic media modules within the two reactors, is aerated passively as wastewater is moved alternately between the reactors during an aeration sequence. Thus as the two reactors empty and fill a number of times during a typical aeration sequence, the biofilm is exposed, in turn, to atmospheric air and wastewater. Furthermore while the PFBR has many of the features of a sequencing batch reactor the fill and discharge from the system typically take place in Reactors 1 and 2 respectively. GPS-X is modular, multi-purpose commercial software that can be used to simulate various wastewater treatment processes. As a relatively new technology a predictive model for the PFBR system has yet to be developed. Indeed for novel passive aeration systems in general, it can be time consuming and difficult to develop new models that accurately describe performance. In this study, using the PFBR as a case study of a biofilm-based PAS, a predictive model, developed using the modelling package GPS-X (Hydromatis Inc.), is presented. The model, which aims to simulate effluent quality only, was developed by modifying standard activated sludge sequencing batch reactor processes. The model was calibrated using experimental data obtained from a laboratory PFBR study. The model was then applied to a second set of independent laboratory data, obtained by operating the PFBR under an alternative wastewater loading regime. The results showed excellent correlation between experimental and modelled effluent results. While future work will focus on developing a unique model for the PFBR (and similar technologies) this study presents an alternative means to efficiently develop initial predictive models for novel passive aeration systems.

Presented by the 1st author at the *IWA 9th International Conference on Biofilm Reactors 2013.* Paris, France. 28th – 31st May 2013

Abstract associated with Chapter 4.

Modelling a Novel Batch Biofilm Passive Aeration Technology Using AQUASIM

Noelle Jones[1], Eoghan Clifford[2]
[1] Civil Engineering, College of Engineering & Informatics, NUI Galway
[2] Ryan Institute, NUI Galway

Abstract. Wastewater Treatment Plant modelling is a effective tool for performing plant capacity assessments and improving plant operations, thus allowing for energy and chemical cost savings. Once implemented and calibrated, a model provides important benefits for planning, designing and optimizing wastewater treatment plants. However, mathematical modelling of biofilm reactors can be very complicated and time-consuming due to the complexity of the biofilms - to combat this a wide range of models from 1D to 3D have been tested to describe the complex conditions that occur in biofilms. The Pumped Flow Biofilm Reactor (PFBR) is a new biofilm-based passive aeration system (PAS) that is an example of a complex biofilm system. The PFBR is a two reactor technology that employs a unique hydraulic regime and enables aerobic, anoxic and anaerobic conditions to be sequenced. Biofilm, growing on plastic media modules within the two reactors, is aerated passively as wastewater is moved alternately between the reactors during an aeration sequence. Thus as the two reactors empty and fill a number of times during a typical aeration sequence, the biofilm is exposed, in turn, to atmospheric air and wastewater. Thus the system, while simple to design and operate, provides a particular challenge to modellers. Given its complexity, due to the passive aeration system achieved using a unique hydraulic flow regime; previous models have only been concerned with simulating the effluent from the PFBR. The results showed excellent correlation between experimental and modelled effluent results. However these models were only suitable to be used at macro scale level (i.e. wastewater characteristics). To date, models for the PFBR technology have not focused on the cycle performance of the PFBR, biofilm thickness or biofilm composition. It is proposed to model the PFBR using the modelling package AQUASIM in order to study the PFBR at a micro-scale level; this will enable the study of cycle performance, biofilm thickness and biofilm composition.

In this study, using the PFBR as a case study of a biofilm-based PAS, a predictive model, developed using the modelling package AQUASIM is presented for two different treatment plants. The results showed good correlation between experimental and modelled results.

Accepted at the 4th *International Conference on Environmental Science and Engineering*. Erzurum, Turkey. April 24th-26th, 2014

Abstract associated with Chapter 6.

The Modelling of a Batch Biofilm Passive Aeration Process using an Activated Sludge Process in GPS-X

Noelle Jones[1], Eoghan Clifford[2]
[1] Civil Engineering, College of Engineering & Informatics, NUI Galway
[2] Ryan Institute, NUI Galway

Abstract. Biofilm-based passive aeration systems (PAS) have attracted recent attention as alternative energy efficient and low maintenance technologies for the treatment of municipal wastewater. However the modelling of biofilm-based PAS offers unique challenges for modellers particularly where new technologies are not easily modelled using existing commercial modelling software. However, if the modeller is concerned only with simulating "macro" plant performance (e.g. key effluent concentrations and cycle analysis) it may be possible to model these technologies using "surrogate" unit process systems (e.g. using an activated sludge process to model a biofilm process). The pumped flow biofilm reactor (PFBR); a batch biofilm technology, is a recent example of a PAS. As a relatively new technology a predictive model for the PFBR system has yet to be developed. Indeed for novel passive aeration systems in general, it can be time consuming and difficult to develop new models that accurately describe performance.The present investigation serves to investigate the possibility of (1) modelling the PFBR (a novel biofilm technology) using an activated sludge object in GPS-X in order to quickly study the PFBR at a macro scale level (2) predicting effluent results and contaminant concentration changes (nitrogen and organic carbon) during individual treatment cycles using the activated sludge object (3) once the model is calibrated modelling different scenarios and thus predicting the optimal scenario i.e. one that meets effluent standards, the most energy efficient and the most cost-effective. The PFBR was modelled and calibrated at laboratory and field scale. In each case, after calibration, the models were verified using independent data. The models resulted in good predictions of effluent results and contaminant concentration changes (nitrogen and organic carbon) during individual treatment cycles and could thus be used for process optimisation; or eventually real time process simulation.

Accepted at the 4th *International Conference on Environmental Science and Engineering*. Erzurum, Turkey. April 24th-26th, 2014

International Proceedings

Jones, N., Clifford, E. (2014) Modelling a Novel Batch Biofilm Passive Aeration Technology Using AQUASIM. Volume 68 of International Proceedings of Chemical, Biological & Environmental Engineering. Volume 68. 50-5

Jones, N., Clifford, E. (2014) Modelling a Novel Batch Biofilm Passive Aeration Technology Using AQUASIM. Volume of Journal (IPCBEE, ISSN: 2010-4618)

Abstract associated with Chapter 4 and 5.

Developing an AQUASIM biofilm model to simulate a novel batch biofilm passive aeration technology

Noelle Jones [1,2], Maebh Grace [1,2], Eoghan Clifford [1,2]
[1] Civil Engineering, College of Engineering & Informatics, NUI Galway, University Road, Galway
[2] Ryan Institute, NUI Galway
n.jones2@nuigalway.ie *eoghan.clifford@nuigalway.ie*

Abstract: Mathematical modelling of biofilm reactors can be complicated and time-consuming due to the complexity of the biofilms and a wide range of models have been developed to simulate biofilm reactors. The Pumped Flow Biofilm Reactor (PFBR) is a new biofilm-based passive aeration system (PAS) that is an example of a complex biofilm system. The PFBR is a two reactor technology that employs a unique hydraulic regime and enables aerobic, anoxic and anaerobic conditions to be sequenced. Biofilm, growing on plastic media modules within the two reactors, is aerated passively as wastewater is moved alternately between the reactors during an aeration sequence. The two reactors (R1 and R2) empty and fill a number of times during a typical aeration sequence, exposing, in turn, the biofilm to atmospheric air and wastewater. Furthermore while the PFBR has many of the features of a sequencing batch reactor the fill and discharge from the system typically take place in reactors 1 and 2 respectively. Thus the system, while simple to design and operate, provides a particular challenge to modellers. Given its complexity, due to the passive aeration system achieved using a unique hydraulic flow regime; previous models have only been concerned with simulating the effluent from the PFBR. The results showed excellent correlation between experimental and modelled effluent results however these models were only suitable to be used at macro scale level (i.e. wastewater characteristics). In this paper the following objectives have been set forth for this investigation: (1) develop a unique biofilm model for the PFBR, (2) calibrate the effluent characteristics and the cycle performance of the PFBR, (3) identify the biofilm composition, (4) model the biofilm thickness using a confined reactor and an unconfined reactor.

Presented at the *7th International Congress on Environmental Modelling and Software*. San Diego, California. June 15th-19th, 2014

Abstract associated with Chapter 6.

Modelling biofilm based technologies with activated sludge unit processes: A short cut to performance simulation?

Noelle Jones [1,2], Maebh Grace [1,2], Eoghan Clifford [1,2]

[1] Civil Engineering, College of Engineering & Informatics, NUI Galway, University Road, Galway

[2] Ryan Institute, NUI Galway

n.jones2@nuigalway.ie *eoghan.clifford@nuigalway.ie*

Abstract: Biofilm-based passive aeration systems (PAS) have attracted recent attention as alternative, energy efficient and low maintenance technologies in the wastewater sector. However the modelling of biofilm-based PAS offers unique challenges for modellers, particularly where new technologies are not easily simulated using existing commercial modelling software. However, if the modeller is concerned only with simulating "macro" plant performance (e.g. key effluent concentrations and cycle analysis) it may be possible to efficiently model these technologies using "surrogate" unit process systems (e.g. using an activated sludge process to model a biofilm process). The pumped flow biofilm reactor (PFBR); a batch biofilm technology, is a recent example of a PAS. As a relatively new technology a predictive model for the PFBR system has yet to be developed. Indeed for novel passive aeration systems in general, it can be time consuming and difficult to develop new models that accurately describe performance. This research investigates the potential for (1) modelling the PFBR (an example of a batch biofilm PAS) using previously developed, simple activated sludge based models (2) predicting effluent results and contaminant concentration changes (nitrogen and organic carbon) during individual treatment cycles using the activated sludge object, and (3) using the calibrated model to predict the optimal operational regimes.

Presented at the *7th International Congress on Environmental Modelling and Software*. San Diego, California. June 15th-19th, 2014

Abstract associated with Chapter 4 and 5.

APPENDIX B

ASM2

Process kinetics and stoichiometry for C oxidation, nitrification, denitrification and P removal in ASM2

Component	index	1	2	3	4	5	6	7	8	9	10	11	12	13	14	15	16	17	18	19	20	Process Rate, ρ
	↓	S_S	S_{O2}	S_F	S_A	S_{NH4}	S_{NO3}	S_{PO4}	S_I	S_{ALK}	S_{N2}	X_I	X_S	X_H	X_{PAO}	X_{PP}	X_{PHA}	X_{AUT}	X_{TSS}	X_{MeOH}	X_{MeP}	$[ML^{-3}T^{-1}]$
1	Aerobic Hydrolysis			$1-f_{SI}$		$v_{1,NH4}$		$v_{1,PO4}$	f_{SI}	$v_{1,ALK}$									$v_{1,TSS}$			$K_H \frac{S_{O2}}{K_{O2}+S_{O2}} \frac{X_S/X_H}{K_X+X_S/X_H} X_H$
2	Anoxic Hydrolysis			$1-f_{SI}$		$v_{2,NH4}$		$v_{2,PO4}$	f_{SI}	$v_{2,ALK}$									$v_{2,TSS}$			$K_H \eta_{NO3} \frac{K_{O2}}{K_{O2}+S_{O2}} \frac{S_{NO3}}{K_{NO3}+S_{NO3}} \frac{X_S/X_H}{K_X+X_S/X_H} X_H$
3	Anaerobic Hydrolysis			$1-f_{SI}$		$v_{3,NH4}$		$v_{3,PO4}$	f_{SI}	$v_{3,ALK}$									$v_{3,TSS}$			$K_H \eta_{fe} \frac{K_{NO3}}{K_{O2}+S_{O2}} \frac{K_{NO3}}{K_{NO3}+S_{NO3}} \frac{X_S/X_H}{K_X+X_S/X_H} X_H$
4	Aerobic growth on S_F		$1-\frac{1}{Y_H}$	$-\frac{1}{Y_H}$								1										$\mu_H \frac{S_{O2}}{K_{O2}+S_{O2}} \frac{S_F}{K_F+S_F} \frac{S_A}{K_{AA}+S_{AA}} \frac{S_{NH4}}{K_{NH4}+S_{NH4}} \frac{S_{PO4}}{K_{PO4}+S_{PO4}} \frac{S_{ALK}}{K_{ALK}+S_{ALK}} X_H$
5	Aerobic growth on S_A		$1-\frac{1}{Y_H}$		$-\frac{1}{Y_H}$							1										$\mu_H \eta_{NO3} \frac{K_{O2}}{K_{O2}+S_{O2}} \frac{S_A}{K_A+S_A} \frac{S_F}{K_F+S_F} \frac{S_{NH4}}{K_{NH4}+S_{NH4}} \frac{S_{PO4}}{K_{PO4}+S_{PO4}} \frac{S_{ALK}}{K_{ALK}+S_{ALK}} X_H$
6	Anoxic growth on S_F Denitrification			$1-f_{SI}$			$-\frac{1-Y_H}{2.86Y_H}$				$\frac{1-Y_H}{2.86Y_H}$											$\mu_H \eta_{NO3} \frac{K_{O2}}{K_{O2}+S_{O2}} \frac{S_F}{K_F+S_F} \frac{S_{NO3}}{K_{NO3}+S_{NO3}} \frac{S_{NH4}}{K_{NH4}+S_{NH4}} \frac{S_{PO4}}{K_{PO4}+S_{PO4}} \frac{S_{ALK}}{K_{ALK}+S_{ALK}} X_H$
7	Anoxic growth on S_A Denitrification			$1-f_{SI}$	$-\frac{1}{Y_H}$		$-\frac{1-Y_H}{2.86Y_H}$				$\frac{1-Y_H}{2.86Y_H}$											$\mu_H \eta_{NO3} \frac{K_{O2}}{K_{O2}+S_{O2}} \frac{S_A}{K_A+S_A} \frac{S_F}{K_F+S_F} \frac{S_{NH4}}{K_{NH4}+S_{NH4}} \frac{S_{PO4}}{K_{PO4}+S_{PO4}} \frac{S_{ALK}}{K_{ALK}+S_{ALK}} X_H$
8	Fermentation		1	-1																		$K_{fe} \frac{S_F}{K_{O2}+S_{O2}} \frac{K_{O2}}{K_F+S_F} \frac{S_F}{K_{NH4}+S_{NH4}} \frac{S_{NH4}}{K_{ALK}+S_{ALK}} \frac{S_{ALK}}{K_{PO4}+S_{PO4}} X_H$
9	Lysis													-1								$b_H X_H$
10	Storage of X_{PHA}				-1			Y_{PO4}									$-Y_{PO4}$	1				$q_{PHA} \frac{S_A}{K_A+S_A} \frac{S_{ALK}}{K_{ALK}+S_{ALK}} \frac{X_{PP}/X_{PAO}}{K_{PP}+X_{PP}/X_{PAO}} X_{PAO}$
11	Storage of X_{PP}							-1									1				$-Y_{PHA}$	$q_{PP} \frac{S_{O2}}{K_{O2}+S_{O2}} \frac{S_{PO4}}{K_{PS}+S_{PO4}} \frac{S_{ALK}}{K_{ALK}+S_{ALK}} \frac{X_{PHA}/X_{PAO}}{K_{PHA}+X_{PHA}/X_{PAO}} \frac{K_{MAX}-X_{PP}/X_{PAO}}{K_{PP}+K_{MAX}-X_{PP}/X_{PAO}} X_{PAO}$
12	Aerobic growth of X_{PAO}		$1-\frac{1}{Y_H}$					$-i_{PBM}$									$-\frac{1}{Y_H}$					$\mu_{PAO} \frac{S_{O2}}{K_{O2}+S_{O2}} \frac{S_{NH4}}{K_{NH4}+S_{NH4}} \frac{S_{PO4}}{K_{PS}+S_{PO4}} \frac{S_{ALK}}{K_{ALK}+S_{ALK}} \frac{X_{PHA}/X_{PAO}}{K_{PHA}+X_{PHA}/X_{PAO}} X_{PAO}$
13	Lysis of X_{PAO}							$v_{13,PO4}$					f_{XI}	$1-f_{XI}$	-1							$b_{PAO} X_{PAO} f_{ALK} (K_{ALK}+S_{ALK})$
14	Lysis of X_{PP}							1							-1							$b_{PP} X_{PP} f_{ALK} (K_{ALK}+S_{ALK})$
15	Lysis of X_{PHA}				1											-1						$b_{PHA} X_{PHA} f_{ALK} (K_{ALK}+S_{ALK})$
16	Aerobic growth of X_{AUT}		$-\frac{4.57-Y_A}{Y_A}$			$-i_{NBM}-\frac{1}{Y_A}$	$\frac{1}{Y_A}$	$-i_{PBM}$										1				$\mu_{AUT} \frac{S_{O2}}{K_{O2}+S_{O2}} \frac{S_{NH4}}{K_{NH4}+S_{NH4}} \frac{S_{ALK}}{K_{ALK}+S_{ALK}} \frac{S_{PO4}}{K_P+S_{PO4}} X_{AUT}$
17	Lysis					$v_{17,NH4}$		$v_{17,PO4}$				f_{XI}	$1-f_{XI}$					-1				$b_{AUT} X_{AUT}$
18	Precipitation							-1		$v_{18,ALK}$											4.87	$k_{PRE} S_{PO4} X_{MeOH}$
19	Redissolution							1		$v_{19,ALK}$										3.45	-4.87	$k_{RED} X_{MeP} S_{ALK} / (K_{ALK}+S_{ALK})$
Observed Conversion Rates $[ML^{-3}T^{-1}]$								$r_i = \sum_j \nu_{ij} \rho_j$														

Stoichiometric Parameters:
Soluble Material: i_{NBS}, i_{NSF}
Particulate Material: i_{NXI}, i_{NXS}, i_{NBM}
Phosphorus (Soluble Material): i_{PBS}, i_{SF}
Phosphorus (Particulate Material): i_{PXI}, i_{PXS}, i_{PBM}
Total SS: i_{TSSXI}, i_{TSSXS}, i_{TSSBM}
Hydrolysis: f_{SI}
Heterotrophs Organisms: f_{XI}, Y_H,
PAOs: Y_{PAO}, Y_{PHA}, Y_{PP}, f_{XI}
Nitrifying Organisms: Y_{AUT}, f_{XI}

Kinetic Parameters:
Hydrolysis: K_H, η_{NO3}, η_{fe}, K_{O2}, K_{NO3}, K_X
Heterotrophic growth and decay: μ_H, q_{fe}, η_{NO3}, K_A, K_{NH4}, K_{PO4}, K_{ALK}, b_H
PAOs: q_{PHA}, q_{PP}, μ_{PAO}, b_{PAO}, b_{PHA}, b_{PP}, K_{ALK}, K_{PS}, K_{PP}, K_{MAX}, K_{IPP}, K_{PHA}
Nitrifiers: μ_{AUT}, b_{AUT}, K_{O2}, K_{NH4}, K_{ALK}, K_P
precipitation: k_{PRE}, K_{RED}, K_{ALK}

APPENDIX C

Some results from initial GPS-X investigations (attached on CD)

APPENDIX D

GPS-X flow control forms

Flow control form Reactor 1

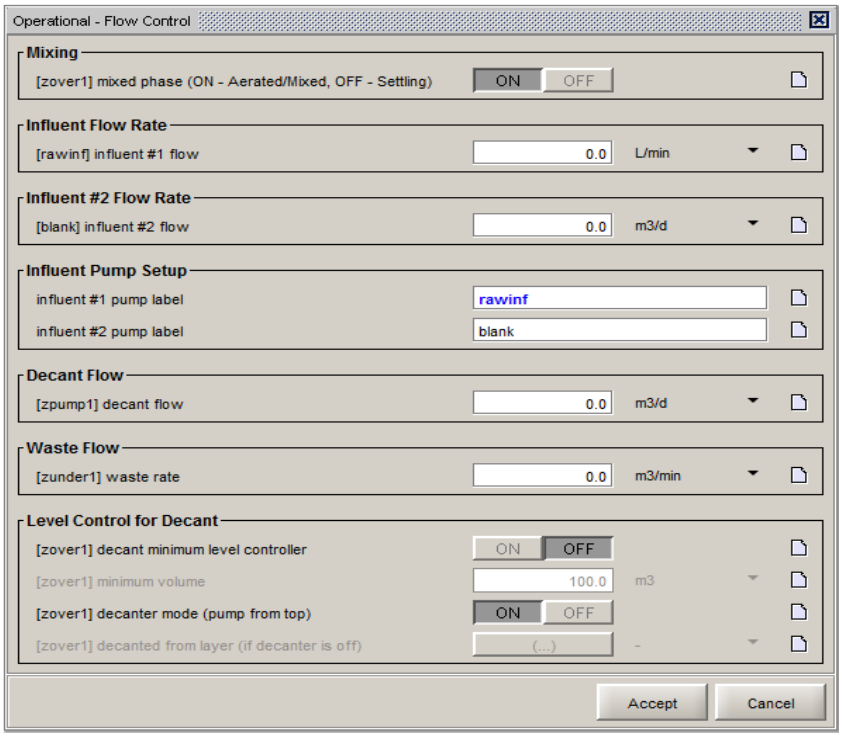

Flow control form Reactor 2

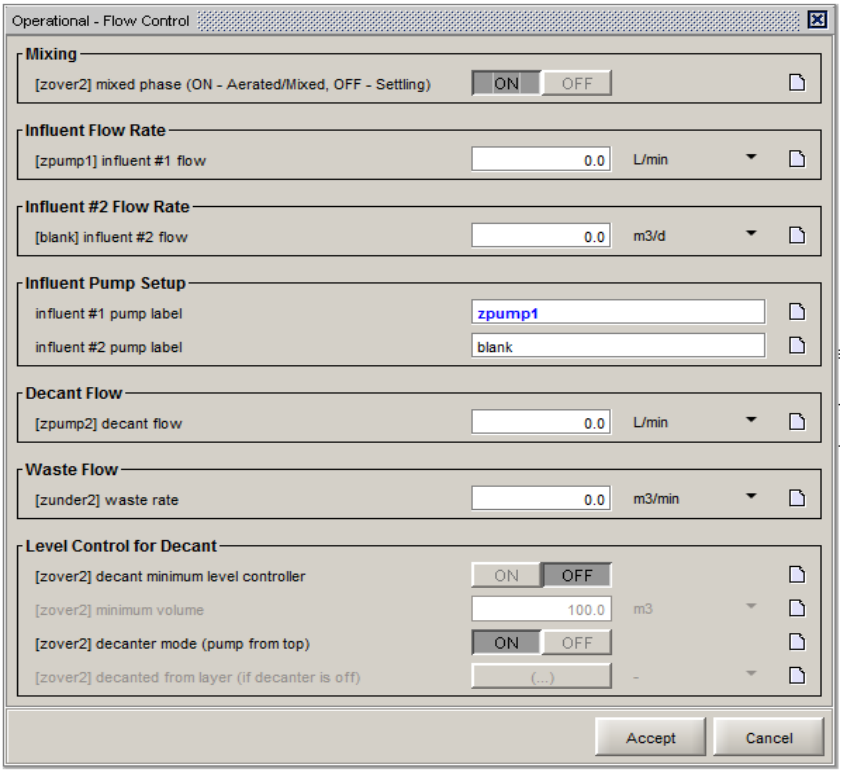

APPENDIX E

Influent advisor in GPS-X

LS-PFBR Influent Advisor

Study 1 modelled influent composition using influent Advisor in GPS-X

Biological Model: asm1		
Influent Composition		
total COD	gCOD/m^3	1020
total suspended solids	g/m^3	0
total nitrogen	gN/m^3	96
Organic Variables		
active autotrophic biomass	gCOD/m^3	0
unbiodegradable particulates from cell decay	gCOD/m^3	0
Dissolved Oxygen		
dissolved oxygen	gO2/m^3	0
Nitrogen Compounds		
nitrate and nitrite	gN/m^3	0
dinitrogen	gN/m^3	0
Alkalinity		
alkalinity	mole/m^3	7
Influent Fractions		
XCOD/VSS ratio	gCOD/gVSS	1.8
BOD5/BODultimate ratio	-	0.66
TSSCOD Model Coefficients		
inert fraction of soluble COD	-	0.2
substrate fraction of particulate COD	-	0.82
heterotrophic fraction of particulate COD	-	0
ammonium/TKN ratio	-	0.66
part. org. N/total org. N ratio	-	0.9
VSS/TSS ratio	gVSS/gTSS	0.75
ASM1 Nutrient Fractions		
N content of active biomass	gN/gCOD	0.086
N content of endogenous/inert mass	gN/gCOD	0.06
Nitrogen Compounds		
free and ionized ammonia	gN/m^3	63.36

Study 2 modelled influent composition using influent Advisor in GPS-X

Biological Model: asm1		
Influent Composition		
total COD	gCOD/m^3	346
total suspended solids	g/m^3	0
total nitrogen	gN/m^3	32
Organic Variables		
active autotrophic biomass	gCOD/m^3	0
unbiodegradable particulates from cell decay	gCOD/m^3	0
Dissolved Oxygen		
dissolved oxygen	gO2/m^3	0
Nitrogen Compounds		
nitrate and nitrite	gN/m^3	0
dinitrogen	gN/m^3	0
Alkalinity		
alkalinity	mole/m^3	7
Influent Fractions		
XCOD/VSS ratio	gCOD/gVSS	1.8
BOD5/BODultimate ratio	-	0.66
TSSCOD Model Coefficients		
inert fraction of soluble COD	-	0.2
substrate fraction of particulate COD	-	0.82
heterotrophic fraction of particulate COD	-	0
ammonium/TKN ratio	-	0.59
part. org. N/total org. N ratio	-	0.9
VSS/TSS ratio	gVSS/gTSS	0.75
ASM1 Nutrient Fractions		
N content of active biomass	gN/gCOD	0.086
N content of endogenous/inert mass	gN/gCOD	0.06
Nitrogen Compounds		
free and ionized ammonia	gN/m^3	18.9

FS-PFBR1 Influent Advisor

Study 3 modelled influent composition using influent advisor in GPS-X

Biological Model: ASM1		
Influent Composition		
total COD	gCOD/m^3	310
filtered COD	gCOD/m^3	186
particulate COD	gCOD/m^3	76
total suspended solids	g/m^3	90
total nitrogen	gN/m^3	40
Organic Variables		
active autotrophic biomass	gCOD/m^3	0
unbiodegradable particulates from cell decay	gCOD/m^3	0
Dissolved Oxygen		
dissolved oxygen	gO2/m^3	0
Nitrogen Compounds		
nitrate and nitrite	gN/m^3	0
dinitrogen	gN/m^3	0
Alkalinity		
alkalinity	mole/m^3	7
Influent Fractions		
XCOD/VSS ratio	gCOD/gVSS	1.4
BOD5/BODultimate ratio	-	0.66
TSSCOD Model Coefficients		
inert fraction of soluble COD	-	0.3
substrate fraction of particulate COD	-	0.82
heterotrophic fraction of particulate COD	-	0
ammonium/TKN ratio	-	0.85
part. org. N/total org. N ratio	-	0.15
VSS/TSS ratio	gVSS/gTSS	0.6
ASM1 Nutrient Fractions		
N content of active biomass	gN/gCOD	0.086
N content of endogenous/inert mass	gN/gCOD	0.06
Nitrogen Compounds		
free and ionized ammonia	gN/m^3	34

Study 4 modelled influent composition using influent advisor in GPS-X

Biological Model: asm1		
Influent Composition		
total COD	gCOD/m^3	310
filtered COD	gCOD/m^3	146
particulate COD	gCOD/m^3	164
total suspended solids	g/m^3	73
total nitrogen	gN/m^3	40
Organic Variables		
active autotrophic biomass	gCOD/m^3	0
unbiodegradable particulates from cell decay	gCOD/m^3	0
Dissolved Oxygen		
dissolved oxygen	gO2/m^3	0
Nitrogen Compounds		
nitrate and nitrite	gN/m^3	0.03
dinitrogen	gN/m^3	0
Alkalinity		
alkalinity	mole/m^3	7
Influent Fractions		
XCOD/VSS ratio	gCOD/gVSS	2.25
BOD5/BOD ultimate ratio	-	0.66
TSSCOD Model Coefficients		
inert fraction of soluble COD	-	0.2
substrate fraction of particulate COD	-	0.82
heterotrophic fraction of particulate COD	-	0
ammonium/TKN ratio	-	0.8
part. org. N/total org. N ratio	-	0.9
VSS/TSS ratio	gVSS/gTSS	1
ASM1 Nutrient Fractions		
N content of active biomass	gN/gCOD	0.086
N content of endogenous/inert mass	gN/gCOD	0.06
Nitrogen Compounds		
free and ionized ammonia	gN/m3	32

FS-PFBR2 Influent Advisor

Study 5 modelled influent composition using influent advisor in GPS-X

Influent Composition		
total COD	$gCOD/m^3$	143
total suspended solids	g/m^3	177
total TKN	gN/m^3	15.2
Organic Variables		
active autotrophic biomass	$gCOD/m^3$	0
unbiodegradable particulates from cell decay	$gCOD/m^3$	0
Dissolved Oxygen		
dissolved oxygen	gO_2/m^3	0
Nitrogen Compounds		
nitrate and nitrite	gN/m^3	0
Alkalinity		
alkalinity	$mole/m^3$	7
Influent Fractions		
XCOD/VSS ratio	gCOD/gVSS	1.8
BOD5/BOD ultimate ratio		0.66
TSSCOD Model Coefficients		
inert fraction of soluble COD	-	0.2
substrate fraction of particulate COD	-	0.82
heterotrophic fraction of particulate COD	-	0.0
ammonium/TKN ratio	-	0.7
part. org. N/total org. N ratio	-	0.9
VSS/TSS ratio	gVSS/gTSS	0.75
ASM1 Nutrient Fractions		
N content of active biomass	gN/gCOD	0.086
N content of endogenous/inert mass	gN/gCOD	0.06

APPENDIX F

DO testing using Redeye oxygen patches (attached on CD)

APPENDIX G

GPS-X sensitivity analysis results LS-PFBR (attached on CD)

APPENDIX H

GPS-X LS-PFBR model results Study 1 and Study 2 (attached on CD)

APPENDIX I

FS-PFBR1 model results Study 3 and Study 4 (attached on CD)

APPENDIX J

AQUASIM sensitivity analysis results FS-PFBR1 (attached on CD)

APPENDIX K

AQUASIM FS-PFBR1 model results for Study 3 and 4 (attached on CD)

APPENDIX L

Comparison between AQUASIM Study 4 confined and unconfined reactor models (attached on CD)

APPENDIX M

KLA analysis FS-PFBR1 GPS-X
(attached on CD)

APPENDIX N

Comparison of features in GPS-X and AQUASIM

Feature	GPS-X	AQUASIM
Model Build	Simple, based on a graphical interface.	Difficult, allows its users to define the spatial configuration of the WWTP as a set of compartments, which can be connected to each other by links.
	It is very user friendly due to its drag and drop interface.	It is not user friendly.
	It has a comprehensive database of unit processes and has 37 process objects to choose from.	It has 6 process objects to choose from.
	It allow users to quickly and easily assemble a treatment plant model.	It time consuming and difficult to assemble a treatment plant model
	Modelling can be carried out quickly to answer any operational questions associated with WWTP.	Modelling can be be carried to answer any operational questions associated with WWTP but it takes more time.
	Over 50 plant layouts are pre-compiled covering many popular activated sludge systems and biofilm systems.	No pre-compiled layouts.
	All GPS-X models are open-code and available to be edited.	AQUASIM compartments are not available to be edited.
	All state variables and transformation processes are active.	The user of the program is free in specifying any set of state variables and transformation processes to be active within the compartments.

Feature	GPS-X	AQUASIM
Activated Sludge models	The user can choose from four influent models (ASM1, ASM2, ASM3, mantis).	ASM family. The user must enter all the ASM equations into the model. This is a very difficult process and can account for a lot of errors.
Input data:	Directly into the GPS-X program 'influent advisor'.	Directly into the model
	GPS-X allows the user to quickly enter characterisation data due to the influent advisor.	It is a very slow process entering characterisation data.
	Influent advisor ensures that the influent data entered by the user is partitioned correctly.	The user must partition the influent data themselves.
	If influent data is entered incorrectly a warning will be issued and information provided about where a potential problem exists.	No warnings issued so you won't know if your influent data is entered correctly or not.
Biofilm modelling	1-dimensional biofilm model with 5 biofilm layers.	1-dimensional biofilm model with a user specified amount of biofilm layers.
	Biomass distribution is heterogeneous	Biomass distribution is heterogeneous
Presentation of output data	GPS-X supports seven types of output displays. X-Y time series plot, X-Y scrolling time series plot, Bar Chart, Bar Chart horizontal, Digital, 3-D Bar Chart, Grayscale. Data files also available. Formatting graphs is not possible	Calculated results can be plotted to the screen (window interface version only), written to a Post-Script file for transfer to a printer, or written to a text file for external post-processing.

Feature	GPS-X	AQUASIM
	GPS-X creates reports directly in Excel format, including images, graphs, parameter settings, and simulation results. Either the default or customized report format can be used for each project.	The `Plot to File', and `List to File' are available in .lis files and must be exported to excel.
Sensitivity Analysis	Yes	Yes
Calibration	Any measured variable can be controlled. An advanced control module is included.	Any measured variable can be controlled.
Ease of calibration	Not difficult	Not difficult
Simulation	It is quick and easy to run simulations.	It is quick and easy to run simulations.
	Both steady-state and dynamic simulations can be run in GPS-X.	Both steady-state and dynamic simulations can be run in GPS-X.
Simulation time	It took 72 minutes for GPS-X to run a 50 day simulation for FS-PRBR1.	It took 20 minutes for AQUASIM to run a 50 day simulation for FS-PRBR1.
Cost	GPS-X requires a site license.	No licence required for AQAUSIM.
Technical Support	Excellent tutorials, webinars and training available on line	AQUASIM don't provide any technical support. An electronic user group list is maintained that facilitates contacts among AQUASIM users.